

Pro-apoptotic TRAIL- and CDK9 inhibition-based cancer therapy

A DISSERTATION
SUBMITTED TO
UNIVERSITY COLLEGE LONDON (UCL)
IN FULFILMENT OF THE REQUIREMENTS
FOR THE DEGREE OF
DOCTOR OF PHILOSOPHY

Itziar Ibone Areso Zubiaur

March 2020

DECLARATION

I, Itziar Ibone Areso Zubiaur, confirm that the work presented in this thesis is my own. Where information has been derived from other sources, I confirm that this has been indicated in the thesis.

ABSTRACT

TRAIL was shown to specifically kill cancer cells *in vivo* without causing toxicity. Based on this, TRAIL-R agonists were developed for clinical use. However, to date, TRAIL-R agonists have only shown limited therapeutic benefit in clinical trials. This is likely attributed to the fact that most primary human cancers are TRAIL-resistant. It is therefore essential to identify potent and cancer-selective TRAIL-sensitising drugs that overcome TRAIL-resistance.

In this thesis it is shown that the CDK9 inhibitor Dinaciclib broadly sensitises different cancer types to TRAIL-induced apoptosis, including, notably, chemo- and targeted therapy-resistant tumour cells. Mechanistically, treatment with Dinaciclib results in RNA polymerase II inhibition, leading to the inhibition of transcriptional elongation. Consequently, this induces the downregulation of FLIP and Mcl-1, two anti-apoptotic proteins that are frequently upregulated in TRAIL-resistant cancer cells. Furthermore, this thesis shows that Dinaciclib, in addition to CDK9, also targets the transcriptional regulator BRD4, and that the combined inhibition of both is required to break TRAIL-resistance in several cancer cell lines.

Moreover, this thesis demonstrates that the combination of TRAIL and Dinaciclib has therapeutic efficacy in different mouse models of NSCLC, including the *Kras* and *Tp53*-driven KP autochthonous mouse model, which recapitulates the histopathological features of the human disease. This combination led to significant tumour regression and prolonged the survival of these mice. Additionally, the effect of this novel combination on the tumour microenvironment was explored. It was found that for its *in-vivo* activity, Dinaciclib requires the action of the adaptive immune system.

Lastly, I propose the development of novel immunogenic mouse models of NSCLC that resemble the mutational burden of human tumours by combining the cancer cell-specific expression of oncogenic drivers with the administration of carcinogens.

In conclusion, this thesis validates the combined use of TRAIL and Dinaciclib as a potent cancer therapy.

IMPACT STATEMENT

In the UK, more than 363,000 people are diagnosed with cancer every year (Cancer Research UK, www.cancerresearchuk.org/health-professional/cancer-statistics). In spite of the research efforts over the last decades to find new treatment options, cancer is still the leading cause of death, accounting for more than a quarter of all deaths in the UK. Among the different cancer types, lung cancer is by far the most common cause of cancer death, responsible for 21% of cancer mortality in the UK. In fact, only 5% of the patients diagnosed with lung cancer survive for 10 years or longer. Therefore, the development of new therapeutic options for this disease is of paramount importance.

In this thesis, the anti-tumour efficacy of a novel combination therapy comprising the death ligand TRAIL and the CDK9 inhibitor Dinaciclib in lung cancer mouse models was demonstrated. It is shown that combined treatment with TRAIL and Dinaciclib reduces tumour burden and prolongs survival of lung cancer-bearing mice. This preclinical validation could be the basis for future clinical development of this combination therapy. If successful in clinical trials, the combination of TRAIL and Dinaciclib could be a novel therapeutic option for lung cancer patients, thus directly influencing the survival of these patients.

Importantly, this work has also shown that TRAIL and Dinaciclib co-treatment can kill many cell lines obtained from various different cancer types including very frequently diagnosed types like breast cancer, but also other less commonly diagnosed types with extremely low survival rates like pancreatic cancer. Thereby, although further preclinical testing in animal models needs to be carried out in these other pathologies, the combination therapy proposed by this thesis has the potential to be an effective treatment option for many cancer patients.

Furthermore, this thesis has highlighted the need for novel mouse models of lung cancer that recapitulate the high mutational burden and heterogeneity observed in the human disease. This thesis proposes the development of immunogenic lung cancer models that combine the cancer cell-specific expression of oncogenic drivers with the administration of carcinogens. Once the characterisation of these models is completed, and if they indeed are more immunogenic, they will be made available to the scientific community. Since these models are expected to more accurately

represent human lung cancer, the responses observed may more closely recapitulate what is observed in patients, thus increasing the translational relevance of the preclinical results obtained with them. Consequently, this should translate into the saving of both resources and time in the development of novel cancer drugs.

TABLE OF CONTENTS

DECLARATION	2
ABSTRACT	3
IMPACT STATEMENT	4
LIST OF FIGURES	11
LIST OF TABLES	14
LIST OF ABBREVIATIONS	15
1. INTRODUCTION.....	23
1.1 TRAIL-R: a member of the TNF-Receptor superfamily.....	23
1.1.1. The TNF-Receptor superfamily	23
1.1.2. The TRAIL/TRAIL-R system in humans and mice	25
1.1.3. TRAIL-induced signalling	28
1.1.3.1. Pro-apoptotic TRAIL signalling	29
1.1.3.2. Non-apoptotic cell death TRAIL signalling.....	35
1.1.3.3. Non-canonical TRAIL signalling.....	37
1.1.4. The role of TRAIL and its receptors in cancer.....	41
1.1.5. TRAIL-R agonists in the clinic	44
1.2. Cyclin-dependent kinases and their role in transcription	52
1.2.1. Cyclin-dependent kinases	52
1.2.2. CDK9: a regulator of transcriptional elongation	53
1.2.3. CDK9 inhibition in cancer therapy	57
1.3. Lung cancer and mouse models of the disease	62
1.3.1. Lung cancer	62
1.3.2. Mouse models of NSCLC.....	64
1.4. Aims of the study	68
2. MATERIALS AND METHODS.....	69
2.1. Materials	69

2.1.1.	Chemicals and reagents	69
2.1.2.	Buffers and solutions	69
2.1.3.	Biological agents.....	73
2.1.4.	Specific inhibitors	73
2.1.5.	Proteolysis targeting chimeras (PROTACs).....	73
2.1.6.	Antibodies	74
2.1.7.	Cell culture media and supplements.....	76
2.1.8.	Cell lines	77
2.1.9.	Ready-to-use kits and solutions.....	79
2.1.10.	Consumables	79
2.1.11.	Instruments	80
2.1.12.	Software.....	82
2.2.	Methods in cell biology	82
2.2.1.	Cell culturing	82
2.2.2.	Generation of cell lines from lung tumours.....	83
2.2.3.	Freezing and thawing of cell lines	83
2.2.4.	siRNA-mediated knockdown	84
2.2.5.	Generation of knockout cells.....	84
2.2.6.	Cell viability assay (CellTiter-Glo)	85
2.2.7.	Cell death assay by SYTOX Green staining	85
2.2.8.	Clonogenic assay.....	86
2.2.9.	Surface staining by fluorescent-associated cell sorting (FACS).....	86
2.3	Methods in biochemistry	86
2.3.1.	Preparation of cell lysates	86
2.3.2.	SDS polyacrylamide gel electrophoresis (SDS-PAGE).....	87
2.3.3.	Coomassie staining of SDS-PAGE gels.....	87
2.3.4.	Western Blotting	87
2.3.5.	Stripping of Western Blot membranes	88

2.3.6. Production of recombinant izmTRAIL	88
2.4. Methods in molecular biology	89
2.4.1. DNA digestion and restriction.....	89
2.4.2. DNA separation using agarose electrophoresis and purification.....	90
2.4.3. DNA fragment ligation	90
2.4.4. Transformation of competent <i>E.coli</i> bacteria.....	90
2.4.5. Isolation of plasmid DNA.....	91
2.4.6. Isolation of genomic DNA.....	91
2.4.7. Polymerase chain reaction (PCR).....	91
2.5. Animal studies	93
2.5.1. Mouse models.....	93
2.5.1.1. Transplantable tumours	93
2.5.1.2. Orthotopic A549 xenograft lung tumours	93
2.5.1.3. Autochthonous lung tumours in the KP model.....	94
2.5.2. Genotyping.....	94
2.5.3. Treatment of mice	95
2.5.4. <i>In vivo</i> bioluminescence imaging	95
2.5.5. Dissection and fixation of tissues for histology.....	95
2.6. <i>Ex vivo</i> studies.....	96
2.6.1. Histological examination and quantification of tumour burden	96
2.6.2. Immunofluorescence.....	96
2.6.3. Immune cell profiling by FACS.....	96
2.6.4. Serum analysis.....	97
2.7. Statistical analysis	97
3. RESULTS.....	98
3.1. Characterisation of Dinaciclib as a potent sensitiser to TRAIL-induced apoptosis	98
3.1.1. Dinaciclib is a more potent sensitiser to TRAIL-induced cell death than SNS-032.....	98

3.1.2. Dinaciclib overcomes TRAIL resistance in multiple cancer types	103
3.1.3. Co-treatment with TRAIL and Dinaciclib overcomes chemo- and targeted therapy resistance	110
3.1.4. TRAIL- and Dinaciclib-induced cell death is apoptotic	116
3.2. Evaluation of the therapeutic potential of the TRAIL and Dinaciclib combination <i>in vivo</i>	121
3.2.1. TRAIL and Dinaciclib treatment is well tolerated <i>in vivo</i>	121
3.2.2. TRAIL and Dinaciclib combination therapy reduces tumour growth and prolongs the survival of NSCLC transplant tumour-bearing mice	123
3.2.3. The combination of TRAIL and Dinaciclib eradicates established orthotopic human NSCLC xenografts	125
3.2.4. Dinaciclib treatment is sufficient to reduce tumour growth and prolong survival in the autochthonous KP model of NSCLC	127
3.2.5. TRAIL and Dinaciclib combined treatment does not synergise with platinum-based chemotherapy in the KP model of NSCLC	130
3.2.6. Dinaciclib equally reduces the viability of KP cell lines derived from chemotherapy-treated or -naïve animals	132
3.3. Investigation of the impact of the TRAIL- and Dinaciclib-comprising therapy on the tumour microenvironment	136
3.3.1. TRAIL- and Dinaciclib-comprising therapy modulates the tumour microenvironment	136
3.3.2. NK cells are not responsible for the anti-tumour response in Dinaciclib-treated mice	138
3.3.3. The adaptive immunity is required for the anti-cancer effect exerted by Dinaciclib	140
3.4. Identification of the Dinaciclib targets that mediate TRAIL resistance	144
3.4.1. CDK9 is the Dinaciclib-target responsible for TRAIL sensitisation in human cells	144
3.4.2. CDK9 downregulation is not sufficient to sensitise KP cells to TRAIL-induced apoptosis	147

3.4.3. Dinaciclib targets BRD4 in addition to CDK9 and combined inhibition of both is required to overcome TRAIL resistance in KP cell lines.....	152
3.4.4. CDK9 inhibition overcomes TRAIL resistance in some cell types, while others required the additional inhibition of BRD4.....	158
3.5. Establishment of immunogenic GEMMs for NSCLC.....	161
3.5.1. Carcinogen exposure after the engineered-induction of NSCLC tumours increases tumour burden	161
3.5.2. Carcinogen exposure before the oncogenic expression of <i>Kras</i> and <i>Tp53</i> increases tumour growth.....	164
4. DISCUSSION.....	168
4.1. The combination of TRAIL and Dinaciclib is an effective anti-cancer therapy	168
4.1.1. Dinaciclib is a potent sensitiser to TRAIL-induced cell death in many cancers.....	169
4.1.2. Dinaciclib breaks the resistance to TRAIL-induced apoptosis by downregulating Mcl-1 and FLIP	172
4.1.3. TRAIL- and Dinaciclib-comprising therapy shows preclinical activity in NSCLC mouse models.....	174
4.2. TRAIL and Dinaciclib treatment modulates the activity of the immune system	177
4.3. Combined inhibition of CDK9 and BRD4 is required to sensitise some cancer cells to TRAIL-induced apoptosis	181
4.4. KP mice treated with urethane could serve as a novel iGEMM for NSCLC	185
4.5. Summary and outlook.....	186
ACKNOWLEDGEMENTS.....	188
REFERENCES.....	190

LIST OF FIGURES

Figure 1.1: Human and mouse TRAIL-receptor systems.	26
Figure 1.2: Structure of apoptotic caspases.	29
Figure 1.3: TRAIL-induced pro-apoptotic signalling pathway.	34
Figure 1.4: TRAIL-induced necroptosis signalling pathway.	37
Figure 1.5: TRAIL-induced non-canonical TRAIL signalling.	40
Figure 1.6: The role of the TRAIL/TRAIL-R system in the tumour and its microenvironment.	43
Figure 1.7: Mammalian CDKs and their cyclin partners.	53
Figure 1.8: The RNA polymerase II transcription cycle.	55
Figure 3.1: Dinaciclib is more efficient than SNS-032 in sensitising cancer cells to TRAIL-induced cell death.	99
Figure 3.2: The combination of TRAIL and Dinaciclib inhibits the clonogenic survival of cancer cells more efficiently than the combination of TRAIL and SNS-032.	101
Figure 3.3: Dinaciclib, similarly to SNS-032, sensitises cancer cells to TRAIL-induced cell death by downregulation of FLIP and Mcl-1.	102
Figure 3.4: Dinaciclib sensitises a panel of NSCLC cell lines to TRAIL-induced cell death.	104
Figure 3.5: Dinaciclib sensitises mesothelioma cell lines to TRAIL-induced cell death.	106
Figure 3.6: Dinaciclib broadly sensitises different cancers to TRAIL-induced cell death.	108
Figure 3.7: Combination of TRAIL and Dinaciclib treatment inhibits the long-term survival of cancer cells.	109
Figure 3.8: Conditioned melanoma cell lines are resistant to chemo- or targeted therapy drugs.	111
Figure 3.9: TRAIL and Dinaciclib combination treatment overcomes chemo- and targeted therapy-resistance.	113
Figure 3.10: Combined TRAIL and Dinaciclib treatment prevents the long-term survival of melanoma cells, including the chemotherapy-resistant ones.	115

Figure 3.11: The cell death induced by TRAIL and Dinaciclib combination can be prevented by the caspase inhibitor zVAD but not by the RIPK1 inhibitor Nec-1s.	117
Figure 3.12: Dinaciclib sensitises cancer cells to TRAIL-induced apoptosis.....	118
Figure 3.13: Dinaciclib synergises with TRAIL to induce apoptosis.	120
Figure 3.14: Dinaciclib sensitises KP802T4 cells to TRAIL-induced apoptosis.....	121
Figure 3.15: The combination of TRAIL and Dinaciclib is well tolerated <i>in vivo</i>	122
Figure 3.16: TRAIL and Dinaciclib co-treatment shows therapeutic efficacy <i>in vivo</i> in a NSCLC tumour transplant model.....	124
Figure 3.17: The combined treatment of TRAIL and Dinaciclib eradicates orthotopic human NSCLC xenografts.	126
Figure 3.18: Dinaciclib treatment reduces the tumour growth of KP mice.....	128
Figure 3.19: TRAIL and Dinaciclib combination prolongs the survival of KP mice.	129
Figure 3.20: TRAIL and Dinaciclib combination treatment does not synergise with the standard-of-care carboplatin.	131
Figure 3.21: Generation of cell lines from chemotherapy-naïve or -treated KP mice.	133
Figure 3.22: Dinaciclib reduces the viability of KP cell lines, including those derived from chemotherapy-treated mice.....	135
Figure 3.23: TRAIL and Dinaciclib treatment modifies the composition of the tumour immune microenvironment.	137
Figure 3.24: NK cells are not responsible for the Dinaciclib-induced anti-tumour response.....	139
Figure 3.25: Experimental control of the treatment of <i>WT</i> and <i>Rag1^{-/-}</i> mice with TRAIL and Dinaciclib therapy.	141
Figure 3.26: Dinaciclib requires the adaptive immunity for its anti-tumour effect <i>in vivo</i>	142
Figure 3.27: CDK9 is the Dinaciclib-target responsible for TRAIL sensitisation in A549 cells.	145
Figure 3.28: Specific CDK9 inhibition sensitises a panel of human cancer cell lines to TRAIL-induced apoptosis.	146

Figure 3.29: Specific CDK9 inhibition breaks TRAIL resistance by downregulating FLIP and Mcl-1.	147
Figure 3.30: Dinaciclib but not SNS-032 or NVP-2 sensitises KP cell lines to TRAIL-induced apoptosis.	148
Figure 3.31: siRNA-mediated CDK9 knockdown is not sufficient to sensitise KP cell lines to TRAIL-induced death.	150
Figure 3.32: shRNA-mediated CDK9 knockdown is not sufficient to sensitise NSCLC PCC8 cells to TRAIL-induced apoptosis.	151
Figure 3.33: BRD4 inhibition in addition to CDK9 downregulation synergises with TRAIL to kill KP cancer cells.	153
Figure 3.34: The combination of CDK9 and BRD4 inhibition is required to sensitise KP cells to TRAIL-induced death.	155
Figure 3.35: Concomitant and selective degradation of CDK9 and BRD4 overcomes TRAIL resistance in KP cells.	157
Figure 3.36: The role of BRD4 in mediating TRAIL resistance is cell type-dependent.	159
Figure 3.37: The injection of urethane after tumour initiation in the KP model increases the tumour burden.	162
Figure 3.38: P mice do not develop tumours, even with the addition of urethane after the Ad-Cre infection.	164
Figure 3.39: The injection of urethane before the induction of the oncogenic expression of <i>Kras</i> and <i>Tp53</i> in the KP model leads to increased tumour burden.	166
Figure 3.40: The injection of urethane before the expression of mutated <i>Tp53</i> does not lead to any tumour formation.	167
Figure 4.1: Model of Dinaciclib-mediated sensitisation to TRAIL-induced apoptosis.	173

LIST OF TABLES

Table 1.1: Completed clinical trials with TRAs.	46
Table 1.2: CDK9 inhibitors in preclinical or clinical development.	58
Table 1.3: Completed clinical trials with Dinaciclib.	61
Table 2.1: Unconjugated primary antibodies for Western Blot.	74
Table 2.2: Unconjugated primary antibodies for immunofluorescence.....	75
Table 2.3: Conjugated primary antibodies for flow cytometry.....	75
Table 2.4: Conjugated secondary antibodies.	76
Table 2.5: Cell lines.....	77
Table 2.6: CRISPR sgRNA sequence.	85
Table 2.7: DNA restriction set-up.	89
Table 2.8: PCR reaction set-up.	92
Table 2.9: PCR cycling parameters.....	92

LIST OF ABBREVIATIONS

ABC	ATP-binding cassette
Ad-Cre	Adenoviral-Cre
ADP	Adenosine diphosphate
AEBSF	4-(2-aminoethyl)benzenesulfonyl fluoride hydrochloride
Ala	Alanine
ALK	Anaplastic lymphoma kinase
ALT	Alanine aminotransferase
AML	Acute myeloid leukaemia
Apaf-1	Apoptosis protease-activating factor-1
APC	Antigen presenting cell
AR	Androgen receptor
Arg	Arginine
AU	Arbitrary unit
Bak	Bcl-2 homologous antagonist killer
BAP1	BRCA1-associated protein 1
Bax	Bcl-2-associated X
BCA	Bicinchoninic acid
Bcl-2	B-cell lymphoma 2
Bcl-XL	B-cell lymphoma extra large
BCRP	Breast cancer resistance protein
Bid	BH3-interacting domain death agonist
Bp	Base pair
BRAF	v-Raf murine sarcoma viral oncogene homolog B,
BRD4	Bromodomain-containing protein 4
BSA	Bovine serum albumin
CARD	Caspase recruitment domain
CCL2	C-C motif chemokine ligand 2
CCR2	C-C motif chemokine receptor 2
CD	Cluster of differentiation
CD95L	CD95 ligand
CDK	Cyclin-dependent kinase
CDKN2A	CDK inhibitor 2A
ciAP	Cellular IAP

CLL	Chronic lymphocytic leukaemia
CPT	Circularly permuted TRAIL
CR	Complete response
CRD	Cysteine-rich domain
CRISPR	Clustered regularly interspaced short palindromic repeats
CTD	Carboxyl-terminal domain
CTL	Cytotoxic lymphocyte
CTL4	Cytotoxic T lymphocyte-associated protein 4
CXCL	C-X-C motif chemokine ligand
Cyc	Cyclin
D	Aspartate
DAMP	Damage-associated molecular pattern
DAPI	4',6-diamidino-2-phenylindole
DC	Dendritic cell
DD	Death domain
ddH ₂ O	Double distilled H ₂ O
DED	Death effector domain
DISC	Death-inducing signalling complex
DMEM	Dulbecco's modified Eagle's medium
DMSO	Dimethyl sulfoxide
DNA	Deoxyribonucleic acid
dNTP	Deoxynucleoside triphosphate
DRB	5,6-Dichloro-1-β-d-ribofuranosylbenzimidazole
Dox	Doxycycline
DPBS	Dulbecco's phosphate-buffered saline
DR	Death receptor
DSIF	DRB sensitivity inducing factor
DTT	Dithiothreitol
e.g.	<i>Exempli gratia</i>
ECL	Enhanced Chemiluminescence Substrate
EDTA	Ethylenediaminetetraacetic acid
EGFR	Epidermal growth factor receptor
EpCAM	Epithelial cell adhesion molecule
ERK	Extracellular regulated kinase
ESCRT	Endosomal sorting complexes required for transport

FACS	Fluorescence-activated cell sorting
FADD	Fas-associated protein with death domain
FasL	Fas ligand
FCS	Fetal calf serum
FLICE	FADD-like ICE
FLIP	FLICE-like inhibitory protein
FLP	Flippase
FMO	Fluorescence minus one
FRT	Flp recognition target
G	Glycine
GEMM	Genetically-modified mouse model
Glu	Glutamic acid
GPI	Glycosylphosphatidylinositol
GTF	General transcription factor
h	Hour
H	Histidine
H&E	Haematoxylin and eosin
HDACi	Histone deacetylase inhibitors
HEXIM1/2	Hexamethylene bisacetamide-inducible protein 1/2
HLA	Human leukocyte antigen
HOIL-1	Heme-oxidized IRP2 ubiquitin ligase-1
HOIP	HOIL-1 interacting protein
HRP	Horseradish Peroxidase
i.e.	<i>Id est</i>
i.p.	intraperitoneal
IAP	Inhibitor of apoptosis proteins
IC ₅₀	Half maximal inhibitory concentration
ICAM-1	Intercellular adhesion molecule 1
ICB	Immune checkpoint blockade
IFN	Interferon
iGEMM	Immunogenic GEMM
IgG	Immunoglobulin G
IKK complex	IκB kinase complex
IL	Interleukin
Ile	Isoleucine

IPTG	Isopropyl β -D-1-thiogalactopyranoside
IZ	Isoleucine zipper
izmTRAIL	IZ murine TRAIL
I κ B	Inhibitor of κ B
JNK	c-Jun N-terminal kinase
kDa	Kilodalton
KEAP1	Kelch-like ECH-associated protein 1
KO	Knockout
<i>KP</i>	<i>KRas</i> ^{LSL-G12D/+} ; <i>p53</i> ^{LSL-R172H/+}
<i>KP</i> ^{null}	<i>KRas</i> ^{LSL-G12D/+} ; <i>p53</i> ^{f/f}
KRAS	Kirsten rat sarcoma
<i>Kras</i> ^{LSL-G12D}	<i>Kras</i> LoxP-Stop-LoxP-G12D
LAC	Lung adenocarcinoma
LAL	<i>Limulus ameobocyte lysate</i>
LARP7	La-related protein 7
LB	Lysogeny broth
LDC	LDC000067
LDS	Lithium dodecyl sulfate
Leu	Leucine
LPS	Lipopolysaccharide
LSL	LoxP-Stop-LoxP
LT α	Lymphotoxin alpha
LUBAC	Linear ubiquitin chain assembly complex
LZ	Leucine zipper
MACH	MORT1-associated CED-3 homologue
MAPK	Mitogen activated protein kinase
Mcl-1	Myeloid cell leukaemia 1
MCP-1	Monocyte chemoattractant protein-1
MDR	Multi-drug resistance
MDR1	Multi-drug resistance protein 1
MDSCs	Myeloid-derived suppressor cells
MEK	MAPK kinase
MePCE	7SK snRNA methylphosphate capping enzyme
min	Minutes
MK	Murine killer

MLKL	Mixed lineage kinase domain like
MM	Multiple myeloma
MNU	Methylnitrosourea
MOMP	Mitochondrial outer membrane permeabilisation
MPD	Membrane-proximal domain
mRNA	Messenger RNA
MS	Median survival
mTOR	Mammalian target of rapamycin
mut	Mutant
NA	Not available
Nec-1s	Necrostatin-1s
NELF	Negative elongation factor
NEMO	NF- κ B essential modulator
NF1	Neurofibromatosis type 1
NF- κ B	Nuclear factor kappa B
NHL	Non-Hodgkin lymphoma
Ni-NTA	Nickel-nitrilotriacetic acid
NK	Natural killer
NNK	4-(methylnitrosamino)-1-(3-pyridyl)-1butanone
NNN	N'-nitrosonornicotine
NR	No responses
NSCLC	Non-small-cell lung carcinoma
NTP	Nucleoside triphosphate
OPG	Osteoprotegerin
P	<i>p53^{LSL-R172H/+}</i>
pA	Practical grade
PARP	Poly-ADP-ribose-polymerase
PBS	Phosphate buffered saline
PBST	PBS Tween
PCM	Plasma cell myeloma
PCR	Polymerase chain reaction
PD-1	Programmed cell death 1
PD-L1	Programmed death ligand 1
PFS	Progression-free survival
Pfu	Plaque-forming unit

PHH	Primary human hepatocytes
PI3K	Phosphoinositide 3-kinase
PI3KCA	PI3K catalytic subunit alpha
PIC	Pre-initiation complex
PID	P-TEFb interacting domain
PIPs	Phosphatidylinositol phosphates
PR	Partial response
Pro	Proline
PROTAC	Proteolysis targeting chimera
pSer2	Phosphorylated serine 2
P-TEFb	Positive transcription elongation factor b
Q	Glutamine
R	Arginine
Rac1	Ras-related C3 botulinum toxin substrate 1
RANK	Receptor for receptor activator of NF- κ B
RANKL	Receptor activator of NF- κ B ligand
Rb	Retinoblastoma
RB1	Retinoblastoma protein
RBC	Red blood cell
RCT	Randomised-controlled trial
RFP	Red fluorescent protein
RHIM	RIP homotypic interaction motif
RIPK	Receptor-interacting serine/threonine protein kinase
RNA	Ribonucleic acid
RNA Pol II	RNA Polymerase II
RNA-seq	RNA sequencing
ROCK	Rho-associated protein kinase
RPMI	Roswell Park Memorial Institute medium
RT	Room temperature
rTTA	Reverse tetracycline-controlled transactivator
s	Second
SCID	Severe combined immunodeficiency
SCLC	Small-cell lung carcinoma
SDS	Sodium dodecyl sulfate
SDS-PAGE	SDS polyacrylamide gel electrophoresis

SEC	Super elongation complex
SEM	Standard error of the mean
Ser	Serine
sgRNA	Single guide RNA
SHARPIN	SHANK-associated RH domain interactor
shRNA	Short hairpin RNA
SMAC	second mitochondria-derived activator of caspase
snRNP	Small nuclear ribonucleoprotein
SOC	Super Optimal broth with Catabolite repression
STAT	Signal transducer and activator transcription
STK11	Serine/threonine kinase 11
STS	Soft tissue sarcoma
TAM	Tumour-associated macrophage
TAPE	Threonine, alanine, proline and glutamine
tBid	Truncated Bid
TCR	T cell receptor
TF	Transcription factor
TGF- β	Transforming Growth Factor- β
THD	TNF homology domain
Thr	Threonine
TKI	Tyrosine kinase inhibitors
TNBC	Triple-negative breast cancer
TNF	Tumour necrosis factor
TNF-R	TNF receptor
TNF-RSC	TNF-R1 signalling complex
TNFR-SF	TNF receptor superfamily
TNF-SF	TNF superfamily
TP53	Tumour protein 53
TRA	TRAIL-R agonist
TRAF2	TNF-receptor associated factor 2
TRAIL	Tumour necrosis factor-related apoptosis-inducing ligand
TRAIL-R	TRAIL receptor
TRE	Tetracycline responsive element
Treg	Regulatory T cell
Tyr	Tyrosine

V	Valine
v/v	Volume/volume
VEGI	Vascular endothelial growth inhibitor
VHL	Von Hippel-Lindau
vs	<i>Versus</i>
w/v	Weight/volume
wt	Wilt type
XIAP	X-linked inhibitor of apoptosis
zVAD	zVAD-FMK

1. INTRODUCTION

1.1 TRAIL-R: a member of the TNF-Receptor superfamily

1.1.1. The TNF-Receptor superfamily

Whilst unknown at that time, tumour necrosis factor (TNF) was first used in the treatment of cancer in 1894 when William Coley showed that bacterial infection caused tumour shrinkage in patients (Nauts et al., 1946). However, it was not until almost a century later that Coley's seminal observation was found to be due to the induction of a factor that caused the necrosis of sarcoma tumours, a feature responsible for the coining of its name (Carswell et al., 1975). Subsequent studies led to the discovery of numerous molecules involved in the regulation of immunity and inflammation that are homologous to TNF and are therefore classified as the TNF superfamily (TNF-SF). With the exception of lymphotoxin alpha (LT α) and vascular endothelial growth inhibitor (VEGI), which are soluble factors, TNFSF members are type II transmembrane proteins and contain an extracellular TNF homology domain (THD) responsible for their homotrimerisation (Warzocha et al., 1995). TNF-SF members bind to a cognate family of receptors, referred to as the TNF receptor superfamily (TNFR-SF). While the TNF-SF consists of 19 ligands, there are 29 receptors in the TNFR-SF and hence, some ligands can bind to multiple receptors (Aggarwal, 2003; Aggarwal et al., 2012). TNFR-SF members are type I transmembrane proteins which bind to their respective ligands through cysteine-rich domains (CRD), hallmark of these receptors (Smith et al., 1994). Moreover, eight TNFR-SF members contain an intracellular domain required for cell death induction and consequently named death domain (DD) (Locksley et al., 2001). This subset of the TNFR-SF is referred to as death receptors (DR), of which the most extensively studied ones are TNF receptor 1 (TNF-R1), cluster of differentiation (CD)95 and tumour necrosis factor-related apoptosis-inducing ligand-receptor 1/2 (TRAIL-R1/2).

Although it contains a DD (Tartaglia et al., 1993), the primary signalling outcome of TNF-R1 is gene expression activation. Upon binding of TNF to TNF-R1, the receptor trimerises and several proteins are recruited to TNF-R1 to form the TNF-R1 signalling complex (TNF-RSC), also known as complex I of TNF-R1 signalling (Micheau and Tschopp, 2003). Gene induction is subsequently achieved through the activation of nuclear factor kappa B (NF- κ B) and mitogen activated protein kinase (MAPK)

signalling (O'Donnell et al., 2007; Walczak et al., 2012). Under certain circumstances, when its gene-activatory arm is obstructed, TNF-R1 can also result in cell death. This occurs via the formation of a secondary cytoplasmic complex, called complex II, which forms subsequently to complex I (Micheau and Tschopp, 2003). Initial enthusiasm following the discovery of the anti-tumourigenic features of TNF was dampened by the demonstration that systemic TNF treatment induced a lethal inflammatory shock syndrome (Tracey et al., 1988).

In search of another protein with similar anti-tumour properties, attention turned into CD95 ligand (CD95L), also known as Fas ligand (FasL). The cell death inducing effects of its receptor, CD95, also known as APO-1 or Fas, were first identified in 1989 independently by the groups of Peter Krammer and Minako Yonehara (Trauth et al., 1989; Yonehara et al., 1989). They showed that cross-linking CD95 with agonistic antibodies killed CD95-expressing cancer cells. Cloning and characterisation of CD95 demonstrated its homology with TNF-R1 as well as it revealed that apoptosis induction is its primary signalling outcome (Itoh et al., 1991; Oehm et al., 1992). Apoptosis is triggered upon the formation of a multimolecular complex of proteins known as the death-inducing signalling complex (DISC) (Kischkel et al., 1995). The main components of this complex are Fas-associated protein with death domain (FADD), also known as MORT1 (Boldin et al., 1995; Chinnaiyan et al., 1995; Kischkel et al., 1995) and caspase-8, which was originally termed FLICE (FADD-like ICE) (Muzio et al., 1996) or MACH (MORT1-associated CED-3 homologue) (Boldin et al., 1996). Attempts to activate CD95 for cancer therapy were hampered by its liver toxicity, since systemic treatment with CD95 agonists was lethal to mice within few hours of treatment (Ogasawara et al., 1993; Kondo et al., 1997).

A third opportunity for the anti-cancer therapeutic use of a TNF-like molecule arose few years later with the discovery of tumour necrosis factor-related apoptosis-inducing ligand (TRAIL). This death ligand, also known as TNFSF10 or APO2L, was first identified in the mid-1990s simultaneously by Raymond Goodwin's and Avi Ashkenazi's laboratories based on its homology with TNF and CD95L (Wiley et al., 1995; Pitti et al., 1996). Importantly, this factor was shown to specifically kill tumour cells without causing the lethal adverse effects encountered with TNF-R1 or CD95 agonists (Ashkenazi et al., 1999; Walczak et al., 1999). These findings placed TRAIL in the centre of attention concerning cancer therapeutics within the TNF-SF.

The following sections will focus on the biology of the TRAIL/TRAIL-R system and its use in the clinic.

1.1.2. The TRAIL/TRAIL-R system in humans and mice

TRAIL is a 35 kDa protein that shares 65% identity between humans and mice (Wiley et al., 1995). Similarly to other members of the TNF-SF, aside from being present in its membrane-bound version, it can be cleaved at the cell surface, resulting in the release of the THD in the form of a soluble fragment of 24 kDa (Mariani et al., 1997). The generation of soluble TRAIL occurs through shedding, although the identity of the protease(s) responsible for its cleavage remains unknown. Interestingly, soluble TRAIL is present in the blood plasma of a healthy adult at around 100 pg/ml, a concentration at which it does not induce apoptosis in cell lines *in vitro* (Gibellini et al., 2007).

This death ligand is composed of three parts: an extracellular region, comprising the THD and an extracellular stalk, which is the part being cleaved to release the soluble form; a transmembrane helix and a small cytoplasmatic domain (Manzo et al., 2009). The active part of TRAIL is at its C-terminus, containing the receptor-binding THD domain and composed by two anti-parallel β -sheets (Cha et al., 1999; Hymowitz et al., 1999; Hymowitz et al., 2000). Like other TNF-SF members, TRAIL forms a homotrimer and, as shown by the crystal structure of TRAIL interacting with TRAIL-R2, each receptor molecule binds to the crevice formed by two monomers of the trimer (Hymowitz et al., 1999). Therefore, the trimer can engage three receptors simultaneously. TRAIL is the only protein of the TNF-SF that trimerises around a zinc atom located at the core of the trimeric structure. This is achieved by a cysteine residue, Cys230, which allows the interaction and stabilisation of the three molecules of TRAIL through the contact of the three cysteines with the zinc atom. This interaction is not required for the folding of TRAIL but it is necessary for its trimerisation and consequent activity. Indeed, point mutations of Cys230 give rise to inactive monomeric or dimeric forms of TRAIL (Bodmer et al., 2000).

Among the TNF-SF, human TRAIL is unique in that it binds to four different membrane receptors and one soluble receptor (Figure 1.1 A). Human TRAIL-Rs can be divided in two classes. On one hand, the ones that contain a full-length intracellular DD and

thus can induce apoptosis: TRAIL-R1 (also known as DR4) (Pan et al., 1997b) and TRAIL-R2 (also known as DR5) (Pan et al., 1997a; Schneider et al., 1997a; Schneider et al., 1997b; Screaton et al., 1997; Sheridan et al., 1997; Walczak et al., 1997; Wu et al., 1997). On the other hand, the alternative receptors, which either lack a DD or contain a truncated one and are hence incapable of transmitting an apoptotic signal: TRAIL-R3 (also known as DcR1) (Degli-Esposti et al., 1997b; MacFarlane et al., 1997; Schneider et al., 1997a; Sheridan et al., 1997), TRAIL-R4 (also known as DcR2) (Degli-Esposti et al., 1997a; Marsters et al., 1997) and the soluble receptor osteoprotegerin (OPG) (Emery et al., 1998). At 37° C, TRAIL was shown to bind to TRAIL-R2 with higher affinity than to the other membrane-expressed TRAIL-Rs, indicating that, under physiological conditions, the interaction of TRAIL with TRAIL-R2 might be favoured (Truneh et al., 2000).

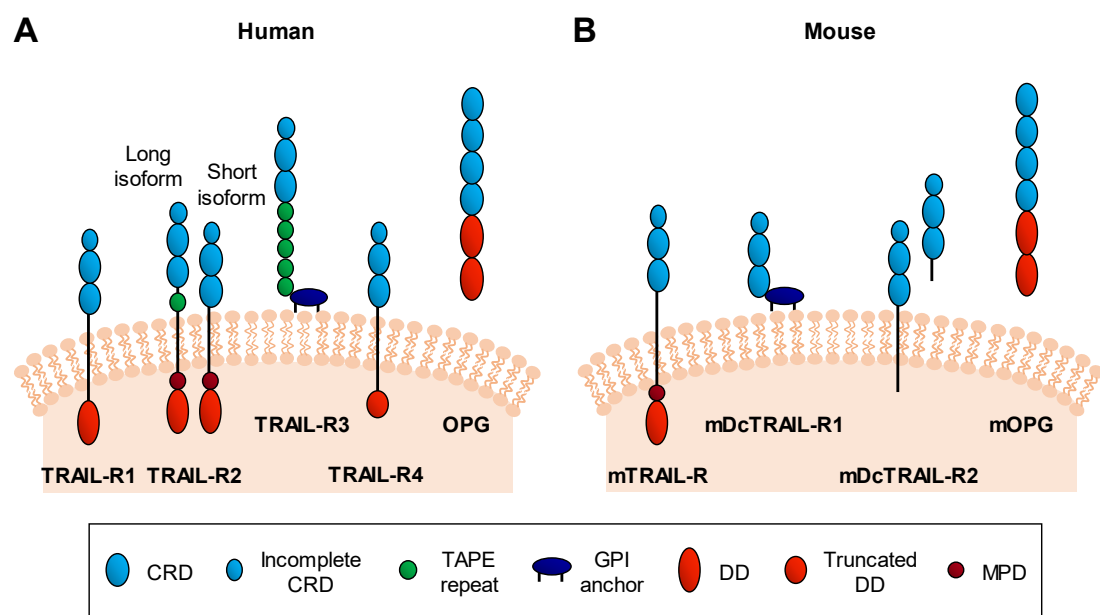


Figure 1.1: Human and mouse TRAIL-receptor systems.

(A) The human TRAIL/TRAIL-R system. Humans express three receptors with an intracellular domain that contains a full DD in the case of TRAIL-R1 and TRAIL-R2 or a truncated DD in the case of TRAIL-R4. TRAIL-R2 is expressed as a long and short isoform, which differ by the presence or absence of a TAPE repeat domain. TRAIL-R3 is attached to the membrane through a GPI anchor, contains five TAPE repeats but it is devoid of an intracellular domain. OPG serves as a soluble receptor for TRAIL.

(B) The mouse TRAIL/TRAIL-R system. mTRAIL-R is homologous to human TRAIL-R1 and TRAIL-R2. mDcTRAIL-R1 and mDcTRAIL-R2, however, differ substantially from human TRAIL-R3 and TRAIL-R4. Moreover, mDcTRAIL-R2 is also found in its soluble form. Similar to human OPG, mOPG is a soluble TRAIL receptor.

Both pro-apoptotic receptors, TRAIL-R1 and TRAIL-R2, share high sequence similarity but the most obvious difference between the two is that there is only one splice variant for TRAIL-R1 whereas TRAIL-R2 exists in two (Wang and Jeng, 2000). The long isoform contains 29 additional extracellular amino acids that are rich in threonine, alanine, proline and glutamine (TAPE), and are therefore referred to as the TAPE domain (Schneider et al., 1997a). Furthermore, TRAIL-R2 contains a membrane-proximal domain (MPD), a short, ten amino-acid-long stretch close to the plasma membrane.

The relative contribution of the two DD-containing TRAIL-Rs to apoptosis induction is not entirely clear and it seems to be cell type-dependent. Despite surface expression of TRAIL-R2, in chronic lymphocytic leukaemia (CLL), mantle cell lymphoma and some pancreatic cancer cells, TRAIL-R1 has been described as the only receptor used by these cells for apoptotic induction (MacFarlane et al., 2005a; MacFarlane et al., 2005b; Lemke et al., 2010; Stadel et al., 2010). On the contrary, TRAIL-R2 has been shown to be the main contributor to apoptosis induction in a wide range of epithelial cancer cells (Kelley and Ashkenazi, 2004; van der Sloot et al., 2006).

TRAIL-R3 and TRAIL-R4 share high homology in their CRD-containing extracellular domains with those of the DRs TRAIL-R1 and TRAIL-R2. However, TRAIL-R3 completely lacks an intracellular DD, and it is linked to the membrane via a glycosylphosphatidylinositol (GPI) anchor (Degli-Esposti et al., 1997b; MacFarlane et al., 1997; Schneider et al., 1997a; Sheridan et al., 1997). TRAIL-R4, on the other hand, contains a truncated DD that can induce NF- κ B and AKT activation but not apoptosis (Marsters et al., 1997; Lalaoui et al., 2011). These alternative receptors have been proposed to act as decoy receptors that inhibit apoptosis induction by TRAIL as a consequence of ligand scavenging (Merino et al., 2006; Morizot et al., 2011). In addition, TRAIL-R4 has been suggested to negatively influence apoptosis activation by forming ligand-independent heterotrimeric complexes with TRAIL-R2 (Merino et al., 2006). Herein, in an overexpression system, the decoy receptor TRAIL-R4 prevented TRAIL-R2 DISC activation by inhibiting the cleavage of the initiator procaspase-8. A more recent report confirmed the inhibitory role of TRAIL-R3 and TRAIL-R4 by short hairpin ribonucleic acid (shRNA) knockdown and monoclonal antibody-mediated blockade, showing that these regulatory receptors limit the apoptosis of hepatic stellate cells (Singh et al., 2017). Nevertheless, the physiological

role of these decoy receptors remains controversial and further work is required to clarify it.

In addition to the membrane-attached or membrane-spanning receptors, human TRAIL can also bind to OPG, albeit with lower affinity, which acts as a soluble receptor (Emery et al., 1998). OPG also functions as a decoy receptor for receptor activator of NF- κ B ligand (RANKL), another TNF-SF member involved in bone remodelling (Simonet et al., 1997; Lacey et al., 1998). By binding to RANKL, OPG makes RANKL unavailable to its natural receptor, RANK, hence blocking osteoclast differentiation and survival. It has been postulated that TRAIL has the capacity to reverse the inhibitory action of OPG on RANKL-RANK binding by interacting with OPG. Thereby, RANK-RANKL binding might be favoured, increasing osteoclastogenesis (Vitovski et al., 2007). However, given that *Trail*-deficient mice do not show any defects in bone remodelling and homeostasis, it seems unlikely that TRAIL plays a major role in these processes under physiological conditions, at least in mice (Cretney et al., 2002).

In contrast to humans, mice only express one DD-containing TRAIL receptor, mTRAIL-R, also known as mouse DR5 or murine killer (MK) (Figure 1.1 B). mTRAIL-R shares similar sequence identity with its human counterparts TRAIL-R1 (43% homology) and TRAIL-R2 (49% homology) and is, consequently, capable of inducing apoptosis (Wu et al., 1999). Additionally, two intracellular DD-lacking mTRAIL-Rs, mDcTRAIL-R1 and mDcTRAIL-R2 have been identified in mice, as well as the soluble mOPG. These murine non-DRs differ substantially in their sequence from human TRAIL-R3 and TRAIL-R4 and do not induce either apoptosis or NF- κ B activation upon overexpression (Schneider et al., 2003). Similar to OPG, mOPG is a soluble TRAIL receptor.

Notably, human TRAIL binds only weakly to mTRAIL-R whereas mouse TRAIL has high affinity for the human TRAIL-Rs (Bossen et al., 2006).

1.1.3. TRAIL-induced signalling

Like other members of the TNF-SF, TRAIL can trigger several biological responses. These include the activation of cell death pathways by apoptosis or necroptosis, as well as non-canonical signalling pathways.

1.1.3.1. Pro-apoptotic TRAIL signalling

Apoptosis is executed by a family of cysteine-dependent aspartate-specific proteases known as caspases (Alnemri et al., 1996). These proteins are expressed as inactive procaspases (zymogens), containing a large and a small subunit of 20 and 10 kDa, respectively. Apoptotic caspases can be divided into two classes: initiator caspases (caspase-2, -8, -9 and -10) and effector caspases (caspase-3, -6, and -7) (Shalini et al., 2015) (Figure 1.2). Structurally, initiator caspases contain an additional prodomain that facilitates homotypic interactions with other proteins containing the same domain. These prodomains contain either a caspase recruitment domain (CARD) in the case of caspase-2 and caspase-9 or two tandem death effector domain (DEDs) in the case of caspase-8 and caspase-10 (Riedl and Shi, 2004).

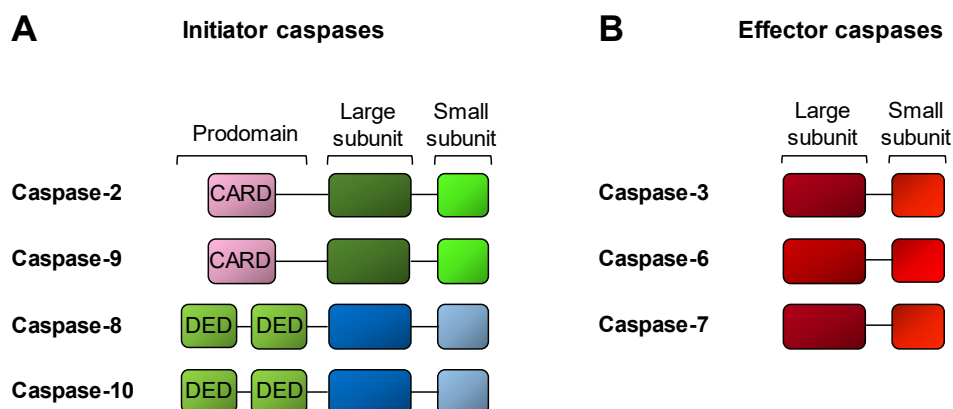


Figure 1.2: Structure of apoptotic caspases.

(A) Initiator apoptotic caspases (caspases-2, -8, -9 and -10) contain a prodomain, a large subunit and a small subunit.

(B) Effector apoptotic caspases (caspases-3, -6 and -7) contain a large subunit and a small subunit.

TRAIL-Rs are present on the cell surface as pre-assembled pre-ligand trimers. TRAIL binding causes a structural reorganisation that allows for interactions between receptor interfaces that are located opposite the ligand-binding interfaces, leading to the multimerisation or crosslinking of neighbouring trimers. Consequently, highly organized receptor networks composed by hexameric honeycomb-like structures are formed (Valley et al., 2012). Interestingly, TRAIL-R1 and TRAIL-R2 can homo- and

heterotrimerise to form higher-order complexes. This model received support from two studies showing that untagged recombinant TRAIL synergised with an agonistic TRAIL-R2-specific antibody (AMG-655) to kill cancer cells by achieving a higher order clustering of TRAIL-R2 (Graves et al., 2014; Tuthill et al., 2015).

Binding of TRAIL induces a spatial reorganisation of the three ligand-cross-linked receptors, enabling the intracellular DDs to adopt a conformational change that allows them to recruit FADD. FADD is an adaptor molecule that contains a DD, which interacts with the DD of the TRAIL-Rs. Subsequently, the DED of FADD becomes available to interact with the DEDs of initiator procaspase-8 and thus recruit it to the signalling platform. The membrane-associated complex that results from these interactions is termed the TRAIL DISC (Kischkel et al., 2000; Sprick et al., 2000; Kischkel et al., 2001; Sprick et al., 2002). According to the model proposed by Dickens and colleagues, FADD may initially recruit one molecule of procaspase-8 through one of its DEDs, facilitating the sequential interaction of the other DED of procaspase-8 with additional molecules to produce a caspase-activating chain (Dickens et al., 2012). These authors reported that the stoichiometry of the DISC components receptor:FADD:procaspase-8 is of approximately 3:1:9.

Upon recruitment to the TRAIL DISC, procaspase-8 forms homodimers, which induces a conformational change that exposes their proteolytic active sites. As a result, intra-molecular autocatalytic cleavage of the small subunit of the caspase occurs, which stabilises the dimer. Subsequently, the caspase-8 intermediate forms in the dimer cleave one another in the region between the DED and the large subunit (Medema et al., 1997). Two large subunits associate with two small subunits to form the active caspase-8 heterodimer that is then released into the cytosol, where it can cleave executioner caspases (Lavrik et al., 2003). Executioner caspase-3 and caspase-7 are constitutively present in the cytosol as homodimers and get activate following cleavage by initiator caspases between their large and small subunits (Riedl and Shi, 2004).

Procaspase-10 is structurally homologous to pro-caspase-8, containing tandem DEDs (Figure 1.2 A) and hence, it is capable of binding to FADD to be recruited to the TRAIL DISC (Sprick et al., 2002). There, it forms homodimers and is activated in the same manner as procaspase-8. Nevertheless, the ability of caspase-10 to compensate for the loss of capase-8 remains controversial. Some reports indicate that in the absence of caspase-8, caspase-10 can induce TRAIL-dependent

apoptosis (Kischkel et al., 2001). This was done by transient expression of caspase-10 in the caspase-8 deficient Jurkat cell line. On the contrary, some other studies reported that, in the same caspase-8 deficient cells, caspase-10 is unable to compensate for the loss of caspase-8 despite effective recruitment to the TRAIL DISC in the absence of caspase-8 (Sprick et al., 2002). The stable expression of caspase-10 at endogenous levels achieved in this latter system might explain the contradictory results, assigning caspase-8 a central role in the initiation of the apoptotic cascade by TRAIL. Nevertheless, more research into the function of caspase-10 at the DISC is required.

In addition to the core components TRAIL-R, FADD, procaspase-8 and procaspase-10, the TRAIL-R DISC is also comprised of other proteins such as receptor-interacting serine/threonine protein kinase (RIPK)1 or FLICE-like inhibitory protein (FLIP) (Thome and Tschopp, 2001). By competing with caspase-8 for its binding to FADD, FLIP acts as a modulator of caspase-8 activation within the DISC. This mechanism is exploited by cancer cells, which frequently upregulate the expression of FLIP in order to mediate resistance to apoptosis (Burns and El-Deiry, 2001; Guseva et al., 2008; Riley et al., 2013; McCann et al., 2018). Three splice variants of FLIP have been identified: a long form (FLIP(L)), and two short forms (FLIP(S) and FLIP(R)), all of which contain tandem DEDs that are homologous to those of procaspase-8 and procaspase-10 and can bind to FADD (Irmeler et al., 1997; Scaffidi et al., 1999; Golks et al., 2005). In addition, FLIP(L) possesses a caspase-like domain at its C-terminus that lacks a critical catalytic cysteine within the active site, rendering this protein catalytically inactive. For the modulation of DISC activation and caspase-8 activity, the ratio of FLIP(L) and FLIP(S) to caspase-8 molecules is crucial (Scaffidi et al., 1999). Although both FLIP(L) and FLIP(S) can bind to FADD, their mechanism of action is different. FLIP(S) inhibits caspase-8 activation in a dominant-negative manner by competing with it for binding to FADD through the formation of heterodimers with procaspase-8 (Irmeler et al., 1997; Scaffidi et al., 1999; Krueger et al., 2001). FLIP(R), although it has not been so well characterised, seems to elicit its anti-apoptotic functions through a similar mechanism (Golks et al., 2005). On the other hand, the role of FLIP(L) is more complex, having been reported to be both an activator and an inhibitor of caspase-8. The first studies showed FLIP(L) to act in the same manner as FLIP(S) (Irmeler et al., 1997). Later, however, it was demonstrated that FLIP(L) forms heterodimers with procaspase-8, resulting in a partially active enzymatic complex (Micheau et al., 2002). In these FLIP(L)/procaspase-8

heterodimers, FLIP(L) can induce the conformational change in procaspase-8 necessary for the self-cleavage between its large and small subunits (Chang et al., 2002; Dohrman et al., 2005). Nevertheless, due to FLIP(L)'s lack of enzymatic activity, it cannot induce the second cleavage of procaspase-8 between the DEDs and the large subunit and therefore the heterodimer remains tethered to the DISC. There, the proteolytic activity of the FLIP(L)/procaspase-8 heterodimers is responsible for the cleavage of a limited number of proximal substrates such as RIPK1 (Yu et al., 2009; Pop et al., 2011). This cleavage of RIPK1 is required to inhibit necroptosis, a novel mode of programmed cell death described in the next section (Oberst et al., 2011; Weinlich et al., 2013). Importantly, cell fate is controlled by the levels of FLIP(L). At physiological levels, when there is less FLIP(L) than procaspase-8, the formation of the FLIP(L)/procaspase-8 heterodimers leads to the assembly and activation of procaspase-8 oligomers, resulting in the activation of apoptosis (Hughes et al., 2016). Conversely, when the levels of FLIP(L) are high, the assembly of procaspase-8 oligomers is inhibited, restricting the activity of FLIP(L)/procaspase-8 and consequently inhibiting cell death.

In some cells, known as type I cells, activation of caspase-8 at the DISC is sufficient to achieve a robust activation of caspase-3 and consequently of apoptosis through the so-called extrinsic pathway (Fulda and Debatin, 2002; Fulda et al., 2002a). On the contrary, in the so-called type II cells, direct activation of caspase-3 by caspase-8 is insufficient to trigger apoptosis. This different outcome is usually explained by higher expression of the caspase-8 inhibitors FLIP and X-linked inhibitor of apoptosis (XIAP) in type II cells (Jost et al., 2009). Therefore, type II cells require the additional activation of the mitochondrial or intrinsic apoptotic pathway in order to amplify the activation of effector caspases (Fulda et al., 2002a) (Figure 1.3). This is achieved through caspase-8-mediated cleavage of BH3-interacting domain death agonist (Bid) to generate truncated Bid (tBid) (Schug et al., 2011). tBid, in turn, activates B-cell lymphoma 2 (Bcl-2)-associated X (Bax) and Bcl-2 homologous antagonist killer (Bak), which oligomerise and form pores in the mitochondrial membrane, triggering mitochondrial outer membrane permeabilisation (MOMP) (Li et al., 1998; Luo et al., 1998; Wei et al., 2000). Upon MOMP, several pro-apoptotic factors are released from the mitochondrial intermembrane space into the cytosol, namely second mitochondria-derived activator of caspase (SMAC), which is also known as DIABLO, and cytochrome c. Once released, cytosolic cytochrome c associates with the CARD-containing adaptor protein apoptosis protease-activating factor-1 (Apaf-1), to induce

the recruitment of procaspase-9 via its respective CARD (Pan et al., 1998). The complex formed is known as the apoptosome, an activation platform for caspase-9 that then activates effector caspases, including caspase-3. These activated effector caspases induce the cleavage of a plethora of substrates, including poly-adenosine diphosphate(ADP)-ribose-polymerase (PARP), ultimately culminating in the execution of apoptosis, which is characterised by deoxyribonucleic acid (DNA) fragmentation, cell shrinkage and membrane blebbing.

Given that the proteolysis exerted by caspases is irreversible, in order to prevent excessive apoptosis induction by TRAIL, several mechanisms that tightly regulate the TRAIL apoptosis pathway have evolved. Caspases are mainly controlled by the members of the inhibitor of apoptosis proteins (IAP) family. The most characterised one is XIAP, which counteracts apoptosis induction by inhibiting initiator caspase-9 and effector caspase-3 and caspase-7 (Deveraux et al., 1997; Bratton et al., 2002). XIAP is, in turn, antagonised by SMAC/DIABLO, which is released from the mitochondria together with cytochrome c after MOMP. Thereby, SMAC/DIABLO abrogates XIAP's caspase-inhibitory effect, allowing the activation of the apoptotic programme to the fullest extent (Chai et al., 2000; Zhang et al., 2001).

Intrinsic apoptosis is additionally regulated by anti-apoptotic members of the Bcl-2 family such as Bcl-2 or B-cell lymphoma extra-large (Bcl-XL), which inhibit MOMP. Type II cancer cells have been demonstrated to acquire resistance to TRAIL by exacerbated expression of these molecules (Hinz et al., 2000; Munshi et al., 2001; Fulda et al., 2002a). Similarly, another member of this family, myeloid cell leukaemia 1 (Mcl-1), also controls this pathway by binding to and inhibiting pro-apoptotic BH3-only proteins such as Bim, Bid, Puma and Bak (Adams and Cory, 2007). Overexpression of Mcl-1 has been shown to cause resistance to TRAIL, whereas its knockdown restores TRAIL sensitivity (Taniai et al., 2004; Clohessy et al., 2006)

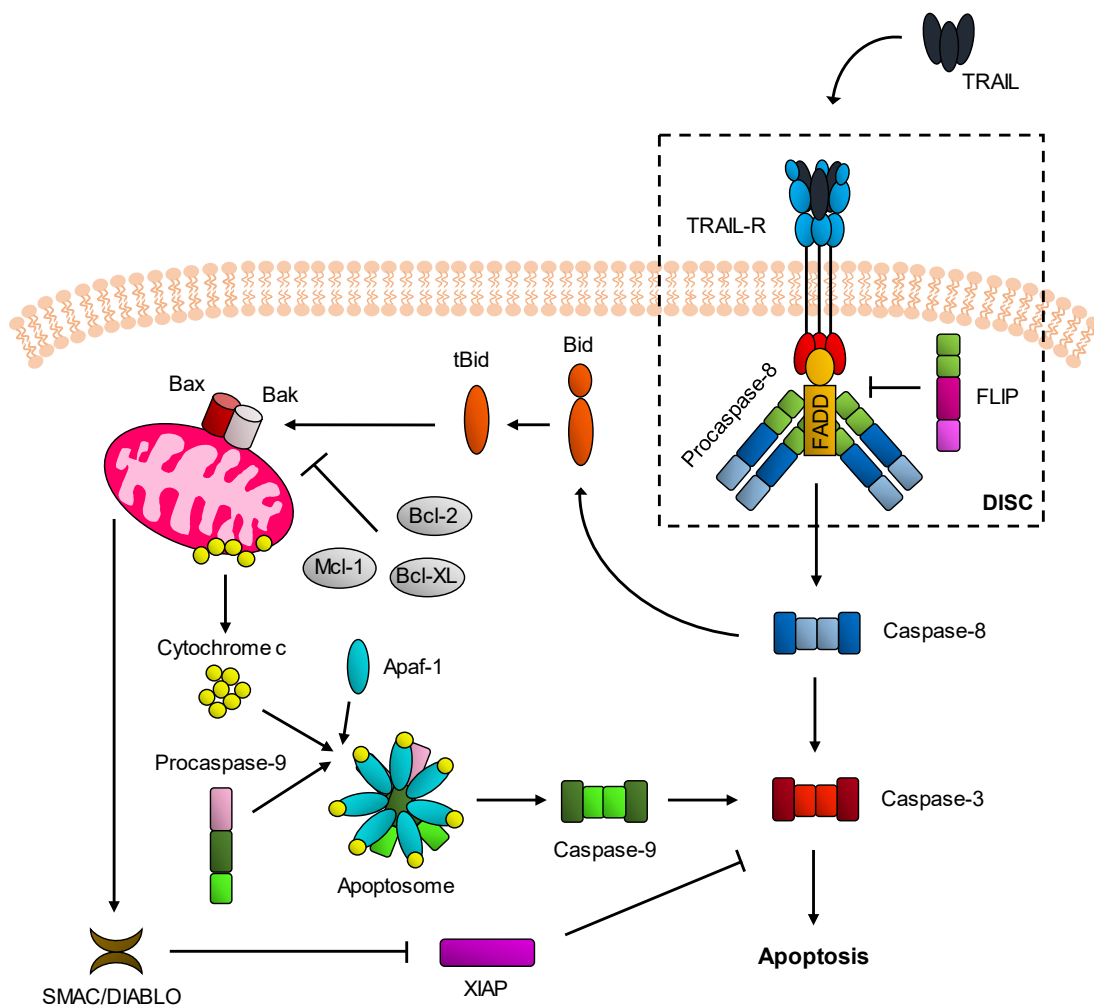


Figure 1.3: TRAIL-induced pro-apoptotic signalling pathway.

Upon binding of TRAIL, TRAIL-R1 and/or TRAIL-R2 adopt a conformation that enables them to recruit FADD, which in turn binds to procaspase-8 to form the TRAIL DISC. DISC formation is regulated by FLIP, which can bind to FADD and form dimers with procaspase-8. In type I cells, DISC-activated caspase-8 is sufficient to cleave and activate effector caspase-3 and hence, trigger apoptosis by the extrinsic pathway. In cells referred to as type II, full activation of caspase-3 is inhibited by XIAP and thus, the activation of the intrinsic apoptosis pathway is required. Caspase-8 cleaves Bid, which, in its truncated form, translocates to the mitochondria to activate Bax and Bak and execute MOMP. This results in the release of SMAC/DIABLO, which is a natural antagonist of XIAP, thereby enabling the full activation of caspase-3. Furthermore, cytochrome c is also released from the mitochondria, which along with Apaf-1 assembles the apoptosome. This platform activates the initiator procaspase-9, which subsequently enhances the activation of caspase-3 and thereby the triggering of apoptosis.

1.1.3.2. Non-apoptotic cell death TRAIL signalling

Besides promoting apoptosis, TRAIL engagement has also been demonstrated to be capable of triggering necroptosis, a caspase-independent type of cell death (Vercammen et al., 1998; Holler et al., 2000; Jouan-Lanhouet et al., 2012; Voigt et al., 2014; Goodall et al., 2016). Necroptosis is a programmed type of necrosis that results in membrane bursting and cellular leakage and is critical in the regulation of immunity and inflammation (Linkermann and Green, 2014; Vanden Berghe et al., 2014). This type of cell death depends on the activities of RIPK1 and RIPK3, which form the core of the necrosome complex (Holler et al., 2000; Degterev et al., 2008; Declercq et al., 2009; Mompean et al., 2018), as well as the pseudokinase mixed lineage kinase domain like (MLKL) (Sun et al., 2012; Zhao et al., 2012; Murphy et al., 2013). Despite an early study reporting that a caspase-8-independent, RIPK1-dependent cell death pathway was induced by CD95L, TRAIL and TNF (Holler et al., 2000), the field has mainly focused so far on investigating necroptosis in the TNF-RSC system.

Necroptosis occurs in scenarios where caspase-8 is absent or its activity is hampered, since caspase-8 has been identified to inhibit necroptosis by cleavage of RIPK1 and RIPK3 (Lin et al., 1999; Feng et al., 2007). In these circumstances, RIPK1 binds to RIPK3 via RIP homotypic interaction motif (RHIM)-mediated interactions (Sun et al., 2002). This interaction, in turn, promotes the recruitment and phosphorylation of MLKL by RIPK3 (Sun et al., 2012; Chen et al., 2013; Murphy et al., 2013; Rodriguez et al., 2016). Subsequently, MLKL is activated by oligomerisation, adopting a conformational change that promotes its translocation to the plasma membrane (Cai et al., 2014; Chen et al., 2014a; Dondelinger et al., 2014; Hildebrand et al., 2014; Wang et al., 2014b; Quarato et al., 2016; Huang et al., 2017). Activation of MLKL results in a rapid flux of calcium into the cell, which is followed by lipid scrambling of the plasma membrane, ultimately leading to membrane disruption and cell death. Recently, it has been discovered that necroptotic cell death is regulated by the endosomal sorting complexes required for transport (ESCRT)-III machinery, which can counteract the MLKL-mediated membrane damage (Gong et al., 2017).

The first time that necroptosis was shown to occur in a system other than TNF-RSC was in the CD95L/CD95 system, which is mechanistically very similar to the

TRAIL/TRAIL-R system (Vercammen et al., 1998). A couple of years later, a RIPK1-dependent cell death was also reported in response to TRAIL (Holler et al., 2000). According to the current model, necroptosis is thought to emanate from complex II, a secondary cytoplasmatic signalling complex that forms subsequently to the DISC upon TRAIL stimulation (Figure 1.4) (Lafont et al., 2017). This complex retains the DISC components FADD and caspase-8 and also contains RIPK1. It is important to note that necrostatin, a small-molecule inhibitor of RIPK1, can block this type of cell death (Degterev et al., 2008). The recruitment of RIPK3 and MLKL to this secondary complex is limited and controlled by the linear ubiquitin chain assembly complex (LUBAC), which is described in the following section (Lafont et al., 2017).

During the last years, necroptosis triggered by TRAIL has been demonstrated to be enabled in circumstances of acidic pH (Meurette et al., 2005; Meurette et al., 2007), or depletion of cellular IAP (cIAP) or TNF-receptor associated factor 2 (TRAF2), two proteins that form part of the DISC and complex II as detailed in the next section (Karl et al., 2014). Furthermore, the combined treatment with TRAIL and certain chemotherapeutic drugs has also been shown to trigger necroptosis in some cancer cell lines (Voigt et al., 2014).

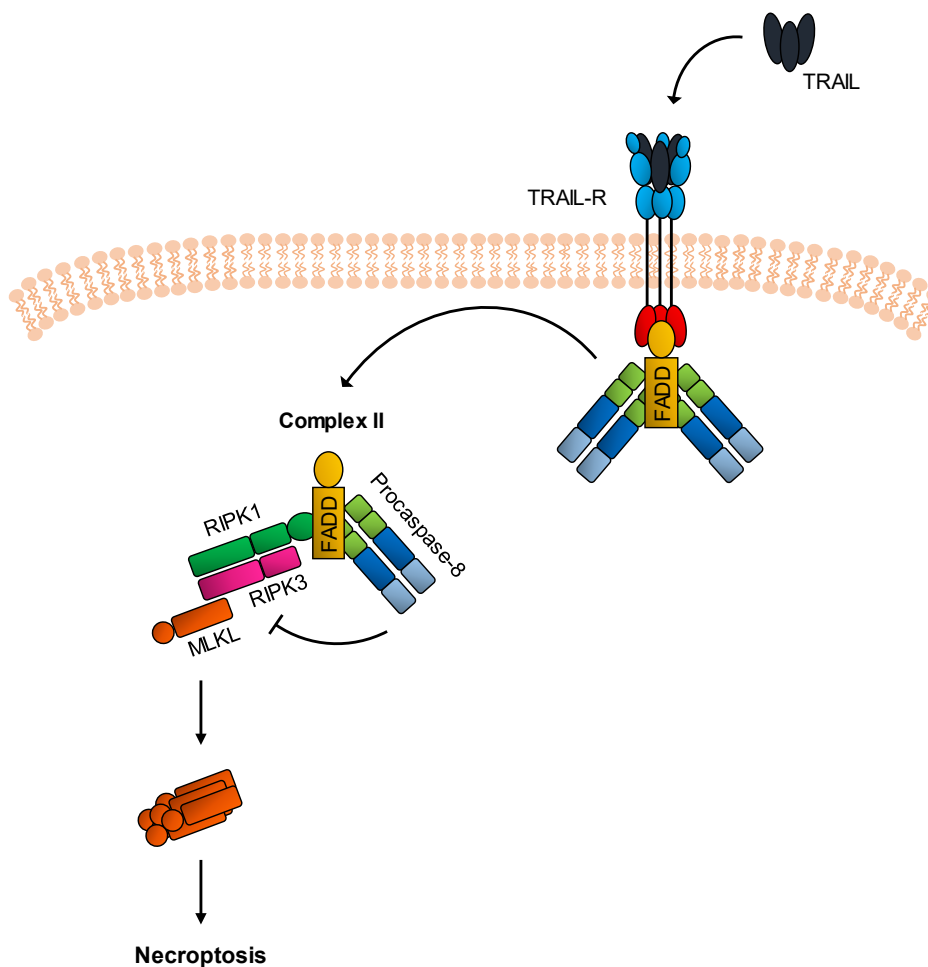


Figure 1.4: TRAIL-induced necroptosis signalling pathway.

Upon TRAIL stimulation, subsequent to the assembly of the DISC, a secondary cytoplasmatic complex can be formed, known as complex II. This secondary complex retains the DISC components FADD and caspase-8 and it also contains RIPK1. In certain circumstances, when caspase-8 is absent or its activity is blocked, RIPK1 recruits RIPK3, which in turn phosphorylates MLKL. Phosphorylated MLKL then oligomerises, which results in the execution of necroptosis.

1.1.3.3. Non-canonical TRAIL signalling

In addition to the induction of cell death, TRAIL has also been demonstrated to induce non-cell death signalling pathways in cancer cells. One of the most characterised one is the activation of NF- κ B, which has been shown to be activated by TRAIL binding to TRAIL-R1, TRAIL-R2 and TRAIL-R4 (Chaudhary et al., 1997; Degli-Esposti et al., 1997a; Schneider et al., 1997b). Interestingly, the transcription factor NF- κ B activates inflammatory and pro-survival pathways that play an important role in pro-inflammatory immune responses (Huet et al., 2014). RIPK1, besides activating

necroptosis as explained before, is also involved in the activation of NF- κ B downstream of TRAIL (Lin et al., 2000). In line with these findings, RIPK1 has been shown to be part of the DISC (Varfolomeev et al., 2005; Li and Lin, 2008). RIPK1 activates the inhibitor of κ B (I κ B) kinase complex (IKK complex), causing the phosphorylation and subsequent degradation of the I κ B, which, in turn, leads to the release and accumulation of NF- κ B (Varfolomeev et al., 2005). NF- κ B then translocates to the nucleus, where it activates the transcription of several anti-apoptotic genes such as *FLIP*, *BCL-XL*, *CIAPs* and *MCL1* (Kreuz et al., 2001; Ravi et al., 2001; Mitsiades et al., 2002; Henson et al., 2003). Consequently, TRAIL-induced NF- κ B activation was initially suggested to simply mediate resistance to apoptosis induction. Nevertheless, more recent evidence demonstrates that it serves other purposes. In fact, in apoptosis-resistant cancer cells, TRAIL can induce NF- κ B-dependent proliferation, migration and invasion (Ehrhardt et al., 2003; Ishimura et al., 2006). Furthermore, NF- κ B activation can activate the induction and secretion of pro-inflammatory cytokines such as C-C motif chemokine ligand 2 (CCL2), interleukin (IL)-8, IL-6, monocyte chemoattractant protein-1 (MCP-1), C-X-C motif chemokine ligand (CXCL)5 and CXCL1 (Varfolomeev et al., 2005; Hartwig et al., 2017; Henry and Martin, 2017). Of note, TRAIL-induced secretion of cytokines, most importantly CCL2, has been shown to induce the recruitment of C-C motif chemokine receptor 2 (CCR2)-expressing myeloid-derived suppressor cells (MDSCs), promoting the formation of a tumour-supportive immune microenvironment (Hartwig et al., 2017).

Mechanistically, a secondary cytoplasmatic complex has been deemed responsible for TRAIL-induced NF- κ B activation. This complex was shown to contain FADD, caspase-8, RIPK1, TRAF2 and NF- κ B essential modulator (NEMO) (also known as IKK γ) (Varfolomeev et al., 2005; Jin and El-Deiry, 2006). The formation of this secondary complex, also known as FADDosome or complex II, was initially reported to be dependent on FADD and caspase-8 activity (Varfolomeev et al., 2005). A more recent report, however, demonstrated that only the scaffold function of caspase-8 and not its activity was required for complex II assembly (Henry and Martin, 2017). According to a revised model of TRAIL signalling, gene activation can emanate from both TRAIL-induced complexes I and II (Lafont et al., 2017) (Figure 1.5). Interestingly, LUBAC, which is composed of SHANK-associated RH domain interactor (SHARPIN), heme-oxidized IRP2 ubiquitin ligase-1 (HOIL-1) and the catalytic component HOIL-1 interacting protein (HOIP), facilitates the recruitment of the IKK complex to both complexes, thereby promoting gene activation (Lafont et al., 2017). LUBAC is the

only ubiquitin E3 ligase known to form linear chains and has been shown to regulate multiple signalling pathways including TNF-RSC (Haas et al., 2009; Tokunaga et al., 2009; Shimizu et al., 2015).

Besides NF- κ B, both the TRAIL DISC and complex II can trigger the activation of other kinase signalling cascades involving MAPKs, mainly c-Jun N-terminal kinase (JNK), p38 and extracellular regulated kinase (ERK)1/2, (Varfolomeev et al., 2005). First, JNK can be activated by TRAIL both in a caspase-dependent and -independent manner (Muhlenbeck et al., 1998), with RIPK1 and TRAF2 being required for its activation (Varfolomeev et al., 2005). JNK activation results in the phosphorylation of the transcription factor AP1, and it has been reported to have opposing effects in TRAIL signalling, inducing both pro-apoptotic (Herr et al., 1999; Werneburg et al., 2007) as well as pro-survival responses (Mucha et al., 2009). Second, the activation of p38 downstream of TRAIL has also been shown to have opposing effects depending on the cell type with pro-apoptotic responses elicited in ovarian tumour cells (Lee et al., 2002) whilst having a pro-survival role in prostate or breast cancer cells (Son et al., 2010). Lastly, the activation of ERK by TRAIL seems to be intimately implicated in the stimulation of cell survival and proliferation of tumour cells (Zhang et al., 2003; Belyanskaya et al., 2008; Vilimanovich and Bumbasirevic, 2008).

All the non-canonical TRAIL-mediated signalling arms reported above are mediated by the TRAIL-R DD. Nevertheless, TRAIL has also been shown to induce non-apoptotic signalling via the TRAIL-R MPD. In fact, it was recently demonstrated that TRAIL-signalling promotes Kirsten rat sarcoma (*KRAS*)-driven cancer progression, invasion and metastasis via the TRAIL-R2 MPD-mediated activation of Ras-related C3 botulinum toxin substrate 1 (Rac1) and Phosphoinositide 3-kinase (PI3K) (von Karstedt et al., 2017).

This non-canonical signalling exerted by the TRAIL/TRAIL-R system highlights its dual function, inducing on one hand the cell death of cancer cells and on the other hand the promotion of tumour growth.

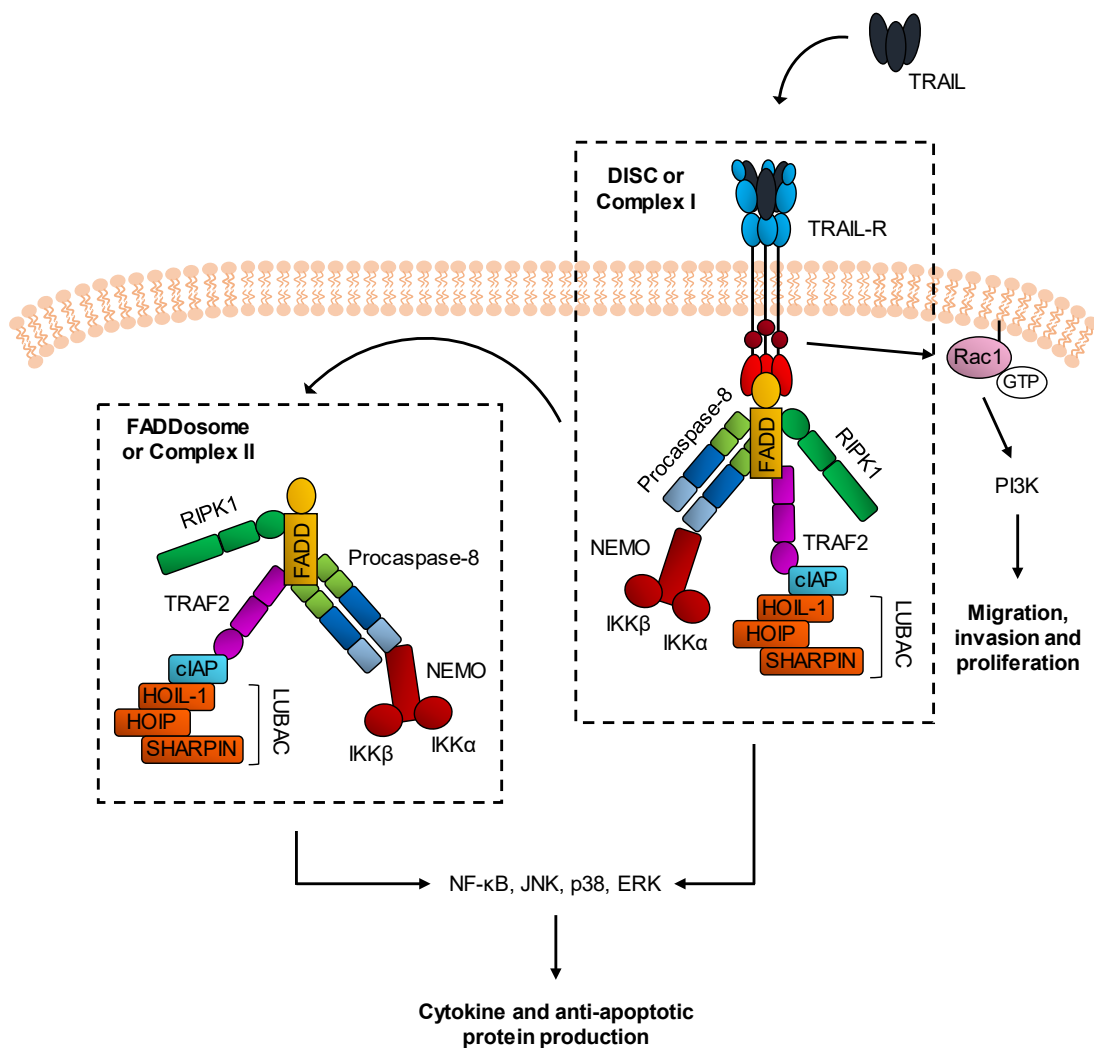


Figure 1.5: TRAIL-induced non-canonical TRAIL signalling.

Following DISC formation upon TRAIL triggering, TRAF2 is recruited to the complex, which in turn binds to cIAP1/2. This promotes the recruitment of LUBAC, enabling the recruitment of the IKK complex. RIPK1 also associates with the DISC when caspase-8 is inhibited. Moreover, TRAIL can trigger the formation of a secondary cytoplasmatic complex retaining caspase-8, FADD, TRAF2, RIPK1 and NEMO. Both this complex II and the DISC activate NF-κB, p38, JNK and ERK, thereby inducing cytokine production and pro-survival gene activation. LUBAC is present in both complexes, where it restricts the activation of caspase-8 and, thus, apoptosis and promotes cytokine production. Independently, TRAIL-R MPD-dependent signalling is mediated via Rac1 and PI3K activation to elicit migration, invasion and proliferation.

1.1.4. The role of TRAIL and its receptors in cancer

TRAIL is mainly expressed on the surface of two main immune effector cells: activated T cells and natural killer (NK) cells (Kayagaki et al., 1999a; Kayagaki et al., 1999b; Takeda et al., 2001). However, it is also found on macrophages, neutrophils and dendritic cells (DCs) after pro-inflammatory cytokine induction (Fanger et al., 1999; Griffith et al., 1999; Koga et al., 2004). In the innate system, TRAIL is involved in the effector mechanisms mediated by these cells. On the other hand, in the adaptive immune cells, the TRAIL/TRAIL-R system has a crucial role in preventing aberrant T cell activation and is required for immune homeostasis (Janssen et al., 2005; Ikeda et al., 2010; Pillai et al., 2011; Lehnert et al., 2014). In contrast to their ligand, TRAIL-Rs are ubiquitously expressed both in cancer cells and in the immune system. It is now clear that the TRAIL/TRAIL-R system plays a critical role in the interplay between cancer cells and the immune system. Nevertheless, the role of this system in cancer biology is complex and, depending on the tumour type and its oncogenic make-up, it can have a tumour-suppressive role mediating immunosurveillance or it can elicit pro-tumorigenic effects (Figure 1.6).

With the aim of deciphering the physiological role of the TRAIL/TRAIL-R system, first *Trail*-deficient (Cretney et al., 2002; Sedger et al., 2002) and later *Trail-r*-deficient (Diehl et al., 2004) mice were generated. Interestingly, both mice were viable and fertile, and neither of them exhibited any obvious phenotype. Nevertheless, the initial evidence for the involvement of the endogenous TRAIL/TRAIL-R system in regulating tumour growth came from the above-mentioned *Trail*-deficient mice, which were more susceptible to transplanted syngeneic A20 lymphoma (Sedger et al., 2002). Numerous subsequent animal studies with either *Trail*-deficient (Cretney et al., 2002; Zerafa et al., 2005), *Trail-r*-deficient (Finnberg et al., 2008; Grosse-Wilde et al., 2008) or mice that were injected with TRAIL neutralising antibodies (Smyth et al., 2001; Takeda et al., 2001; Takeda et al., 2002) have confirmed the tumour-suppressive role of the TRAIL/TRAIL-R system. This protective role of TRAIL in cancer development has been mainly attributed to the cytotoxic function of NK cells. In fact, the increase in metastasis formation observed upon treatment with anti-TRAIL antibodies in mice was abolished by NK cell depletion (Takeda et al., 2001). Furthermore, the protective effect of TRAIL is dependent on the interferon (IFN) γ -mediated upregulation of TRAIL expression on NK cells (Smyth et al., 2001). Whilst NK cells play a crucial role in killing cancer cells via TRAIL-R-mediated apoptosis, TRAIL has also been

demonstrated to participate in tumour-specific cytotoxic lymphocytes (CTLs)-mediated cell death (Dorothee et al., 2002). Importantly, in addition to the direct killing of cancer cells, TRAIL also contributes to the death of tumour-supportive immune cells that are present in the immune microenvironment. Indeed, TRAIL has been reported to induce apoptosis in MDSCs (Condamine et al., 2014) and regulatory T cells (Tregs) (Diao et al., 2013).

Cancer cells employ different strategies to escape from the immune system and TRAIL can contribute to their survival by promoting an immunosuppressive microenvironment. For example, TRAIL-induced stimulation of TRAIL-Rs on cancer cells has recently been shown to lead to a secretome that promotes the recruitment and accumulation of a MDSC-rich tumour-supportive microenvironment via CCR2 (Hartwig et al., 2017). Moreover, TRAIL has been implicated in the immunosuppressive functions of Tregs. A study by Pillai *et al.* demonstrated that Tregs lacking the expression of IL-10 and IL-35, which is usually required for their function, upregulated the expression of TRAIL, rendering these cells functionally dependent on the death ligand (Pillai et al., 2011). In line with this, upregulation of TRAIL on Tregs has been reported to mediate their cytotoxicity against CD4⁺ T cells (Ren et al., 2007).

Besides developing resistance against TRAIL-mediated immune cell death, cancer cells hijack the TRAIL/TRAIL-R non-canonical signalling in order to support invasion and migration, mainly in the presence of certain oncogenic mutations. TRAIL was shown to stimulate the invasion of colorectal tumour cells and liver metastases in a KRAS-dependent way (Hoogwater et al., 2010). The authors demonstrated that oncogenic KRAS and its effector RAF1 could switch the signalling of the DR into invasion-promoting through the suppression of the Rho-associated protein kinase (ROCK)/LIM kinase pathway. In addition, a kinome profiling of the TRAIL-induced non-canonical pathway in TRAIL-resistant non-small-cell lung cancer (NSCLC) cells revealed that Src and signal transducer and activator of transcription (STAT)3 are activated downstream of RIPK1 and TRAIL-R2 to promote migration and invasion of these cells (Azijli et al., 2012). Similarly, cancer cell-expressed endogenous mTRAIL-R was shown to promote the progression, invasion and metastasis of autochthonous *Kras*-driven pancreatic and lung cancer in a cell-autonomous manner through the activation of RAC1 (von Karstedt et al., 2017).

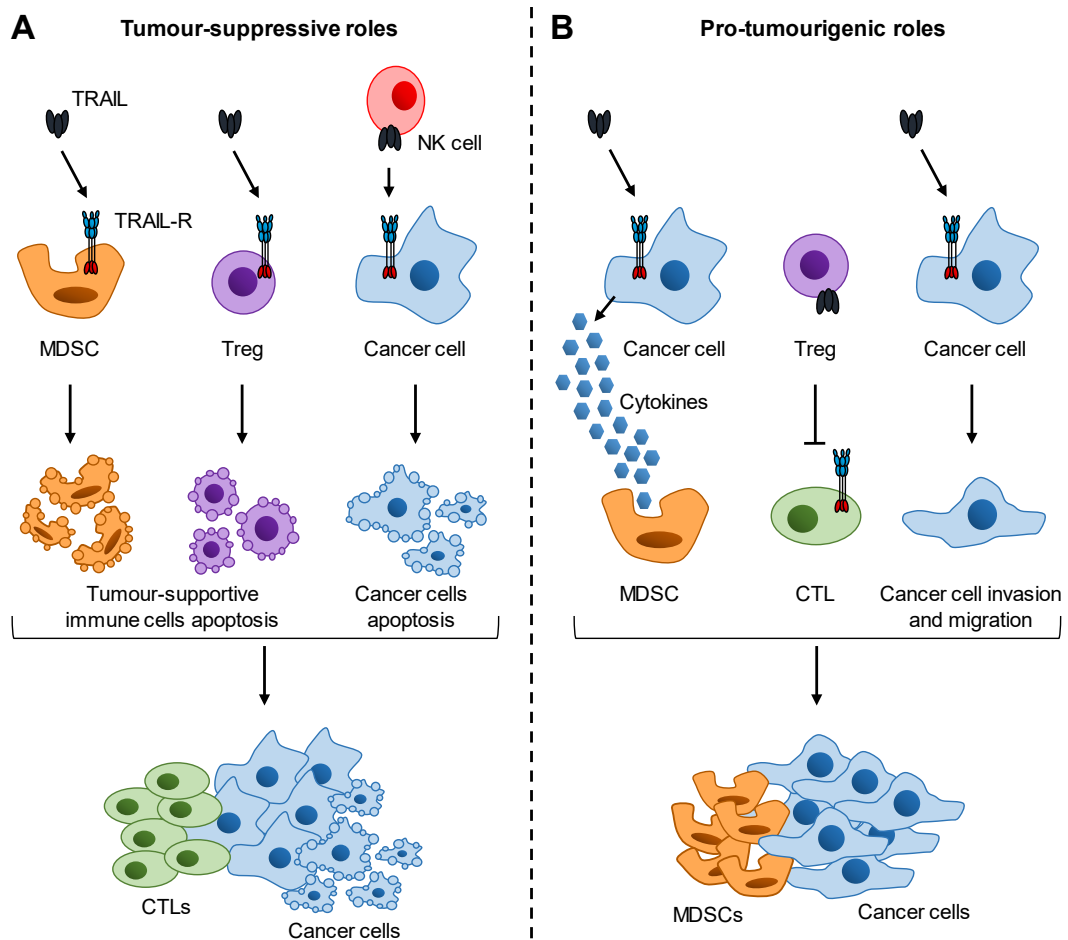


Figure 1.6: The role of the TRAIL/TRAIL-R system in the tumour and its microenvironment.

(A) The TRAIL/TRAIL-R system can induce direct killing of tumour-supportive immune cells such as MDSCs and Tregs by promoting their apoptosis. Furthermore, TRAIL-expressing NK cells can induce TRAIL-R-mediated apoptosis in cancer cells. Collectively, these effects lead to the accumulation of CTLs in the tumour microenvironment, facilitating the immunosurveillance against the tumour.

(B) The TRAIL/TRAIL-R system can facilitate an immunosuppressive cancer microenvironment that contributes to the tumour growth. Cancer cells can secrete several cytokines upon the stimulation of TRAIL-R by TRAIL that regulate the recruitment of MDSCs. Moreover, TRAIL on Tregs can suppress CTL activation and oncogenic mutation-bearing cancer cells can use the TRAIL-TRAIL-R system to promote their invasion and migration.

1.1.5. TRAIL-R agonists in the clinic

The discovery that systemic treatment of xenograft tumour-bearing mice with recombinant forms of TRAIL resulted in tumour regression without causing any toxicity highlighted the cancer selectivity of this death ligand (Ashkenazi et al., 1999; Walczak et al., 1999). This unique property suggested TRAIL therapy to be a promising new avenue for cancer therapy and led to worldwide efforts for the clinical development of TRAIL-R agonists (TRAs). Currently tested TRAs in the clinic comprise two categories of pharmacological agents: recombinant forms of TRAIL and specific agonistic antibodies against TRAIL-R1 or TRAIL-R2.

The use of recombinant TRAIL, as opposed to agonistic antibodies specific for only one TRAIL-R, has the advantage of triggering both TRAIL-R1 and TRAIL-R2, likely resulting in a stronger death signal. On the other hand, recombinant TRAIL may also engage the alternative non-apoptosis-inducing TRAIL-Rs, which could hamper its apoptotic activity. Given that the trimerisation of TRAIL is of crucial importance for its biological activity, several recombinant TRAIL formulations have been developed with the aim of increasing its stability such as adding various tags to its N-terminal including poly-histidine (His-TRAIL) (Pitti et al., 1996) and FLAG epitope (FLAG-TRAIL) (Wiley et al., 1995). Nevertheless, these constructs demonstrated toxicity given their ability to kill primary human hepatocytes (PHH), most likely due to the supramolecular aggregates formed by the interaction of the tags (Jo et al., 2000; Ichikawa et al., 2001; Ganten et al., 2006). Alternatively, an improved version of TRAIL was engineered, containing a leucine zipper (LZ) or isoleucine zipper (IZ) trimerisation motif at the end of the N-terminus of the extracellular domain. These forms of recombinant TRAIL showed high activity both *in vitro* and *in vivo* and, importantly, caused neither PHH toxicity *ex vivo* nor systemic toxicity *in vivo* in mice (Walczak et al., 1999; Ganten et al., 2006; Rozanov et al., 2009). Various other strategies have been designed to stabilise the trimeric conformation of TRAIL such as the incorporation of the tenascin-C oligomerisation domain (Berg et al., 2007) or the fusion of TRAIL to the Fc portion of human immunoglobulin G (IgG) (Wang et al., 2014a). Nevertheless, only two forms of recombinant TRAIL have entered clinical testing so far. First, the non-tagged Dulanermin (also known as APO2L.0 or AMG-951), which comprises amino acids 114-281 of the extracellular domain of TRAIL (Ashkenazi et al., 1999). Although encouraging preclinical results were obtained with this TRA (Ashkenazi et al., 1999; Kelley et al., 2001; Lawrence et al., 2001; Ganten

et al., 2006), clinical trials have failed to show any significant anti-cancer activity (Table 1.1). The main features of Dulanermin responsible for this failure are most likely its short half-life *in vivo*, of approximately 30 minutes (Kelley *et al.*, 2001; Xiang *et al.*, 2004), and its poor trimer stability, which explains its weak ability to induce higher-order clustering of TRAIL-Rs (Graves *et al.*, 2014; Tuthill *et al.*, 2015). Second, circularly permuted TRAIL (CPT), a new generation of mutant recombinant TRAIL is now under evaluation in clinical trials. The main characteristic of this TRA is that the N-terminus of amino acids 121-135 of TRAIL is connected to the C-terminus of amino acids 135-281 by a flexible linker, which allows it to form stable homotrimers. Following promising results in mouse xenografts (Fang *et al.*, 2005; Wu *et al.*, 2017), CPT entered clinical trials for multiple myeloma (MM). However, the results of the completed trials so far have not demonstrated any significant clinical benefit (Table 1.1).

Antibodies developed as specific TRAIL-R1 or TRAIL-R2 agonists are more stable and present improved pharmacokinetic properties, with substantially longer lives when compared to recombinant forms of TRAIL. Whilst only one agonistic TRAIL-R1 antibody has entered clinical testing to date, Mapatumumab (HGS-ETR1), several agonistic antibodies targeting TRAIL-R2 have done so, including Conatumumab (AMG-655), Tigatuzumab (CS-1008), Lexatumumab (HGS-ETR2), Drozitumumab (PRO95780) and DS-8273a (Table 1.1). Overall, although anti-cancer efficacy was demonstrated in preclinical *in vivo* models for all of the aforementioned agonistic TRAIL-R1 or TRAIL-R2 antibodies, the results of the clinical trials completed so far in a number of malignancies have failed to achieve statistically significant anti-tumour activity in randomised-controlled trials (RCT). Nevertheless, phase 1 testing revealed safety and broad tolerability when these antibodies were administered alone or in combination with chemotherapy or other standard therapies. This poor cell death induction is probably due to the bivalent nature of the antibodies, which only allows the crosslinking of two TRAIL-Rs instead of the three that would be required for optimal activation of TRAIL-Rs, as explained before. In order to overcome this, novel TRAs are being designed with the aim of forming stable high-order complexes. The first one of this new generation of TRAs to reach the clinic was TAS266, a tetrameric TRAIL-R2-activating nanobody. It consists of four identical humanised high-affinity heavy chain domain antibody fragments, occurring naturally in camelid species, connected via three 35 amino acid-linkers. TAS266 was reported to be more effective than soluble TRAIL or agonistic antibodies both *in vitro* and *in vivo* since it has the

potential to cluster four TRAIL-R2 molecules simultaneously, leading to robust DISC formation and apoptosis induction (Huet et al., 2014). Despite these promising preclinical results, the phase 1 clinical study that was set to evaluate its safety had to be terminated early due to acute toxicity in three patients (Papadopoulos et al., 2015). This toxicity appeared to be owing to the patients having pre-existing anti-camelid antibodies, which bound to TAS266, causing an anti-drug antibody response. The clinical benefit of other novel TRAs that have shown exciting preclinical results like APG350 awaits assessment (Legler et al., 2018).

Table 1.1: Completed clinical trials with TRAs.

Dulanermin (recombinant TRAIL)				
In combination with	Cancer	Phase	Outcome	Reference
-	Various	1a	NA	(Pan et al., 2011)
-	Various	1	NA	(Herbst et al., 2010a)
Rituximab	Lymphoma	1b/2	NR	NCT00400764 (Cheah et al., 2015)
FOLFOX + Bevacizumab	Colorectal	1b	13 PR (n=23)	NCT00873756 (Wainberg et al., 2013)
Paclitaxel + Carboplatin + Bevacizumab	NSCLC	1b	1 CR, 13 PR (n=213)	NCT00508625 (Soria et al., 2010)
Camptosar + Erbitux or FOLFIRI	Colorectal	1b	NA	NCT00671372
Paclitaxel + Carboplatin + Bevacizumab	NSCLC	2 (RCT)	Negative	NCT00508625 (Soria et al., 2011)
Vinorelbine + Cisplatin	NSCLC	3 (RCT)	Positive	(Ouyang et al., 2018)
CPT (recombinant TRAIL)				
In combination with	Cancer	Phase	Outcome	Reference
-	MM	1b	1 CR, 4 PR (n=27)	(Hou et al., 2018)
-	MM	2	9 PR (n=27)	(Leng et al., 2016)
Thalidomide	MM	2	2 CR, 7 PR (n=41)	(Geng et al., 2014)
Thalidomide + Dexamethasone	MM	2 (RCT)	Negative	(Leng et al., 2017)

Mapatumumab (TRAIL-R1 agonistic antibody)				
In combination with	Cancer	Phase	Outcome	Reference
-	Solid	1	NR	(Tolcher et al., 2007)
-	Solid	1	NR	(Hotte et al., 2008)
-	NHL	1b/2	2 CR, 1 PR (n=40)	NCT00094848 (Younes et al., 2010)
-	Colorectal	2	NR	(Trarbach et al., 2010)
-	NSCLC	2	NR	NCT00092924 (Greco et al., 2008)
Gemcitabine + Cisplatin	Solid	1	NR	NCT01088347 (Mom et al., 2009)
Carboplatin + Paclitaxel	Solid	1	5 PR (n=27)	(Leong et al., 2009)
Sorafenib	Liver	1b	NA	NCT00712855
Cisplatin + radiotherapy	Cervical	1b/2	NA	NCT01088347
Bortezomib	Myeloma	2 (RCT)	Negative	NCT00315757 (Belch et al., 2010)
Carboplatin + Paclitaxel	NSCLC	2 (RCT)	Negative	NCT00583830 (von Pawel et al., 2014)
Sorafenib	Liver	2 (RCT)	Negative	NCT01258608 (Ciuleanu et al., 2016)
Tigatuzumab (TRAIL-R2 agonistic antibody)				
In combination with	Cancer	Phase	Outcome	Reference
-	Various	1	NR	NCT00320827 (Forero-Torres et al., 2010)
-	Colorectal	1	1 PR (n=19)	NCT01220999 (Ciprotti et al., 2015)
FOLFIRI	Colorectal	1	NA	NCT01124630
Carboplatin + Paclitaxel	Ovarian	2	NA	NCT00945191
Gemcitabine	Pancreatic	2	8 PR (n=61)	NCT00521404 (Forero-Torres et al., 2013)
Sorafenib	Liver	2 (RCT)	Negative	NCT01033240 (Cheng et al., 2015)
Abraxane	TNBC	2 (RCT)	Negative	NCT01307891 (Forero-Torres et al., 2015)

Carboplatin + Paclitaxel	NSCLC	2 (RCT)	Negative	NCT00991796 (Reck et al., 2013)
Conatumumab (TRAIL-R2 agonistic antibody)				
In combination with	Cancer	Phase	Outcome	Reference
-	Solid	1	NR	(Doi et al., 2011)
-	Solid	1	1 PR (n=37)	(Herbst et al., 2010b)
Birinapant	Ovarian	1b	NA	NCT01940172
Bortezomib or Vorinostat	Lymphoma	1	NA	NCT00791011
Panitumumab	Colorectal	1b/2	NA	NCT00630786
Doxorubicin	STS	1b/2 (RCT)	Negative	NCT00626704 (Demetri et al., 2012)
FOLFOX + Bevacizumab	Colorectal	1b/2	Negative	NCT00625651 (Fuchs et al., 2013)
Carboplatin + Paclitaxel	NSCLC	2 (RCT)	Negative	NCT00534027 (Paz-Ares et al., 2013)
FOLFIRI	Colorectal	2 (RCT)	Negative	NCT00813605 (Cohn et al., 2013)
Gemcitabine	Pancreatic	2 (RCT)	Negative	NCT00630552 (Kindler et al., 2012)
Drozitumab (TRAIL-R2 agonistic antibody)				
In combination with	Cancer	Phase	Outcome	Reference
-	Various	1	NR	(Camidge et al., 2010)
FOLFOX + Bevacizumab	Colorectal	1b	2 PR (n=9)	NCT00851136 (Rocha Lima et al., 2012)
Cetuximab + Irinotecan or FOLFIRI + Bevacizumab	Colorectal	1b	NA	NCT00497497
Rituximab	NHL	2	NA	NCT00517049
Carboplatin + Paclitaxel + Bevacizumab	NSCLC	2 (RCT)	NA	NCT00480831
Lexatumumab (TRAIL-R2 agonistic antibody)				
In combination with	Cancer	Phase	Outcome	Reference
-	Solid	1	NR	(Plummer et al., 2007)
-	Solid	1	NR	(Wakelee et al., 2010)

-	Solid paediatric	1	NR	(Merchant et al., 2012)
DS-8273a (TRAIL-R2 agonistic antibody)				
In combination with	Cancer	Phase	Outcome	Reference
-	Solid	1	NR	NCT02076451 (Forero et al., 2017)

-, TRA alone; CR, complete response; CPT, circularly permuted TRAIL; MM, multiple myeloma; n, number of patients; NA, not available; NHL, non-Hodgkin lymphoma; NR, no responses; NSCLC, non-small-cell lung cancer; PR, partial response; RCT, randomised-controlled trial; STS, soft tissue sarcoma; TNBC, triple-negative breast cancer.

Outcome was considered positive when the addition of the TRA significantly improved the primary endpoint of the trial as compared with the standard therapy.

In summary, the initial optimism after promising anti-cancer activity achieved in preclinical models by TRAs has been dampened by the results obtained in the clinical trials to date. In addition to the previously mentioned insufficient agonistic activity of some of the TRAs tested so far, it appears that there are two main pitfalls to the current TRA-based treatment approaches. On one hand, there is a lack of biomarkers that can predict which patients are likely to respond to a certain TRA-based therapy (Ashkenazi, 2015). On the other hand, it is now well established that most primary cancers are resistant to monotherapy with TRAs (Ehrhardt et al., 2003; Todaro et al., 2008; Koschny et al., 2010; Graves et al., 2014; Tuthill et al., 2015). As described in section 1.1.2.1, resistance mainly occurs through the exacerbated expression of different TRAIL-induced apoptosis pathway regulators such as FLIP, XIAP, Bcl-2, Bcl-XL or Mcl-1. Nonetheless, alternative resistance mechanisms have also been demonstrated, like the epigenetic silencing of *CASP8*, which is commonly present in small-cell lung cancer (SCLC) (Hopkins-Donaldson et al., 2003).

Consequently, efforts are being made to identify sensitisers that can break the intrinsic TRAIL resistance of many cancer cells. In this regard, numerous TRAIL-sensitising strategies are being devised and tested constantly. For example, TRAs have been successfully combined with commonly used chemotherapeutic agents such as doxorubicin or cisplatin to kill TRAIL-resistant cancer cell lines both *in vitro* and *in vivo* (El-Zawahry et al., 2005; Shamimi-Noori et al., 2008). Different mechanisms have been proposed to underlie the chemotherapy-induced sensitisation to TRAIL-mediated apoptosis, including increased DISC formation,

upregulation of pro-apoptotic factors and suppression of anti-apoptotic proteins. However, as explained above, none of the RCTs conducted to date with this combination showed clinical activity (Table 1.1). Similarly, the proteasome inhibitor Bortezomib, which is used in MM treatment, has been shown to sensitise a range of tumour cells to TRAIL-mediated apoptosis by downregulating FLIP (Sayers et al., 2003), although higher doses of Bortezomib can also sensitise PHH to TRAIL (Koschny et al., 2007). Yet, a completed RCT in MM comparing the treatment with Bortezomib alone or in combination with the TRA Mapatumumab showed no additive therapeutic benefit (Belch et al., 2010).

Moreover, SMAC and BH3 mimetics have been widely tested as sensitisers to TRAIL-induced cell death. SMAC mimetics mimic the XIAP-binding site of the endogenous XIAP-antagonist SMAC, thereby antagonising IAPs. They have shown broad preclinical activity as TRAIL sensitisers in various cancer cell lines (Fulda et al., 2002b; Li et al., 2004; Fakler et al., 2009; Lecis et al., 2010). The clinically most advanced SMAC mimetic, Birinapant, has been tested in a Phase 1b clinical trial in combination with the TRA Conatumumab in ovarian cancer, but the results are not available yet. Likewise, BH3 mimetics were developed to antagonise anti-apoptotic Bcl-2 family members. To date, seven such compounds have reached clinical evaluation: the Bcl-2, Bcl-XL and Bcl-W inhibitors ABT-737 and ABT-263 (Navitoclax); the Bcl-2-specific inhibitors ABT-199 (Venetoclax) and S55746; and the Mcl1-inhibitors AMG176, AZD5991 and S64315 (Merino et al., 2018). Whilst the development of Mcl-1 inhibitors has been slower and they have only recently reached the clinic, the other BH3-mimetics have already demonstrated impressive clinical activity (Kipps et al., 2015; Fischer et al., 2019; Jain et al., 2019). Indeed, Venetoclax is currently approved for the treatment of refractory CLL. Interestingly, Bcl-2/XL inhibition by ABT-263 or ABT-737 has been reported to sensitise cancer cells to TRAIL *in vitro* and *in vivo* (Huang and Sinicrope, 2008; Cristofanon and Fulda, 2012; Wang et al., 2012a). Nevertheless, only future clinical testing will be able to conclude if these combinations are efficient at breaking the resistance of tumours to TRAIL.

Furthermore, the combination of histone deacetylase inhibitors (HDACi) and TRAIL has been shown to be synergistic in killing TRAIL-resistant cancer cells (Inoue et al., 2004; MacFarlane et al., 2005b; Nebbioso et al., 2005) and has shown efficacy *in vivo* (Frew et al., 2008; Srivastava et al., 2010). HDACi have been reported to enhance TRAIL-induced cell death by coordinating the upregulation of the pro-apoptotic

proteins caspase-8, caspase-3, Bid, Bak, Bax and Bim as well as the TRAIL-R1 and TRAIL-R2 while downregulating at the same time the anti-apoptotic proteins Bcl-XL, Mcl-1, XIAP and FLIP (Elmallah and Micheau, 2019). So far, only one clinical trial has been conducted to determine the safety and tolerability of combining a TRA with an HDACi. Conatumumab was combined with Vorinostat in lymphoma patients where, despite demonstrating a safety profile, the overall response rate was only of 9% (AMGEN Clinical study report 20060340).

Recent work in our laboratory discovered cyclin-dependent kinase (CDK)9 inhibition as the most potent strategy to break TRAIL resistance of cancer cells identified to date (Lemke et al., 2014b). CDK inhibitors like Flavoparidol or Selecciclib had previously been shown to synergise with TRAIL (Kim et al., 2003; Kim et al., 2004; Palacios et al., 2006; Fandy et al., 2007; Ortiz-Ferron et al., 2008; Molinsky et al., 2013). However, at that point it remained unclear which of the CDK inhibited by these pan-CDK inhibitors was responsible for that effect. The study by Lemke *et al.* identified CDK9 as the target responsible for sensitisation to TRAIL by performing a kinome-wide screen of the targets of PIK-75, a compound they showed to sensitise cells to TRAIL-induced apoptosis (Lemke et al., 2014a). In this work, the CDK9 inhibitor SNS-032 exquisitely sensitised a panel of NSCLC to TRAIL-induced apoptosis, whereas not causing toxicity in PHH within a considerable therapeutic window. Mechanistically, CDK9 inhibition resulted in downregulation of FLIP and Mcl-1 and concomitant downregulation of both anti-apoptotic factors was required and sufficient for CDK9-mediated TRAIL sensitisation. Importantly, the potency of this combination was underlined by the fact that established orthotopic lung cancer xenografts were eradicated upon treatment with izTRAIL and SNS-032.

1.2. Cyclin-dependent kinases and their role in transcription

1.2.1. Cyclin-dependent kinases

CDKs are a family of serine/threonine kinases that require binding to a regulatory cyclin partner protein for their enzymatic activity. CDKs were first identified in the 1980s in genetic screens in yeast (Russell and Nurse, 1986). These studies showed that CDKs must associate with cyclins to form complexes in which the CDK is the effector subunit and the cyclin serves as an activator (Jeffrey et al., 1995). Cyclins receive that name from the observation that they were synthesised and degraded at each cleavage division in sea urchin eggs (Evans et al., 1983). The discovery that these proteins rise and fall led to the realisation that cell cycle is controlled by specific proteins. However, since these initial studies, it has been clearly established that the CDK protein family does not only modulate cell division but also gene transcription.

There are 20 CDKs in mammals, which can be divided in two main groups based on their functions (Malumbres, 2014). First, the CDKs that regulate the cell cycle: CDK1, CDK2, CDK3, CDK4, CDK5, CDK6, CDK14, CDK15, CDK16, CDK17 and CDK18. Second, CDKs that are involved in the regulation of transcription, whose role will be described in the next section: CDK7, CDK8, CDK9, CDK10, CDK11, CDK12, CDK13, CDK19 and CDK20. Nevertheless, both activities are present in some CDKs such as CDK7 (Fisher, 2005). Similarly to most cyclins, which associate with one or two CDKs, most CDKs also pair with one or two cyclins. Figure 1.7 summarises the interactions between CDKs and their respective cyclins.

For the purpose of this thesis, the next section will focus on the CDKs controlling transcription, more specifically on CDK9.

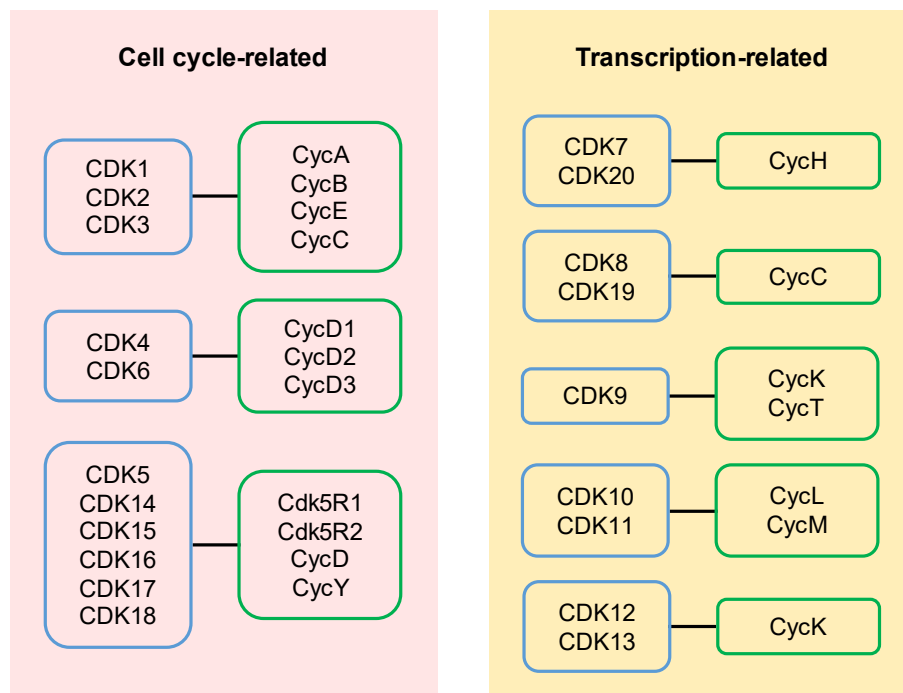


Figure 1.7: Mammalian CDKs and their cyclin partners.

Classification of the mammalian CDKs according to their function. The cyclin partner of each CDK is indicated. CDK, cyclin-dependent kinase; Cyc, cyclin.

1.2.2. CDK9: a regulator of transcriptional elongation

CDK9 was initially isolated in the 1990s as a 42 kDa serine/threonine kinase and it was originally designated PITALRE because of its characteristic Pro-Ile-Thr-Ala-Leu-Arg-Glu cyclin binding motif (Grana et al., 1994). CDK9 exists in two isoforms, the originally identified CDK9₄₂, and a minor, less studied, 55 kDa protein (CDK9₅₅) that is 17 amino acids longer at the N-terminus (Shore et al., 2003). Both isoforms are expressed in the cells albeit at different levels, with the short form being more abundant (Liu and Herrmann, 2005). While CDK9₅₅ is essentially localised in the nucleus (Shore et al., 2005), CDK9₄₂ is present both in the cytoplasm and in the nucleus (Falco et al., 2002). Both isoforms can form heterodimers with cyclin T and cyclin K. Interestingly, CDK9 is very conserved among different species, with 99% sequence homology between human and mouse. In addition, it is broadly distributed in all types of human and murine tissues, with particularly high levels of expression in terminally differentiated cells (Bagella et al., 1998; Bagella et al., 2000; Lin et al., 2002b).

CDK9 is the catalytic subunit of the positive transcription elongation factor-b (P-TEFb) and plays a crucial role in regulating global (non-ribosomal) transcription (Peng et al., 1998; Wei et al., 1998). This is achieved by the phosphorylation of the carboxyl-terminal domain (CTD) of RNA polymerase II (RNA Pol II) to promote transcriptional elongation. The Price laboratory was the first to demonstrate the role of P-TEFb in transcription and CTD phosphorylation using *Drosophila melanogaster* as a model organism (Marshall and Price, 1995; Zhu et al., 1997; Peng et al., 1998).

The transcription of protein-coding genes is a complex biological process orchestrated by RNA Pol II with the help of various transcriptional factors and several other CDKs. It can be divided in four main distinct sequential phases: initiation, pausing, elongation and termination (Figure 1.8).

Transcription starts by the activation of a gene, when DNA is unwound in the area where the gene-to-be-transcribed is located. Subsequently, the pre-initiation complex (PIC) is formed. First, transcription factor (TF)IID binds to the promoter region of the DNA (Davison et al., 1983; Sawadogo and Roeder, 1985). Then, the rest of the general TFs (GTFs) (TFIIA, TFIIB, TFIIE and TFIIIF) are recruited, stabilising the binding of TFIID to the promoter (Buratowski et al., 1989). This is followed by the recruitment of the mediator complex, which is formed by several molecules, including CDK8, and serves as a scaffold to recruit RNA Pol II (Tsai et al., 2013; Plaschka et al., 2016). Once it is assembled, the PIC adopts an inactive, or closed, state in which it is unable to initiate transcription. The PIC is activated by the recruitment of TFIIH, which contains CDK7. This TF stabilises RNA Pol II, opens up the DNA and brings it closer to the RNA Pol II, thereby changing the conformation of the PIC from closed to open to initiate transcription (He et al., 2013; Gupta et al., 2016). Following the activation of the PIC, RNA Pol II starts to recruit the first nucleoside triphosphates (NTPs) according to the DNA sequence and produces the first phosphodiester bond. When the transcript has reached a length of about 15 nucleotides, RNA Pol II can escape the promoter and enter in the elongation phase.

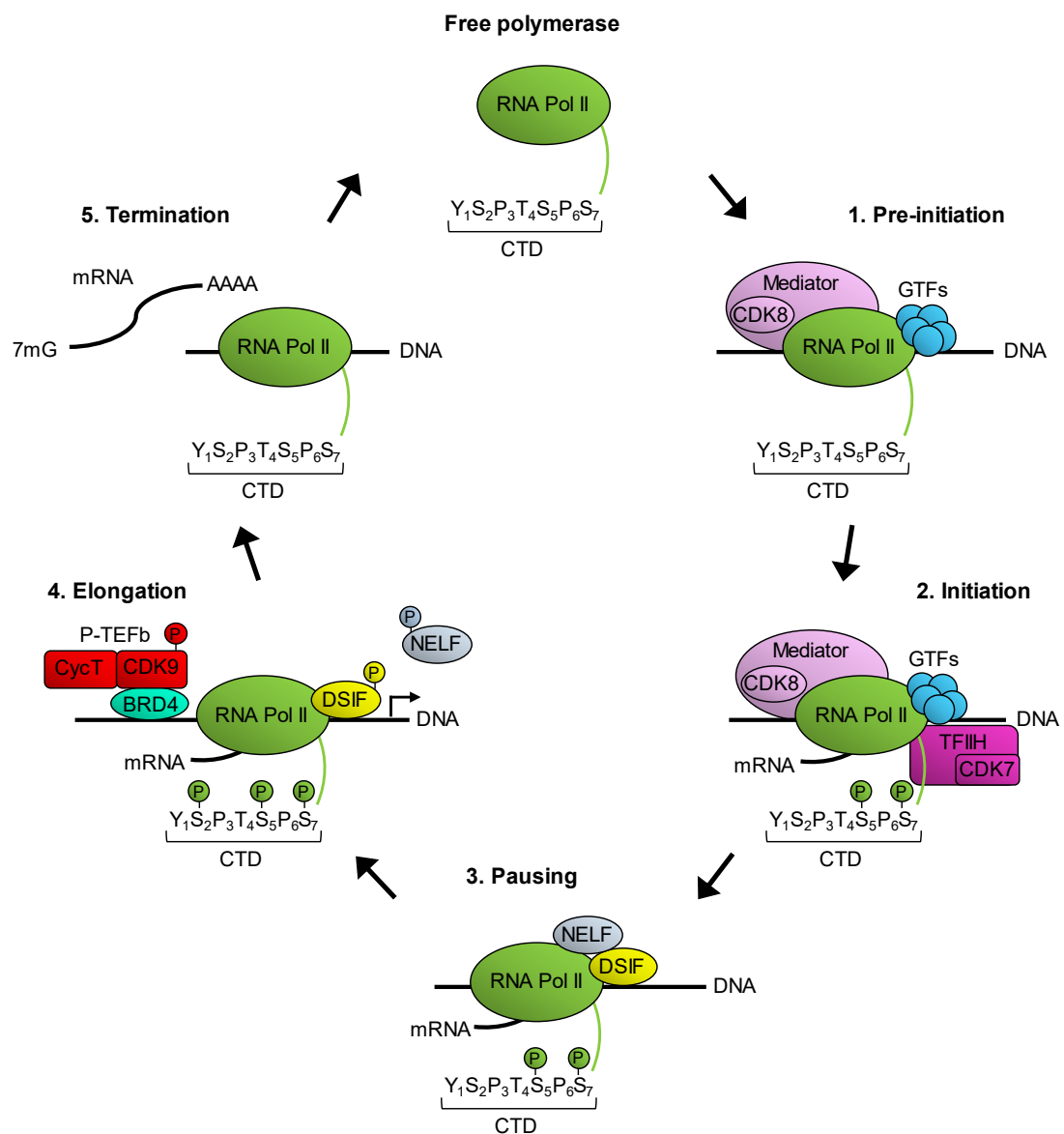


Figure 1.8: The RNA polymerase II transcription cycle.

Transcription starts with the activation of a gene and the recruitment of the mediator complex, GTFs and RNA Pol II to the promoter. TFIIH is then recruited and its catalytically active subunit CDK7 phosphorylates the CTD of RNA Pol II on Ser5 and Ser7. RNA Pol II subsequently starts the transcription of mRNA until the recruitment of DSIF and NELF leads to its pausing. To allow transcriptional elongation, CDK9, which is part of the P-TEFb, is recruited via BRD4 to phosphorylate DSIF, NELF and the Ser2 of the CTD. Consequently, the transcription of the nascent mRNA continues until termination. In order to enter a new cycle of transcription, all remaining CTD phosphorylations are removed by phosphatases.

One of the most critical domains of RNA Pol II, involved in the tight control of its activity, is the CTD. It consists of tandem heptad 52 repeats of the consensus sequence Tyr-Ser-Pro-Thr-Ser-Pro-Ser ($Y_1S_2P_3T_4S_5P_6S_7$) (Buratowski, 2003). Importantly, this domain is dynamically phosphorylated throughout the transcription cycle, controlling the whole process. When RNA Pol II is recruited to the PIC in the pre-initiation, its CTD is hypophosphorylated. After the activation of the PIC, the CTD undergoes its first modification, the phosphorylation of Ser5 and Ser7 by CDK7 (Akhtar et al., 2009; Glover-Cutter et al., 2009; Larochelle et al., 2012; Rimel and Taatjes, 2018). This CDK7-mediated phosphorylation is required for the efficient release of RNA Pol II from the PIC, thus facilitating promoter escape (Sogaard and Svejstrup, 2007; Jeronimo and Robert, 2014; Wong et al., 2014). Simultaneously, the PIC is partially disassembled, which can be used again in new transcription processes (Yudkovsky et al., 2000).

Once it is released from the PIC, RNA Pol II initiates the elongation. However, around 20-100 base pairs downstream of the transcription start site, the polymerase is paused. Thereby, the transcription rate is regulated and the cell ensures that both basal and signal-induced genes are expressed at the right times (Gilchrist et al., 2010). The pausing of RNA Pol II is facilitated by negative elongation factors 5,6-Dichloro-1- β -d-ribofuranosylbenzimidazole (DRB) sensitivity inducing factor (DSIF) and negative elongation factor (NELF) (Wada et al., 1998; Yamaguchi et al., 1999).

The elongation pause is overcome as a consequence of the recruitment of the P-TEFb and the phosphorylation and subsequent activation of CDK9 by CDK7 (Paparidis et al., 2017). CDK9 then facilitates productive elongation by phosphorylating DSIF and NELF, which causes the dissociation of the latter from the complex and the conversion of DSIF into a positive elongation factor (Fujinaga et al., 2004). Furthermore, CDK9 also phosphorylates the CTD of RNA Pol II on Ser2, enabling RNA Pol II to progress through transcriptional elongation. (Ahn et al., 2004; Yamada et al., 2006)

A tight regulation of the P-TEFb activity is essential to maintain transcriptional homeostasis. Most of the P-TEFb present in the cell is sequestered in a 7SK small nuclear ribonucleoprotein (snRNP) complex, which inhibits its kinase activity (Li et al., 2005). In addition to 7SK snRNA, this complex also contains hexamethylene bisacetamide-inducible protein 1/2 (HEXIM1/2), La-related protein 7 (LARP7) and

7SK snRNA methylphosphate capping enzyme (MePCE) (Nguyen et al., 2001; Yang et al., 2001; Barboric et al., 2009).

In order to activate transcriptional elongation, P-TEFb must be recruited at a precise genomic location at the right time. Bromodomain-containing protein 4 (BRD4) has been shown to be implicated in CDK9 delivery to the transcription site (Jang et al., 2005; Yang et al., 2005). Bromodomains are a common characteristic of chromatin-binding proteins, which usually bind acetylated histone tails. Indeed, this has also been observed for BRD4, which contains a bromodomain at its N-terminus. (Dey et al., 2003). Additionally, BRD4 contains a P-TEFb interacting domain (PID) at its C-terminus, which mediates the association to CDK9 (Bisgrove et al., 2007). According to the current model, BRD4 recruits and activates P-TEFb from its inactive complex and subsequently binds to the acetylated lysine residues in histones 3 and 4 of the gene being transcribed, consequently bringing P-TEFb in close proximity with RNA Pol II.

Elongation continues until the termination of transcription and the full synthesis of mRNA. Of note, the CTD of RNA Pol II is dephosphorylated to allow the termination and the recycling of the polymerase for new transcription cycles (Cho et al., 2001; Lin et al., 2002a).

1.2.3. CDK9 inhibition in cancer therapy

Given the importance of maintaining transcriptional homeostasis for appropriate cell function, it is not surprising that dysregulation of CDK9 signalling has critical implications for the development and/or progression of a malignant phenotype. Aberrant function of the CDK9 pathway has been observed in a variety of human tumours, most often by the induction of an increased expression of oncogenic factors. For instance, CDK9 regulates the transcription of short-lived anti-apoptotic proteins like Mcl-1, Bcl-2 and XIAP. Inhibition of CDK9 and thus, inhibition of the phosphorylation of Ser (pSer2) of the RNA Pol II CTD reinstates the ability of cancer cells to undergo apoptosis. This has been particularly demonstrated for haematological malignancies like lymphoma and leukaemia (Chen et al., 2005; MacCallum et al., 2005; Bettayeb et al., 2007; Gregory et al., 2015). Moreover, in prostate cancer, CDK9 has been shown to phosphorylate androgen receptor (AR)

and enhance AR-mediated transcription (Lee et al., 2001). Similarly, P-TEFb has been shown to be required for the *MYC* oncogene to promote transcription elongation of its target genes (Eberhardy and Farnham, 2001; Kanazawa et al., 2003; Rahl et al., 2010). In line with this, a more recent study identified CDK9 to be required for the maintenance of MYC-driven hepatocellular carcinoma (Huang et al., 2014). Furthermore, CDK9 has been demonstrated to have an additional role at maintaining epigenetic gene silencing and its inhibition has been shown to reactivate tumour-suppressor genes (Zhang et al., 2018).

The aforementioned observations encouraged the development of CDK9 inhibitors as potential anti-cancer therapeutics. An array of CDK9 inhibitors has been studied in preclinical and clinical settings. Despite usually displaying activity against several CDKs, CDK9 inhibitors are referred to as such because they typically exhibit increased half maximal inhibitory concentration (IC_{50}) values for CDK9 compared to other CDKs. Flavopiridol (Alvocidib) was the first CDK9 inhibitor to be enter clinical trials and has been the most studied thus far (Senderowicz et al., 1998). Nevertheless, to date, many other inhibitors have been developed and tested. Table 1.2 summarises the CDK9 inhibitors that have reached the clinic or have been evaluated in preclinical studies, including their CDK inhibition profiles.

Table 1.2: CDK9 inhibitors in preclinical or clinical development.

Agent	CDK inhibition profile (IC_{50})	Development stage	Reference
AT7519	CDK9: <10 nM CDK2: 47 nM CDK4: 100 nM CDK5: 13 nM CDK6: 179 nM	Phase 2	(Squires et al., 2009)
AZD4573	CDK9: 14 nM CDK1: 37 nM CDK2: >10 μ M CDK4: >10 μ M CDK7: 1.1 μ M	Phase 1	(Cidado et al., 2019)
BAY-1143572	CDK9: <1 μ M 50 fold selectivity against other CDKs	Phase 1	(Narita et al., 2017)
CDKI-73	CDK9: 6 nM CDK1: 8 nM CDK2: 3 nM	Preclinical	(Walsby et al., 2014)

	CDK4: 8 nM CDK6: 37 nM CDK7: 134 nM		
Dinaciclib	CDK9: 4 nM CDK1: 3 nM CDK2: 1 nM CDK5: 1 nM	Phase 3	(Parry et al., 2010)
Flavopiridol	CDK9: 6 nM CDK4: 10 nM CDK5: 110 nM CDK7: 23 nM CDK11: 57 nM	Phase 2	(Park et al., 1996)
LDC000067	CDK9: 32.7 nM CDK1: 5.5 μ M CDK2: 2.4 μ M CDK4: 9.2 μ M CDK6: >10 μ M CDK7: >10 μ M	Preclinical	(Albert et al., 2014)
LY2857785	CDK9: 11 nM CDK7: 246 nM CDK8: 16 nM	Preclinical	(Yin et al., 2014)
NVP-2	CDK9: <0.5 nM CDK1: 584 nM CDK2: 706 nM CDK5: 1.05 μ M CDK7: >10 μ M CDK8: >10 μ M	Preclinical	(Olson et al., 2018)
Seliciclib	CDK9: 0.79 μ M CDK1: 0.65 μ M CDK2: 0.7 μ M CDK5: 0.2 μ M CDK7: 0.49 μ M	Phase 2	(Havlicek et al., 1997; Meijer et al., 1997)
SNS-032	CDK9: 4 nM CDK2: 38 nM CDK7: 62 nM	Phase 1	(Conroy et al., 2009)
TG02	CDK9: 3 nM CDK1: 9 nM CDK2: 5 nM CDK3: 8 nM CDK5: 4 nM CDK7: 37 nM	Phase 2	(Goh et al., 2012)
Voruciclib	CDK9: 2 nM CDK1: 9 nM CDK4: 4 nM CDK6: 3 nM	Phase 1	(Dey et al., 2017)

Among all the CDK9 inhibitors, Dinaciclib (also known as SCH 7279656) is the most advanced in the clinic, having reached phase 3 testing. It is an ATP-competitive inhibitor of CDK1, CDK2, CDK5 and CDK9 that was developed by Merck as a result of a drug development program seeking to build on Flavopiridol by improving its safety and increasing its therapeutic index (Parry et al., 2010). During its preclinical characterisation, Dinaciclib was shown to suppress retinoblastoma (Rb) phosphorylation and induce cell cycle arrest and apoptosis activation in a broad panel of 100 tumour cell lines (Parry et al., 2010). Similarly, it has also been demonstrated to deplete Mcl-1 and Bcl-XL, leading to apoptosis in various solid and haematological cancers (Johnson et al., 2012; Booher et al., 2014; Gregory et al., 2015). Moreover, this CDK9 inhibitor has been shown to elicit a potent anti-tumour response in multiple cancer mouse models including ovarian cancer (Parry et al., 2010), acute myeloid leukaemia (AML) (Baker et al., 2016), melanoma (Desai et al., 2013), B cell lymphoma (Gregory et al., 2015) and pancreatic cancer (Feldmann et al., 2011).

Table 1.3 summarises the completed clinical trials conducted with Dinaciclib to date. In Phase 2 RCTs for breast cancer or NSCLC patients, Dinaciclib was generally well tolerated (Mita et al., 2014; Stephenson et al., 2014). Nevertheless, Dinaciclib monotherapy did not show significant anti-cancer activity as compared to the randomised control arm of the trial, which was the chemotherapeutic drug Capecitabine for breast cancer and the epidermal growth factor receptor (EGFR) inhibitor Erlotinib for NSCLC. The only phase 3 trial performed so far with Dinaciclib showed improved progression-free survival (PFS) in CLL patients, with a median PFS of 13.7 months in Dinaciclib-treated patients in comparison to 5.9 months in the patients that received the anti-CD20 antibody Ofatumumab (Ghia et al., 2017). It is important to note, however, that this trial was terminated early due to program prioritisation and, hence, the limited sample size precluded any statistical analysis. The termination of the trial was unrelated to safety since Dinaciclib had an acceptable safety and tolerability, with adverse effects similar to those identified in previous trials including neutropenia, thrombocytopenia and decreased neutrophil count. Currently, Dinaciclib is in clinical testing in combination with immunotherapy (Pembrolizumab) in breast cancer and haematological malignancies. Furthermore, ongoing studies are evaluating the efficacy of the combination of Dinaciclib with the Bcl-2 inhibitor Venetoclax in AML.

Table 1.3: Completed clinical trials with Dinaciclib.

In combination with	Cancer	Phase	Outcome	Reference
-	Various	1	NA	NCT00871910 (Mita et al., 2017)
-	Various	1	NA	NCT00871663 (Nemunaitis et al., 2013)
-	CLL	1	28 PR (n=52)	NCT00871663 (Flynn et al., 2015)
-	MM	1/2	3 PR (n=27)	NCT01096342 (Kumar et al., 2015)
-	NSCLC	2 (RCT)	Negative	NCT00732810 (Stephenson et al., 2014)
-	Breast	2 (RCT)	Negative	NCT00732810 (Mita et al., 2014)
-	CLL	3 (RCT)	Positive*	NCT01580228 (Ghia et al., 2017)
Bortezomib	PCM	1	NA	NCT01711528
Akt inhibitor MK2206	Pancreatic	1	NA	NCT01783171
Rituximab	CLL	1	NA	NCT01650727 (Fabre et al., 2014)
Epirubicin	Breast	1	NA	NCT01624441 (Mitri et al., 2015)
Ofatumumab	CLL	2	14 PR (n=36)	NCT01515176

-, Dinaciclib alone; CLL, chronic lymphocytic leukaemia; MM, multiple myeloma; n, number of patients; NA, not available; NR, no responses; NSCLC, non-small-cell lung cancer; PCM, plasma cell myeloma; PR, partial response; RCT, randomised-controlled trial.

Outcome was considered negative when the addition of Dinaciclib did not significantly improve the primary endpoint of the trial as compared with the standard therapy.

*Trial was terminated early and the small sample size prevented statistical analysis. However, the outcome was considered positive because there was a robust difference in PFS between the Dinaciclib and the standard therapy arms.

1.3. Lung cancer and mouse models of the disease

1.3.1. Lung cancer

Lung cancer is the leading cause of cancer-related death worldwide, being the second most common cancer for men and women, after prostate and breast cancer, respectively (Siegel et al., 2019). Despite significant progress in the treatment of this malignancy in the last decade, its prognosis remains poor, with a 5-year survival rate of only 18% (Schrank et al., 2018).

Lung cancer is classified in two major subtypes based on histologic features: NSCLC, which accounts for 85% of lung cancers, and SCLC, which accounts for the other 15%. NSCLC is a heterogeneous disease and can be further subdivided into lung adenocarcinoma (LAC) (50% of NSCLC), squamous-cell carcinoma (40%) and large-cell lung cancer (Herbst et al., 2008). Tobacco smoking is a risk factor for nearly 90% of lung cancer, but it is most strongly linked to SCLC and squamous cell carcinoma (Khuder, 2001; Khuder and Mutgi, 2001; Alexandrov et al., 2016). Interestingly, smoking is particularly associated with a higher frequency of mutations in *KRAS* (Rodenhuis and Slebos, 1992). For the purpose of this thesis, this section will focus on NSCLC, more specifically on LAC.

Molecular characterisation of LAC during the last decade has revealed a number of recurrent alterations that are likely to act as oncogenic drivers. The most commonly mutated oncogenes in LAC are *KRAS* (in 33% of tumours), *EGFR* (in 14%), v-Raf murine sarcoma viral oncogene homolog B (*BRAF*) (in 10%), PI3K catalytic subunit alpha (*PIK3CA*) (in 7%) and *MET* (in 8%). These mutations result in constitutive activation of downstream signalling cascades such as the PI3K-AKT-mammalian target of rapamycin (mTOR) and the RAS-RAF-MAPK kinase (MEK)-ERK pathways, promoting cell survival, proliferation, migration and invasion (Drosten and Barbacid, 2016). Furthermore, tumour-suppressors are often found mutated, including tumour protein 53 (*TP53*) (in 46%), serine/threonine kinase 11 (*STK11*) (also known as *LKB1*) (in 17%), Kelch-like ECH-associated protein 1 (*KEAP1*) (in 17%), neurofibromatosis type 1 (*NF1*) (in 11%) and *RB1* (in 4%). Moreover, CDK inhibitor 2A (*CDKN2A*) is deleted in 20% of the LAC and rearrangements in anaplastic lymphoma kinase (*ALK*), *ROS1* and *RET* are also present in these tumours (in 3-8%, 2% and 1%, respectively)

(Luo and Lam, 2013; Cancer Genome Atlas Research, 2014; Chen et al., 2014b; Swanton and Govindan, 2016).

KRAS mutations, which are the most common oncogenic driver alteration, are strongly associated with smoking (Govindan et al., 2012; Cancer Genome Atlas Research, 2014). Activating *KRAS* mutations primarily occur in the glycine (G) of codons 12 (G12, 91%) and 13 (G13, 6%) and the glutamine (Q) of codon 61 (2%). Among the G12 mutations, the most common substitution is by cysteine (C) (G12C, 44%), followed by valine (V) (G12V, 23%) and aspartate (D) (G12D, 17%) (Campbell et al., 2016; Jordan et al., 2017).

The discovery of these mutations has led to the development of targeted therapies. For instance, *EGFR*-mutations bearing patients are susceptible to therapeutic intervention with tyrosine kinase inhibitors (TKI) such as Afatinib, Erlotinib and Gefitinib (Godin-Heymann et al., 2008; Ray et al., 2009; Solca et al., 2012; Yu et al., 2013; Engle and Kolesar, 2014). Similarly, NSCLC patients carrying *ALK* or *ROS1* rearrangements can be treated with the TKI Crizotinib (Bang, 2011; Kazandjian et al., 2014). Additionally, treatment with Dabrafenib (BRAF inhibitor) and Trametinib (MEK inhibitor) has been recently approved for the treatment of NSCLC patients harbouring *BRAF* mutations (Khunger et al., 2018; Odogwu et al., 2018). However, prolonged treatment with these targeted therapies often results in the development of acquired drug resistance that limits the duration of their clinical benefit (Schrank et al., 2018).

Despite *KRAS* mutations being very common, no targeted therapy exists in the clinic yet for *KRAS*-mutated NSCLC patients. Indeed, this oncoprotein has been considered an undruggable target for a long time (McCormick, 2015). Recent studies, however, have demonstrated that *KRAS G12C* mutations can be selectively targeted and that these *KRAS (G12C)* inhibitors show preclinical anti-tumour efficacy (Janes et al., 2018; Canon et al., 2019). One of these inhibitors, AMG510, is currently under clinical evaluation in solid tumours (clinicaltrials.gov identifier NCT03600883).

Similar to other cancer types, it is now clear that NSCLC establishes an immunosuppressive tumour microenvironment conducive to tumour growth, which has led to the development of immunotherapies for this disease (Carbone et al., 2015). For instance, immune checkpoint blockade (ICB) has been the biggest paradigm shift in lung cancer therapy in the last decade. This therapy relies on the removal of inhibitory signals of T cell activation, which enables tumour-reactive T cells

to overcome regulatory mechanisms and mount an effective anti-tumour response that recognises tumour antigens. ICB can be achieved by antibodies blocking the cytotoxic T lymphocyte-associated protein 4 (CTLA-4) or the programmed cell death 1 (PD-1) pathway. CTLA-4 is upregulated on T cells following T cell receptor (TCR) engagement and acts as a negative regulator outcompeting CD28 for binding to costimulatory molecules B7 on antigen presenting cells (APCs), resulting in the attenuation of T cell activation (Walunas et al., 1994; Leach et al., 1996; Brunner et al., 1999). PD-1 is expressed on T cells upon activation and acts primarily to dampen T cell activation in the periphery (Agata et al., 1996). Inflammation-induced expression of programmed cell death ligand 1 (PD-L1) on tumour cells, or other immune cells in the tumour microenvironment, results in PD-1-mediated T cell exhaustion, hence inhibiting the anti-tumour cytotoxic T cell response (Freeman et al., 2000; Keir et al., 2006; Yokosuka et al., 2012). In NSCLC, the use of monoclonal antibodies against PD-1 first showed unprecedented rates of long-lasting tumour responses in 2015 (Borghaei et al., 2015; Brahmer et al., 2015). Since then, four ICB therapies have been approved for the treatment of NSCLC: the anti-PD-1 antibodies Nivolumab (Kazandjian et al., 2016) and Pembrolizumab (Larkins et al., 2017; Paischerf et al., 2017) and the anti-PD-L1 antibodies Atezolizumab (Weinstock et al., 2017) and Durvalumab (Antonia et al., 2018).

1.3.2. Mouse models of NSCLC

Mouse models of human cancer have been widely used as preclinical platforms for the understanding of the basic biology of cancer, as well as for the development of novel therapeutics and the elucidation of drug resistance mechanisms. Murine cancer models include xenograft or allograft (syngeneic) transplantation, carcinogen-induced mouse models and genetically-engineered mouse models (GEMMs). In transplanted models of lung cancer, cancer cells are injected either subcutaneously or orthotopically to establish tumours. In xenograft models, immunocompromised recipient mice must be used to avoid the immune response against foreign cells. Syngeneic models can overcome this disadvantage but they still rely on the transplantation of a large number of fully progressed homogenous cells in the animal. Consequently, they do not recapitulate the natural course of tumour progression (Sausville and Burger, 2006). In stark contrast, carcinogen-induced models and

GEMMs generate lung tumours that are initiated and progress in their natural microenvironment, and thus recapitulate the histological progression of precancerous lesions to invasive cancers. This may explain why critical differences in immunosurveillance and therapeutic response have been described between equivalent autochthonous and transplanted tumours (DuPage et al., 2011).

Carcinogen-induced mouse models of NSCLC likely represent the most realistic model of tobacco smoke-induced tumourigenesis. Nevertheless, they often require extended time periods for tumour development and the variability in the administration technique leads to discrepancies in the results. The most commonly used carcinogens are urethane (also known as ethyl carbamate) (You et al., 1989; Nuzum et al., 1990; Kawano et al., 1995), benzo(a)pyrene (You et al., 1989; Hecht et al., 1994), vinyl carbamate (Foley et al., 1991; Massey et al., 1995), methylnitrosourea (MNU) (You et al., 1989), 4-(methylnitrosamino)-1-(3-pyridyl)-1butanone (NNK) and N'-nitrosornicotine (NNN) (Vikis et al., 2013). Overall, the vast majority of carcinogen-induced mouse models represent *KRAS* mutant LAC. For example, in the most commonly employed urethane-induced lung tumourigenesis model, the most prominent genetic changes found are *Kras* Q61 and *Tp53* mutations (You et al., 1989; Ohno et al., 2001; Westcott et al., 2015). It is noteworthy that the frequency and latency of lung cancer incidence strongly depend on the inbred strain. For instance, A/J and SWR strains are the most susceptible ones, while BALB/c and FVB have intermediate susceptibility and C57BL/6, DBA and AKR strains are relatively resistant (Shimkin and Stoner, 1975; Manenti and Dragani, 2005).

GEMM models of NSCLC have mostly focused on *KRAS* mutant LAC. The first of this mouse models was developed in the laboratory of Tyler Jacks, who has notably contributed to the advance of this field. They generated mutant *Kras* alleles, designated *Kras*^{LA1} and *Kras*^{LA2}, which, upon spontaneous somatic recombination, activated the expression of the *Kras*^{G12D} oncogene (Johnson et al., 2001). These mice develop LAC with 100% incidence, as well as thymic lymphomas and papillomas with reduced prevalence, as *Kras*^{G12D} expression is not limited to the lung. Tumourigenesis was accelerated when the *Kras*^{LA1} mice were crossed into a strain carrying a germline *Tp53* deletion. More sophisticated models followed, allowing for temporal and spatial control of the oncogene expression. In fact, soon thereafter, a conditional *Kras*^{G12D} allele was developed by the same group, the *Kras* *LoxP-Stop-LoxP-G12D* (*Kras*^{LSL-G12D}) mouse strain (Jackson et al., 2001). In this strain, the endogenous *Kras* locus is

targeted with a LoxP-Stop-LoxP (LSL) cassette and therefore, endogenous levels of the oncogenic KRAS G12D protein are expressed after the excision of the Stop element. This is achieved by intranasal instillation of the adenoviral Cre recombinase (Ad-Cre), inducing lung-specific recombination. It is noteworthy that, since the LSL cassette prevents the expression of the mutant allele until the stop elements are removed, it creates a null version of the gene. Given that *Kras* deficient mice are embryonically lethal (Johnson et al., 1997), these mice can only be heterozygous for *Kras*^{LSL-G12D}.

Using the aforementioned Cre-LoxP system, Jacks and colleagues generated conditional knock-in mice that, in addition to the *Kras*^{LSL-G12D} allele, also harbour a *Tp53*^{FL} allele (*Kras*^{LSL-G12D/+}; *Tp53*^{FL/FL} mice, here referred to as KP^{null} mice) (Jackson et al., 2005; DuPage et al., 2009). In these mice, the endogenous *Tp53* exons 2 to 10 are flanked by two LoxP sites that are deleted after Cre-mediated recombination, abolishing p53 function (Jonkers et al., 2001). Before the recombination, however, the *Tp53* locus is maintained in its wildtype (wt) state and p53 activity is normal. In this model, p53 expression loss strongly promoted the progression of KRAS-induced LAC (Jackson et al., 2005; DuPage et al., 2009). In human lung tumours, however, *TP53* is rarely deleted. Instead, human LAC usually harbours *TP53* mutations at the arginine (R) of codon 175, which is substituted by histidine (H). Consequently, *Kras*^{LSL-G12D/+}; *Tp53*^{R172H/+} (KP) mice were generated (Jackson et al., 2005; Kasinski and Slack, 2012) (*Tp53*^{R172H} is the mouse orthologue of human *TP53*^{R175H} (Brosh and Rotter, 2009)). KP mice recapitulate many of the histopathological features of human LAC, including the adenoma to adenocarcinoma transition (Kasinski and Slack, 2012).

More recently, a dual recombinase system using the Cre and flippase (Flp) recombinases has been developed. By inserting Flp recognition target (FRT) sites instead of LoxP sites, the *Kras*^{FSF-G12D/+} strain was generated, in which *Kras*^{G12D} was expressed upon Flp recombination (Young et al., 2011). Similarly, *Tp53*^{FRT/FRT} mice have also been developed (Lee et al., 2012). By combining these two strains, it is possible to uncouple tumour induction, which is controlled in a time and tissue-specific manner by Flp recombination, from target inactivation or any other genetic manipulation, which can be manipulated at a different time and in a different tissue(s) via Cre-mediated recombination.

Although the GEMMs described above recapitulate most of the histologic features of human NSCLC, they display a more limited mutational complexity than the tumours they are intended to model. Comprehensive sequencing efforts over the last years have demonstrated the heterogeneous and clonal nature of human NSCLC (Alexandrov et al., 2013; de Bruin et al., 2014). In contrast, whole exome sequencing of LAC GEMMs revealed that they acquire few somatic mutations and thereby, they have a low mutational burden as compared to human cancers (Westcott et al., 2015; McFadden et al., 2016). Interestingly, carcinogen-induced mouse models have been shown to harbour a higher mutational landscape than GEMMs (Westcott et al., 2015). These discrepancies in tumour mutational burden between GEMMs and human cancer have important implications for the use of these mouse models for the testing of new therapeutics since the tumour mutation burden has been recently correlated with the efficacy of immunotherapy (Snyder et al., 2014; Rizvi et al., 2015; Hugo et al., 2016; Carbone et al., 2017). In accordance with their low mutational burden, NSCLC GEMMs have been shown to be poorly infiltrated with T cells and, consequently to be resistant to ICB (DuPage et al., 2011; Lastwika et al., 2016; Pfirschke et al., 2016; Akbay et al., 2017). Altogether, these studies highlight the need for novel mouse models that can more faithfully mimic the human disease.

1.4. Aims of the study

The TRAIL/TRAIL-R system has been the focus of many translational cancer research efforts in the last 20 years since the discovery that it can selectively kill tumour cells without affecting normal cells. Nevertheless, the success of TRAIL agonists in the clinic to date has been impeded by the inherent or acquired resistance to TRAIL-induced apoptosis of most cancer cells. In order to overcome this, it is crucial to identify new sensitising strategies that can break the resistance and render TRAIL-based therapies effective.

Previous work in our laboratory has demonstrated that CDK9 inhibition by SNS-032 synergises with TRAIL to induce apoptosis in a panel of NSCLC cell lines. Considering the advanced clinical status of the CDK9 inhibitor Dinaciclib, the goal of this work was to evaluate the therapeutic potential of the combination of TRAIL and Dinaciclib. Specifically, the aims of this thesis were:

1. To test if Dinaciclib sensitises cancer cells to TRAIL-induced apoptosis and determine the applicability of this combination to multiple cancer types.
2. To evaluate the preclinical efficacy of the combined TRAIL and Dinaciclib treatment in mouse models of NSCLC.
3. To investigate the impact of the TRAIL- and Dinaciclib-comprising therapy on the immune microenvironment.
4. To identify the mechanism by which Dinaciclib breaks the resistance to TRAIL-induced apoptosis.

Furthermore, given the lack of mouse models that can faithfully recapitulate the tumour mutational burden observed in human NSCLC, the last aim of this study was:

5. To develop novel NSCLC mouse models that can mimic the immunogenicity of the human disease.

2. MATERIALS AND METHODS

2.1. Materials

2.1.1. Chemicals and reagents

All reagents were purchased from the following companies unless stated otherwise: Abcam, Biovision, Merck, Invitrogen, Pierce, R&D systems, Roche, Roth and Sigma-Aldrich.

2.1.2. Buffers and solutions

Blocking buffer	2.5% milk powder (w/v) 0.05% Tween-20 in phosphate buffered saline (PBS)
Borax buffer	0.1% Borax (w/v) in H ₂ O
Coomassie staining solution	0.1% Coomassie (w/v) 40% methanol (v/v) 10% acetic acid (v/v)
Coomassie destaining solution	20% methanol (v/v) 10% acetic acid (v/v)
Crystal violet fixing solution	75% methanol (v/v) 25% acetic acid (v/v)
Crystal violet staining solution	0.5% crystal violet (v/v) 20% methanol
FACS buffer	5% fetal calf serum (FCS) (v/v) in PBS
Freezing medium (for cells)	90% FCS (v/v)

	10% dimethyl sulfoxide (DMSO) (v/v)
Genotyping lysis buffer	25 mM NaOH 0.2 mM ethylenediaminetetraacetic acid (EDTA)
Genotyping neutralising buffer	40 mM Tris HCl
Hydroxyapatite equilibration buffer (pH 7.4)	50 mM potassium phosphate buffer 100 mM NaCl 0.02% Tween-20 (v/v) 2 mM β -mercaptoethanol
Hydroxyapatite wash buffer (pH 7.4)	200 mM potassium phosphate buffer 100 mM NaCl 0.02% Tween-20 (v/v) 0.1% Triton X-114 2 mM β -mercaptoethanol
Hydroxyapatite elution buffer (pH 7.4)	400 mM potassium phosphate buffer 100 mM NaCl 0.02% Tween-20 (v/v) 2 mM β -mercaptoethanol
Immunofluorescence blocking buffer	0.2 % bovine serum albumin (BSA) (v/v) in PBS
Lysogeny broth (LB) media (pH 7.4)	10 g/l tryptone 10 g/l NaCl 5 g/l yeast extract
Lysis buffer (for mammalian cells)	30 mM Tris-Base (pH 7.4) 120 mM NaCl 2 mM EDTA 2 mM KCl

	10% Glycerol (v/v)
	1% Triton X-100 (v/v)
	cOmplete protease inhibitor cocktail
	phosphatase inhibitor cocktail
Lysis buffer (for bacteria) (pH 7.4)	50 mM potassium phosphate buffer
	200 mM NaCl
	100 mM KCl
	10% glycerol (v/v)
	0.5% Triton X-100 (v/v)
	70 μ M 4-(2-aminoethyl)benzenesulfonyl fluoride hydrochloride (AEBSF)
	5 μ M E-64
	1.2 μ g/ml aprotinin
	50 μ g/ml lysozyme
	5 U/ml benzonase
	2 mM dithiothreitol (DTT)
Nickel-nitrilotriacetic acid (Ni-NTA) equilibration buffer (pH 7.4)	50 mM Tris-HCl
	200 mM NaCl
	100 mM KCl
	10% glycerol (v/v)
	0.5% Triton X-100 (v/v)
	2 mM β -mercaptoethanol
Ni-NTA wash buffer (pH 7.4)	50 mM Tris-HCl
	200 mM NaCl
	100 mM KCl
	10% glycerol (v/v)
	0.5% Triton X-100 (v/v)
	0.1% Triton-X114 (v/v)
	2 mM β -mercaptoethanol
Ni-NTA elution buffer (pH 8)	20 mM Tris-HCl

	300 mM NaCl
	50 mM imidazole
	0.02% Tween-20 (v/v)
	2 mM β -mercaptoethanol
PBS (pH 7.4)	137 mM NaCl
	8.1 mM Na_2HPO_4
	2.7 mM KCl
	1.5 mM KH_2PO_4
PBS Tween (PBST)	PBS
	0.05% Tween-20 in PBS (v/v)
Ponceau S solution	0.1% Ponceau S (w/v)
	5% acetic acid (v/v)
Primary antibody solution	2.5% BSA (w/v)
	0.1% sodium azide (w/v) in PBST
Storage buffer (pH 7.4)	20 mM Tris-HCl
	100 mM NaCl
	0.5 M arginine
	0.005% Tween-20 (v/v)
	2 mM β -mercaptoethanol
Stripping buffer (pH 2.3)	50 mM glycine in H_2O
Tris/Glycine/ Sodium dodecyl sulfate (SDS) running buffer (pH 8.3)	25 mM Tris
	192 mM glycine
	0.1% SDS (w/v)

2.1.3. Biological agents

Iz-TRAIL	Previously produced in <i>E. coli</i> and purified in our laboratory.
Iz-mTRAIL	Produced and purified as explained in this thesis (section 2.3.6)

2.1.4. Specific inhibitors

AEBSF	Sigma-Aldrich
BAY-1143572	Active Biochem
Benzonase	Sigma-Aldrich
Carboplatin	R & D systems
Cisplatin	Selleckchem
cOmplete EDTA-free Protease Inhibitor Cocktail	Roche
Dabrafenib	Selleckchem
Dinaciclib (for <i>in vitro</i> use)	Selleckchem
Dinaciclib (for <i>in vivo</i> use)	Insight Biotechnology
E-64	Sigma-Aldrich
iBET151	ChemieTek
JQ1	Sigma-Aldrich
LDC000067	Selleckchem
Lysozyme	Sigma-Aldrich
Necrostatin-1s	Biovision
NVP-2	S. Lowe
Phosphatase Inhibitor Cocktail	Sigma-Aldrich
SNS-032	Selleckchem
Trametinib	Selleckchem
zVAD.FMK	R & D systems

2.1.5. Proteolysis targeting chimeras (PROTACs)

MZ1	Tocris
-----	--------

Thal-SNS-032

Tocris

2.1.6. Antibodies

Table 2.1: Unconjugated primary antibodies for Western Blot.

Antibody (clone)	Isotype	Manufacturer	Catalogue #
Bak	Rabbit	Cell Signaling	3814
Bax (D2E11)	Rabbit	Cell Signaling	5023
Bcl2 (C2)	Mouse IgG1	Santa Cruz	sc-7382
Bcl-XL (54H6)	Rabbit	Cell Signaling	2764
Bid	Rabbit	Cell Signaling	2002
Bid	Goat	R & D systems	AF860
BRD4	Rabbit	Bethyl Laboratories	A301-985A100
Caspase-3	Goat	R & D systems	AF605
Caspase-8 (C15)	Mouse IgG2b	Custom-made	-
Caspase-8 (5F7)	Mouse IgG2b	Enzo	ADI-AAM-118-E
Caspase-8 (IG12)	Rat	Enzo	ALX-804-447
Caspase-9 (5B4)	Mouse IgG1	MBL	M054-3
Caspase-10 (E35)	Rabbit	Epitomics	1035-1
CDK1	Rabbit	Cell Signaling	77055
CDK2 (78B2)	Rabbit	Cell Signaling	2546
CDK5 (1H3)	Mouse IgG1	Cell Signaling	12134
CDK7	Rabbit	Cell Signaling	2090
CDK9 (C12F7)	Rabbit	Cell Signaling	2316
cIAP1/2	Mouse IgG2a	R & D systems	MAB3400
Cleaved caspase-8 (Asp387)	Rabbit	Cell Signalling	9429
Caspase 3 cleaved (Asp175)	Rabbit	Cell Signalling	9661

FADD (A66-2)	Mouse IgG1	BD Bioscience	556402
FADD (G-4)	Mouse IgG2b	Santa Cruz	sc-271748
FLIP (Dave-2)	Rat	Adipogen	AG-20B-0005
FLIP (NF6)	Mouse IgG1	Custom-made	-
FLIP (7F10)	Mouse IgG1	Enzo	ALX-804-961-0100
MCL1 (D35A5)	Rabbit	Cell Signaling	5453
pSer2 RNA Pol II (H5)	Mouse IgM	Biologend	920204
PARP (C2-10)	mIgG1	BD Bioscience	556362
RNA Pol II RPB1 (8WG16)	mIgG2a	Biologend	664906
XIAP	Rabbit	Cell Signaling	2042
α -Tubulin (DM1A)	mIgG1	Sigma-Aldrich	T9026
β -Actin (AC-15)	mIgG1	Sigma-Aldrich	A1978

Table 2.2: Unconjugated primary antibodies for immunofluorescence.

Antibody	Isotype	Manufacturer	Catalogue #
CD45	Rat	BD Bioscience	550539

Table 2.3: Conjugated primary antibodies for flow cytometry.

Antibody	Fluorophore	Manufacturer	Catalogue #
CD11b	PerCP	Biologend	101230
CD11c	BV711	Biologend	117349
CD206	FITC	Biologend	141703
CD3	Percp/Cy5.5	Biologend	100328
CD4	BUV496	BD Bioscience	564667
CD45	Alexa Fluor 700	Biologend	103128

CD8	PE/Cy7	Biolegend	100722
F4/80	BV786	Biolegend	123141
Foxp3	AF700	eBioscience	56-5773-82
GR-1	PE-Cy7	Biolegend	108416
Ki-67	FITC	BD Bioscience	556026
Ly6C	BV450	BD Bioscience	560594
Mouse CD262 (mTRAIL-R)	PE	BD Bioscience	12-5883-81
Mouse CD326 (EpCAM)	PE	BD Bioscience	12-5791-82
Mouse IgG1 isotype control	PE	Biolegend	400139
NKp46	BV421	Biolegend	137611

Table 2.4: Conjugated secondary antibodies.

Antibody	Manufacturer
Donkey-anti-goat-IgG- horseradish peroxidase (HRP)	Southern Biotech
Goat-anti-mIgG1-HRP	Southern Biotech
Goat-anti-mIgG2a-HRP	Southern Biotech
Goat-anti-mIgG2b-HRP	Southern Biotech
Goat-anti-mouse-IgM-HRP	Southern Biotech
Goat-anti-rabbit-IgG-HRP	Southern Biotech
Goat-anti-rat-IgG-HRP	Southern Biotech
Alexa Fluor 594 goat anti-rat IgG	Invitrogen

2.1.7. Cell culture media and supplements

DMEM/F-12

Thermo Fisher Scientific

Doxycycline	Sigma-Aldrich
Dulbecco's phosphate-buffered saline (DPBS)	Invitrogen
Dulbecco's Modified Eagle Medium (DMEM)	Invitrogen
FCS	Sigma-Aldrich
Glutamine	Invitrogen
Iscove's Modified Dulbecco's Medium	Thermo Fisher Scientific
PBS	Invitrogen
Penicillin/Streptomycin	Invitrogen
Roswell Park Memorial Institute medium (RPMI) 1640	Invitrogen
Sodium Pyruvate	Invitrogen
Trypsin/EDTA	Invitrogen

2.1.8. Cell lines

Table 2.5: Cell lines.

Name	Species	Cancer type	Culture Medium	Provider
4T1	Mouse	Breast	RPMI	ATCC
A375	Human	Melanoma	RPMI	Prof. D. Kulms
A549-luc	Human	NSCLC	RPMI	ATCC
B16 WT	Mouse	Melanoma	DMEM	Prof. S. Quezada
Calu-1	Human	NSCLC	RPMI	Prof. J. Downward
Colo 357	Human	Colorectal	RPMI	Prof. A. Trauzold
H320	Human	NSCLC	RPMI	Prof. J. Downward
H322	Human	NSCLC	RPMI	Prof. J. Downward
H460	Human	NSCLC	RPMI	Prof. J. Downward
HCT-116	Human	Colorectal	DMEM	Prof. B. Vogelstein
HeLa	Human	Cervical	RPMI	

Hep3B	Human	Liver	DMEM	
IGR-37	Human	Melanoma	RPMI	Prof. D. Kulms
JHH4	Human	Liver	DMEM	
KP394T4	Mouse	NSCLC	RPMI	Prof. T. Jacks
KP59	Mouse	NSCLC	RPMI	Produced in-house
KP802T4	Mouse	NSCLC	RPMI	Prof. T. Jacks
KPC1	Mouse	NSCLC	RPMI	Produced in-house
KPC2	Mouse	NSCLC	RPMI	Produced in-house
KPC3	Mouse	NSCLC	RPMI	Produced in-house
KPC4	Mouse	NSCLC	RPMI	Produced in-house
KPV1	Mouse	NSCLC	RPMI	Produced in-house
KPV2	Mouse	NSCLC	RPMI	Produced in-house
KPV3	Mouse	NSCLC	RPMI	Produced in-house
KPV4	Mouse	NSCLC	RPMI	Produced in-house
Malme3M	Human	Melanoma	RPMI	Prof. D. Kulms
MDA-MB-231	Human	Breast (TNBC)	DMEM	
Panc-89	Human	Pancreatic	RPMI	Prof. A. Trauzold
PCC8	Mouse	NSCLC	RPMI	Prof. S. Lowe
PEA2	Human	Ovarian	RPMI	
RP250.3	Mouse	SCLC	RPMI	Prof. C. Reinhardt
RP252.7	Mouse	SCLC	RPMI	Prof. C. Reinhardt
RP280.1	Mouse	SCLC	RPMI	Prof. C. Reinhardt
Skmel147	Human	Melanoma	RPMI	Prof. D. Kulms
Skmel2	Human	Melanoma	RPMI	Prof. D. Kulms
VMC12	Human	Mesothelioma	RPMI	Dr. B. Hegedus
VMC40	Human	Mesothelioma	RPMI	Dr. B. Hegedus
VMC45	Human	Mesothelioma	RPMI	Dr. B. Hegedus
VMC6	Human	Mesothelioma	RPMI	Dr. B. Hegedus
WM3248	Human	Melanoma	RPMI	Prof. D. Kulms

2.1.9. Ready-to-use kits and solutions

BCA protein assay	Thermo Fisher Scientific
Chemoluminescent Substrate SuperSignal West Femto	Thermo Fisher Scientific
DharmaFECT .1 Transfection Reagent	Dharmacon
E.Z.N.A. Plasmid Maxi Kit	OMEGA bio-tek
E.Z.N.A. Plasmid Mini Kit I	OMEGA bio-tek
Western Lightning Plus-ECL	PerkinElmer
GenElute Mammalian Genomic DNA Miniprep Kit	Sigma-Aldrich
Lipofectamine 2000	Invitrogen
NuPAGE lithium dodecyl sulfate (LDS) Sample Buffer	Thermo Fisher Scientific
Luciferin (<i>in vivo</i>)	Caliper Life Science
MinElute PCR Purification Kit	Qiagen
Opti-MEM	Invitrogen
Pierce LAL Chromogenic Endotoxin Quantitation Kit	Thermo Fisher Scientific
Popidium Iodide	Sigma-Aldrich
QIAquick Gel Extraction Kit	Qiagen
SeeBlue Plus2 Pre-Stained Standards	Invitrogen
SOC medium	Thermo Fisher Scientific
SYBR Safe DNA gel stain	Invitrogen
SYTOX Green nucleic acid stain	Thermo Fisher Scientific
TrypanBlue	Serva

2.1.10. Consumables

4–15% Criterion TG Midi Gels	Sigma-Aldrich
4–15% Mini-PROTEAN TG Gels	Sigma-Aldrich
50 ml Reagent Reservoir	Corning
Cell Culture Petri dishes	TPP

Cell Culture Test Plates (6-, 12-, 24-well)	TPP
Cell Sieve (40 and 70 µm pore size)	Becton Dickinson
Conical tubes (15 ml and 50 ml)	TPP
Cryogenic vials	Nunc
Dialysis membrane	KMF
DNA purification columns	Syd labs
Glassware	Schott
Microtainer tube	BD Biosciences
PCR Tubes	StarLab
Pipette tips (0.1-10, 1-200, 100-1000 µl)	StarLab
Plastic pipettes (5 ml, 10 ml and 15 ml)	Becton Dickinson
Polypropylene round bottom tube (5 ml)	Becton Dickinson
Reflotron ALT test strip	Roche
Round and flat bottom 96-well test plates	TPP
Safe-Lock Reaction Tubes (1,5 ml, 2 ml)	Eppendorf
Single-Use Needles	Becton Dickinson
Single-Use Scalpel	Feather
Single-Use Syringe (1 ml, 2 ml)	Becton Dickinson
Single-Use Syringe (5 ml, 30 ml, 50 ml)	Terumo
SmartLadder DNA Standards	Eurogentec
Sterile filter (0.22 µm)	Millipore
Tissue Culture flasks (25, 75, 150 cm ²)	TPP
Trans-Blot Turbo Mini and Midi Nitrocellulose	Bio-Rad
Transfer Packs	
Vivaspin Concentrator MWCO 5000	Sartorius
X-Ray film 18 x 24 cm	Scientific laboratory supplies

2.1.11. Instruments

Accuri C6	BD Biosciences
Äkta Prime	GE Healthcare
Avanti J-26S XPI Centrifuge	Beckman Coulter
Blotting system	Bio-Rad

Class II Biological Safety Cabinet	Esco
Countless II Automated Cell Counter	Thermo Fisher Scientific
Dark Reader DR46B Transilluminator	Clare Chemical Research
FACS Aria Fusion Sorter	BD Biosciences
FORTESSA X-20	BD Biosciences
FACSymphony	BD Biosciences
Freezer -20° C	Liebherr
Freezer -80° C	Forma Scientific
GBox	Syngene
Ice machine	Scotsman
Incubator Stericult 2000	Forma Scientific
IncuCyte FLR	Essen Bioscience
Ivis Spectrum	Caliper Life Science
Light Microscope	Zeiss
Mastercycler pro PCR machine	Eppendorf
Microwave	AEG
Mithras LB 940	Berthold Technologies
Multichannel pipettes	Micronic Systems
Multifuge 3S-R	Heraeus
Multiskan Ascent	Thermo Labsystems
NanoDrop Spectrophotometer ND-1000	NanoDrop Technologies
pH Meter	Mettler
Pipetboy	Integra Bioscience
Pipettes (10 µl, 100 µl, 200 µl, 1 ml)	Gilson
Power Supply for agarose gels	Biorad
Reflovet Analyzer	Roche
Scanner (CanoScan LiDE 110)	Canon
SRX-101A Tabletop Film Processor	Konica Minolta
Table Centrifuge Biofuge	Heraeus
Thermomixer compact	Eppendorf
Trans-Blot Turbo Transfer System	Bio-Rad
Vortex	Heidolph

2.1.12. Software

Adobe Photoshop CC	Adobe
ApE	Wayne Davis (University of Utah)
Ascent Software Version 2.6	Thermo LabSystems
CanoScan	Canon
EndNote	Thomson Reuters
FACSDiva	BD Biosciences
FlowJo 7.6.5	TriStar
GaphPad Prism 6	GaphPad
IncuCyte Software	Essen Bioscience
Ivis Spectrum Software	Caliper Life Science
Microsoft Excel 2010	Microsoft
Microsoft Powerpoint 2010	Microsoft
Microsoft Word 2010	Microsoft
MikroWin 2000	Berthold Technologies
SnapGene	GSL Biotech

2.2. Methods in cell biology

2.2.1. Cell culturing

All cell lines used in this thesis were adherent and cultured in a 5% CO₂-humidified atmosphere at 37° C. Cells were cultured in the medium indicated in Table 2.5, supplemented with 10% FCS and 1% penicillin-streptomycin, except for the melanoma cell lines, which were cultured in the absence of antibiotics. Cells were passaged before reaching confluence. To do so, cells were washed with PBS and detached using 1 x trypsin/ EDTA solution and diluted either 1/10 or 1/15 depending on the cell line's growth rate. For seeding, cell numbers were determined using the Countless II Automated Cell Counter.

2.2.2. Generation of cell lines from lung tumours

Tumour-bearing KP mice were euthanized when they reached their humane endpoint. Lungs were extracted in sterile conditions inside a tissue culture hood and washed in a Petri dish with PBS. Depending on the size of the tumours, the whole lung was taken or only the tumour was removed. The selected portion of the lung was placed in 1 ml of RPMI medium in a Petri dish and cut in 2-3 mm pieces using scalpels. Subsequently, the tissue was homogenised using the flat surface of a 5 ml syringe and re-suspended in a final volume of 3 ml of medium. The homogenate was then passed through a 40 µm strainer and centrifuged at 1500 rpm for 3 min. The cell pellet was subsequently re-suspended in RPMI medium supplemented with 10% FCS, 50 units/ml penicillin and 50 µg/ml streptomycin and transferred into a T-25 or a T-75 flask. The following day, the medium was replaced to wash the dead cells. After two passages, cells were stained for epithelial cell adhesion molecule (EpCAM), which is a marker of epithelial cells, as explained in section 2.2.9. EpCAM-positive cells, containing the tumour cells, were sorted using the FACS Aria Fusion (BD Bioscience).

2.2.3. Freezing and thawing of cell lines

For freezing, cells were harvested by trypsinisation, centrifuged at 1500 rpm for 3 min and re-suspended at $1-2 \times 10^6$ cells/ml in freezing medium containing DMSO to prevent the formation of crystals during the thawing process. The cell suspension was then transferred to cryogenic vials and placed at -80°C for short term storage. 24-48 h later, frozen cells were transferred to liquid nitrogen (-196°C) for long-term storage.

Thawing of frozen cells was achieved by suspending them in 10 ml of pre-warmed medium. In order to remove residual DMSO, cells were spun down at 1500 rpm for 3 min and re-suspended in fresh medium before being transferred to a T-75 culture flask containing the appropriate medium.

2.2.4. siRNA-mediated knockdown

Transient knockdown of protein expression was achieved by reverse transfection of cells with siRNA smart-pools purchased from Thermo Scientific. Dharmafect (Dharmacon) was used as transfection reagent. Briefly, 1.5 μ l Dharmafect and 200 μ l FCS-free RPMI were mixed per condition and incubated 5 min at room temperature (RT). Subsequently, 2.2 μ l of siRNA (from a previously prepared 20 μ M stock) were added to 200 μ l of transfection mix, mixed and incubated for further 30 min at RT. After this time, 200 μ l of the siRNA containing mix were mixed with 1.5×10^5 cells. From those cells mixed with the siRNA, 7×10^3 cells were seeded into a 96-well plate for a viability assay, which were then incubated for 24 or 48 h before treating them with different inhibitors and/or TRAIL and assessing their viability.

The rest of the cells mixed with siRNA were seeded in a 6-well plate were incubated for 48 h, after which the efficiency of the knockdown was assessed by Western Blotting.

2.2.5. Generation of knockout cells

CDK9 and BRD4 knockout (KO) cells were generated *via* clustered regularly interspaced short palindromic repeats (CRISPR)/Cas9 technology. Single guide RNAs (sgRNAs) were designed using the CHOPCHOP online design tool (<https://chopchop.cbu.uib.no/>) (Table 2.6) and ligated into the transient expression CRISPR vector pSpCas9(BB)-2A-mCherry, which is a version of the PX458 vector (Addgene) (Ran et al., 2013) modified by Dr. Peter Draber. Cells were seeded at 60% confluency in 10 cm dishes and transfected the following day with 15 μ g of the sgRNA-containing plasmid using Lipofectamine 2000 (Invitrogen) and Opti-MEM (Invitrogen). 48 h later, transfected cells were selected for mCherry positivity and single cell sorted into 96-well plates using the FACS Aria Fusion (BD Bioscience). Sorted cells were cultured with medium containing 50% conditioned medium from the parental cells for 3-4 weeks until single cell colonies were detected. These clones were expanded and the loss of expression of the target protein was validated by Western Blot and sequencing.

Table 2.6: CRISPR sgRNA sequence.

Target	Sequence
Mouse <i>Brd4</i>	5'-GGCCTGCGTTGTAGACATTT
Mouse <i>Cdk9</i>	5'-GGCCCGCCCATTGACCTTTG

2.2.6. Cell viability assay (CellTiter-Glo)

Cell viability was assessed using the CellTiter-Glo Luminescent Cell Viability Assay kit (Promega) following the manufacturer's instructions. This method enables the measurement of viable cells by quantifying the ATP present in them, as a representation of metabolically active cells. For this purpose, $1-2 \times 10^4$ cells/well were seeded in advance in 96-well plates. The following day, cells were treated appropriately and 24 or 48 h later, cell viability was tested. Briefly, 100 μ l CellTiter-Glo reagent diluted 1:5 in PBS was added to the each well after the removal of the treatment-containing medium. After 10 min of incubation at RT in the dark, 80 μ l were transferred to a whitewall plate to enhance measurement of luminescence. The absolute bioluminescence was measured using the Mithras (Berthold Technologies) plate reader. The percentage viability was then calculated as relative to the untreated control.

2.2.7. Cell death assay by SYTOX Green staining

SYTOX Green stains nucleic acids and can penetrate cells with a compromised plasma membrane but does not cross the plasma membrane of live cells. Thus, it serves as a marker for dead cells. For this assay, cells were seeded at $2-4 \times 10^5$ cells/well, depending on the cell line, in 12-well plates. The following day, they were treated with the appropriate inhibitors and/or TRAIL and SYTOX Green (Thermo Fisher Scientific) was added to the medium in a dilution of 1:10,000 (to achieve a final concentration of 0.5 μ M). Dead cells were detected by time-lapse live imaging in the IncuCyte FLR (Essen Bioscience). Pictures were collected every 2 h and the fluorescent objects per well at each time point were quantified by the IncuCyte

software. The percentage death per condition was normalised to the one in which maximum dead was achieved.

2.2.8. Clonogenic assay

Clonogenic assays were performed to assess long-term survival. Cells were seeded into 6-well plates at a density of $1-2 \times 10^5$ cells/well and treated the following day with the appropriate inhibitors and/or TRAIL. 24 h after the treatment, dead cells were washed away and surviving cells were cultured for additional 7 days in fresh medium without any treatment. Subsequently, cells were washed with PBS, fixed with crystal violet fixing solution and subsequently stained with crystal violet staining solution. The plates were then thoroughly washed with water and dried overnight before taking pictures.

2.2.9. Surface staining by fluorescent-associated cell sorting (FACS)

In order to assess the surface expression of EpCAM or m-TRAIL-R in murine cell lines obtained from lung tumours, flow cytometry was employed. After trypsinisation, 10^6 cells per sample were washed twice with PBS to remove the medium and incubated with 10 µg/ml antibody against EpCAM, m-TRAIL-R or the appropriate isotype control in 100 µl of PBS for 30 min at 4° C in the dark. Cells were then washed twice with FACS buffer and re-suspended in 300 µl of FACS buffer before being analysed using the Accuri C6 cytometer (BD Bioscience). An unstained sample was used as a control.

2.3 Methods in biochemistry

2.3.1. Preparation of cell lysates

Cells previously seeded and treated in 6-well plates were washed twice with cold PBS and the plates were stored at -20° C with 80-100 µl lysis buffer per well containing 1 x cComplete protease inhibitor (Roche) and 1 x phosphatase inhibitor cocktail (Sigma-Aldrich). Following thawing of the plates on ice, cells were scraped in lysis buffer and

the cell suspension was incubated on ice for 20 min. Subsequently, the cell suspension was centrifuged for 30 min at 13×10^3 rpm at 4° C and the cleared supernatants were transferred into a new tube.

In order to determine the protein concentration in the lysates, the colorimetric bicinchoninic acid (BCA)-containing protein assay (Thermo Fisher Scientific) was employed. In brief, 2 µl of lysate were incubated with 100 µl of BCA solution, containing 49 parts of component A and 1 part of component B, at 37° C for 30 min. After this time, a violet colour was clearly visible in all samples and absorbance at 560 nm was measured using a Multiskan Ascent plate reader (Thermo LabSystems). Lysates were then equilibrated to the least concentrated sample.

2.3.2. SDS polyacrylamide gel electrophoresis (SDS-PAGE)

Lysates were mixed with NuPAGE LDS Sample Buffer (Thermo Fisher Scientific) containing 50 mM DTT (Roche) and heated at 92 °C for 10 min. Separation of proteins according to their size was achieved by SDS-PAGE using pre-cast 4–15% Mini-PROTEAN TGX (up to 15 samples) or Criterion TGX Midi (up to 26 samples) gels (both from Sigma-Aldrich) and Tris/Glycine/SDS running buffer (Bio-Rad). As a molecular weight standard, SeeBlue Plus2 Pre-Stained marker Buffer (Thermo Fisher Scientific) was used. The electrophoretic separation was achieved by applying a constant voltage of 80 V for 10 min and subsequently 180 V for 30-40 min.

2.3.3. Coomassie staining of SDS-PAGE gels

Proteins separated by SDS-PAGE were visualised by incubating the gel in Coomassie staining solution for 1 h and then in Coomassie destaining solution overnight at RT.

2.3.4. Western Blotting

The transfer of proteins to a membrane allows their detection with specific antibodies. For this purpose, a pre-packed 0.2 µM nitrocellulose membrane assembly (Trans-Blot Turbo Mini or Midi Nitrocellulose Transfer Packs, Bio-Rad) was used. The setup

was composed of a layer of filter papers at the anode of the apparatus, on top a nitrocellulose membrane, the gel and lastly another layer of filter papers. Protein transfer was carried out at a constant 20 V for 7 or 10 min. After transfer completion, membranes were stained with Ponceau S solution to confirm successful protein transfer, washed with PBST and blocked with blocking buffer for 1 h at RT. Subsequently, membranes were subjected to immunoprobings with primary antibody overnight at 4° C. Next day, membranes were washed three times with PBST for 10 min and incubated with the respective HRP-conjugated antibody for at least 1 h at RT. Membranes were then washed at least three times with PBST and antibody binding was visualised using Western Lightning Plus-Enhanced Chemiluminescence Substrate (ECL) (PerkinElmer) and X-ray films (Scientific laboratory supplies).

2.3.5. Stripping of Western Blot membranes

In order to re-blot with a different antibody, the membranes were incubated with stripping buffer for 15 min at RT to remove previous primary and secondary antibodies. The low pH of the stripping buffer alters protein conformation, resulting in the release of antibody/antigen-binding. Subsequently, membranes were washed three times with PBST and incubated with blocking buffer for 30 min at RT before adding a new primary antibody as described in section 2.3.4.

2.3.6. Production of recombinant izmTRAIL

Murine isoleucine zipper TRAIL (izmTRAIL) was produced in the Rosetta strain of *E.coli* and purified using a two-step affinity purification system with the Äkta Prime (GE Healthcare). In brief, bacteria were transformed with the izmTRAIL-encoding plasmid and they were grown in LB medium containing 30 µg/ml kanamycin (Roth). IzmTRAIL expression was induced by the addition of 1 mM isopropyl β-D-1-thiogalactopyranoside (IPTG) (Sigma-Aldrich) and incubation overnight at 18° C. The following day, the cultures were centrifuged at 4600 rpm for 30 min at 4° C and the bacteria pellets were lysed in lysis buffer (50 ml of lysis buffer per litre of bacteria culture). Following re-suspension of the bacteria pellets in lysis buffer, lysates were sonicated and ultra-centrifuged at $15 \times 10^3 \times g$ for 30 min at 4° C. Cleared supernatants were then passed through a 0.22 µm filter and applied to a pre-

equilibrated hydroxyapatite column (GE Healthcare). The column was washed with hydroxyapatite wash buffer and then the soluble protein was eluted with hydroxyapatite elution buffer. Subsequently, the eluted protein was applied into a pre-equilibrated Ni-NTA column (GE Healthcare). The column was then washed with Ni-NTA wash buffer and eluted with Ni-NTA elution buffer containing 50 mM imidazole. The eluted protein was dialyzed against storage buffer and the concentration was measured using NanoDrop Spectrophotometer ND-1000 (NanoDrop Technologies). Protein concentration was achieved using Vivaspin concentrator MWCO 5000 (Sartorius) until a final concentration of 2-3 mg/ml was reached. The absence of Lipopolysaccharide (LPS) was confirmed using the Pierce *Limulus amoebocyte lysate* (LAL) Chromogenic Endotoxin Quantitation Kit (Thermo Fisher Scientific) and the aliquots were stored at -80° C.

2.4. Methods in molecular biology

2.4.1. DNA digestion and restriction

Sequence-specific cleavage of vector or insert DNA for cloning purposes was achieved using FastDigest restriction endonucleases (Thermo Fisher Scientific). The reaction was prepared as explained in Table 2.7 and incubated at 37° C for 1 h.

Table 2.7: DNA restriction set-up.

Reagent	Vector restriction (volume)	Insert restriction (volume)
DNA	3 µl	10 µl
Buffer green	3 µl	3 µl
Enzyme (s)	1 µl	1 µl
Fast AP	1 µl	-
ddH ₂ O	Until a total of 30 µl	Until a total of 30 µl

2.4.2. DNA separation using agarose electrophoresis and purification

Analysis of restricted vector DNA or DNA fragments was performed by separation *via* agarose gel electrophoresis. Depending on the expected fragment sizes, gels with 0.5 – 2% agarose were prepared in borax buffer containing SYBR Safe DNA gel stain (Invitrogen) (1: 10,000) and poured in gel casting trays (Bio-Rad). After polymerisation, samples were loaded in gel pockets and electrophoresis was carried out in borax buffer. DNA was visualised employing the Dark Reader DR46B Transilluminator (Clare Chemical Research). After separation, the DNA fragment-containing piece of gel was excised with a scalpel and DNA was recovered using the QIAquick Gel Extraction Kit (Qiagen) according to the manufacturer's instructions. DNA was purified using the provided spin columns and eluted in ddH₂O

2.4.3. DNA fragment ligation

Linearized vectors and DNA fragments with compatible overhangs or blunt ends were ligated using T4 DNA ligase (Thermo Fisher Scientific). The insertion of DNA fragments originating from PCR reactions or DNA restriction in vectors was performed in a ratio of 4:1 (insert:vector). The ligation reaction contained 1 µl T4 DNA ligase, 1 µl T4 ligase buffer (Thermo Fisher Scientific), the vector and fragment DNA solutions and ddH₂O until a total volume of 10 µl. The ligation reaction was incubated overnight at RT.

2.4.4. Transformation of competent *E.coli* bacteria

For plasmid DNA expression in bacteria, different strains of chemically-competent *E.coli* were used depending on the purpose: DG1 *E.coli* (Eurogentec) for propagation of plasmid DNA and BL21 (DE3) *E.coli* (New England Biolabs) for protein expression. For transformation, 25 µl of competent bacteria were mixed with 2 µl (approximately 10 ng) of plasmid DNA and incubated on ice for 20 min. In order to enhance plasmid uptake, reaction tubes containing the bacteria were exposed to a heat-shock in a water bath set at 42° C for 90 s and then incubated on ice for 1 min. Subsequently, 200 µl of Super Optimal broth with Catabolite repression (SOC medium) (Thermo Fisher Scientific) were added and bacteria were allowed to grow at 37° C with gentle

agitation for at least 1 h before plating them on LB agar plates containing the antibiotic to which the plasmid provided resistance. Plates were incubated at 37° C overnight and the following day individual colonies were picked and incubated in LB medium for further amplification.

2.4.5. Isolation of plasmid DNA

Positively transformed selected bacteria colonies were individually grown in 5 ml LB medium containing the appropriate antibiotic overnight at 37° C and then cultures were collected and pelleted by centrifugation at 4600 rpm for 15 min. Subsequently, plasmid DNA was isolated using the E.Z.N.A. Plasmid Mini Kit I (OMEGA bio-tek) according to the manufacturer's instruction. In this way, approximately 30 µg of plasmid DNA were eluted in water.

In cases where more plasmid DNA yield was required, the 5 ml bacteria cultures were transferred into 300 ml of LB medium containing the appropriate antibiotic and incubated overnight at 37° C. Cells were then centrifuged at 4600 rpm for 30 min at 4° C and DNA was purified using the E.Z.N.A. Plasmid Maxi Kit I (OMEGA bio-tek) according to the manufacturer's instructions.

2.4.6. Isolation of genomic DNA

Genomic DNA from cultured cells was isolated using GenElute Mammalian Genomic DNA Miniprep Kit (Sigma-Aldrich), according to the manufacturer's instructions. For this purpose, 2×10^6 cells were trypsinised as explained above, centrifuged at 1500 rpm for 3 min, and washed twice with PBS before re-suspending them in the re-suspension solution provided in the kit.

2.4.7. Polymerase chain reaction (PCR)

PCR amplifications for cloning purposes were set up using the Phusion High-Fidelity DNA Polymerase (New England Biolabs). Reactions were set up as described in Table 2.8 and placed in a Mastercycler pro PCR machine (Eppendorf).

Table 2.8: PCR reaction set-up.

Reagent	Volume
5X Phusion HF Buffer	10 μ l
ddH ₂ O	31 μ l
dNTPs	1 μ l
DMSO	1.5 μ l
Forward primer (10 μ M)	2.5 μ l
Reverse primer (10 μ M)	2.5 μ l
Phusion DNA polymerase	0.5 μ l
Template DNA (~ 250 ng/ μ l)	1 μ l

The standard thermocycling conditions are shown in Table 2.9. The final product was either separated in an agarose gel as described in section 2.4.2 or directly purified using the MinElute PCR Purification Kit (Qiagen) following the manufacturer's instructions.

Table 2.9: PCR cycling parameters.

Step	Number of cycles	Temperature	Duration
Initial denaturation	1	98° C	30 s
Denaturation	31	98° C	10 s
Annealing	31	60-72° C	15 s
Elongation	31	72° C	1 min
Final elongation	1	72° C	5 min

2.5. Animal studies

All animal experiments were conducted under an appropriate UK project license in accordance with the regulations of UK home office for animal welfare according to ASPA (animal (scientific procedure) Act 1986).

2.5.1. Mouse models

2.5.1.1. Transplantable tumours

Female C57BL/6 mice were purchased from Charles River UK. *Rag1*^{-/-} mice were kindly provided by Prof. Caetano Reis e Sousa. The experiment was started when the mice were 6-8 weeks old. Mice were shaved a small area in their right flank the day before the injection of the cells. KP802T4 or KP59 cells were washed with DPBS, trypsinised and counted. Cells were then washed in DPBS and diluted to a concentration of 2.5×10^6 cells/ml for KP802T4 cells and 1.5×10^6 cells/ml for KP59 cells. Mice were injected with 5×10^5 KP802T4 cells or 3×10^5 KP59 cells in 100 μ l of DPBS intradermally in the right flank using 27 gauge needles and 1 ml syringes. Seven days after tumour injection, tumours were palpable and they were measured using a caliper. Tumour volume was calculated using the following formula: volume = (width² x length) / 2. Tumours were measured every 2-3 days throughout the experiment.

2.5.1.2. Orthotopic A549 xenograft lung tumours

Female Fox Chase® severe combined immunodeficiency (SCID) Beige mice were purchased from Charles River UK and the experiment was started when they were 12 weeks old. A549-luc cells were washed with DPBS, trypsinised and counted. Cells were then washed 3 times in DPBS and diluted to a concentration of 10×10^6 cells/ml. Mice were warmed up to 37° C in a heating chamber prior to injection. Once tail veins were clearly visible, 2×10^6 cells were slowly injected into the lateral tail vein in 100 μ l DPBS using 27 gauge needles and 1 ml syringes.

2.5.1.3. Autochthonous lung tumours in the KP model

Kras^{LSL-G12D} and *Tp53*^{LSL-R172H} mice on C57BL/6 background were kindly provided by Prof. D. Tuveson. Lung tumours were initiated in 6-12 week old mix-gender *Kras*^{LSL-G12D/+}; *Tp53*^{LSL-R172H/+} (KP) mice as described previously (DuPage et al., 2009). The delivery of the Cre recombinase into the lungs was achieved using an adenoviral system (Ad-Cre). Mice were anaesthetised by the intraperitoneal (i.p.) injection of 60 mg/kg ketamine (Vetalar, Zoetis) and 0.3 mg/kg medetomidine (Dormitor, Orion Pharma). Mice were then intranasally instilled with 2.5×10^7 plaque-forming units (pfu) of Ad-Cre in 50 μ l. To recover from the anaesthesia, mice were placed in a 37° C heating chamber and injected i.p. with 1 mg/kg atipamezole (Antisedan, Orion Pharma).

2.5.2. Genotyping

KP mice were ear sampled at 2-3 weeks of age for genotyping. Ear samples were lysed in genotyping lysis buffer at 95° C for 45 min and subsequently neutralised with genotyping neutralising buffer. Samples were preserved at 4 °C until use. PCR mix was prepared with 5 μ l Prime master mix or Dream Taq and appropriate sets of primers:

<i>Kras</i> wt	GTCGACAAGCTCATGCGGG
<i>Kras</i> mutant (mut)	CCATGGCTTGAGTAAGTCTGC
<i>Kras</i> common	CGCAGACTGTAGAGCAGCG
<i>Tp53</i> wt	TTACACATCCAGCCTCTGTGG
<i>Tp53</i> mut	AGCTAGCCACCATGGCTTGAGTAAGTCTGCA
<i>Tp53</i> common	CTTGGAGACATAGCCACA CTG

PCR products were run in a 2% agarose gel at 180 V for 30 min. Gels were visualised with GBox (Syngene).

2.5.3. Treatment of mice

All therapeutic compounds were administered i.p. using 27 gauge needles and 1 ml syringes in doses of 200 μ l. IzTRAIL (previously produced by Dr. Antonella Montinaro and Dr. Silvia von Karstedt) was administered in 10% (2-Hydroxypropyl)- β -cyclodextrin (Sigma-Aldrich) at a dose of 2.5 mg/kg. IzmTRAIL (produced and purified during this thesis as explained in section 2.3.6) was administered in 10% (2-Hydroxypropyl)- β -cyclodextrin at a dose of 5 mg/kg. Dinaciclib (Insight Biotechnology) was stored in a 30 mg/ml stock in DMSO and then administered in 10% (2-Hydroxypropyl)- β -cyclodextrin at a dose of 15 mg/kg or 30 mg/kg depending on the experiment. Carboplatin was administered in 10% (2-Hydroxypropyl)- β -cyclodextrin at a dose of 25 mg/kg. Urethane (Sigma-Aldrich) was dissolved in DPBS and administered at a dose of 1 g/kg. Anti-NK1.1 antibody (clone PK136 from Bio X Cell) was prepared in DPBS to a dose of 200 μ g/mouse. All treatment solutions were syringe-filtered through 0.22 μ m.

2.5.4. *In vivo* bioluminescence imaging

All mice bearing A549 lung xenografts were imaged weekly for bioluminescence. D-luciferin (GoldBio) was dissolved in DPBS at a final concentration of 30 mg/ml and syringe filtered at 0,2 μ m. Prior to imaging, each mouse was anaesthetised by 4% isoflurane gas and received 100 μ l subcutaneous injection of 3 mg luciferin per 20 g mouse. To maintain anaesthesia, the isoflurane dose was reduced to 1,5 %. Bioluminescence images were acquired 10 min after luciferin injection using the IVIS Lumina® at 1 min exposure time (Caliper Life Science). Afterwards, mice recovered from anaesthesia in a 37° C heating chamber. Photons per second were quantified using the IVIS software.

2.5.5. Dissection and fixation of tissues for histology

For preparation of lung tissue sections, mice were euthanized when they reached the experimental endpoint. From each mouse, the upper lobe of the left lung was removed, fixed in 10% formalin (Sigma-Aldrich) overnight and then transferred to 70% ethanol.

2.6. *Ex vivo* studies

2.6.1. Histological examination and quantification of tumour burden

Paraffin embedding, cutting into 4 μm sections and haematoxylin and eosin (H&E)-staining was performed by the histological staining service of Ms. Lorraine Lawrence at the Imperial College London Research Histology Facility.

H&E stainings were pathologically examined, as part of a collaboration, by Dr. Mona A. El-Bahrawy (Imperial College London), who was blinded to the study. Tumour burden was quantified as percentage of tumour tissue in the lung.

2.6.2. Immunofluorescence

4 μm formalin-fixed paraffin-embedded lung sections were stained following standard protocols. Sections were boiled in Retrievalgen A (BD Biosciences) in the microwave for 10 min. Slides were blocked in immunofluorescence blocking buffer for 30 min followed by incubation with the primary antibody overnight at 4° C. Next, slides were incubated with the secondary antibody at RT for 1 h. Sections were counterstained with 4',6-diamidino-2-phenylindole (DAPI) (Roche). At least ten images (40x) per slide were acquired and blind quantification was performed using ImageJ Software on monochrome images as the percentage of cells positive for the specific staining in relation to the total number of DAPI-positive cells.

2.6.3. Immune cell profiling by FACS

To stain lung immune cell infiltrates, murine lungs were mechanically disrupted with the top of a syringe piston at 4° C. The cell suspension was filtered through a 70 μm cell strainer, washed with PBS and centrifuged at 1500 rpm for 5 min. The pellet was re-suspended in 5 ml red blood cell (RBC) lysis buffer (BioLegend) at RT and incubated for 5 min. The reaction was stopped by addition of 30 ml PBS followed by centrifugation. Cells were then labelled with fixable viability dye eFluor780 (eBioscience) for 30 min in the dark at RT, followed by addition of Fc block (BD Biosciences). Samples were then stained with the conjugated antibodies at 4 °C for

30 min. Intracellular staining was performed using an Intracellular Fixation and Permeabilization Buffer Set (eBioscience) according to the manufacturer's instructions. Fluorescence minus one (FMO) controls were used to distinguish between positively and negatively stained cells. Flow cytometric analysis was performed with a FORTESSA X-20 (BD) or FACSymphony (BD) flow cytometer. Flow cytometry reference beads (Cell Sorting Set-up Beads, UV laser, BD) were added to the samples before the analysis for quantification of infiltrating leukocytes in the lungs. For example the absolute number of CD45+ cells was calculated using the following formula: (number of beads added to each samples x count of CD45 cells/count of beads). Data analysis was conducted using FlowJo software.

2.6.4. Serum analysis

Blood was withdrawn from the submandibular vein using a lancet and collected into microtainer tubes with separation gels (BD Biosciences). Sampled blood was kept on ice and spun to isolate serum at 3000 rpm for 10 min. Isolated serum was diluted 1:10 in PBS and 30 μ L of the diluted serum were placed on a Reflotron GPT test strip (Roche) and the alanine aminotransferase (ALT) levels were determined in a Reflovet Analyzer (Roche).

2.7. Statistical analysis

Data were analysed with GraphPad Prism 6 software (GraphPad Software). Statistical analysis was performed using one-way ANOVA multiple comparisons followed by the Bonferroni post-test when comparing more than one experimental group or condition and unpaired t-test two tailed (Student's t test) when comparing only two conditions. Statistical significance in survival curves was determined using a log-rank test. A p value ≤ 0.05 was considered significant and indicated with one asterisk (*), $p \leq 0.01$ (**), $p \leq 0.001$ (***) and $p \leq 0.0001$ (****).

3. RESULTS

3.1. Characterisation of Dinaciclib as a potent sensitiser to TRAIL-induced apoptosis

TRAIL has the ability to induce apoptosis selectively in cancer cells (Ashkenazi et al., 1999; Walczak et al., 1999). However, most cancer cells are either intrinsically resistant or acquire resistance to TRAIL (Zhang and Fang, 2005; Lemke et al., 2014b; Tuthill et al., 2015). Therefore, there is an urgent need for novel sensitising therapeutics that can render the tumour cells TRAIL-sensitive. In light of previous work in the laboratory showing that CDK9 inhibition synergises with TRAIL to induce apoptosis (Lemke et al., 2014a), the therapeutic potential of the combination of TRAIL and the clinically most advanced CDK9 inhibitor, Dinaciclib, was evaluated.

3.1.1. Dinaciclib is a more potent sensitiser to TRAIL-induced cell death than SNS-032

In order to determine the ability of Dinaciclib to act as a TRAIL sensitiser, its efficacy was first compared with the previously reported CDK9 inhibitor SNS-032 (Lemke et al., 2014a). To do so, SNS-032 and Dinaciclib in combination with our highly active form of recombinant TRAIL, izTRAIL, were titrated in three different TRAIL-resistant cell lines: A549 and H322 NSCLC cells and Malme3M melanoma cells, which are derived from a metastatic lung site. Whereas only concentrations of 200-300 nM of SNS-032 were capable of a profound sensitisation of cells to TRAIL-induced cell death (Figure 3.1 A), Dinaciclib achieved maximal killing in combination with TRAIL at concentrations as low as 25 nM (Figure 3.1 B). This is interesting given that both SNS-032 and Dinaciclib have the same IC_{50} for CDK9, 4 nM (Table 1.2). Importantly, the concentration of either CDK9 inhibitor at which synergy with TRAIL was achieved correlated with the concentration at which the phosphorylation of Ser2 of RNA Pol II was inhibited (Figure 3.1 C). These results suggest that Dinaciclib inhibits CDK9 more potently than SNS-032 and consequently, it is a stronger sensitiser to TRAIL-induced cell death.

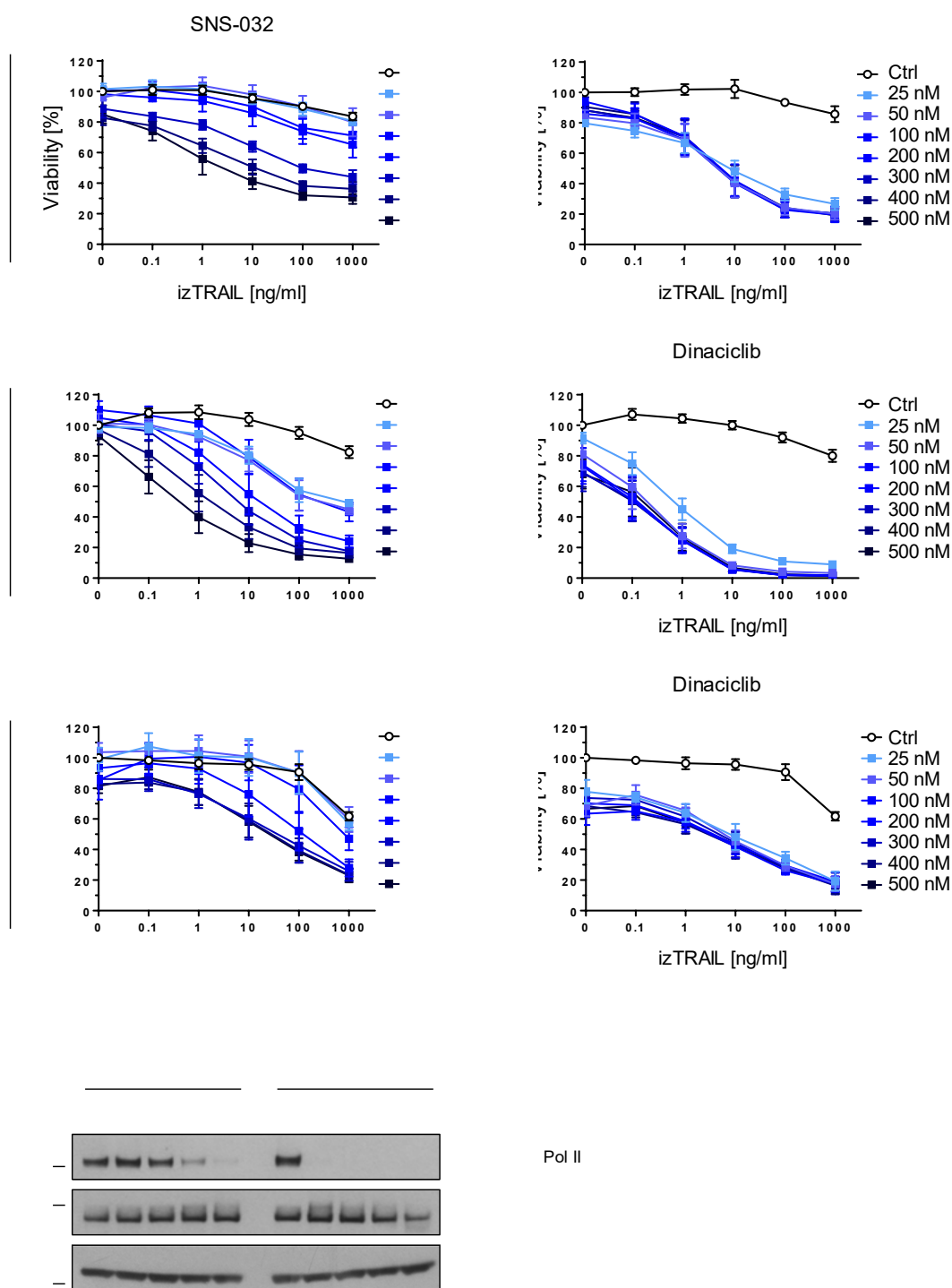


Figure 3.1: Dinaciclib is more efficient than SNS-032 in sensitising cancer cells to TRAIL-induced cell death.

(A-B) A549, Malme3M and H322 cells were pre-incubated with the indicated concentrations of SNS-032 (A) or Dinaciclib (B) for 15 min and subsequently treated with the indicated concentrations of izTRAIL. Cell viability was quantified 24 h later. Data represent means \pm SEM of at least three independent experiments. *(Figure legend continues on next page)*

(C) A549 cells were treated with SNS-032 or Dinaciclib at the indicated concentrations and 24 h later cells were lysed and analysed by Western blotting. Representative Western blots of two independent experiments are shown.

To corroborate these findings, the ability of the two CDK9 inhibitors to synergise with TRAIL to inhibit the long-term survival of cancer cells was compared side-by-side. In line with the previous results, SNS-032 only synergised with TRAIL to deplete the colony formation of all cell lines at 300 nM and not at 25 nM (Figure 3.2). On the contrary, Dinaciclib at 25 nM in combination with TRAIL completely inhibited the survival of clones. Interestingly, after treatment with Dinaciclib alone at 300 nM, no colonies were detected in any cell line and the addition of TRAIL had no effect.

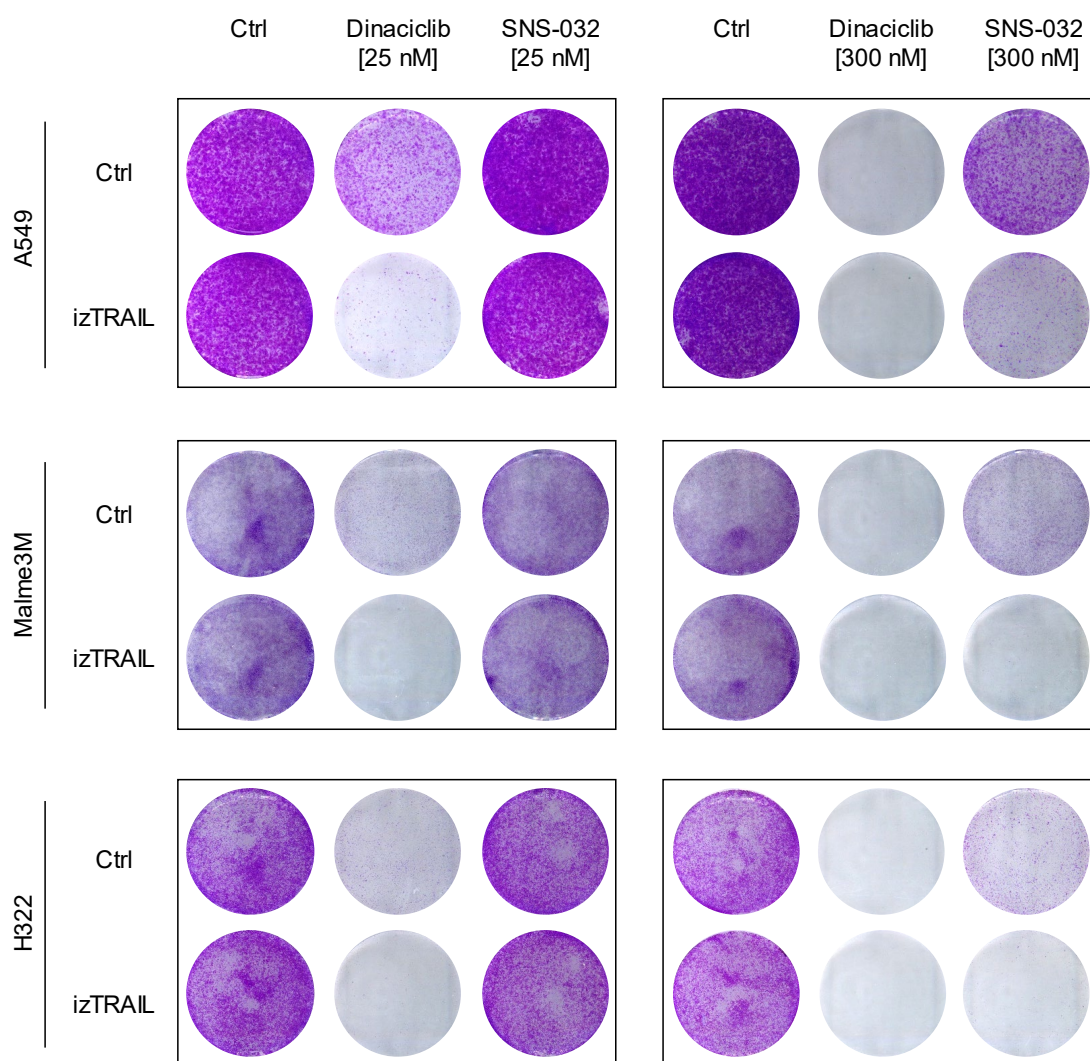


Figure 3.2: The combination of TRAIL and Dinaciclib inhibits the clonogenic survival of cancer cells more efficiently than the combination of TRAIL and SNS-032.

A549, Malme3M and H322 cells were treated with the indicated concentration of SNS-032 or Dinaciclib and subsequently treated with 10 ng/ml izTRAIL for 24 h. 7 days later, long-term survival was visualised by crystal violet staining. One of two independent experiments is shown.

Some years ago, work in our laboratory showed that CDK9 mediates TRAIL resistance by promoting concomitant transcription of FLIP and Mcl-1 (Lemke et al., 2014a). With the aim of testing whether Dinaciclib, as SNS-032, downregulates these two anti-apoptotic factors, a kinetic experiment was performed in A549 cells. As soon as 3 h after the treatment with Dinaciclib or SNS-032, the inhibition of the phosphorylation of Ser2 of RNA Pol II was observed, indicating that CDK9 inhibition was efficient from that time-point (Figure 3.3). As expected, while the majority of the

components of the DISC as well as the downstream pro- and anti-apoptotic factors remained unchanged, FLIP and Mcl-1 were suppressed by both CDK9 inhibitors.

In conclusion, these data show that Dinaciclib is a more potent inhibitor of CDK9 than SNS-032.

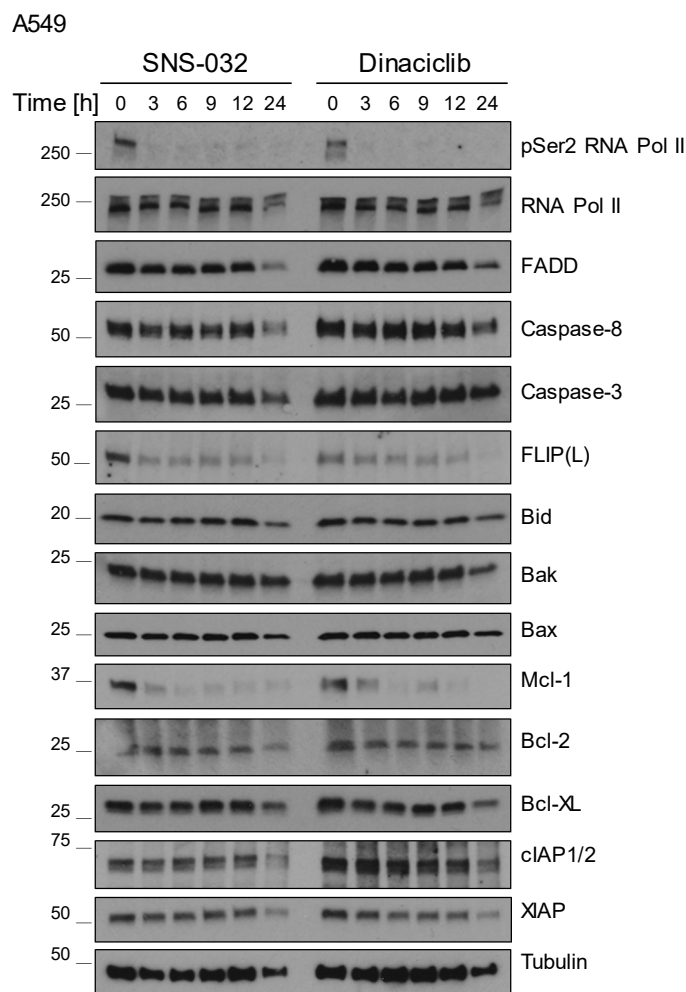


Figure 3.3: Dinaciclib, similarly to SNS-032, sensitises cancer cells to TRAIL-induced cell death by downregulation of FLIP and Mcl-1.

A549 cells were treated with 300 nM SNS-032 or 25 nM Dinaciclib for the indicated time before cell lysis and analysis of the lysates by Western Blotting. Data are presented as representative Western blots of two independent experiments.

3.1.2. Dinaciclib overcomes TRAIL resistance in multiple cancer types

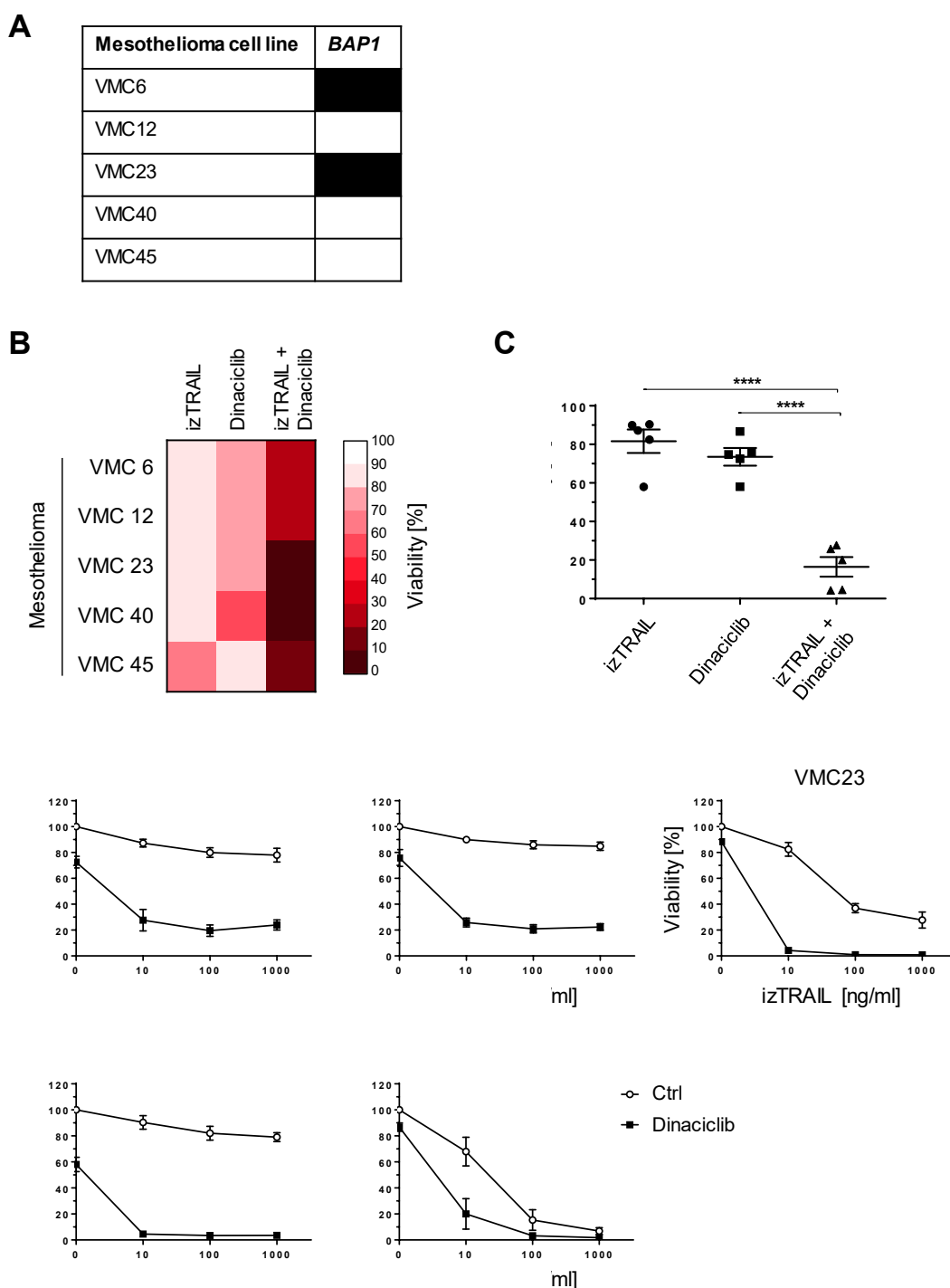
With the aim of evaluating the ability of Dinaciclib to break TRAIL-resistance in different tumour types, a panel of five NSCLC cell lines bearing different oncogenic mutations (Figure 3.4 A) was first selected, based on the fact that these cell lines had been previously demonstrated to be sensitised to TRAIL-induced cell death by the use of the CDK9 inhibitor SNS-032 (Lemke et al., 2014a). Cells were treated with increasing concentrations of TRAIL, in the presence or absence of Dinaciclib. All five cell lines were resistant to low concentrations of TRAIL [10 ng/ml]. However, the combination of 10 ng/ml of TRAIL with 25 nM Dinaciclib readily killed NSCLC cells. (Figure 3.4 B and C). When treated with higher concentrations of TRAIL, some cell lines, namely Calu-1, H322 and H460, showed some decrease in viability. Nonetheless, the addition of Dinaciclib profoundly increased the TRAIL-sensitivity of all tested cell lines (Figure 3.4 D). Of note, Dinaciclib monotreatment had only marginal effects on the cell viability in most of the cell lines.

(C) Cells were treated as in B. Values are means \pm SEM. Each dot represents the mean of at least three independent experiments for one cell line. Statistical analysis was performed using one-way ANOVA.

(D) The indicated NSCLC cell lines were pre-incubated with or without 25 nM Dinaciclib for 15 min and then treated with the indicated concentrations of izTRAIL. Cell viability was quantified after 24 h. Data represent means \pm SEM of at least three independent experiments.

*** $p \leq 0.001$, **** $p \leq 0.0001$.

The results in Figure 3.4 demonstrate that Dinaciclib is a potent sensitiser to TRAIL-induced death in NSCLC. To evaluate whether the applicability of this novel therapy could be broadened to cancers from different origins, it was next tested in a panel of mesothelioma cell lines. Mesothelioma is a rare type of cancer that arises mainly in the pleura of the lungs. In this disease, the expression of the nuclear deubiquitinase BRCA1-associated protein 1 (BAP1) is often lost (Bott et al., 2011). The combination of TRAIL and Dinaciclib was tested in three BAP1 positive and two BAP1 negative cell lines (Figure 3.5 A). VMC23 (BAP1 negative) and VMC45 (BAP1 positive) cell lines were sensitive to high concentrations of TRAIL, whereas the rest of the cell lines remained resistant. Importantly, irrespective of the BAP1 status, TRAIL and Dinaciclib strongly synergised to reduce the viability of all the mesothelioma cell lines tested (Figure 3.5 B-D).



(C) Cells were treated as in B. Values are means \pm SEM. Each dot represents the mean of at least three independent experiments for one cell line. Statistical analysis was performed using one-way ANOVA.

(D) The indicated mesothelioma cell lines were pre-incubated with or without 25 nM Dinaciclib for 15 min and then treated with the indicated concentrations of izTRAIL. Cell viability was quantified after 24 h. Data represent means \pm SEM of at least three independent experiments. **** $p \leq 0.0001$

TRAIL and Dinaciclib combination treatment was then tested in a wide range of solid tumour types including cervical, breast, ovarian, liver, colorectal and pancreatic cancers. As shown in Figure 3.6, Dinaciclib sensitised cells from all origins to TRAIL-induced cell death. Importantly, in TRAIL-sensitive cell lines like JHH4 and HCT-116, the combination with Dinaciclib achieved over 80% reduction in viability at concentrations of TRAIL as low as 1 ng/ml, at which TRAIL monotherapy did not significantly affect these cells (Figure 3.6 B).

Although a profound reduction in cells subjected to the highest concentration of TRAIL and Dinaciclib was observed, some remaining live cells were still present after 24 h treatment. In order to investigate the potential of these TRAIL- and Dinaciclib-surviving cells to outgrow, the clonogenic survival of four representative cell lines (A549, H322, Panc-89 and Colo 357) was next assessed upon TRAIL treatment in the presence or absence of Dinaciclib. Whilst multiple clones survived and continued to grow after TRAIL or Dinaciclib monotherapy, the combination of both completely abrogated the clonogenic survival of the four cell lines (Figure 3.7).

Taken together, the results shown so far establish Dinaciclib as an effective sensitiser to TRAIL-induced cell death across multiple solid tumour types.

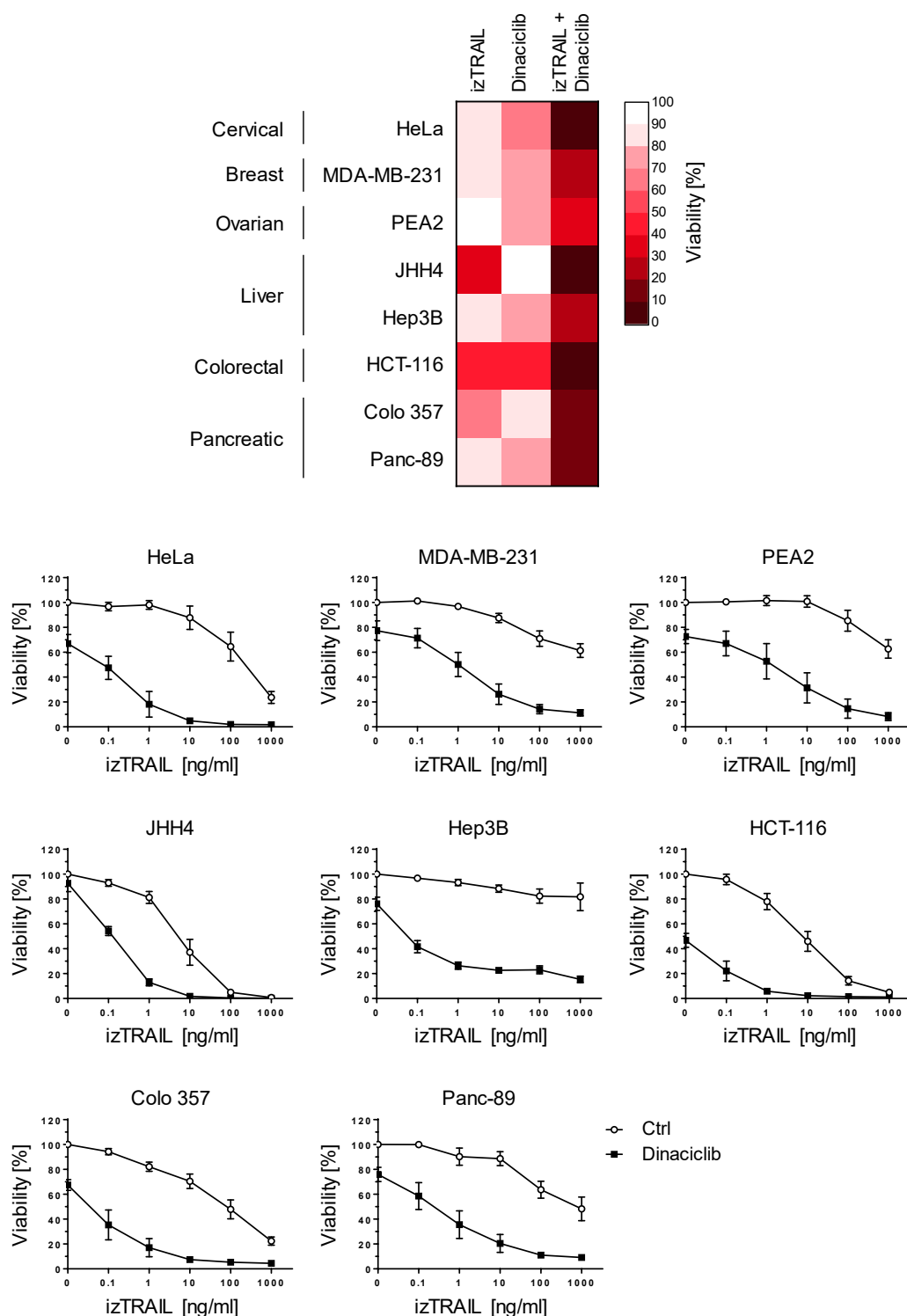


Figure 3.6: Dinaciclib broadly sensitises different cancers to TRAIL-induced cell death.

(A) The indicated cell lines were pre-incubated with or without Dinaciclib [25 nM] for 15 min and subsequently stimulated with izTRAIL [10 ng/ml] or fresh media. Cell viability was quantified after 24 h and normalised to the untreated control.

(Figure legend continues on next page)

Heat map representing colour-coded viability levels of the different cell lines upon the indicated treatments. Values are means of at least three independent experiments.

(B) The cell lines in A were pre-incubated with or without 25 nM Dinaciclib for 15 min and then treated with the indicated concentrations of izTRAIL. Cell viability was quantified after 24 h. Data represent means \pm SEM of at least three independent experiments.

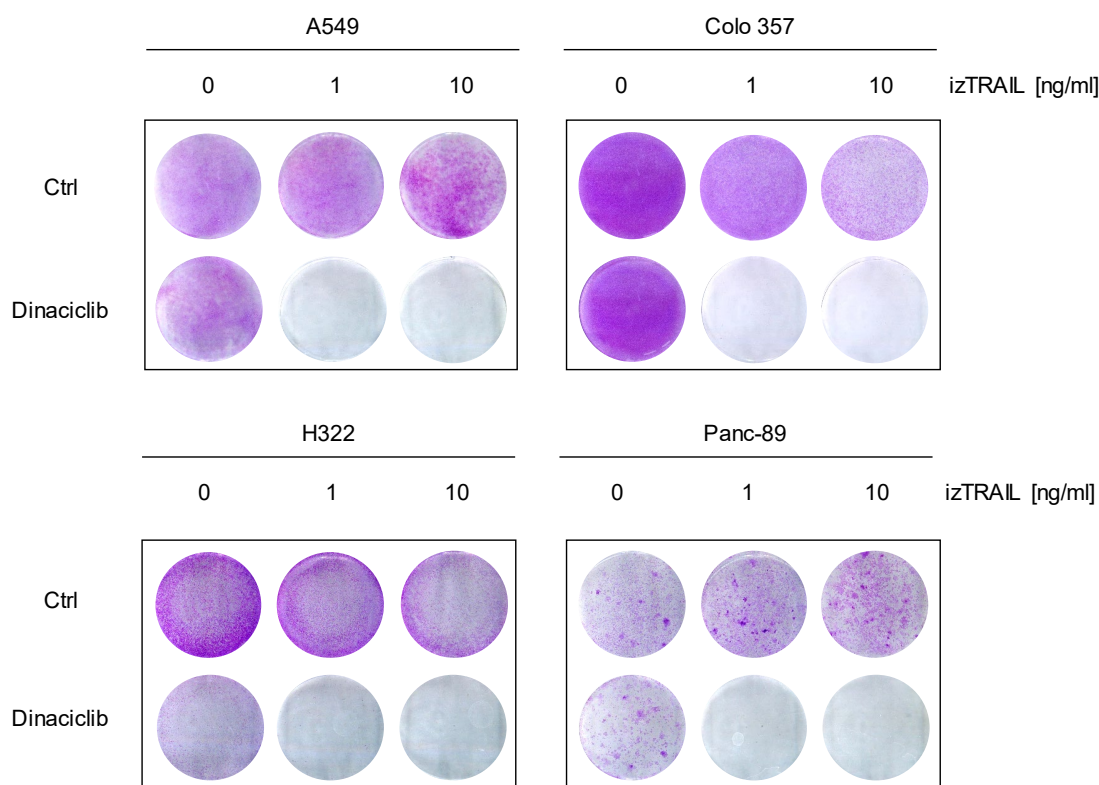


Figure 3.7: Combination of TRAIL and Dinaciclib treatment inhibits the long-term survival of cancer cells.

A549, Colo 357, H322 and Panc-89 cell lines were treated with or without 25 nM Dinaciclib and the indicated concentration of izTRAIL. After 7 days, cells were stained with crystal violet and the stained plates scanned. Representative images of two independent experiments are shown.

3.1.3. Co-treatment with TRAIL and Dinaciclib overcomes chemo- and targeted therapy resistance

As our understanding of the molecular biology of cancer has evolved, new agents that target specific molecular alterations have emerged in the recent years. These targeted therapies, together with conventional chemotherapy, are currently the first-line treatment for most cancers. Nevertheless, resistance to chemotherapy and targeted therapies is a pervasive problem facing current cancer research (Holoohan et al., 2013).

Given the prevalence of cancer drug resistance, the effectiveness of the novel TRAIL and Dinaciclib combination treatment in chemotherapy- and targeted therapy-resistant cell lines was investigated. To this end, a panel of matched parental and therapy-resistant (conditioned) melanoma cell lines was employed. Conditioned cell lines were generated in the laboratory of Prof. D. Kulms by treating them with the indicated agent for 6 months. *BRAF*-mutant WM3248 and Malme3M cells were treated with the B-raf inhibitor Dabrafenib, *NRAS*-mutant Skmel2 and Skmel147 cells with the MEK inhibitor Trametinib and *BRAF*-mutant A375 and IGR-37 cells with the chemotherapeutic agent Cisplatin (Figure 3.8 A). Resistance of all the conditioned cell lines was confirmed as shown in Figure 3.8 B-D. All parental cells remained sensitive to the different therapies, albeit with variable efficacies.

A

Melanoma cell line	<i>BRAF</i>	<i>NRAS</i>	<i>TP53</i>	Conditioned
WM3248				Dabrafenib [1 μ M]
Malme3M				Dabrafenib [1 μ M]
Skmel2				Trametinib [1 nM]
Skmel147				Trametinib [1 nM]
A375				Cisplatin [1 μ M]
IGR-37				Cisplatin [1 μ M]

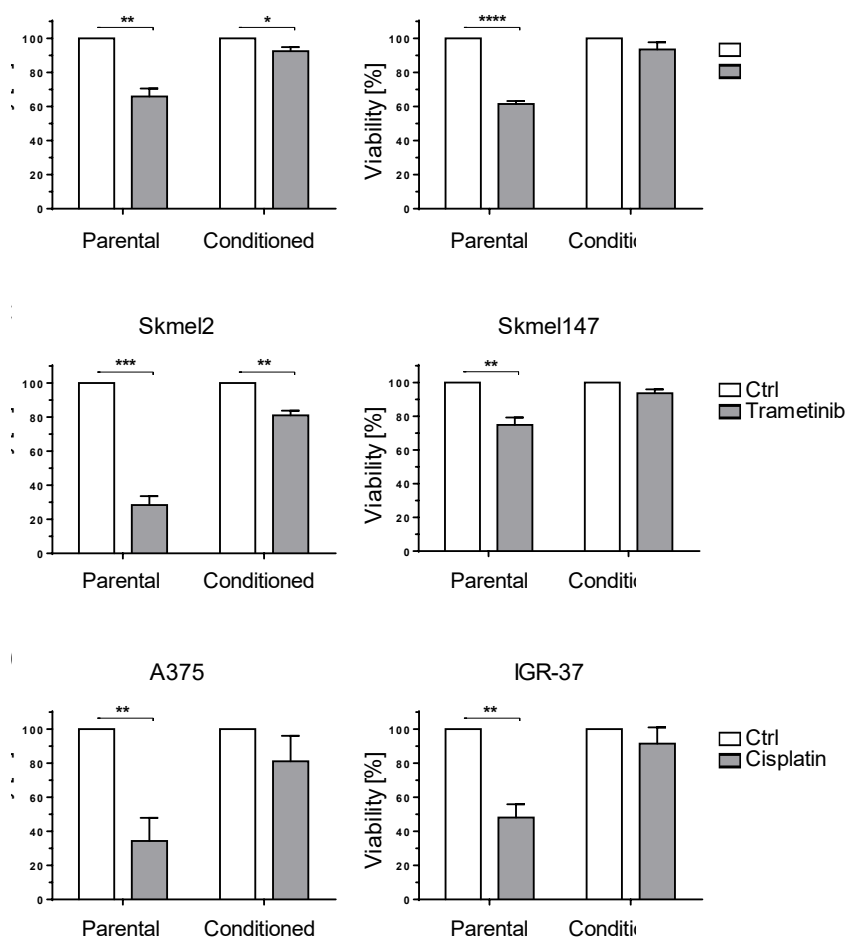


Figure 3.8: Conditioned melanoma cell lines are resistant to chemo- or targeted therapy drugs.

(A) Mutations in *BRAF*, *NRAS* and/or *TP53* of the cell lines included in the melanoma panel are indicated with a black box. Conditioned cell lines were generated by treating the parental lines with the indicated chemotherapeutic or targeted agents at the indicated concentrations continuously for 6 months.

(Figure legend continues on next page)

(B) Parental and conditioned VWM3248 and Malme3M cells were treated with or without Dabrafenib [10 μ M].

(C) Parental and conditioned Skmel2 and Skmel147 cells were treated with or without Trametinib [10 nM].

(D) Parental and conditioned A375 and IGR-37 cells were treated with or without Cisplatin [10 μ M].

(B, C, D) Cell viability was quantified 24 h after the treatment and normalised to the untreated control. Data represent means \pm SEM of three independent experiments. Statistical analysis was performed using Student's t-test. * $p \leq 0.05$, ** $p \leq 0.01$, *** $p \leq 0.001$, **** $p \leq 0.0001$.

Parental and therapy-conditioned melanoma cell lines were stimulated with increasing concentrations of TRAIL in the presence or absence of Dinaciclib. TRAIL and Dinaciclib synergised to efficiently diminish cell viability in both parental and conditioned melanoma cell lines, even at low concentrations of TRAIL [10 ng/ml] (Figure 3.9 A and B). Overall, conditioned cells responded to TRAIL, Dinaciclib or the combined treatment similarly to their parental counterparts. The only exception was the A375 pair of cell lines, in which parental cells were TRAIL-resistant while conditioned cells were sensitive to TRAIL-induced cell death (Figure 3.9 C).

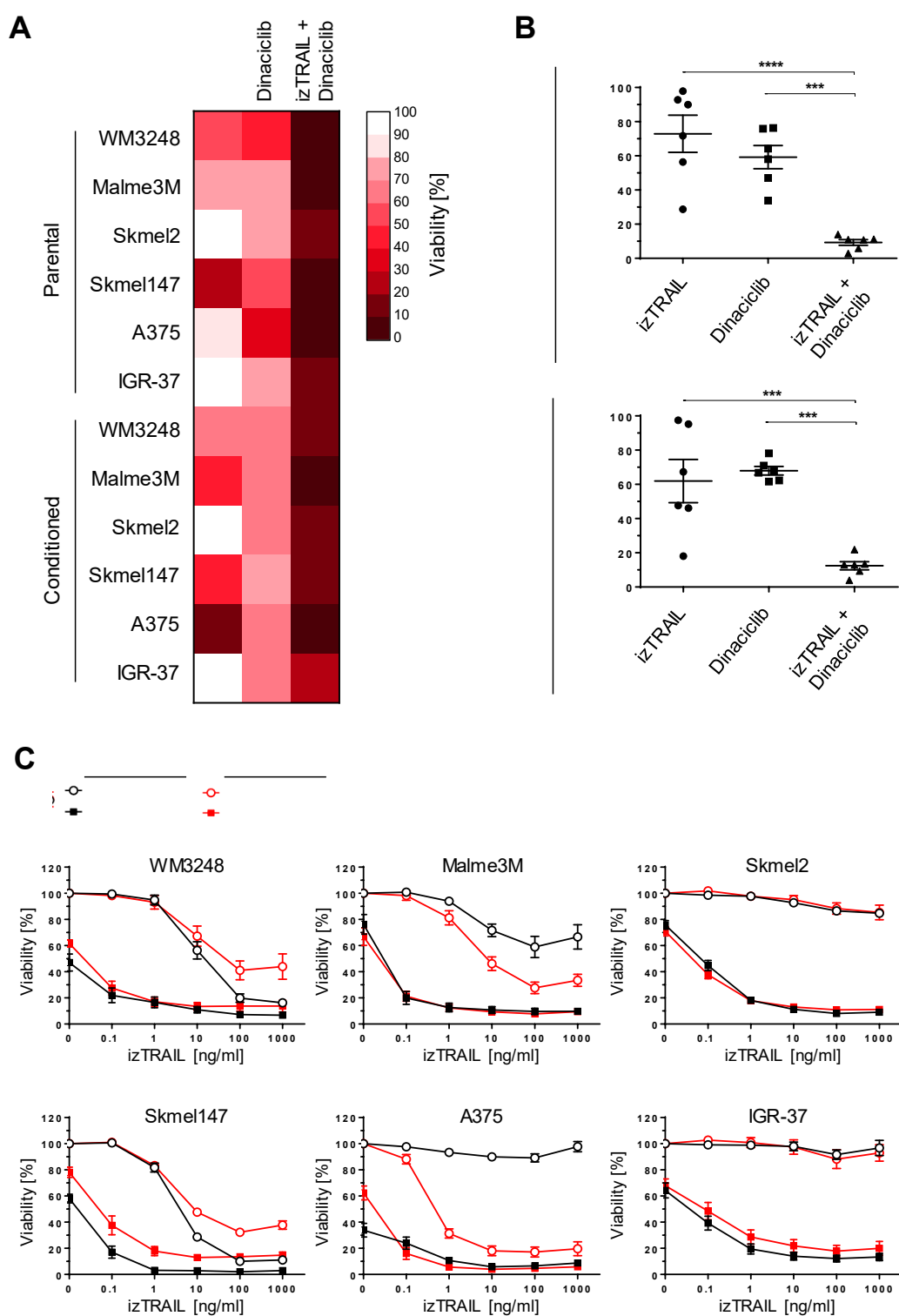


Figure 3.9: TRAIL and Dinaciclib combination treatment overcomes chemo- and targeted therapy-resistance.

(A) Six parental and their corresponding chemotherapy-conditioned melanoma cell lines were pre-incubated with or without Dinaciclib [25 nM] for 15 min and subsequently stimulated with izTRAIL [10 ng/ml] or fresh media. *(Figure legend continues on next page)*

Cell viability was quantified after 24 h and normalised to untreated control. Heat map representing colour-coded viability levels of the different cell lines upon the indicated treatments. Values are means of three independent experiments.

(B) Cells were treated as in A. Values are means \pm SEM. Each dot represents the mean of at least three independent experiments for one cell line. Statistical analysis was performed using one-way ANOVA.

(C) Parental and conditioned melanoma cell lines were pre-incubated with or without 25 nM Dinaciclib for 15 min and then treated with the indicated concentrations of izTRAIL. Cell viability was quantified after 24 h. Data represent means \pm SEM of three independent experiments. *** $p \leq 0.001$, **** $p \leq 0.0001$.

The sensitisation of chemo- and targeted therapy-resistant cells to TRAIL-induced cell death by Dinaciclib was confirmed in colony formation assays (Figure 3.10). Conditioned melanoma cell lines responded in a similar manner than the parental cell lines. Although Dinaciclib monotreatment reduced the clonogenic survival of some of the cell lines, predominantly in the A375 and IGR-37 pairs, the combined treatment with TRAIL and Dinaciclib led to many less surviving clones.

Thus, TRAIL and Dinaciclib therapeutic combination is effective in overcoming resistance to chemotherapy as well as to targeted therapy.

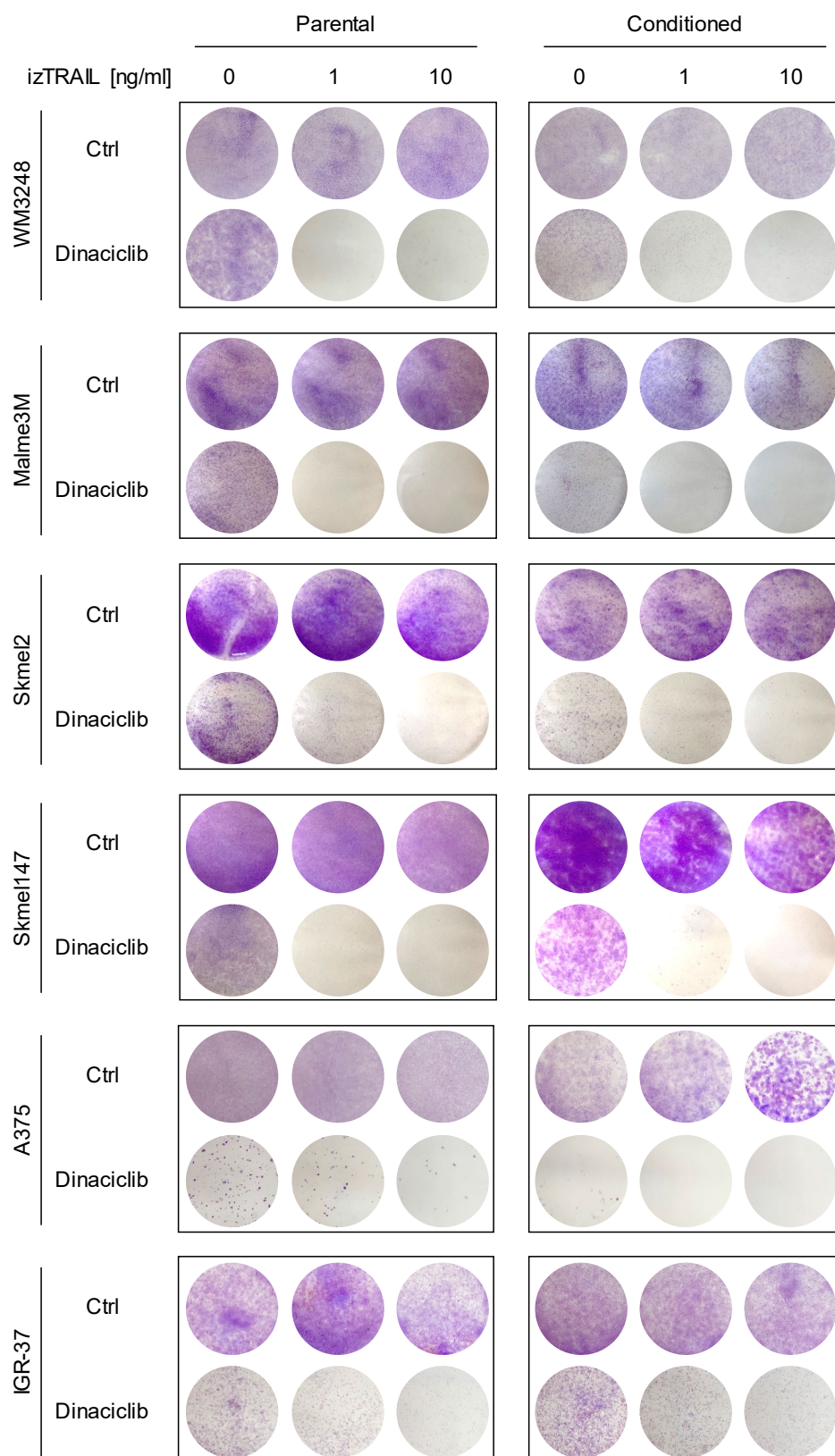


Figure 3.10: Combined TRAIL and Dinaciclib treatment prevents the long-term survival of melanoma cells, including the chemotherapy-resistant ones.

(Figure legend continues on next page)

The indicated parental or conditioned cell lines were treated with the indicated concentration of izTRAIL in the presence or absence of 25 nM Dinaciclib. After 7 days, cells were stained with crystal violet and the stained plates scanned. Representative images of three independent experiments are shown.

3.1.4. TRAIL- and Dinaciclib-induced cell death is apoptotic

TRAIL can trigger different modes of programmed cell death, i.e. caspase-dependent apoptosis and RIPK1-dependent necroptosis (section 1.1.3.2). To decipher the type of TRAIL-induced cell death to which Dinaciclib sensitises cancer cells, A549, Malme3M and H322 cells were treated with TRAIL and Dinaciclib in the presence of apoptosis or necroptosis inhibitors. The caspase inhibitor zVAD.FMK (zVAD) was used to block apoptotic cell death whilst the RIPK1 inhibitor Necrostatin-1s (Nec-1s) was employed to prevent necroptosis. As shown in Figure 3.11, treatment with Nec-1s did not have any effect on the viability of cells stimulated with TRAIL and Dinaciclib. The addition of zVAD, however, completely prevented the decrease in viability observed upon TRAIL and Dinaciclib co-treatment, suggesting that the Dinaciclib-sensitised cells undergo apoptosis in response to TRAIL.

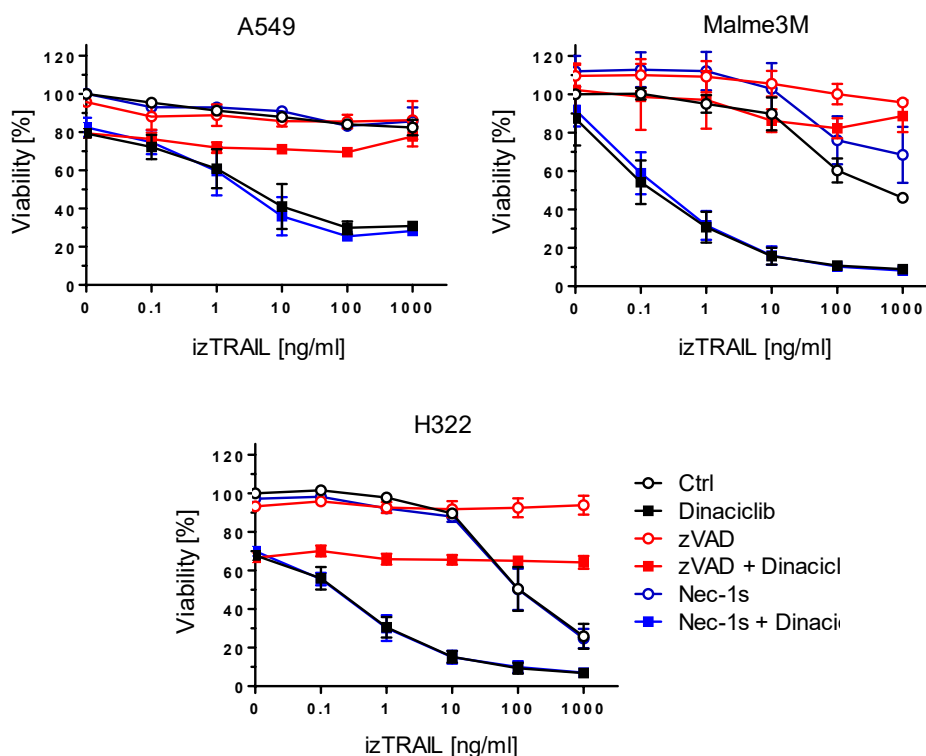


Figure 3.11: The cell death induced by TRAIL and Dinaciclib combination can be prevented by the caspase inhibitor zVAD but not by the RIPK1 inhibitor Nec-1s.

A549, Malme3M and H322 cells were pre-incubated with zVAD [20 μ M] or Nec-1s [10 μ M] for 1 h and subsequently treated with Dinaciclib [25 nM]. After 15 min, cells were stimulated with the indicated concentrations of izTRAIL and cell viability was quantified 24 h later. Values are means \pm SEM of three independent experiments.

In order to validate the previous results and explore the kinetics of the cell death happening upon TRAIL and Dinaciclib treatment, A549, Malme3M and H322 cells were stained with the cell impermeable nucleic acid stain SYTOX Green and cell death was quantified over 24 h. In all three cell lines, an increase in cell death was observed as soon as 4 h after the stimulation with TRAIL and Dinaciclib, which continued to augment until it plateaued after around 20 h (Figure 3.12). Importantly, this cell death was rescued by zVAD, confirming the previous results. It is noteworthy that TRAIL and Dinaciclib monotreatment resulted in 40 and 50% cell death in Malme3M cells, respectively. Interestingly, this cell death was also caspase-dependent since it was prevented by zVAD.

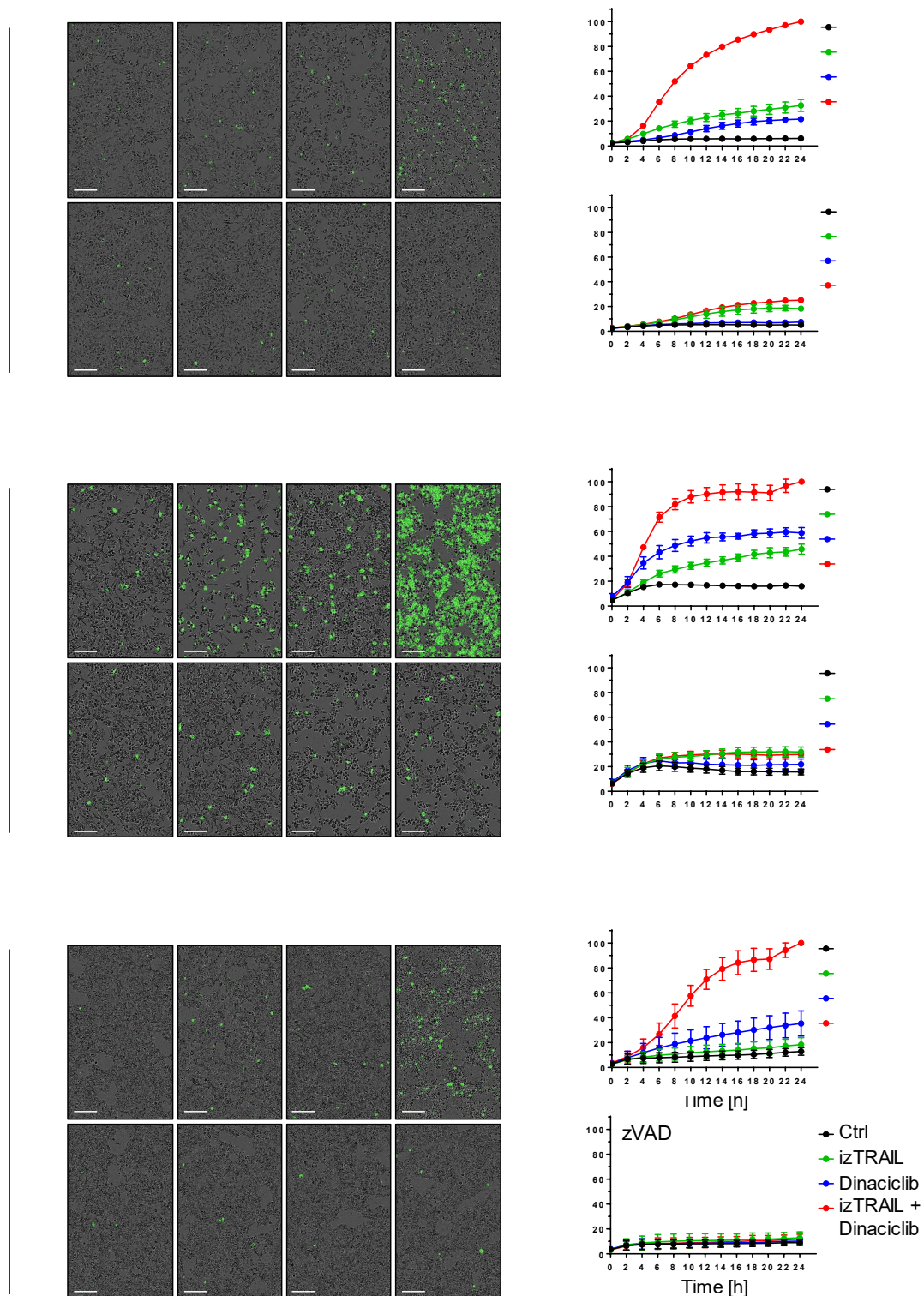


Figure 3.12: Dinaciclib sensitises cancer cells to TRAIL-induced apoptosis.

A549, Malme3M and H322 cells were treated with 100 ng/ml izTRAIL and 25 nM Dinaciclib, in the presence or absence of 20 μ M ZVAD, which was added 1 h before.

(Figure legend continues on next page)

(A) Death cells were imaged in real-time using SYTOX Green and the Incucyte FLR. Representative images of the cells following the indicated treatments after 20 h are shown. White scale bar equals 200 μm .

(B) Cell death was quantified every 2 h as fluorescent objects per well, and percentage cell death was calculated by normalising to the izTRAIL and Dinaciclib treated condition at 24 h. Data represent means \pm SEM of three independent experiments.

Next, it was of interest to investigate the activation of the apoptotic caspase cascade after TRAIL and/or Dinaciclib stimulation. After treating A549 cells with TRAIL for 3 or 6 h in the presence of Dinaciclib, activation of both caspase-8 and caspase-3 was observed, as seen by the decrease in the inactive zymogenic caspase precursor and the activation of the executioner caspase-3, which is indicated by the cleavage of caspase-3 (Figure 3.13). Moreover, TRAIL and Dinaciclib induced the cleavage of PARP, which is a substrate of caspase-3, thus further confirming the activation of this caspase. In line with the previous data, caspase activation and PARP cleavage were completely abrogated by treatment with zVAD. Of note, some active caspase-3 could be detected after treatment with TRAIL alone, indicating that TRAIL can trigger some apoptosis in A549 cells, which correlates with the 20-30% cell death detected previously (Figure 3.12 B). Nevertheless, the activation of caspase-3 induced by TRAIL was minute in comparison with the one induced by the combination of TRAIL and Dinaciclib (Figure 3.13).

Therefore, it can be concluded that Dinaciclib sensitises tumour cells to TRAIL-induced apoptosis, which can be blocked by the caspase inhibitor zVAD.

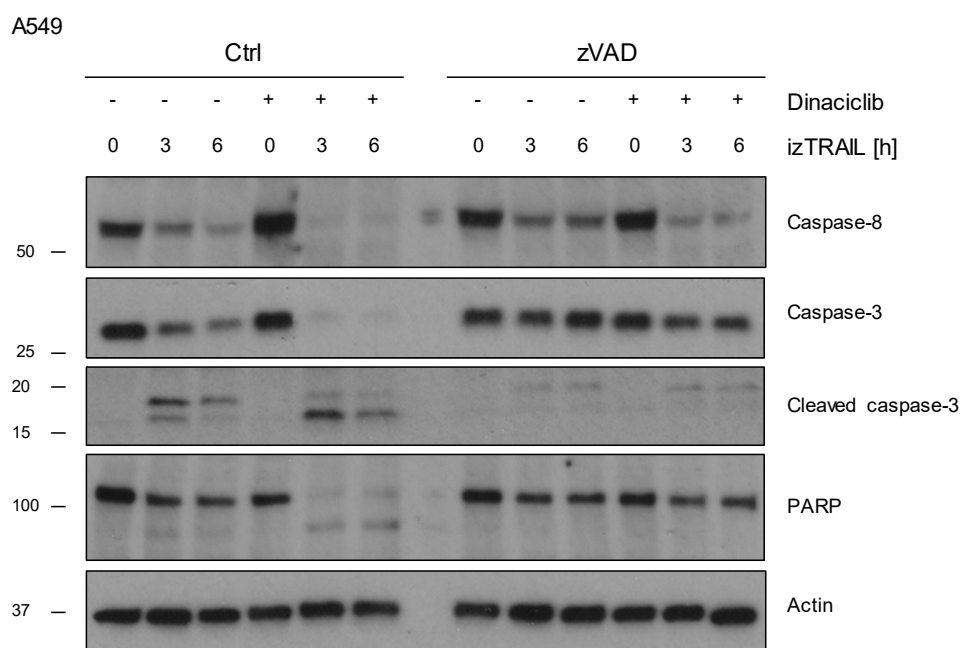


Figure 3.13: Dinaciclib synergises with TRAIL to induce apoptosis.

A549 cells were pre-incubated with or without ZVAD [20 μ M] for 1 h and subsequently treated with or without Dinaciclib [25 nM]. 2 h later, cells were stimulated with izTRAIL [100 ng/ml] for the indicated times before cell lysis and analysis by Western blotting. Representative Western blots of two independent experiments are shown.

3.2. Evaluation of the therapeutic potential of the TRAIL and Dinaciclib combination *in vivo*

Considering the remarkable sensitisation observed with the novel combination of TRAIL and Dinaciclib in a plethora of cancer types *in vitro*, the potency of this combination in mouse models of NSCLC *in vivo* was next assessed.

3.2.1. TRAIL and Dinaciclib treatment is well tolerated *in vivo*

For the initial evaluation of the therapeutic efficacy of the novel therapy, an allogenic transplant tumour model was selected, since it allowed for easy tumour monitoring throughout the experiment. For this purpose, KP802T4 cells were employed. These cells were generated in the laboratory of Prof. T. Jacks from a KP^{null} lung tumour. The model was initially validated *in vitro* by the measurement of cell viability following TRAIL and Dinaciclib co-treatment. Figure 3.14 A shows that these cells were sensitised to TRAIL-induced apoptosis by Dinaciclib. This was achieved at a concentration of Dinaciclib [100 nM] at which the phosphorylation of Ser2 of RNA Pol II was inhibited (Figure 3.14 B).

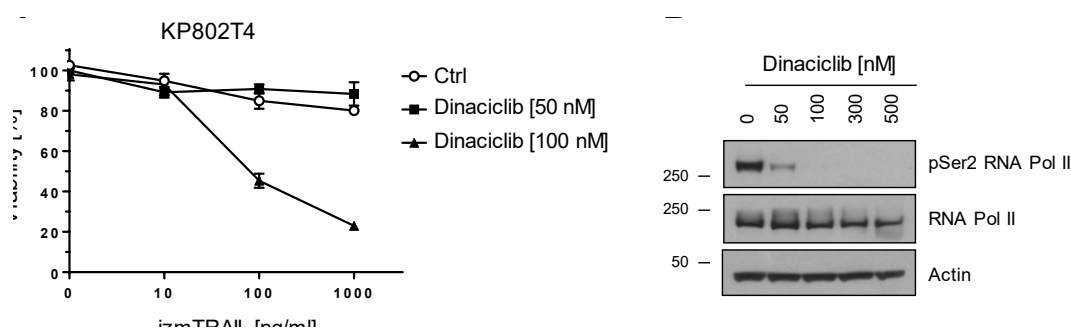


Figure 3.14: Dinaciclib sensitises KP802T4 cells to TRAIL-induced apoptosis.

(A) KP802T4 cells were treated with 50 nM or 100 nM Dinaciclib for 15 min and subsequently stimulated with izmTRAIL at the indicated concentrations. Cell viability was quantified 48 h later. Data represent means \pm SEM of three independent experiments.

(B) KP802T4 cells were treated with the indicated concentration of Dinaciclib. Lysates were obtained 24 h later and analysed by Western blotting. Representative Western blots of two independent experiments are shown.

To determine the efficacy of TRAIL and Dinaciclib combinatorial treatment *in vivo*, KP802T4 cells were injected intradermally in the flank of *Rag1*^{-/-} mice and the treatment was started one week later, once the tumours were visible. Mice received three doses per week during two consecutive weeks of either vehicle, TRAIL, Dinaciclib, or TRAIL and Dinaciclib (Figure 3.15 A). The bodyweight of the mice did not drop during the course of the treatment, indicating that it was well tolerated (Figure 3.15 B). Similarly, the hepatotoxicity was evaluated by measuring the levels of ALT, a hepatic enzyme released to the circulation only when liver cells are damaged. With the exception of an outlier in the TRAIL-treated group, none of the treatments caused a significant elevation in the ALT levels in serum, which implies that the novel TRAIL and Dinaciclib combination is nontoxic in mice (Figure 3.15 C).

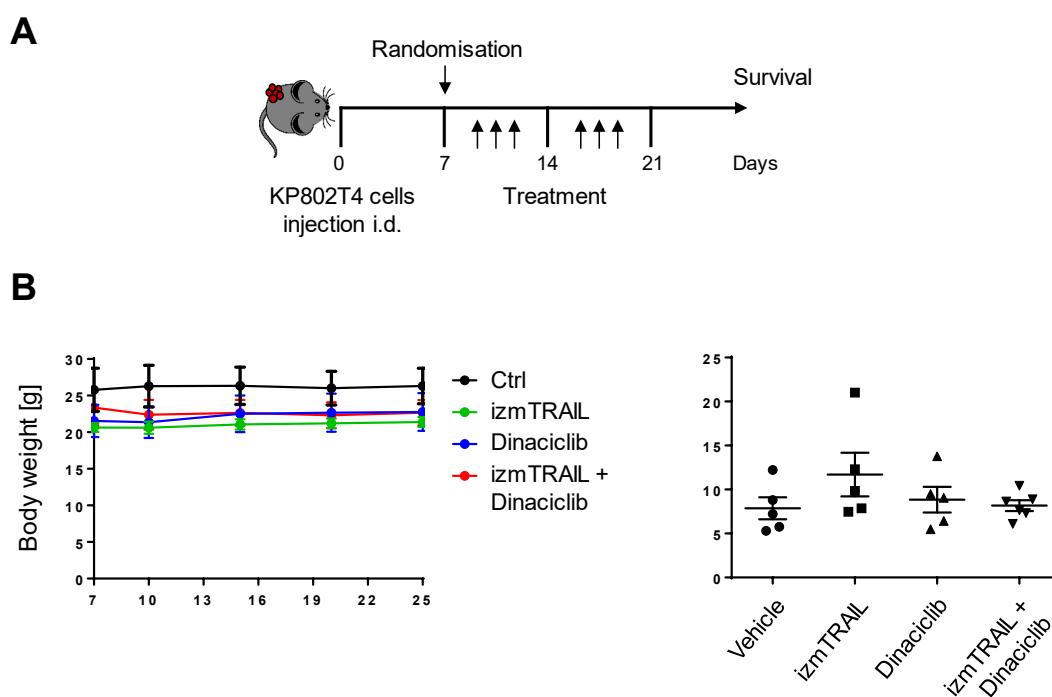


Figure 3.15: The combination of TRAIL and Dinaciclib is well tolerated *in vivo*.

(A) Experimental treatment schedule is shown. KP802T4 cells were injected intradermally in the flank of *Rag1*^{-/-} mice. Mice were treated with Dinaciclib at 30 mg/kg and/or izmTRAIL at 5 mg/kg at the indicated times (vehicle, izmTRAIL, Dinaciclib: n=5 mice per group; izmTRAIL + Dinaciclib: n=6 mice).

(B) Mice were weighted throughout the course of the treatment. Data are shown as means ± SEM of each treatment group. (Figure legend continues on next page)

(C) Serum from the mice receiving the indicated treatments was analysed at day 25 for ALT levels. Data are shown as means \pm SEM. Each dot represents an individual mouse. Statistical analysis was performed using one-way ANOVA.

3.2.2. TRAIL and Dinaciclib combination therapy reduces tumour growth and prolongs the survival of NSCLC transplant tumour-bearing mice

Once the KP802T4 intradermal tumours were of a measurable size, they were randomised into the treatment groups (Figure 3.16 A and B). Following the treatment schedule described in Figure 3.16A, a significant reduction in the growth of KP802T4 intradermal tumours was observed (Figure 3.16 C and D). Treatment with TRAIL or Dinaciclib alone, on the contrary, had no effect on the tumour growth. Furthermore, after the last dose of the treatment, mice were maintained alive until they reached their humane endpoint. As shown in Figure 3.16 E, survival upon TRAIL and Dinaciclib therapy was significantly prolonged from a median survival (MS) of 25-26 days in the vehicle-, TRAIL- or Dinaciclib-treated mice to 36 days in mice that received the TRAIL and Dinaciclib combinatorial regime. These results indicate that this novel combination is effective *in vivo*.

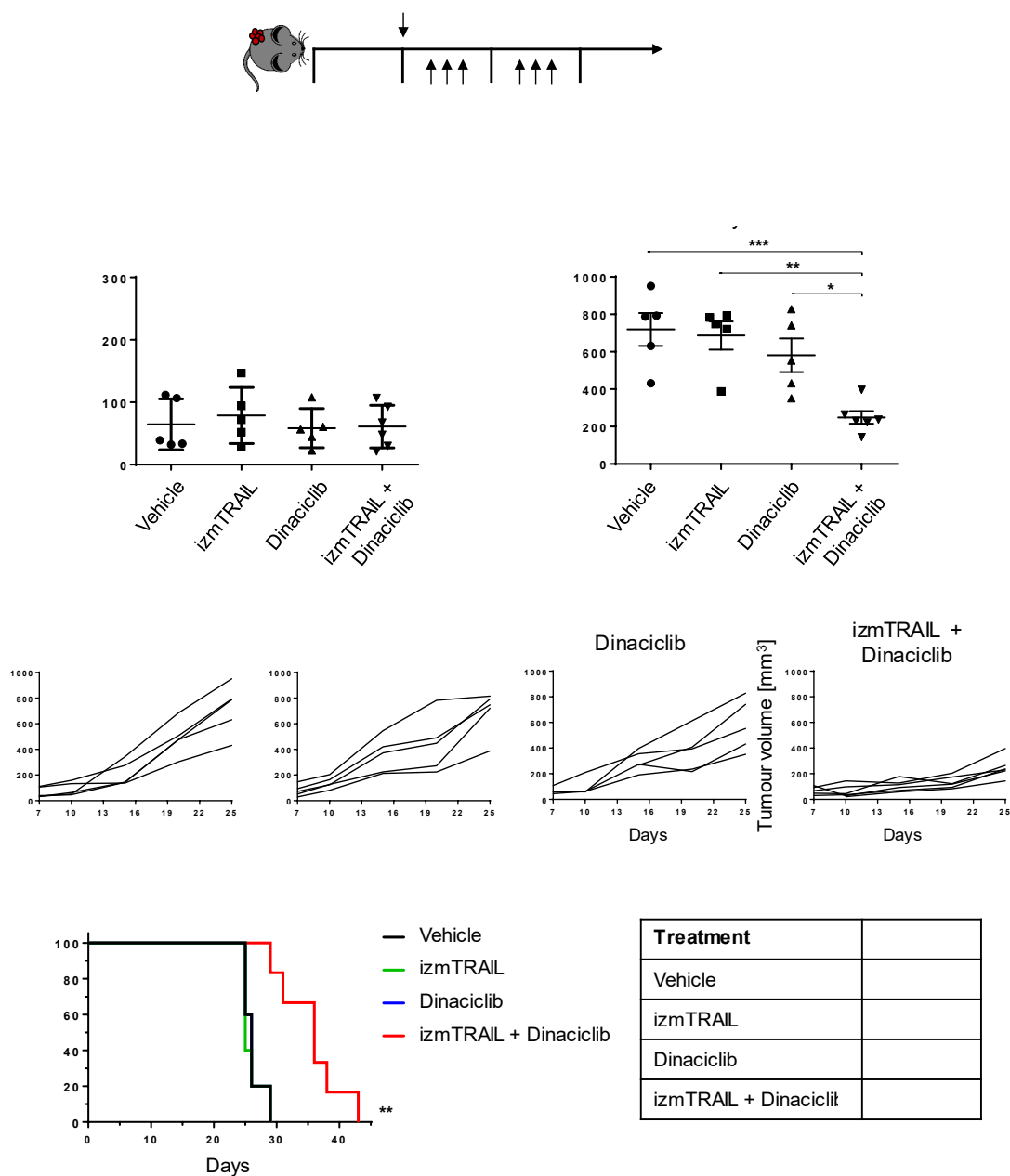


Figure 3.16: TRAIL and Dinaciclib co-treatment shows therapeutic efficacy *in vivo* in a NSCLC tumour transplant model.

(A) Experimental treatment schedule is shown. KP802T4 cells were injected intradermally in the flank of *Rag1*^{-/-} mice. Mice were treated with Dinaciclib at 30 mg/kg and/or izmTRAIL at 5 mg/kg at the indicated times (vehicle, izmTRAIL, Dinaciclib: n=5 mice per group; izmTRAIL + Dinaciclib: n=6 mice).

(B) Tumour volume was measured one week after the injection of the cells and mice were randomised into the treatment groups.

(C) Tumour volume was measured on day 25. Data are presented as means ± SEM. Dots represent individual mice. Statistical analysis was performed using one-way ANOVA.

(D) Mice were individually tracked and tumour volume was measured every 3 days. Each line represents one mouse.

(Figure legend continues on next page)

(E) Kaplan-Meier survival curve of the mice receiving the indicated treatments. MS is indicated for each group. Statistical analysis was performed using log-rank test. * $p \leq 0.05$, ** $p \leq 0.01$, *** $p \leq 0.001$.

3.2.3. The combination of TRAIL and Dinaciclib eradicates established orthotopic human NSCLC xenografts

The main disadvantage of the previous transplantable mouse model is that the NSCLC tumours grow in the flank of the animals instead of in the lungs, which have a substantially different microenvironment. Consequently, the novel therapeutic option was next evaluated in a more physiologically relevant orthotopic lung tumour model. In this model, A549-luc cells are intravenously injected into the tail vein of immunocompromised SCID Beige mice, from which they migrate to and invade the lungs. Importantly, A549-luc cells express luciferase and thus, upon luciferin administration, the tumour cells can be tracked by *in vivo* luminescence using the photon flux as a direct measure of tumour burden.

The analysis of the efficiency of the TRAIL and Dinaciclib combinatorial strategy was performed as outlined in Figure 3.17 A. Lung orthotopic tumours were established one week following tumour cell injection, as detected by luminescence signal (Figure 3.17 B). At this point, the animals were randomised to create treatment groups with comparable tumour burden. Subsequently, a three-day treatment regime was started with either vehicle, TRAIL, Dinaciclib or the combination of TRAIL and Dinaciclib. While TRAIL alone had a significant growth inhibitory effect and Dinaciclib only marginally affected lung tumour burden, combined treatment with TRAIL and Dinaciclib induced a drastic anti-tumour response, leading to the regression of the initially detected lung tumour. As such, the TRAIL- and Dinaciclib-comprising therapy completely eradicated established lung tumours in most mice, as determined by *in vivo* bioluminescence imaging (Figure 3.17 B and C) and subsequent histopathological examination of the lungs (Figure 3.17 D and E).

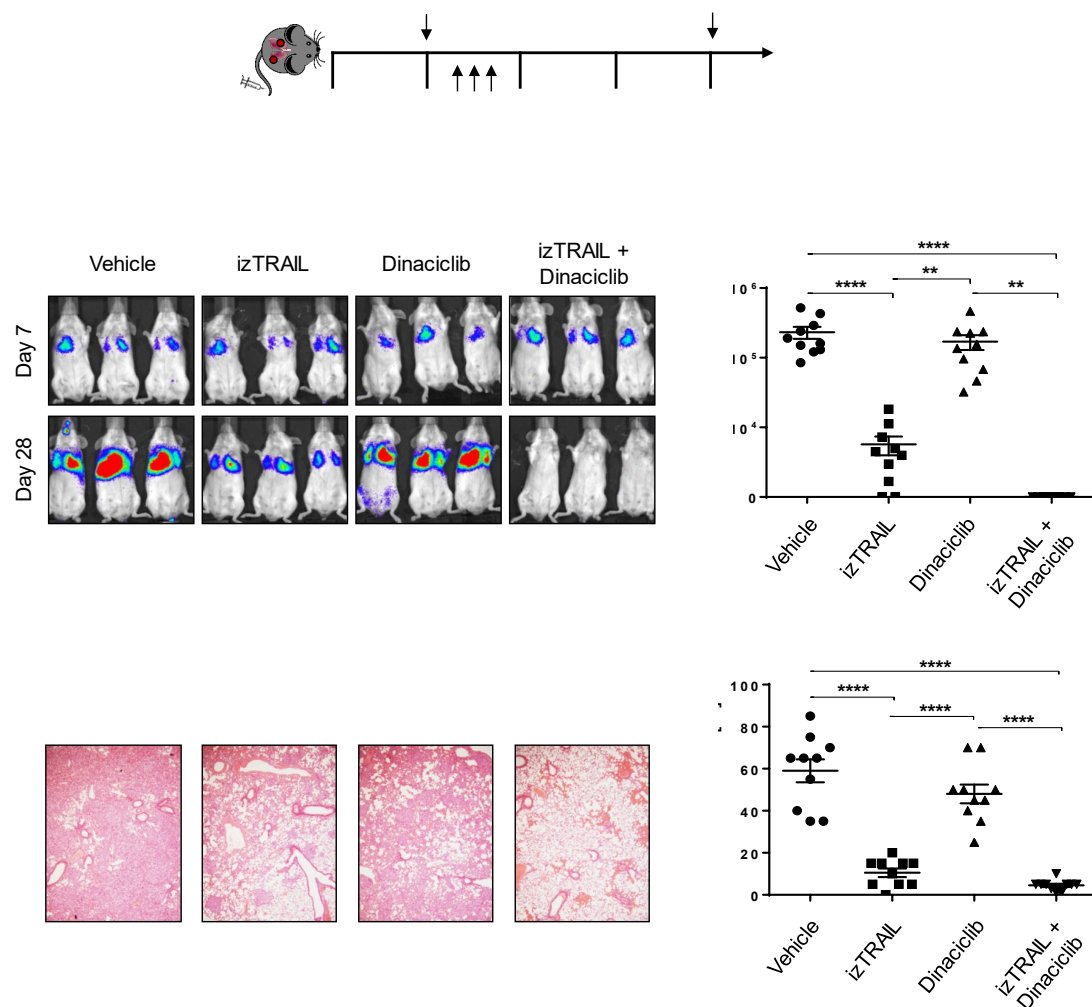


Figure 3.17: The combined treatment of TRAIL and Dinaciclib eradicates orthotopic human NSCLC xenografts.

(A) Experimental treatment schedule is shown. SCID Beige mice were injected with luciferase-expressing A549 cells into the lateral tail vein. Mice were treated with Dinaciclib at 15 mg/kg and/or izTRAIL at 2.5 mg/kg at the indicated times (n=10 mice per group).

(B) Mice were subjected to bioluminescence imaging at the indicated times. Images of three representative mice per group are shown.

(C) Photon flux was quantified by bioluminescence imaging on day 28. Data are presented as means \pm SEM. Dots represent individual mice.

(D) Representative histological images of H&E-stained paraffin-embedded lung sections are shown.

(E) H&E-stained lung sections were subjected to pathological examination to quantify the tumour burden as the percentage of total lung area occupied by tumour tissue. Data are shown as means \pm SEM. Dots represent lungs from individual mice.

Statistical analysis was performed using one-way ANOVA. **p<0.01, ****p<0.0001.

3.2.4. Dinaciclib treatment is sufficient to reduce tumour growth and prolong survival in the autochthonous KP model of NSCLC

After the previous encouraging results, it was next decided to test the novel combination therapy in an autochthonous model of NSCLC, the KP mouse (Jackson et al., 2001), which was already established in the laboratory. To this end, a variant of this GEMM was employed, in which oncogenic *Kras*^{G12D} and *Tp53*^{R172H} are expressed from their respective endogenous loci upon Ad-Cre intranasal instillation (Kasinski and Slack, 2012). Thereby, these mice give rise to lung tumours that progress in their natural environment.

Previous work in our laboratory has demonstrated that, 12 weeks following tumour initiation, animals exhibit macroscopic lesions in the lungs (Walczak laboratory, unpublished data). Therefore, to assess the potency of the anti-cancer combinatorial regimen, mice were treated at this point with three doses of vehicle, TRAIL, Dinaciclib or the combination of TRAIL and Dinaciclib in two alternate weeks, that is 12 and 14 weeks after the Ad-Cre infection (Figure 3.18 A). Mice were sacrificed one week after the last treatment dose and the lungs were collected and weighed as an indication of tumour content. TRAIL monotherapy only had a slight impact on lung weight. Dinaciclib alone or in combination with TRAIL, however, largely decreased the weight of the lungs (Figure 3.18 B). Upon histopathological analysis, only mice receiving TRAIL in combination with Dinaciclib showed a statistically significant reduction in actual tumour burden as compared to the vehicle-treated mice (Figure 3.18 C and D).

Importantly, some KP mice treated as above were kept for survival analysis until they reached their humane endpoint. All three treatments prolonged the survival of mice as compared to the vehicle-receiving group (Figure 3.19). Yet, the combined treatment of TRAIL and Dinaciclib showed the most robust benefit in survival, increasing the MS of the KP mice from 200 days in the mice treated with vehicle to 222 days in the mice treated with TRAIL and Dinaciclib. On the other hand, TRAIL-treated mice had a MS of 210.5 days and Dinaciclib-treated mice 208 days.

Taken together, these data show that TRAIL and Dinaciclib combination therapy is effective in the autochthonous KP model of NSCLC and thus, could be a promising therapeutic option. Although treatment with Dinaciclib seems sufficient to achieve a partial anti-tumour effect, the addition of TRAIL leads to a more robust effect and improves overall survival.

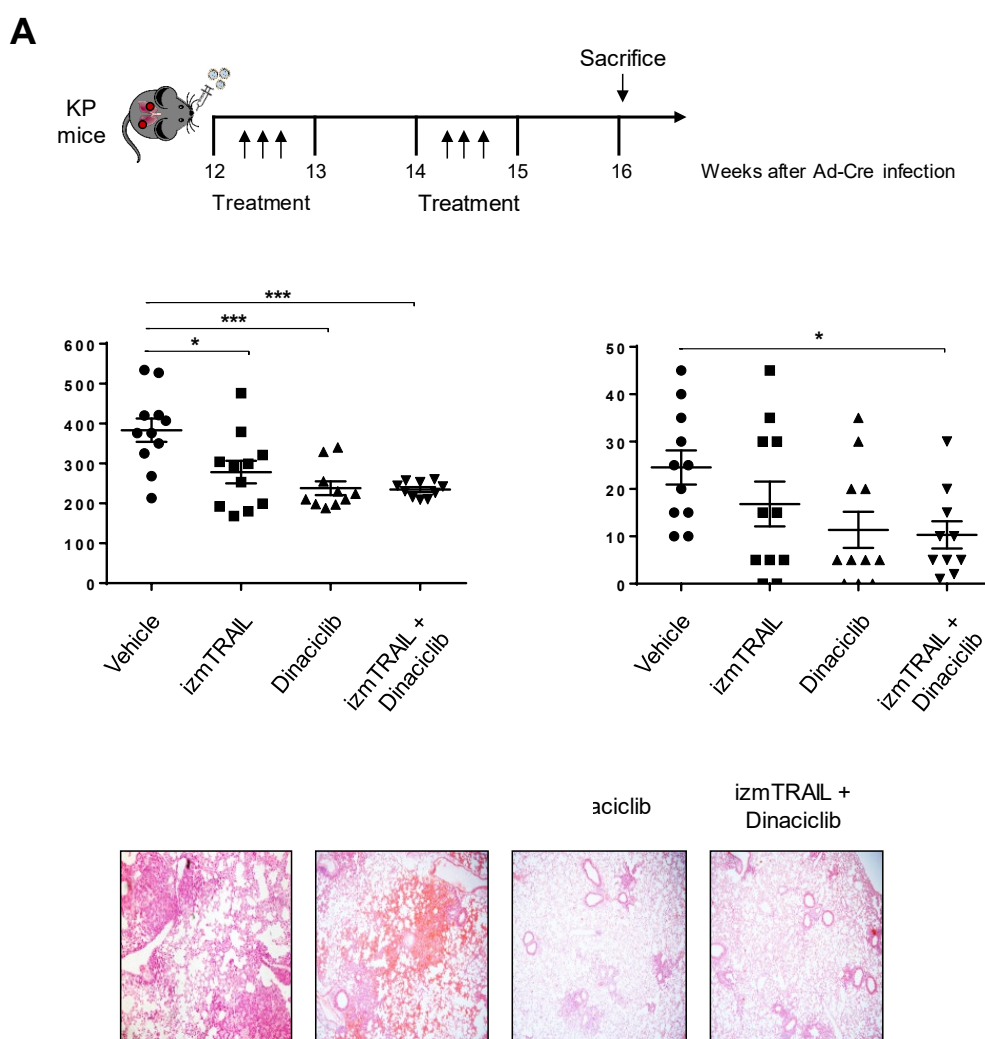


Figure 3.18: Dinaciclib treatment reduces the tumour growth of KP mice.

(A) Experimental treatment schedule is shown. KP mice were subjected to intranasal administration of Ad-Cre to induce the expression of oncogenic *Kras*^{G12D} and *Tp53*^{R172H}. Mice were treated with Dinaciclib at 30 mg/kg and/or izmTRAIL at 5 mg/kg at the indicated times after Ad-Cre delivery (vehicle, izmTRAIL, Dinaciclib: n=11 mice per group; izmTRAIL + Dinaciclib: n=10 mice).

(B) Mice were sacrificed 16 weeks after Ad-Cre administration and the lungs were weighted. Data are shown as means \pm SEM. Dots represent lungs from individual mice.

(C) Paraffin-embedded sections of lungs collected 16 weeks after Ad-Cre administration from all mice were stained with H&E and subjected to pathological examination for tumour burden quantification as percentage of total lung area occupied by tumour tissue. Data are presented as means \pm SEM. Dots represent lungs from individual mice.

(D) Representative histological images of H&E-stained paraffin-embedded lung sections are shown.

Statistical analysis was performed using one-way ANOVA. *p<0.05, ***p<0.001.

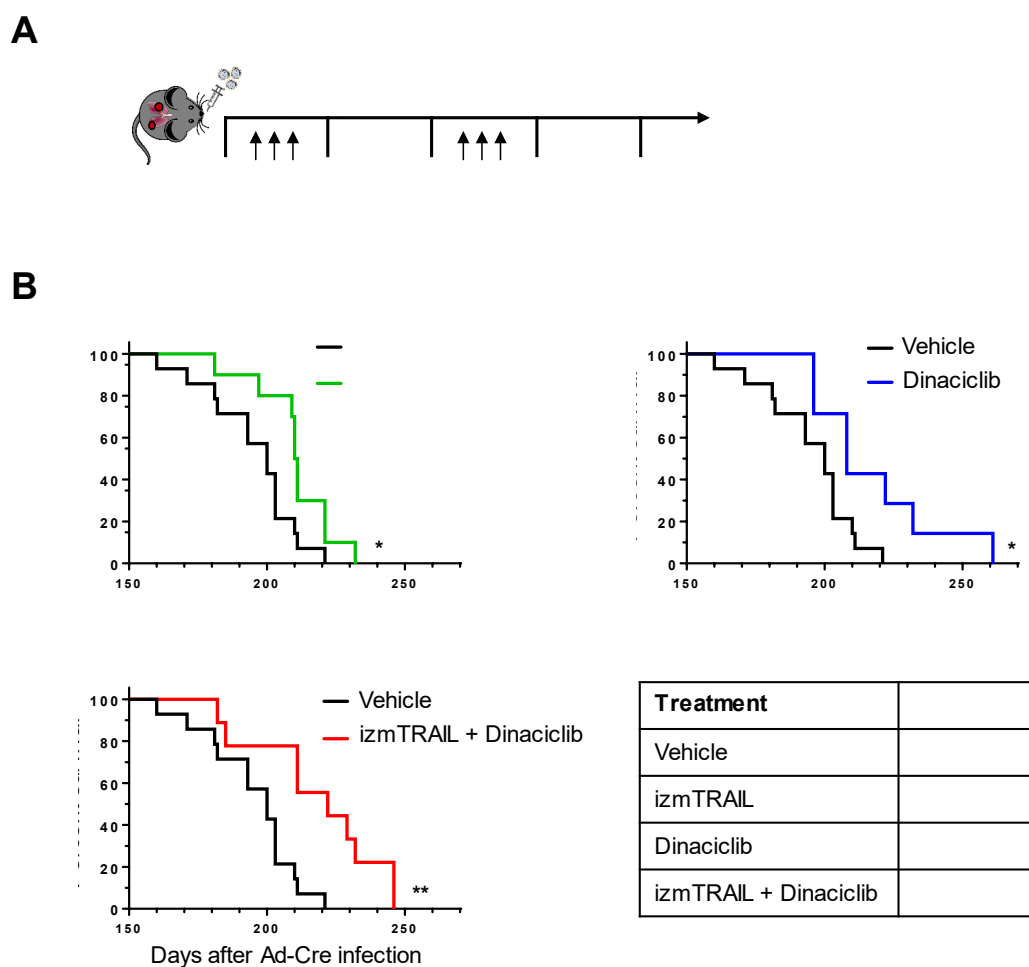


Figure 3.19: TRAIL and Dinaciclib combination prolongs the survival of KP mice.

(A) Experimental treatment schedule is shown. KP mice were subjected to intranasal administration of Ad-Cre to induce the expression of oncogenic *Kras*^{G12D} and *Tp53*^{R172H}. Mice were treated with Dinaciclib at 30 mg/kg and/or izmTRAIL at 5 mg/kg at the indicated times after Ad-Cre delivery (vehicle: n= 14 mice; izmTRAIL: n=10 mice; Dinaciclib: n=7 mice; izmTRAIL + Dinaciclib: n=9 mice).

(B) Kaplan-Meier survival curves of mice receiving the indicated treatments. MS is indicated for each group. Statistical analysis was performed using log-rank test. *p≤0.05, **p≤0.01.

3.2.5. TRAIL and Dinaciclib combined treatment does not synergise with platinum-based chemotherapy in the KP model of NSCLC

The current first-line therapy for advanced NSCLC patients that lack targetable mutations (e.g. *EGFR*, *ALK* or *ROS1*) and have a tumour proportion score for PD-L1 lower than 50% is platinum-based chemotherapy (Hanna et al., 2017; Gandhi et al., 2018). However, this treatment often shows very limited effect and the combination of chemotherapy with other therapeutic strategies is under constant evaluation. Therefore, it was next investigated whether the anti-tumour efficacy of the combined treatment of TRAIL and Dinaciclib could improve current chemotherapy. To this end, Carboplatin was chosen as a commonly used platinum-based chemotherapeutic agent.

KP mice were treated with Carboplatin alone, the combination of TRAIL and Dinaciclib, or the triple treatment starting 12 weeks after Ad-Cre administration following the schedule shown in Figure 3.20 A. Treated animals were allowed to reach their humane endpoint. Carboplatin treatment resulted in a mild increase in the survival of the mice as compared to vehicle-treated mice (Figure 3.20 B). The group size, however, was too small to obtain statistically significant results. Similarly, although mice treated with TRAIL and Dinaciclib survived slightly longer than Carboplatin-treated mice, the big variability and the small number of experimental animals in the Carboplatin group prevent any conclusion.

For the assessment of the synergistic potential of TRAIL and Dinaciclib with Carboplatin, two different doses of Dinaciclib were tested, 15 mg/kg and 30 mg/kg. In both cases, the triple combination of TRAIL, Dinaciclib and Carboplatin decreased the survival of the mice as compared to the TRAIL- and Dinaciclib-treated ones, although this decrease was not significant (Figure 3.20 B). Overall, these results suggest that the combination of TRAIL, Dinaciclib and Carboplatin is not synergistic and a different treatment regime should be tested.

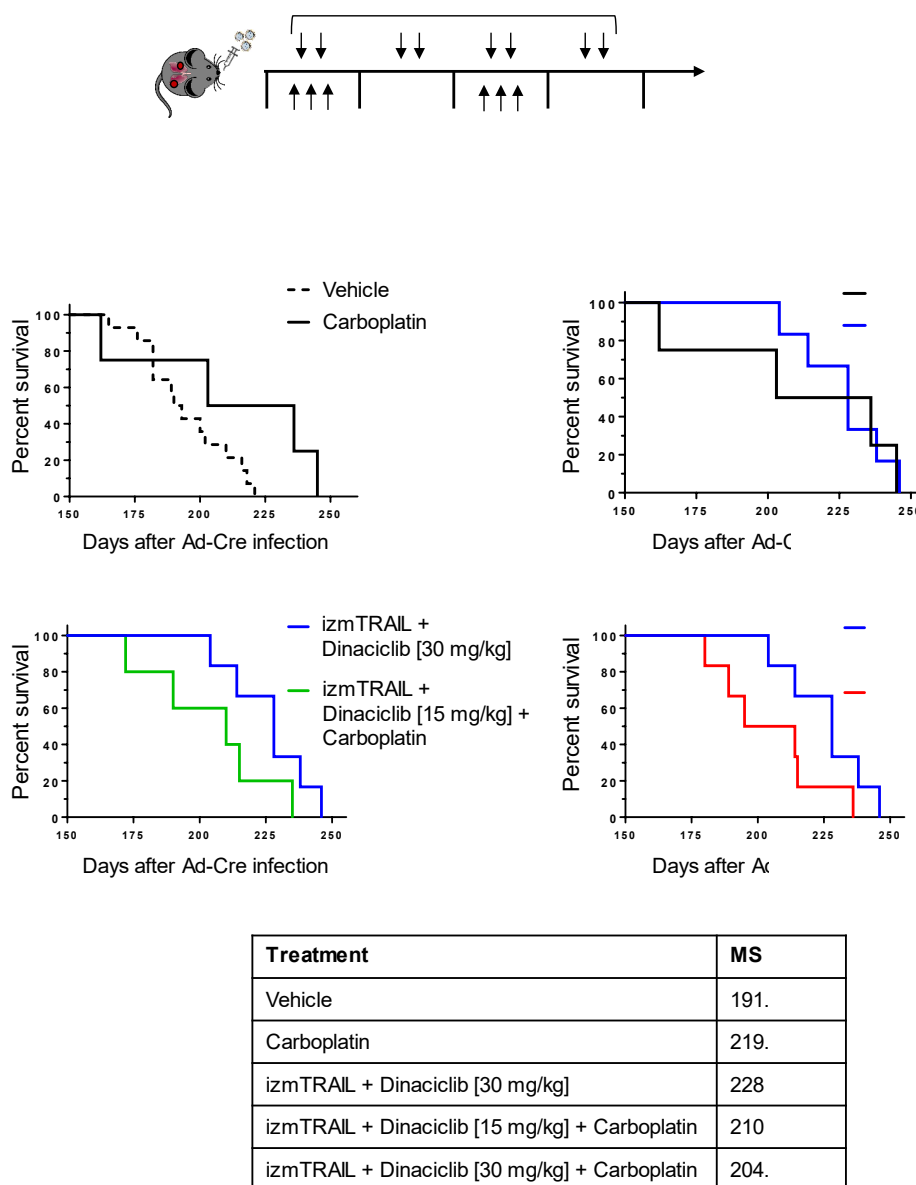


Figure 3.20: TRAIL and Dinaciclib combination treatment does not synergise with the standard-of-care carboplatin.

(A) Experimental treatment schedule is shown. KP mice were subjected to intranasal administration of Ad-Cre to induce the expression of oncogenic *Kras*^{G12D} and *Tp53*^{R172H}. Mice were treated with Dinaciclib at 30 mg/kg or 15mg/kg as indicated, izmTRAIL at 5 mg/kg and/or Carboplatin at 25 mg/kg at the indicated times after Ad-Cre delivery (vehicle: n=14 mice; Carboplatin: n=4 mice; izmTRAIL + Dinaciclib: n=6 mice; izmTRAIL + Dinaciclib [15 mg/kg] + Carboplatin: n=5 mice; izmTRAIL + Dinaciclib [30 mg/kg] + Carboplatin: n=6 mice).

(B) Kaplan-Meier survival curves of mice receiving the indicated treatments. Median survival for each group is indicated. Statistical analysis was performed using log-rank test.

3.2.6. Dinaciclib equally reduces the viability of KP cell lines derived from chemotherapy-treated or -naïve animals

As explained above, the first treatment option NSCLC patients most often receive is chemotherapy and novel therapies are often tested in patients that have received such treatment. In order to test whether the novel combination studied in this thesis is still effective in chemotherapy-treated tumours, cell lines were generated from tumours of Carboplatin- or vehicle-treated KP mice. For this purpose, KP mice were treated with Carboplatin or vehicle at weeks 12 and 14 following Ad-Cre delivery (Figure 3.21 A). Mice were sacrificed 9 weeks after the last chemotherapeutic dosage (week 27 following Ad-Cre administration), when they started showing signs of distress. At this point, there was no difference in weight between vehicle or Carboplatin-treated lungs (Figure 3.21 B). Four cell lines were generated from each group: KPV1, KPV2, KPV3 and KPV4 from vehicle-treated lung tumours and KPC1, KPC2, KPC3 and KPC4 from Carboplatin-treated lung tumours (Figure 3.21 C). To confirm the exclusive presence of cancer cells, cells were sorted for their EpCAM positivity, which is a transmembrane glycoprotein overexpressed in solid tumours of epithelial origin such as NSCLC (Piyathilake et al., 2000; Went et al., 2004) (Figure 3.21 D). Similarly, the expression of oncogenic *Kras*^{G12D} and *Tp53*^{R172H} (Figure 3.21 E) as well as the surface expression of mTRAIL-R was also verified in these cells (Figure 3.21 F).

Following the establishment of the cell lines, KPV and KPC cells were treated with increasing concentrations of Carboplatin to determine their sensitivity *in vitro*. A 50% reduction in the viability of KPV cells was observed after 50 µM Carboplatin and these cells were completely killed by 100 µM Carboplatin after 72 h (Figure 3.21 G). KPC cells, however, were significantly less sensitive to 50 µM Carboplatin but died upon 100 µM Carboplatin and thus, were partially resistant.

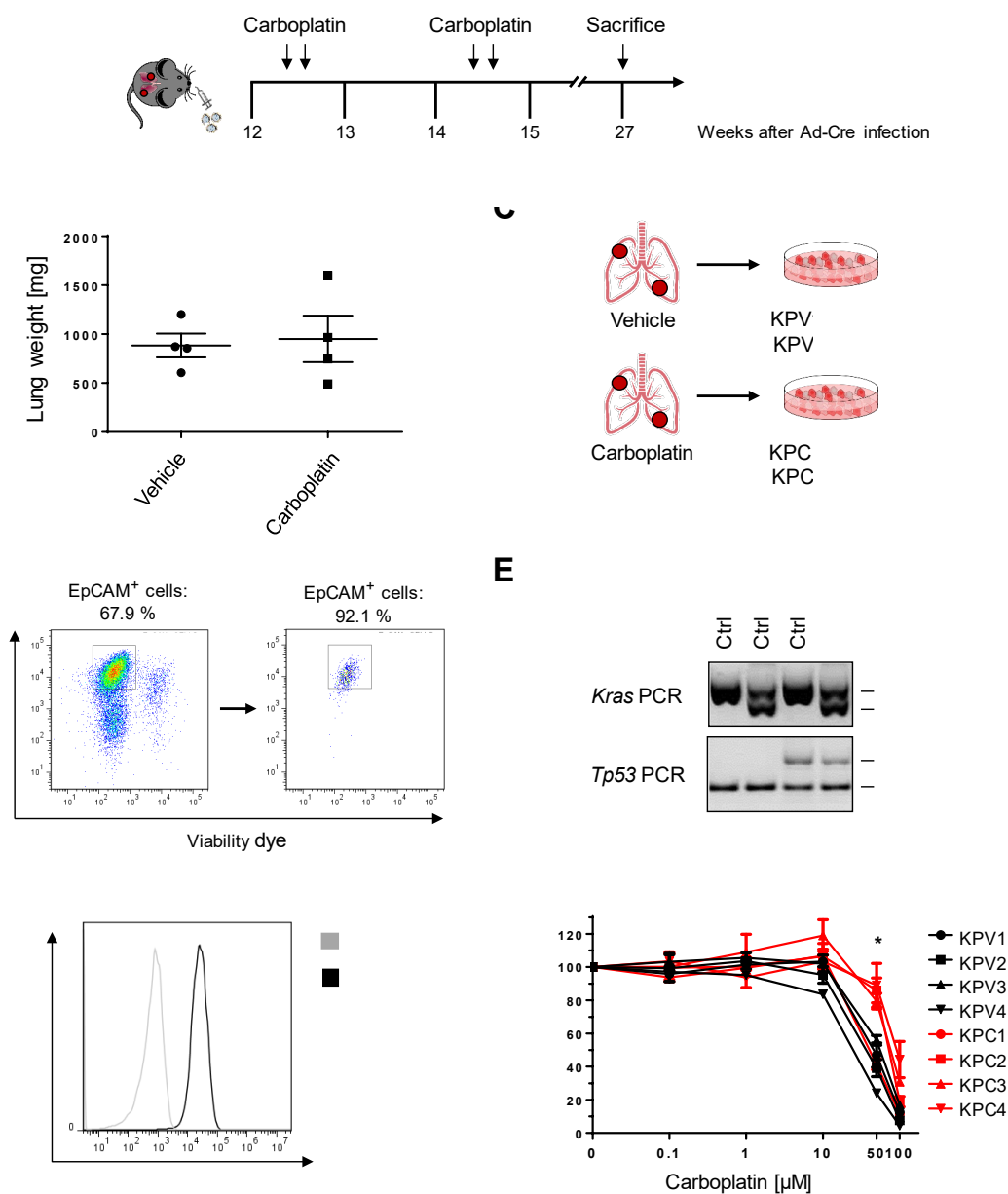


Figure 3.21: Generation of cell lines from chemotherapy-naïve or -treated KP mice.

(A) Experimental treatment schedule is shown. KP mice were subjected to intranasal administration of Ad-Cre to induce the expression of oncogenic *Kras*^{G12D} and *Tp53*^{R172H}. Mice were treated with Carboplatin at 25 mg/kg at the indicated times (n=4 mice per group).

(B) Mice were sacrificed at the humane endpoint and the lungs were weighted as a measure of their tumour content. Data are shown as means \pm SEM. Dots represent lungs of individual mice. Statistical analysis was performed using one-way ANOVA.

(C) Lung tumours were incubated in cultured dishes for the generation of cell lines.

(D) KP lung tumour-derived cell lines were sorted for their EpCAM positivity. Representative FACS profile of a cell line before and after sorting, gated on its EpCAM positive live cells.

(Figure legend continues on next page)

(E) The genotype of established cell lines was confirmed by PCR. Three control samples and a representative cell line is shown. *wt*: wild-type; *mut*: mutated.

(F) The expression of mTRAIL-R was confirmed by FACS. Representative FACS profile is shown.

(G) Cell lines derived from vehicle- and Carboplatin-treated KP mice were treated with carboplatin at the indicated concentrations. 72 h later, cell viability was quantified. Data represent means \pm SEM of three independent experiments. Statistical analysis was performed using Student's t-test. KPV cell lines were compared to KPC cell lines at each Carboplatin concentration. * $p \leq 0.05$.

Next, the KPV and KPC cell lines were treated with increasing concentrations of TRAIL in the presence or absence of Dinaciclib. Strikingly, treatment with Dinaciclib alone had a big impact on the viability of all cell lines (Figure 3.22). Nevertheless, the addition of TRAIL significantly decreased the viability of most of the cell lines, indicating that the combination of TRAIL and Dinaciclib might be a better therapeutic strategy.

Interestingly, there were no differences between the response of KPV and KPC cell lines to Dinaciclib monotherapy or combined TRAIL and Dinaciclib treatment, suggesting that these treatment options could be effective in cancers that have been exposed to chemotherapy.

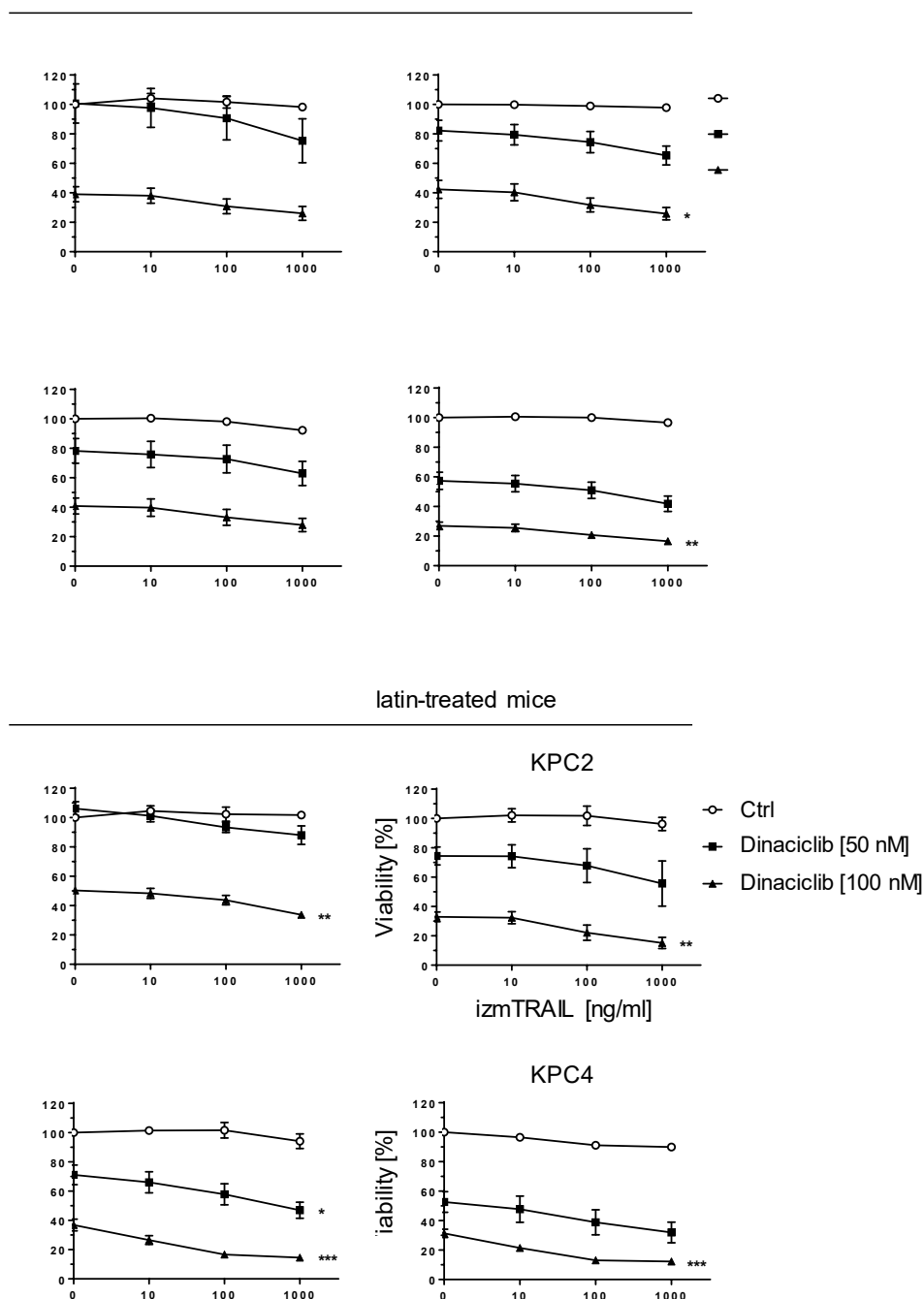


Figure 3.22: Dinaciclib reduces the viability of KP cell lines, including those derived from chemotherapy-treated mice.

The indicated KP cell lines derived from (A) vehicle- or (B) Carboplatin-treated mice were pre-incubated with 50 nM or 100 nM Dinaciclib for 15 min and subsequently stimulated with izmTRAIL at the indicated concentration. Cell viability was quantified 48 h later. Data are shown as means \pm SEM of three independent experiments. Statistical analysis was performed using Student's t-test. In each cell line, for each Dinaciclib concentration, the viability at 0 ng/ml izmTRAIL was compared to the viability at 1000 ng/ml izmTRAIL. * $p \leq 0.05$, ** $p \leq 0.01$, *** $p \leq 0.001$.

3.3. Investigation of the impact of the TRAIL- and Dinaciclib-comprising therapy on the tumour microenvironment.

It is now well established that the immune system plays a crucial role both during tumour progression and treatment response (Hanahan and Weinberg, 2011; Balkwill and Mantovani, 2012). Consequently, new strategies to target the tumour immune microenvironment are constantly being devised. Interestingly, although Dinaciclib did not show any benefit as a single agent treatment in a phase 2 NSCLC trial (Stephenson et al., 2014), some of the drug-related adverse effects observed included neutropenia and leukopenia, suggesting that Dinaciclib might be affecting the immune system. Similarly, as detailed in the introduction, TRAIL is also a known immunomodulator (Beyer et al., 2019). It was therefore of interest to assess the impact of TRAIL and Dinaciclib combination therapy on the tumour microenvironment.

3.3.1. TRAIL- and Dinaciclib-comprising therapy modulates the tumour microenvironment

To this end, the autochthonous KP model was used as, in these mice, lung tumours are initiated and develop in their natural environment, even though, as explained later in section 3.5, it does not fully recapitulate the immunogenicity of human NSCLC. KP mice were treated with TRAIL and/or Dinaciclib three times during two alternating weeks, starting 12 weeks after Ad-Cre administration, and subsequently sacrificed at week 16 (Figure 3.23 A). Determination of the CD45 positivity in the lung sections revealed that there was a drastic reduction in the number of tumour-infiltrating leukocytes upon TRAIL, Dinaciclib or their combination (Figure 3.23 B and C). These results were confirmed by flow cytometry immune-profiling, showing that the number of CD45 positive cells was significantly decreased in the tumour-bearing lungs of mice treated with Dinaciclib alone or in combination with TRAIL (Figure 3.23 D). TRAIL treatment, albeit more modestly, also led to a reduction in the number of CD45 positive cells.

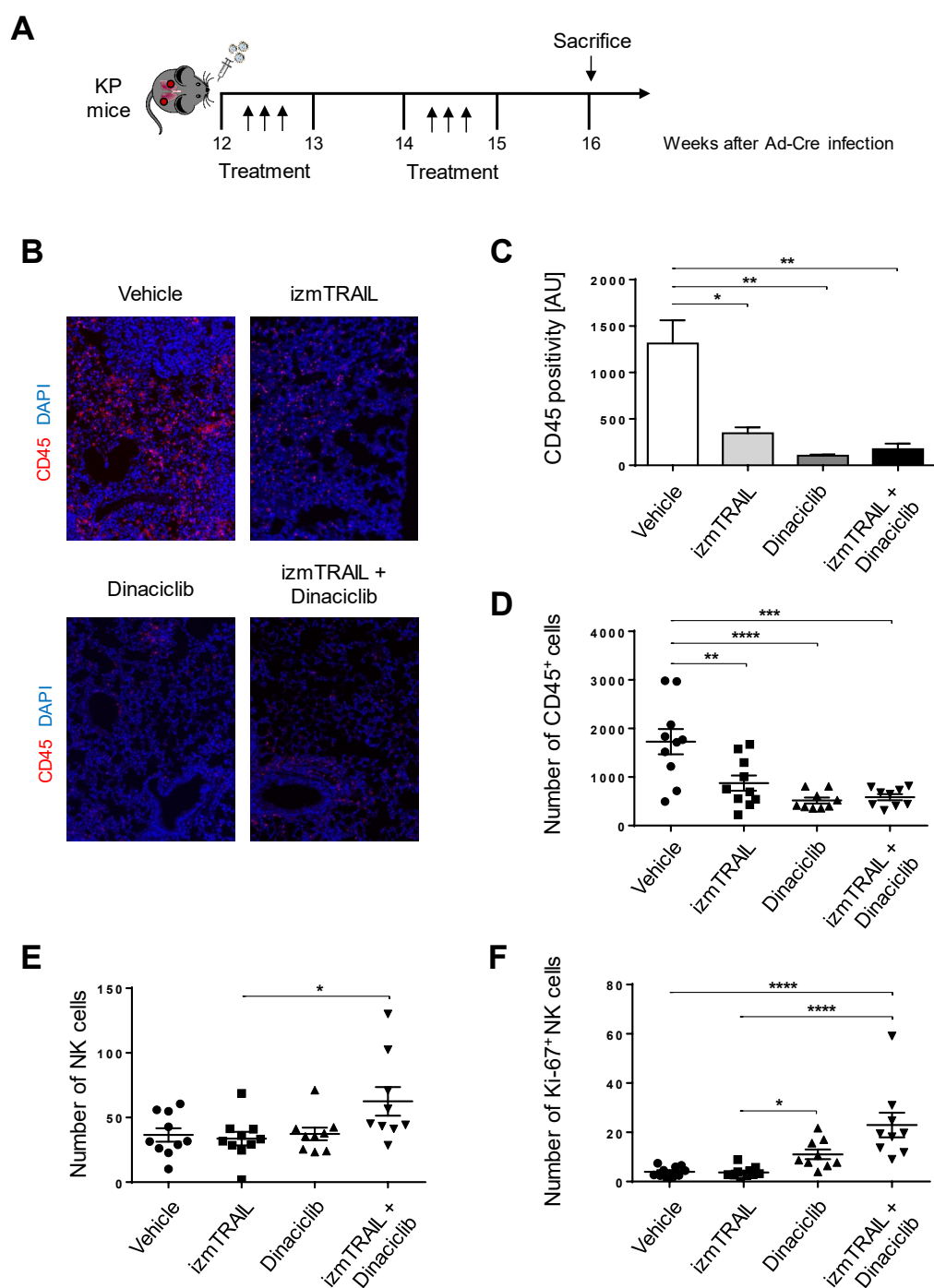


Figure 3.23: TRAIL and Dinaciclib treatment modifies the composition of the tumour immune microenvironment.

(A) Experimental treatment schedule is shown. KP mice were subjected to intranasal administration of Ad-Cre to induce the expression of oncogenic *Kras*^{G12D} and *Tp53*^{R172H}. Mice were treated with Dinaciclib [30 mg/kg] and/or izmTRAIL [5 mg/kg] at the indicated times. (B) Representative immunofluorescence images (40x) of lung sections from mice receiving the indicated treatments and stained with for CD45 (red). Nuclei were stained with DAPI (blue) (n=3 mice per treatment).

(Figure legend continues on next page)

(C) Quantification of CD45 positivity (arbitrary units (AU)) in the lung sections of mice treated as indicated. 10 microscopic fields were analysed per mouse for 3 mice per group. Results are presented as mean values \pm SEM.

(D, E, F) Flow cytometry analysis of the indicated immune cell subpopulations of lung homogenates from mice treated as indicated. Graphs show the absolute number of the indicated subpopulations per mg of lung tissue. NK cells were gated as NKp46⁺ CD3⁻ from CD45⁺ live cells. (vehicle, izmTRAIL: n=10 mice per group; Dinaciclib, izmTRAIL + Dinaciclib: n=9 mice per group).

Statistical analysis was performed using one-way ANOVA. * $p \leq 0.05$, ** $p \leq 0.01$, *** $p \leq 0.001$, **** $p \leq 0.0001$.

Experiments and analyses were performed in collaboration with Dr. Antonella Montinaro.

Furthermore, the individual immune subsets were analysed. Overall, while the number and relative percentage of all major immune cell subtypes were reduced in the lungs of mice treated with TRAIL and Dinaciclib combination therapy, the number of NK cells infiltrated in the tumours of mice treated with the combined treatment were increased (Figure 3.23 E). Interestingly, the therapy also induced the proliferation of NK cells in the lungs of these animals, as quantified by the Ki-67 positive NK cells (Figure 3.23 F). Altogether, these data demonstrate that the combination of TRAIL and Dinaciclib modulates the tumour microenvironment in KP mice.

3.3.2. NK cells are not responsible for the anti-tumour response in Dinaciclib-treated mice

In view of the previous results, it was hypothesised that the increased infiltration and proliferation of NK cells was responsible for the anti-neoplastic effects observed in KP mice after Dinaciclib treatment. To investigate whether the absence of NK cells abrogated the efficacy of the therapeutic strategies tested so far, NK cells were pharmacologically depleted in this model. KP mice were treated with anti-NK1.1 antibody starting 12 weeks after Ad-Cre administration and subsequently treated with vehicle, Dinaciclib or the TRAIL and Dinaciclib combination following the schedule depicted in Figure 3.24 A. The efficiency of the depletion of NK cells was confirmed at the experimental end-point by flow cytometry (Figure 3.24 B). In mice bearing NK cells, treatment with Dinaciclib only or its combination with TRAIL resulted in a decrease in lung weight, reflecting a reduction in the tumour burden (Figure 3.24 C). Surprisingly, depletion of NK cells did not affect the reduction in lung weight upon single or combination treatments (Figure 3.24 C).

It can, thereby, be concluded that despite the increased infiltration of NK cells in lungs of tumour-bearing mice following Dinaciclib treatment, these immune cells do not mediate, at least strongly, the anti-tumour response elicited by Dinaciclib when administered alone or in combination with TRAIL to KP mice.

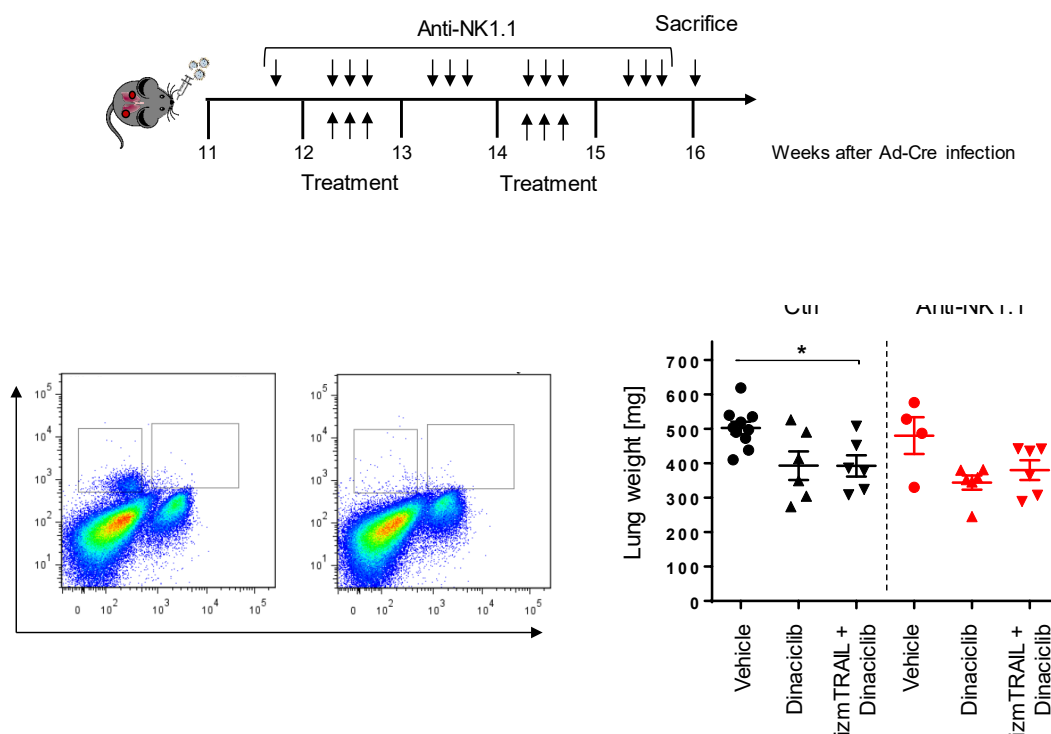


Figure 3.24: NK cells are not responsible for the Dinaciclib-induced anti-tumour response.

(A) Experimental treatment schedule is shown. KP mice were subjected to intranasal administration of Ad-Cre to induce the expression of oncogenic *Kras*^{G12D} and *Tp53*^{R172H}. Mice were treated with Dinaciclib [30 mg/kg], izmTRAIL [5 mg/kg] and/or anti-NK1.1 antibody [200 µg/mouse] at the indicated times (ctrl/vehicle: n=10 mice; ctrl/Dinaciclib, ctrl/izmTRAIL + Dinaciclib, anti-NK1.1/Dinaciclib, anti-NK1.1/izmTRAIL + Dinaciclib: n=6 mice per group; anti-NK1.1/vehicle: n=4 mice).

(B) The depletion efficacy of the anti-NK1.1 antibody was confirmed by flow cytometry. NK cells were gated as NKp46⁺ CD3⁻ from CD45⁺ live cells. Representative dot-plots are shown. (C) 16 weeks after Ad-Cre infection, mice were sacrificed and their lungs weighted as a measure of their tumour content. Data are presented as means ± SEM. Dots represent individual mice. Statistical analysis was performed using one-way ANOVA. *p<0.05.

3.3.3. The adaptive immunity is required for the anti-cancer effect exerted by Dinaciclib

Since NK cells were not responsible for the anti-tumour effect exerted by Dinaciclib *in vivo*, the role of other subsets of the immune system was next addressed. When comparing the different mouse models employed so far for the assessment of the therapeutic potential of the TRAIL and Dinaciclib combination, an interesting observation was made. While Dinaciclib monotreatment led to a significant reduction in the tumour burden of KP mice (Figure 3.18), it did not have a marked impact on the tumours of A549 xenografts in SCID Beige mice, which lack NK, T and B cells (Figure 3.17). This was intriguing because it suggested that, for its efficacy *in vivo*, Dinaciclib requires the presence of NK, T and/or B cells, which are the immune subsets that SCID Beige mice lack. Since the requirement of NK cells had already been excluded, and considering that CDKs, including the Dinaciclib-targeted CDK1, CDK2 and CDK5 have been shown to play a role in T cell proliferation and migration (Wells and Morawski, 2014), the involvement of the adaptive immunity in the response to TRAIL and/or Dinaciclib *in vivo* was investigated.

To do so, KP59 cells, which were generated from a KP C57BL/6 mouse, as described before, were firstly assessed for their sensitivity to TRAIL and Dinaciclib combination treatment *in vitro*. As shown in Figure 3.25 A, the viability of KP59 cells was reduced by Dinaciclib treatment *in vitro*. Yet, this was further decreased by the addition of TRAIL. These cells were then injected intradermally in the flank of *WT* or *Rag1*^{-/-} mice, which produce no mature T or B cells (Mombaerts et al., 1992) (Figure 3.25 B). One week after cell injection, tumours were detected and the mice were randomised (Figure 3.25 C). KP tumour-bearing mice received three doses of vehicle, TRAIL, Dinaciclib, or the combination of TRAIL and Dinaciclib during three consecutive weeks (Figure 3.26 A). In *WT* mice, treatment with TRAIL and Dinaciclib or Dinaciclib alone, significantly reduced the growth of KP59 tumours (Figure 3.26 B and C). The anti-tumour effect exerted by Dinaciclib was, nevertheless, prevented in *Rag1*^{-/-} mice. In these animals, tumours treated with Dinaciclib only grew comparably to the vehicle-treated tumours, demonstrating that the adaptive immunity is required for the anti-cancer effect that Dinaciclib mediates *in vivo*. Interestingly, the anti-tumour effect of the combination of TRAIL and Dinaciclib was only partially rescued in *Rag1*^{-/-} mice, suggesting that the combined therapy triggers an additional mechanism independent of T and B cells and hence, it works differently than Dinaciclib alone.

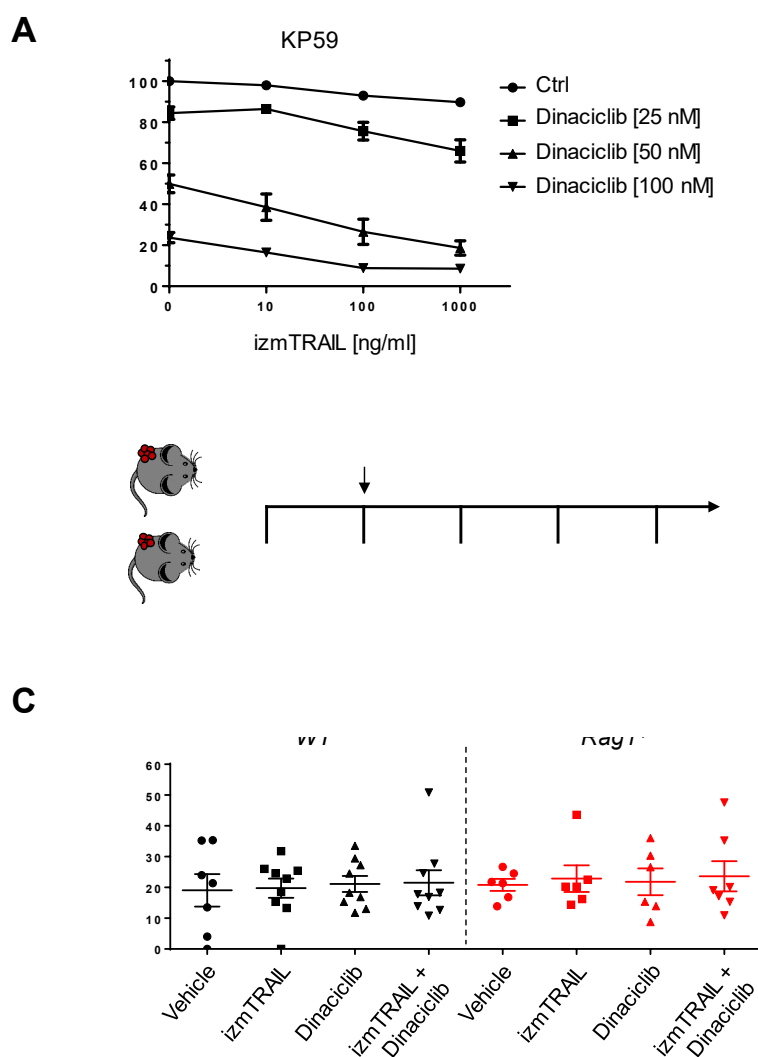


Figure 3.25: Experimental control of the treatment of *WT* and *Rag1*^{-/-} mice with TRAIL and Dinaciclib therapy.

(A) KP59 cells were pre-incubated with the indicated concentration of Dinaciclib for 15 min and subsequently stimulated with the indicated concentration of izmTRAIL. 48 h later, cell viability was quantified. Data are shown as means \pm SEM of three independent experiments. (B) Experimental treatment schedule is shown. KP59 cells were injected intradermally in the flank of *WT* or *Rag1*^{-/-} mice. (C) Tumour volume was measured one week after the injection of the cells and mice were randomised into the treatment groups. Data are presented as means \pm SEM. Dots represent individual mice. Statistical analysis was performed using one-way ANOVA.

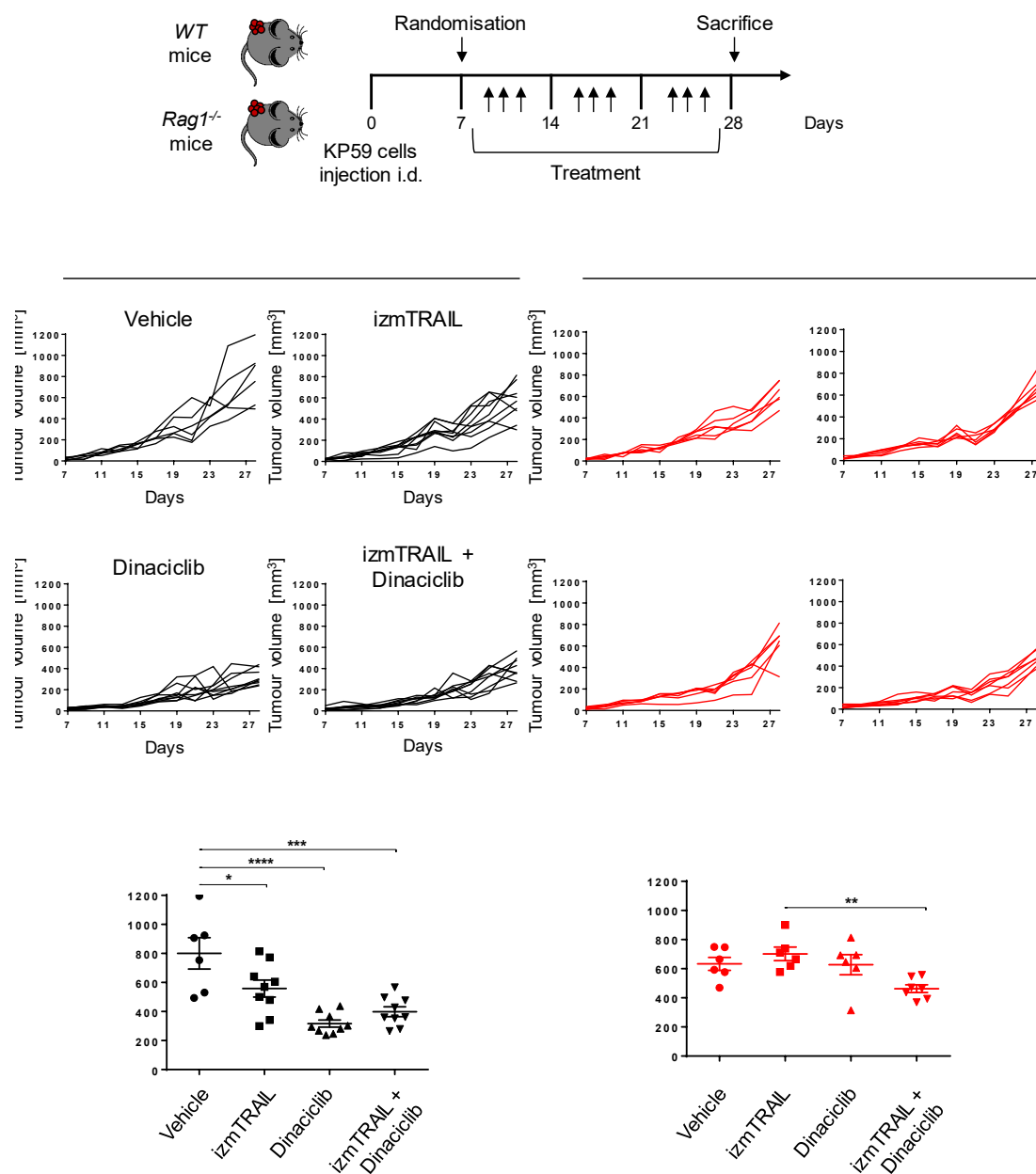


Figure 3.26: Dinaciclib requires the adaptive immunity for its anti-tumour effect *in vivo*.

(A) Experimental treatment schedule is shown. KP59 cells were injected intradermally in the flank of WT or Rag1^{-/-} mice. Mice were treated with Dinaciclib at 30 mg/kg and/or izmTRAIL at 5 mg/kg at the indicated times (WT/vehicle: n=6 mice; WT/izmTRAIL, WT/Dinaciclib, WT/izmTRAIL + Dinaciclib: n=9 mice per group; Rag1^{-/-}/vehicle, Rag1^{-/-}/izmTRAIL, Rag1^{-/-}/Dinaciclib: n=6 mice per group; Rag1^{-/-}/izmTRAIL + Dinaciclib: n=7 mice).

(B) Mice were individually tracked and tumour volume was measured every 2-3 days. Each line represents one mouse.

(C) Mice were sacrificed at day 28 and tumour volume was measured. Data are shown as means \pm SEM. Dots represent individual mice. Statistical analysis was performed using one-way ANOVA. *p<0.05, ***p<0.001, ****p<0.0001, **p<0.01.

Overall, the results presented in this section show that TRAIL and Dinaciclib modulate the tumour immune microenvironment. Whilst T and/or B cells play a crucial role in the anti-tumour effects mediated by Dinaciclib, the combined treatment with TRAIL and Dinaciclib exerts some additional, adaptive immunity-independent anti-tumour activity.

3.4. Identification of the Dinaciclib targets that mediate TRAIL resistance

Work by Lemke *et al.*, demonstrated that selective CDK9 inhibition overcomes TRAIL resistance (Lemke et al., 2014a). In the present study, it has so far been shown that the CDK9 inhibitor Dinaciclib sensitises to TRAIL-induced apoptosis in a wide variety of cancers and that this combination is effective *in vivo*. Nonetheless, as noted previously, Dinaciclib inhibits other CDKs in addition to CDK9, namely CDK1, CDK2 and CDK5 (Parry et al., 2010). Thereby, it was of interest to validate whether the Dinaciclib target responsible for TRAIL sensitisation was CDK9 and not an additional CDK or a combination thereof.

3.4.1. CDK9 is the Dinaciclib-target responsible for TRAIL sensitisation in human cells

Using A549 as a model cell line, the impact of knocking down CDK1, CDK2, CDK5 or CDK9 on TRAIL sensitivity was tested (Figure 3.27 A and B). Although the knockdown of CDK1 reduced slightly the viability of A549 cells, it did not sensitise them to TRAIL-induced apoptosis more than the control cells. Similarly, silencing of CDK2 or CDK5 had no impact on the sensitisation to TRAIL. The downregulation of CDK9, however, achieved a similar decrease in viability than Dinaciclib when combined with TRAIL. Moreover, treatment with the CDK9-specific inhibitor NVP-2 (Olson et al., 2018) sensitised A549 cells to TRAIL-induced cell death to the same degree as treatment with Dinaciclib, suggesting that CDK9 is the Dinaciclib target mediating TRAIL resistance in A549 cells (Figure 3.27 C and D).

With the purpose of validating these results in cell lines from different tissue origins, a panel of ten different cell lines were treated side-by-side with NVP-2 or Dinaciclib in the presence of increasing concentrations of TRAIL. In line with the previous data, NVP-2 and Dinaciclib equally sensitised all the cell lines to TRAIL-induced apoptosis (Figure 3.28).

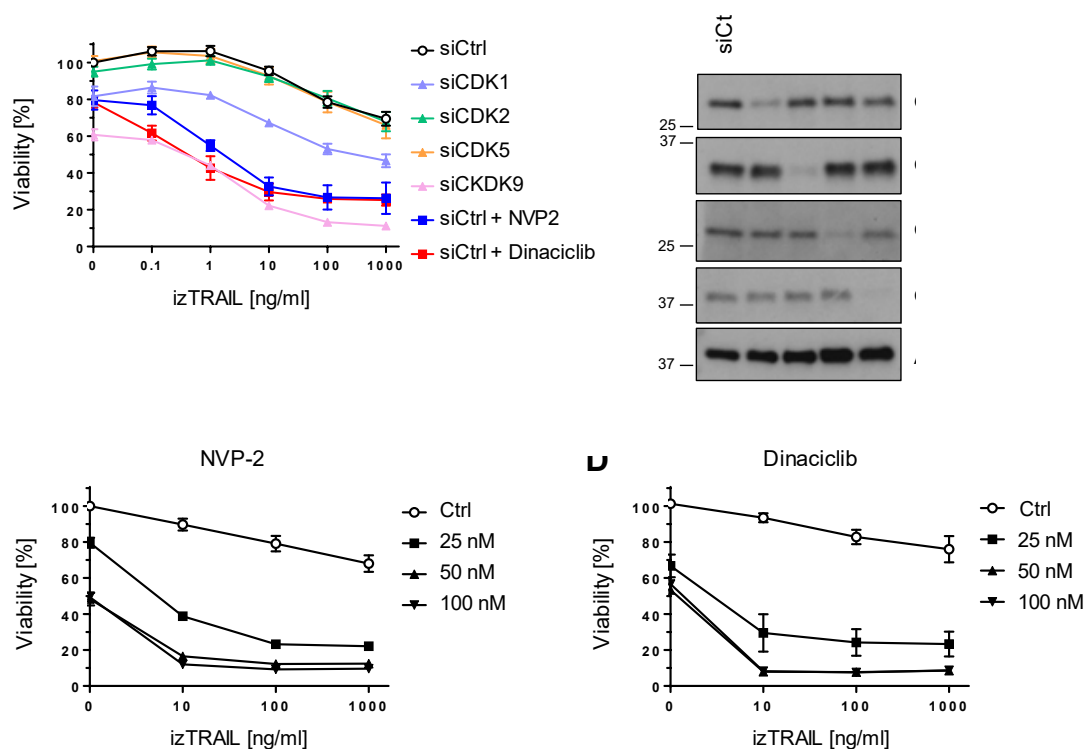


Figure 3.27: CDK9 is the Dinaciclib-target responsible for TRAIL sensitisation in A549 cells.

(A) A549 cells were transiently transfected with the indicated siRNAs for 48 h and subsequently stimulated with Dinaciclib [25 nM], NVP-2 [25 nM] and/or izTRAIL at the indicated concentrations. Cell viability was determined 24 h later. Data are presented as means \pm SEM of three independent experiments.

(B) 48 h after transfection with siRNA, cells were lysed and the knockdown efficiency was analysed by Western Blotting. Representative western blots of three independent experiments are shown.

(C, D) A549 cells were treated with NVP-2 or Dinaciclib at the indicated concentrations for 15 min and subsequently stimulated with izTRAIL at the indicated concentrations. Cell viability was quantified 48 h later. All values are means \pm SEM of three independent experiments.

Of note, NVP-2 treatment inhibited the phosphorylation of Ser2 of RNA Pol II and, consequently, downregulated the expression of FLIP and Mcl-1 with the same efficiency observed for Dinaciclib, without affecting any other components of the DISC or downstream pro- and anti-apoptotic factors (Figure 3.29).

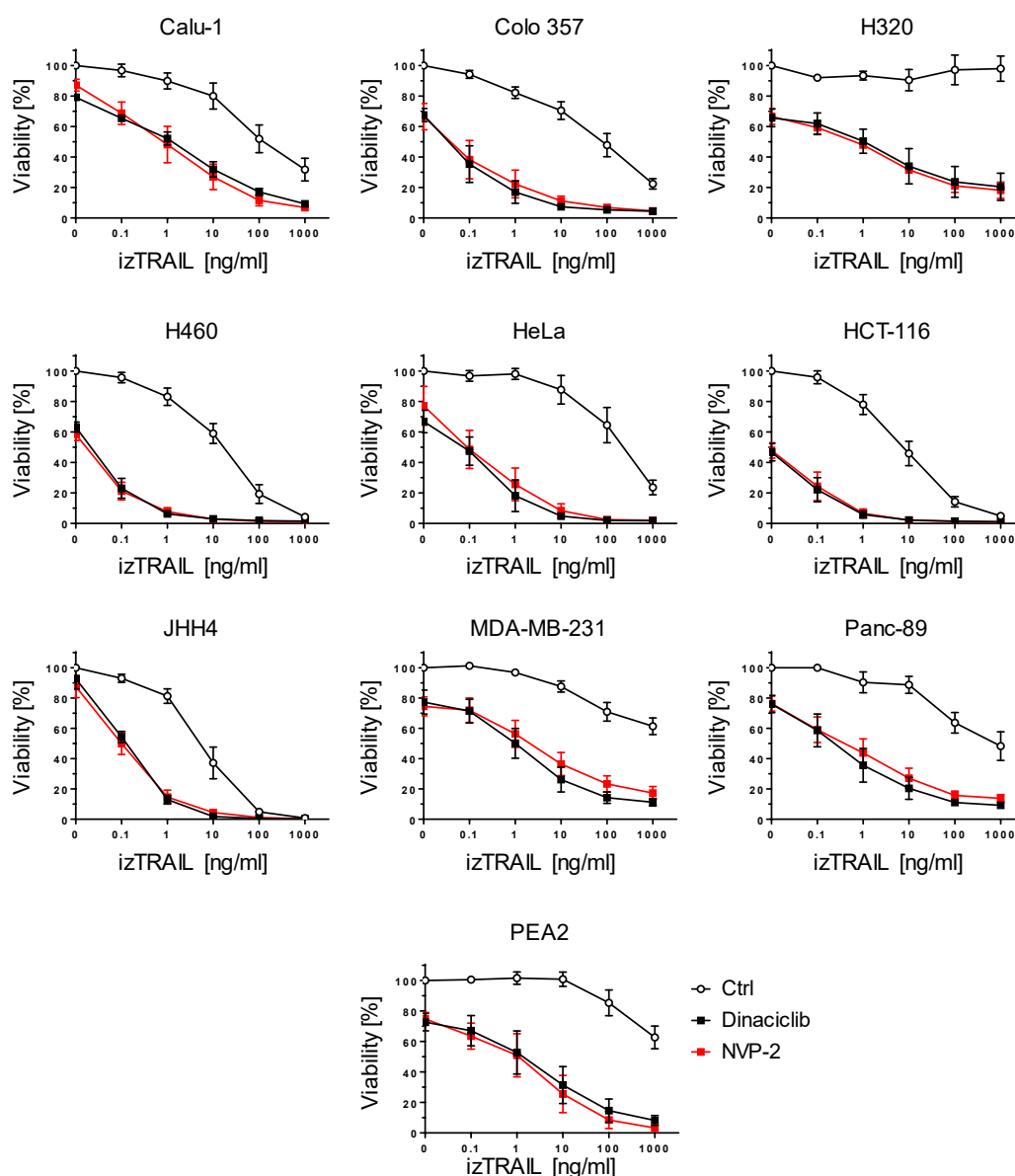


Figure 3.28: Specific CDK9 inhibition sensitises a panel of human cancer cell lines to TRAIL-induced apoptosis.

Cells were pre-incubated with or without 25 nM Dinaciclub or 25 nM NVP-2 for 15 min and then treated with the indicated concentrations of izTRAIL. Cell viability was quantified after 24 h. Data represent means \pm SEM of three independent experiments.

Taken together, these results show that CDK9 is the Dinaciclub target responsible for TRAIL sensitisation, in all the human cancer cells tested in this study.

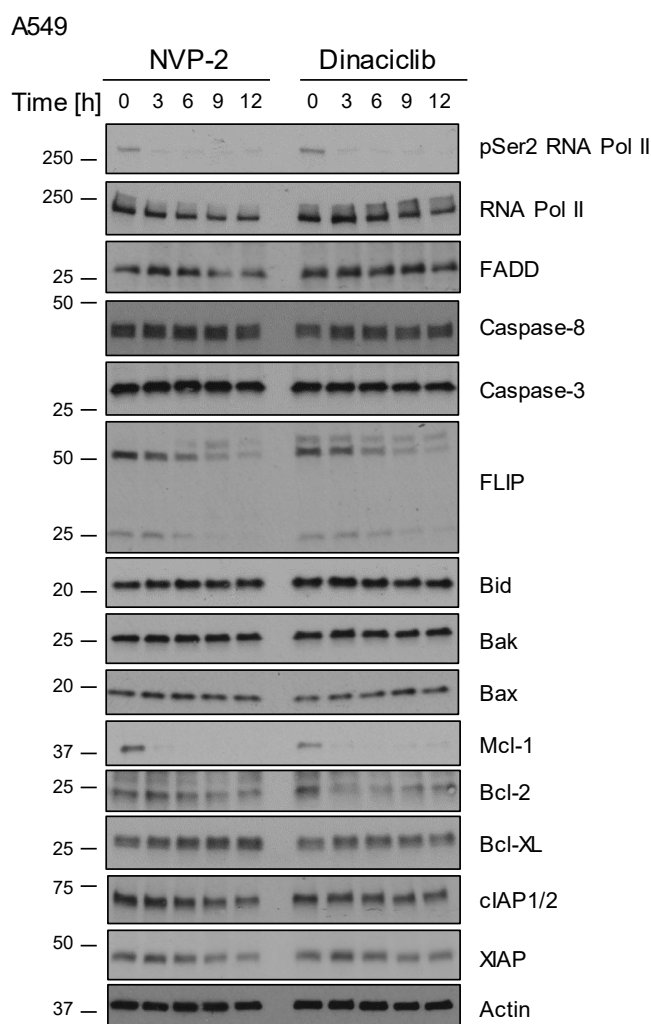


Figure 3.29: Specific CDK9 inhibition breaks TRAIL resistance by downregulating FLIP and Mcl-1.

A549 cells were treated with 25 nM NVP-2 or 25 nM Dinaciclib for the indicated time before cell lysis and analysis of the lysates by Western Blotting. Blots from one of two independent experiments are shown.

3.4.2. CDK9 downregulation is not sufficient to sensitise KP cells to TRAIL-induced apoptosis

During the testing of different CDK9 inhibitors in cell lines derived from the KP mouse model, an unexpected observation was made: the CDK9 inhibitor SNS-032 did not sensitise KP802T4 and KP59 cells to TRAIL even at concentrations of 500 nM (Figure 3.30 A and C). This was surprising, since Dinaciclib sensitised both cell lines to TRAIL-induced cell death. While Dinaciclib inhibited the phosphorylation of RNA Pol

II at 100 nM, treatment with SNS-032 did not influence this phosphorylation (Figure 3.30 B).

Additionally, the highly specific CDK9 inhibitor NVP-2 did also not break the resistance of KP59 cells to TRAIL, suggesting that inhibiting CDK9 was not sufficient to sensitise these cells to TRAIL-induced apoptosis (Figure 3.30 D).

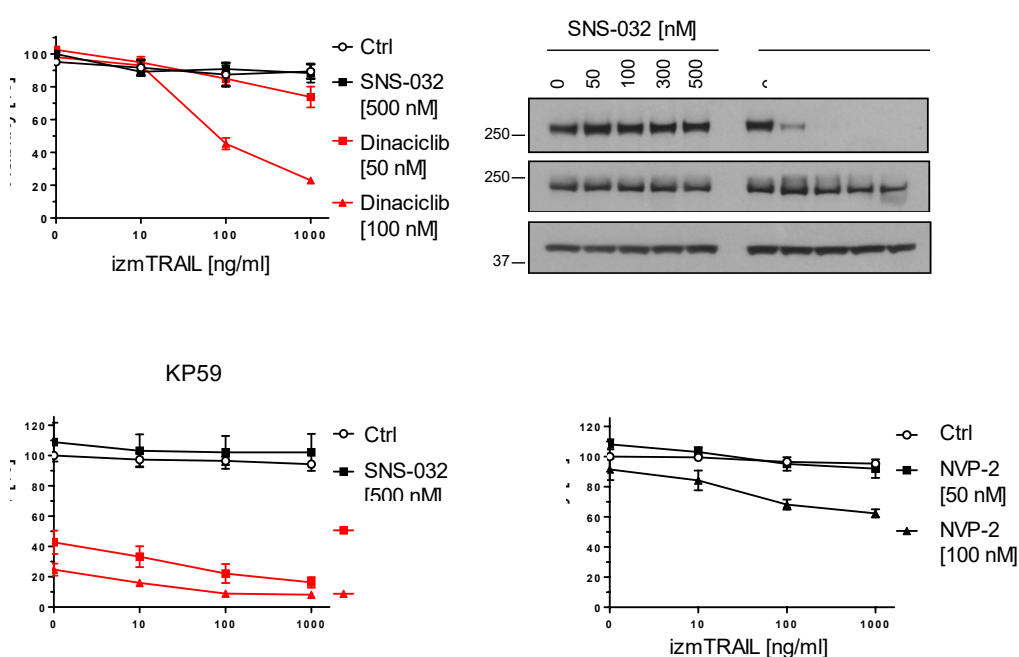


Figure 3.30: Dinacliclib but not SNS-032 or NVP-2 sensitises KP cell lines to TRAIL-induced apoptosis.

(A) KP802T4 cells were pre-incubated with the indicated concentrations of Dinacliclib or SNS-032 for 15 min and subsequently stimulated with the indicated concentrations of izmTRAIL. Cell viability was quantified 24 h later. Data represent means \pm SEM of three independent experiments.

(B) KP802T4 cells were treated with SNS-032 or Dinacliclib at the indicated concentrations and 24 h later cells were lysed and analysed by Western Blotting. Representative Western blots of three independent experiments are shown.

(C, D) KP59 cells were pre-incubated with the indicated concentrations of Dinacliclib, SNS-032 or NVP-2 for 15 min and subsequently stimulated with the indicated concentrations of izmTRAIL. Cell viability was quantified 48 h later. Data represent means \pm SEM of three independent experiments.

Since pharmacological inhibition of CDK9 by SNS-032 or NVP-2 was not sufficient to synergise with TRAIL, it was of interest to test if the knockdown of CDK9 was sufficient to achieve so. Although the siRNA-mediated CDK9 knockdown in KP394T4 and KP59 cells was profound (Figure 3.31 B and D), the viability of CDK9-silenced cells was not affected by co-stimulation with TRAIL (Figures 3.31 A and C). The concomitant downregulation of CDK9 with either of the other targets of Dinaciclib was also attempted. However, none of these combinations sensitised KP394T4 cells to TRAIL (Figure 3.31 A).

It is possible that the absence of sensitisation observed was due to remaining levels of CDK9 protein after an incomplete siRNA-mediated knockdown. In order to overcome this technical difficulty, the first approach was to try to generate CDK9 KO KP cells using the CRISPR/Cas9 technology. Nevertheless, whilst different guide RNAs targeting different regions of CDK9 were used, no CDK9 KO cells were obtained, most likely because the presence of this protein is essential for cell survival.

Alternatively, an inducible shRNA system was employed. PCC8 KP cells stably expressing CDK9-targeting shRNA and red fluorescent protein (RFP) under the control of a tetracycline-dependent promoter were obtained from Prof. S. Lowe. PCC8 cells were transfected with three different shRNAs: shRenilla as a control and two CDK9-targeting shRNA clones (shCDK9.60 and shCDK9.21). Both parental non-transfected PCC8 cells and shRNA-transfected non-induced PCC8 cells were markedly sensitised to TRAIL-induced apoptosis upon treatment with Dinaciclib (Figure 3.32 A, B). To maximise the efficiency of the downregulation of CDK9, shRNA-transfected PCC8 cells were sorted for the highest shRNA expressers after Doxycycline (Dox) administration (Figure 3.32 C). Treatment of shCDK9-expressing PCC8 cells with TRAIL after Dox induction only marginally reduced cell viability in the shCDK9.21-expressing cells, without affecting the viability of the shCDK9.60 expressing cells (Figure 3.32 D). Although in both shCDK9-expressing PCC8 cells an efficient knockdown was achieved, this was not sufficient to inhibit the phosphorylation of RNA Pol II at Ser2 as it was upon Dinaciclib treatment (Figure 3.32 E). The fact that the shCDK9.21-expressing cells showed a higher sensitivity to TRAIL may be explained by the bigger downregulation of CDK9 achieved upon Dox induction.

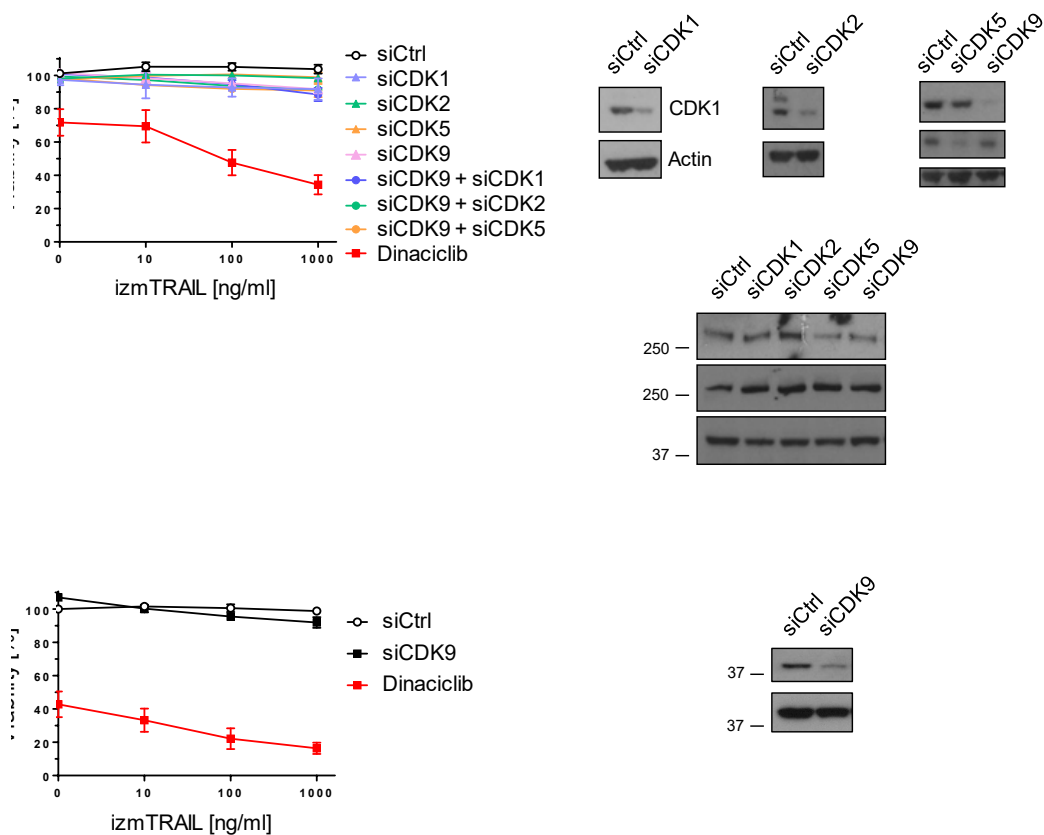


Figure 3.31: siRNA-mediated CDK9 knockdown is not sufficient to sensitise KP cell lines to TRAIL-induced death.

(A, C) KP394T4 or KP59 cells were transiently transfected with siRNA targeting the indicated CDKs or siCtrl for 48 h and subsequently treated with Dinaciclib and/or izmTRAIL at the indicated concentrations. Cell viability was determined 24 h later. Data are presented as means \pm SEM of three independent experiments.

(B, D) 48 h after transfection with siRNA, cells were lysed and the knockdown efficiency was analysed by Western Blotting. Representative Western Blots of three independent experiments are shown.

In conclusion, these results suggest that CDK9 downregulation is not sufficient to sensitise murine KP cancer cells to TRAIL-induced apoptosis. Importantly, this is independent of the cells carrying a mutated or a null *Tp53* allele, since some of the KP cells, namely KP59 and PCC8, were derived from KP mice and thus express a mutated form of *Tp53* and the others, i.e. KP802T4 and KP394T4, were generated from a KP^{null} mouse and consequently do not express *Tp53*.

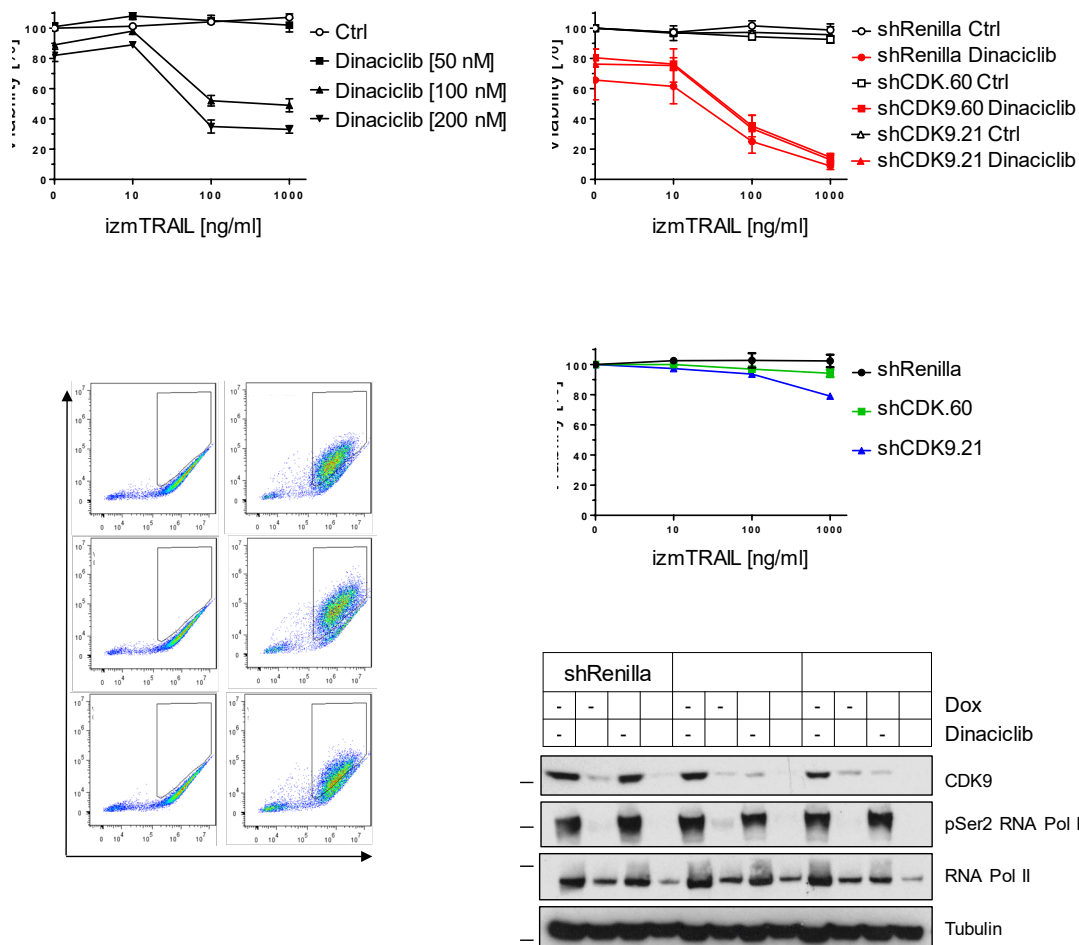


Figure 3.32: shRNA-mediated CDK9 knockdown is not sufficient to sensitise NSCLC PCC8 cells to TRAIL-induced apoptosis.

(A, B) Parental PCC8 cells or non-induced PCC8 cells expressing the indicated shRNAs were pre-incubated with the indicated concentrations of Dinacilib (100 nM Dinacilib in (B)) for 15 min and subsequently treated with izmTRAIL at the indicated concentrations. 24 h later cell viability was determined. Data represent means \pm SEM of three independent experiments.

(C) Representative FACS profile of PCC8 cells expressing the indicated shRNAs before and after 5 day induction with Doxycycline, gated on their RFP and Venus expression levels. TRE, tetracycline response element; rTTA, reverse tetracycline-controlled transactivator.

(D) shRenilla or shCDK9-expressing PCC8 cells were induced with Doxycycline [1 μ g/ml] for 5 days and subsequently treated with the indicated concentrations of izmTRAIL. 24 h later cell viability was measured. Data are shown as means \pm SEM of three independent experiments.

(E) PCC8 cells expressing the indicated shRNAs were induced with Doxycycline for 5 days and subsequently treated with 100 nM Dinacilib. 24 h later cells were lysed and analysed by Western Blotting. Representative Western blots of three independent experiments are shown.

3.4.3. Dinaciclib targets BRD4 in addition to CDK9 and combined inhibition of both is required to overcome TRAIL resistance in KP cell lines

In view of the results obtained upon CDK9 knockdown in KP tumour cells, and considering that Dinaciclib sensitised these cells to TRAIL-induced apoptosis, it seemed likely that Dinaciclib targets some additional protein(s) that is/are required to break the resistance to TRAIL.

Transcription is also controlled by BRD4, which binds to highly acetylated chromatin (Wu and Chiang, 2007) and recruits the P-TEFb complex, consisting of CDK9 and CycT1, to promoters (Jang et al., 2005; Yang et al., 2005; Bisgrove et al., 2007). Interestingly, Dinaciclib has been shown to bind to the acetyl-lysine recognition site of bromodomains, including BRD4 (Martin et al., 2013; Ember et al., 2014; Mishra et al., 2014). Consequently, it was hypothesised that concomitant inhibition of CDK9 and BRD4 are necessary to sensitise KP cells to TRAIL-induced apoptosis.

To test this, BRD4 was pharmacologically targeted in addition to the downregulation of CDK9 and cells were subsequently stimulated with TRAIL. For BRD4 inhibition, the BET bromodomain inhibitor JQ1 was employed (Filippakopoulos et al., 2010). In the previously described shRNA-transfected PCC8 cells, BRD4 inhibition synergised with CDK9 knockdown and sensitised PCC8 cells to TRAIL-induced apoptosis (Figure 3.33 A). Furthermore, JQ1 treatment in combination with CDK9 inhibition mediated by SNS-032, LDC000067 (LDC) or the CDK9-specific NVP-2 also sensitised KP59 cells to TRAIL (Figure 3.33 C, D and E). Notably, other than Dinaciclib (Figure 3.31C), neither of the CDK9 inhibitors sensitised KP59 cells to TRAIL-induced apoptosis. Therefore, both CDK9 and BRD4 appear to mediate TRAIL resistance, which can be overcome by treatment with Dinaciclib.

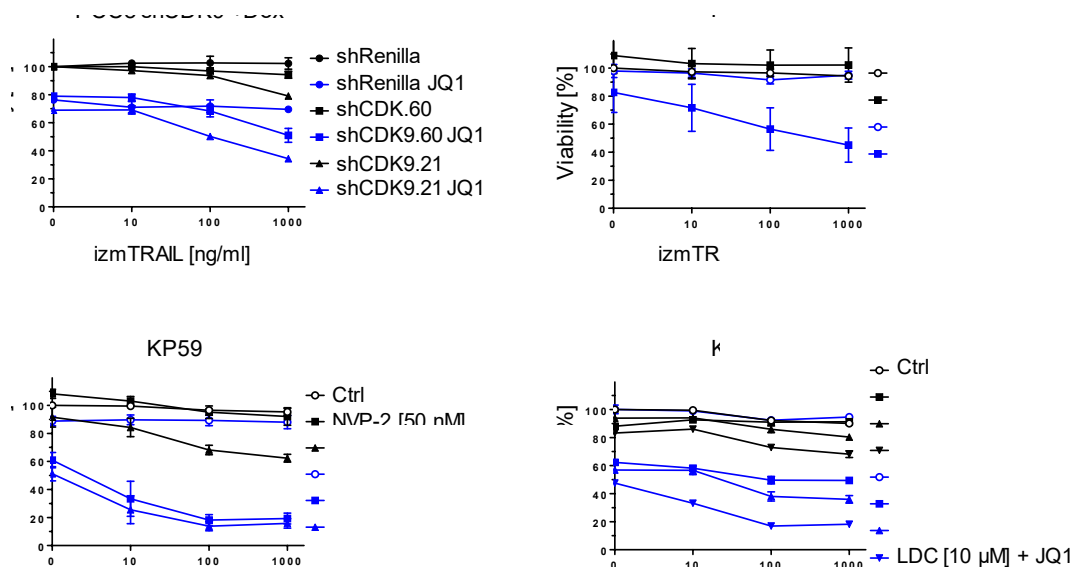


Figure 3.33: BRD4 inhibition in addition to CDK9 downregulation synergises with TRAIL to kill KP cancer cells.

(A) shRenilla- or shCDK9-expressing PCC8 cells were treated with 1 μ g/ml doxycycline. 5 days later, cells were pre-incubated for 15 min with 1 μ M JQ1 and then stimulated with izmTRAIL at the indicated concentrations. 24 h later cell viability was determined.

(B-D) KP59 cells were treated with Dinaciclib [50 nM], SNS-032 [500 nM], NVP-2 [50 or 100 nM], LDC [1, 5 or 10 μ M], JQ1 [1 μ M] or a combination of these as indicated and then treated with the indicated concentrations of izmTRAIL. 48 h later cell viability was determined.

Data represent means \pm SEM of three independent experiments.

With the aim of confirming the previous results in a different KP cell line, an alternative strategy was employed. In addition to NVP-2 treatment for CDK9 inhibition, KP802T4 cells were also stimulated with MZ1, a proteolysis targeted chimera (PROTAC) that tethers JQ1 to a ligand for the E3 ubiquitin ligase von Hippel-Lindau (VHL) to trigger proteasomal degradation of BRD4 (Zengerle et al., 2015). Treatment with neither MZ1 nor JQ1 sensitised KP802T4 cells to TRAIL-induced apoptosis (Figure 3.34 A), despite the efficient degradation of BRD4 induced by MZ1 (Figure 3.34 C).

Similarly, CDK9 inhibition upon stimulation with NVP-2 was not sufficient to sensitise these cells to TRAIL (Figure 3.34 A). As observed before, only concomitant inhibition of CDK9 and BRD4 overcame TRAIL resistance. Consistent with this, phosphorylation of RNA Pol II at Ser2 was abrogated after NVP-2 and JQ1 or MZ1 treatment and consequently, Mcl-1 and FLIP levels were downregulated (Figure 3.34

C). Interestingly, BRD4 inhibition in addition to Dinaciclib treatment did not significantly further reduce the viability of KP802T4 cells after TRAIL stimulation, suggesting that BRD4 is already targeted by Dinaciclib.

Additionally, the impact of the inhibition of CDK9 and/or BRD4 on the long-term survival of KP802T4 cells was tested. NVP-2 or MZ1 treatment alone or in combination with TRAIL did not influence the colony forming ability of these cells (Figure 3.34 B). Dinaciclib, however, greatly reduced the number of surviving clones, and this effect was noticeably more pronounced when TRAIL was added on top. Strikingly, combined stimulation with NVP-2 and MZ1 completely abrogated the long-term survival of KP802T4 cells, which did not form colonies either in the absence or in the presence of TRAIL.

The fact that concomitant pharmacological inhibition of CDK9 and BRD4 sensitises KP tumour cells to TRAIL demonstrates that both proteins mediate resistance to TRAIL. Nonetheless, these data do not formally prove that the downregulation of these two factors is sufficient to sensitise to TRAIL-induced apoptosis because there could still be other off-target proteins which, when inhibited by the drugs used, also participate in the sensitisation to TRAIL-induced apoptosis. In order to exclude this possibility, the best experiment would be to generate CDK9 and BRD4 double KO cells, which according to this hypothesis, should be sensitive to TRAIL. However, obtaining viable CDK9 cells was not possible. Unfortunately, when *Brd4*-targeted clones were generated by CRISPR/Cas9, only clones that had a deletion leading to a new open reading frame were obtained. This new reading frame produced a truncated version of BRD4, with the same sequence but only lacking the first few amino acids. Thereby, alternative strategies had to be sought.

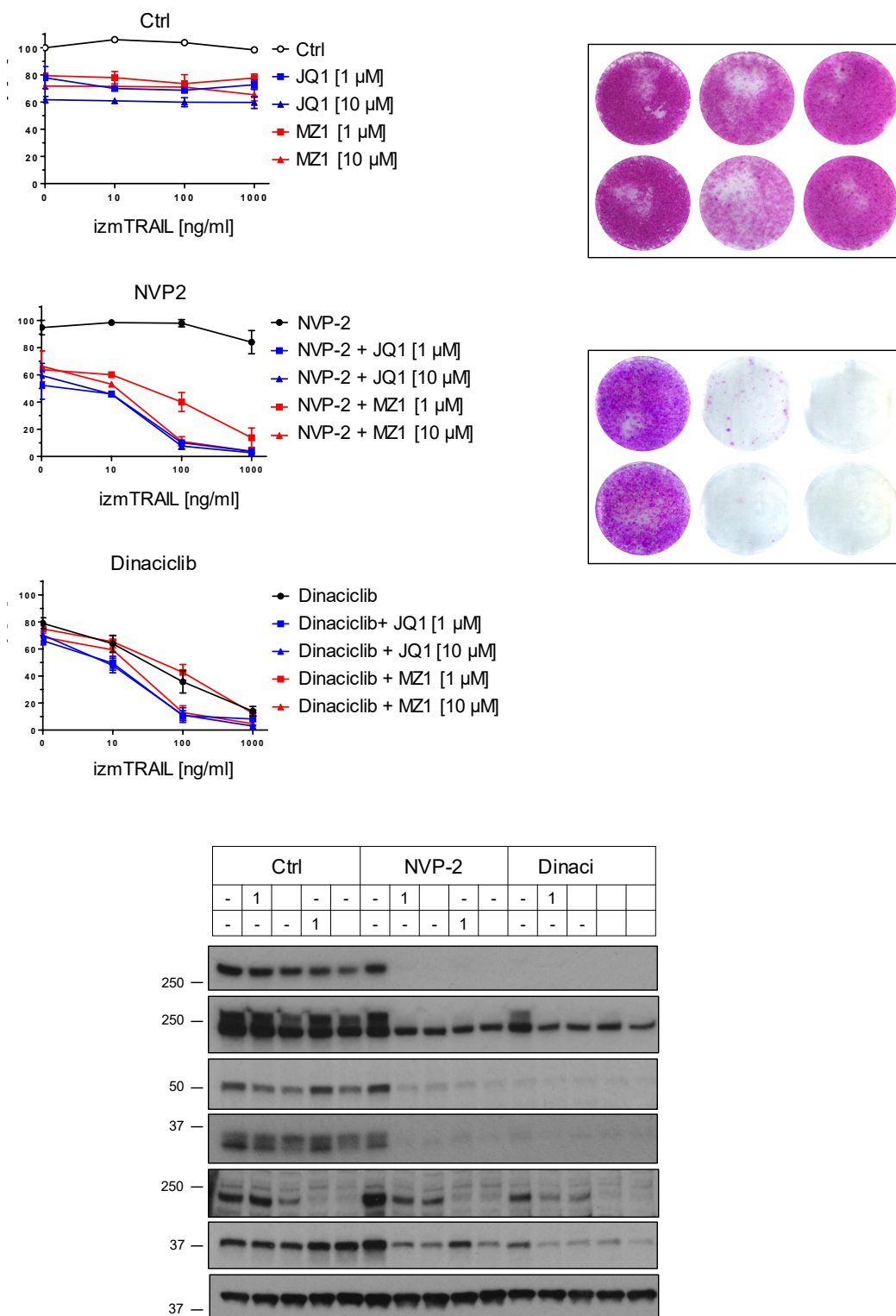


Figure 3.34: The combination of CDK9 and BRD4 inhibition is required to sensitise KP cells to TRAIL-induced death.

(A,) KP802T4 cells were pre-incubated for 15 min with Dinaciclib [100 nM] or NVP-2 [100 nM] (Figure legend continues on next page)

in combination with JQ1 or MZ1 at the indicated concentrations and subsequently stimulated with different concentrations of izmTRAIL as indicated. Cell viability was quantified 48 h later. Data represent means \pm SEM of three independent experiments.

(B) KP802T4 cells were treated with NVP-2 [100 nM], MZ1 [1 μ M], Dinaciclib [100 nM], izmTRAIL [100 ng/ml] or a combination of these as indicated for 24 h. 7 days later, long-term survival was visualised by crystal violet staining. One of two independent experiments is shown.

(C) KP802T4 cells were treated with 100 nM Dinaciclib or 100 nM NVP-2 in combination with JQ1 or MZ1 as indicated. 24 h later cells were lysed and analysed by Western blotting. Representative Western blots of three independent experiments are shown.

As such, PROTACs were employed in order to obtain KP cells in which CDK9 and BRD4 are concomitantly degraded. For BRD4 degradation, the previously introduced MZ1 was used. For selective CDK9 proteolysis, THAL-SNS-032 was selected, which is a selective CDK9 degrader consisting of SNS-032 conjugated to thalidomide that induces Cereblon-dependent degradation (Olson et al., 2018).

First, the selectivity of THAL-SNS-032 for CDK9 was tested. KP802T4 were treated with increasing concentrations of the PROTAC and the degradation of CDK2, CDK7 and CDK9, the primary targets of THAL-SNS-032, was analysed. While CDK2 and CDK7 showed little change in protein levels at any of the tested concentrations, CDK9 was markedly degraded at 2 μ M and completely absent at 5 μ M of THAL-SNS-032 (Figure 3.35 A). Nevertheless, in accordance with the previous results, treatment with 5 μ M THAL-SNS-032 did not sensitise KP802T4 cells to TRAIL (Figure 3.35 B). This correlated with some phosphorylation of the Ser2 of RNA Pol II still being present, albeit very reduced (Figure 3.35 A).

Next, the concomitant and selective degradation of CDK9 and BRD4 was induced in KP802T4 cells. Upon treatment with 5 μ M THAL-SNS-032 and MZ, no expression of CDK9 or BRD4 was detected (Figure 3.35 A). This combined degradation of CDK9 and BRD4 completely prevented the phosphorylation of the Ser2 of RNA Pol II and, as a consequence, sensitised these cells to TRAIL to the same level than Dinaciclib (Figure 3.35 B). From these data, it can be concluded that the concomitant inhibition of CDK9 and BRD4, which is only achieved by Dinaciclib, is required and sufficient to sensitise KP cells to TRAIL-induced apoptosis.

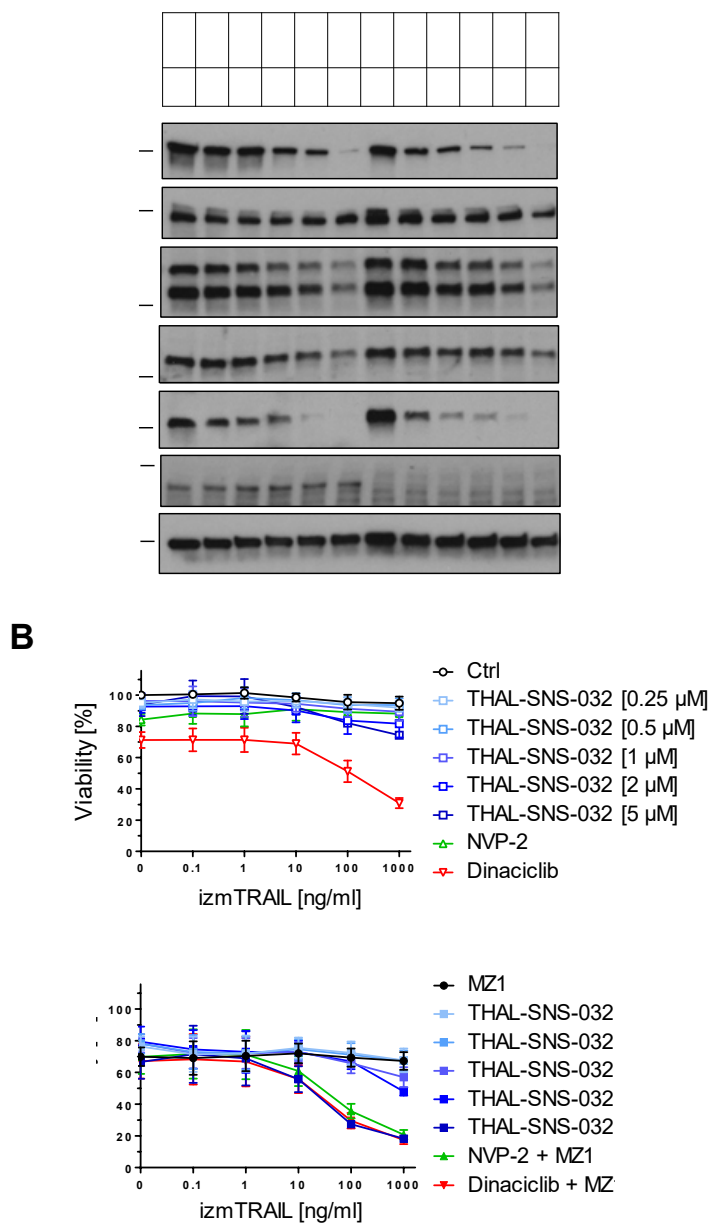


Figure 3.35: Concomitant and selective degradation of CDK9 and BRD4 overcomes TRAIL resistance in KP cells.

(A) KP802T4 cells were treated with Dinacliclib [100 nM] or THAL-SNS-032 at the indicated concentrations in the presence or absence of MZ1 [1 μM]. 10 h later cells were lysed and lysates were analysed by Western blotting. Representative Western blots of two independent experiments are shown.

(B) KP802T4 cells were treated with THAL-SNS-032 at the indicated concentrations, NVP-2 [100 nM] or Dinacliclib [100 nM] in the presence or absence of MZ1 [1 μM] for 15 min and subsequently stimulated with various concentrations of izmTRAIL as indicated. Cell viability was determined 48 h later. Data represent means ± SEM of three independent experiments.

3.4.4. CDK9 inhibition overcomes TRAIL resistance in some cell types, while others required the additional inhibition of BRD4

The results shown in the last sections were intriguing. On one hand, all human cell lines tested, from different origins, were sensitised to TRAIL-induced apoptosis by specific inhibition of CDK9. On the other hand, in murine NSCLC KP cells, the concomitant CDK9 and BRD4 inhibition was required to overcome the resistance to TRAIL. In order to investigate whether this was also the case in murine cell lines derived from different cancer types, a panel of eight different cell lines was selected including melanoma, breast cancer, SCLC and NSCLC (Figure 3.36 A). To test whether selective CDK9 inhibition sensitised these cells to TRAIL-induced apoptosis or whether, instead, combined CDK9 and BRD4 inhibition was required, cells were treated with NVP-2, Dinaciclib or NVP-2 and JQ1 in combination with TRAIL.

From the cell lines tested, Dinaciclib, as well as NVP-2 or its combination with JQ1 very significantly reduced the cell viability of B16 melanoma and 4T1 breast cancer cells in the absence of TRAIL, leaving less than 20% of the cells alive (Figure 3.36 B). These results suggest that, in some cancer cells, CDK9 inhibition could be used as a therapeutic agent in a monotherapy, although this would need to be validated *in vivo*.

In the SCLC and NSCLC cell lines, the results obtained were variable and cell line-dependent. Interestingly, RP280.1 and KPC3 cells were equally sensitised to TRAIL-induced apoptosis by NVP-2 alone or in combination with JQ1 or Dinaciclib treatment. Other cell lines, like KPC2 or RP250.3, behaved like the previously studied KP802T4 cells (Figure 3.35) and CDK9 inhibition by NVP-2 did not break their resistance to TRAIL (Figure 3.36). The combined stimulation with NVP-2 and JQ1 or Dinaciclib, however, markedly sensitised them to TRAIL-induced apoptosis.

Taken together, these results demonstrate that CDK9 inhibition alone is not sufficient to sensitise all cell lines to TRAIL-induced apoptosis and that, in some, concomitant inhibition of BRD4 is required to achieve so. Dinaciclib seems to target both CDK9 and BRD4 and, thus, it possibly constitutes the best therapeutic approach to overcome TRAIL-resistance.

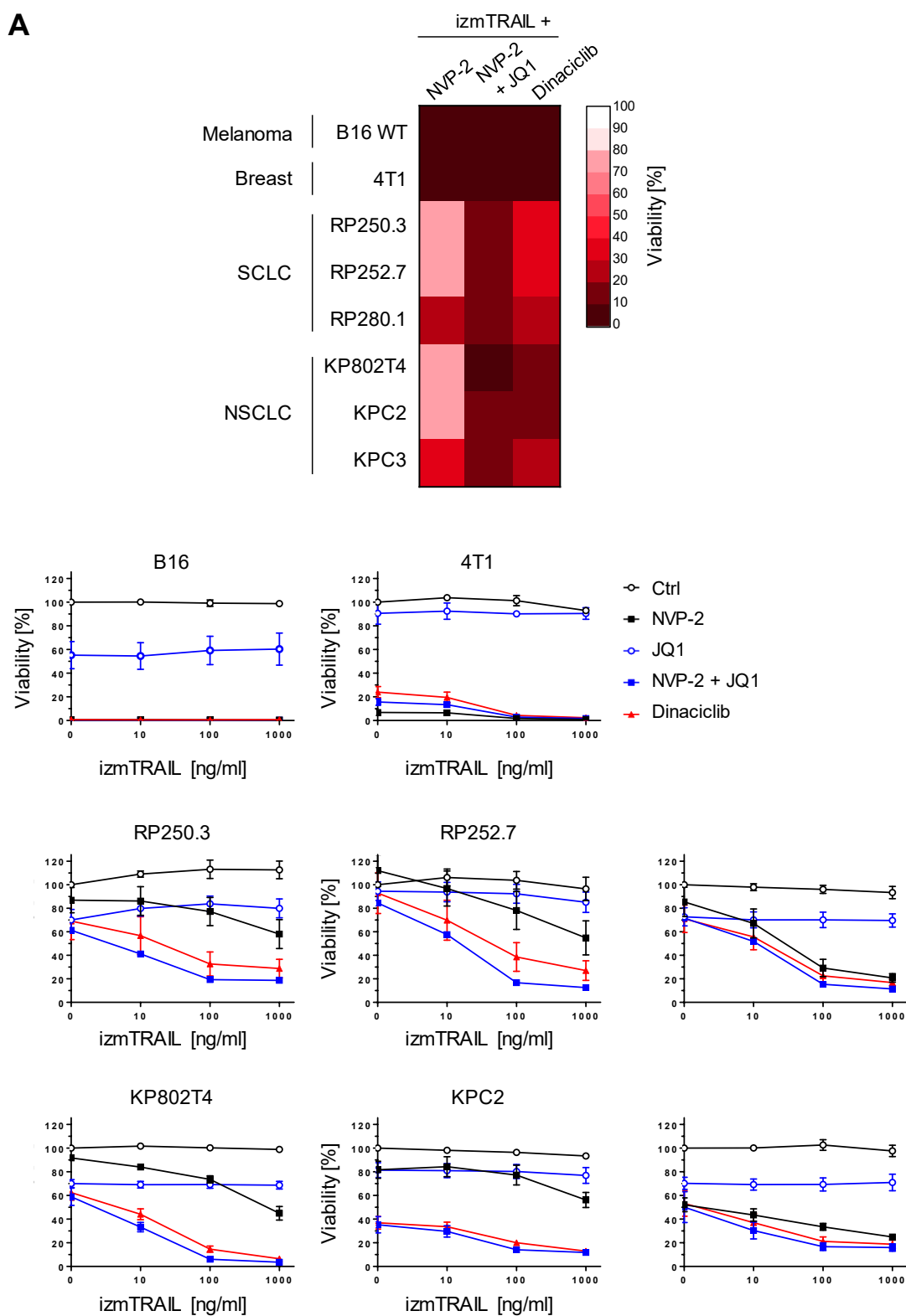


Figure 3.36: The role of BRD4 in mediating TRAIL resistance is cell type-dependent.

(A) The indicated murine cancer cell lines were pre-incubated with NVP-2 [100 nM], NVP-2 [50 nM] and JQ1 [1 μ M] or Dinaciclib [100 nM] for 15 min and subsequently stimulated
(Figure legend continues on next page)

with izmTRAIL [100 ng/ml]. 48 h later cell viability was quantified and normalised to untreated control. Heat map representing colour-coded viability levels of the different cell lines upon the indicated treatments. Values are means of three independent experiments.

(B) Cell lines in A were treated with NVP-2 [100 nM], JQ1 [1 μ M], NVP-2 [50 nM] and JQ1 [1 μ M] or Dinaciclib [100 nM] for 15 min and subsequently stimulated with the indicated concentrations of izmTRAIL. Cell viability was determined 48 h later.

3.5. Establishment of immunogenic GEMMs for NSCLC

One of the biggest shortcomings of currently used lung cancer GEMMs is the poor recapitulation of the heterogeneous and clonal nature of this cancer (Gerlinger et al., 2012; de Bruin et al., 2014). For the successful preclinical development of novel cancer therapies, particularly those that affect the tumour immune microenvironment like the TRAIL and Dinaciclib therapy studied in this thesis, it is imperative to develop mouse models with intrinsically high mutational rates and intratumour heterogeneity, similar to what is found in humans (Alexandrov et al., 2013; Wolf et al., 2019). To address this, the development of mouse models that combine the genetic and chemical induction of NSCLC was decided, since this has been shown to resemble the mutational burden encountered in human lung cancers more closely (Westcott et al., 2015). Using urethane as the carcinogen of choice, the effect of carcinogen induction before or after the induction of the oncogenic expression of *Kras*^{G12D} and *Tp53*^{R172H} in the KP model was explored. Due to their predicted immunogenic nature, these novel models will be referred to as immunogenic GEMMs (iGEMMs).

3.5.1. Carcinogen exposure after the engineered-induction of NSCLC tumours increases tumour burden

First, the effect of the exposure to urethane once the tumour was initiated by the engineered expression of mutated *Kras* and *Tp53* was explored. In order to develop this iGEMM, KP mice received an i.p. injection of urethane 5 and 6 weeks after the Ad-Cre administration (Figure 3.37 A). Mice were euthanized upon signs of moderate distress, which occurred around 32 weeks after Ad-Cre instillation. The lungs of Ad-Cre and urethane-treated mice were bigger than the lungs of Ad-Cre-only- or urethane-only-treated mice, the latter being macroscopically healthy (Figure 3.37 B). Similarly, the tumour burden in the lungs of Ad-Cre and urethane-treated mice was slightly bigger than in the Ad-Cre only mice, although the variability within the group prevented its statistical significance (Figure 3.37 C and D).

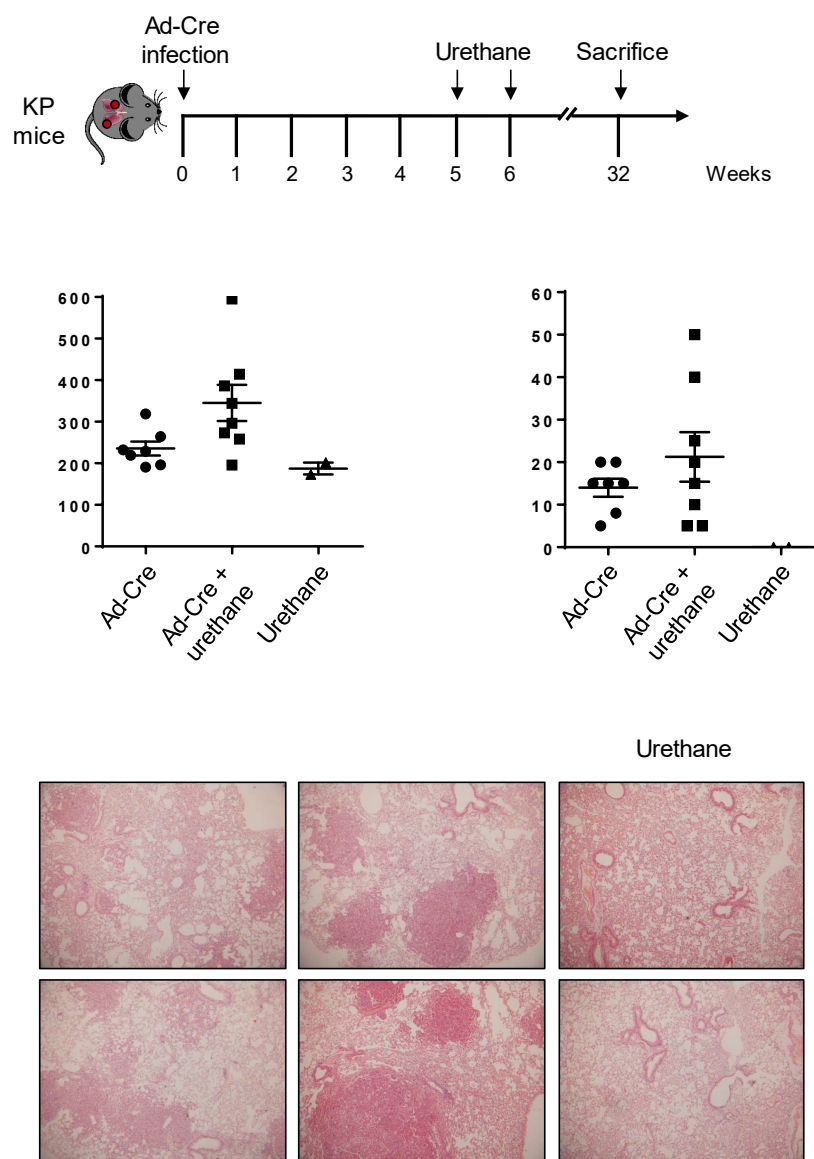


Figure 3.37: The injection of urethane after tumour initiation in the KP model increases the tumour burden.

(A) Experimental treatment schedule is shown. KP mice were subjected to intranasal administration of Ad-Cre to induce the expression of oncogenic *Kras*^{G12D} and *Tp53*^{R172H}. Mice were injected urethane at 1 g/kg at the indicated times (Ad-Cre: n=7 mice; Ad-Cre + urethane: n=8 mice; urethane: n=2 mice).

(B) Mice were sacrificed at the humane endpoint and the lungs were weighted as a measure of their tumour content. Data are shown as means \pm SEM. Dots represent lungs of individual mice. Statistical analysis was performed using one-way ANOVA.

(C) Paraffin-embedded sections of lungs from all mice were stained with H&E and subjected to pathological examination to quantify the tumour burden as the percentage of total lung area occupied by tumour tissue. Data are presented as means \pm SEM. Dots represent individual mice.

(D) Representative histological images of H&E-stained paraffin-embedded lung sections of two mice per group are shown.

Carcinogen treatment of mice in which the expression of oncogenic *Kras* and *Tp53* was not induced did not lead to the development of any tumour. This observation is in line with previous reports showing that C57BL/6 mice, which is the background strain of our colony and the most widely used one, are resistant to urethane-induced lung tumour formation (Malkinson, 1989).

In sum, the previous results show that urethane treatment increases the growth of tumours in the KP model if administered after the initiation of the tumours.

Tumours induced by urethane exposure that arise in susceptible strains have been shown to be initiated by oncogenic mutations in *Kras*, mostly *Kras*^{Q61L} (You et al., 1989; Westcott et al., 2015). It was thereby hypothesised that the mutation in *Kras* as a consequence of urethane treatment could induce tumours in *Tp53*^{SL-R172H/+} (P) mice. To test this, P mice were treated with urethane 5 and 6 weeks after the administration of Ad-Cre sacrificed 26 weeks later (Figure 3.38 A). As expected, the expression of mutated *Tp53* did not lead to the development of any tumour, at least at this time-point (Figure 3.38 B and C). Interestingly, P mice were not susceptible to urethane-induced tumours as indicated by the absence of tumours at the time of euthanasia, highlighting that the mechanisms driving susceptibility to lung tumour are p53 independent.

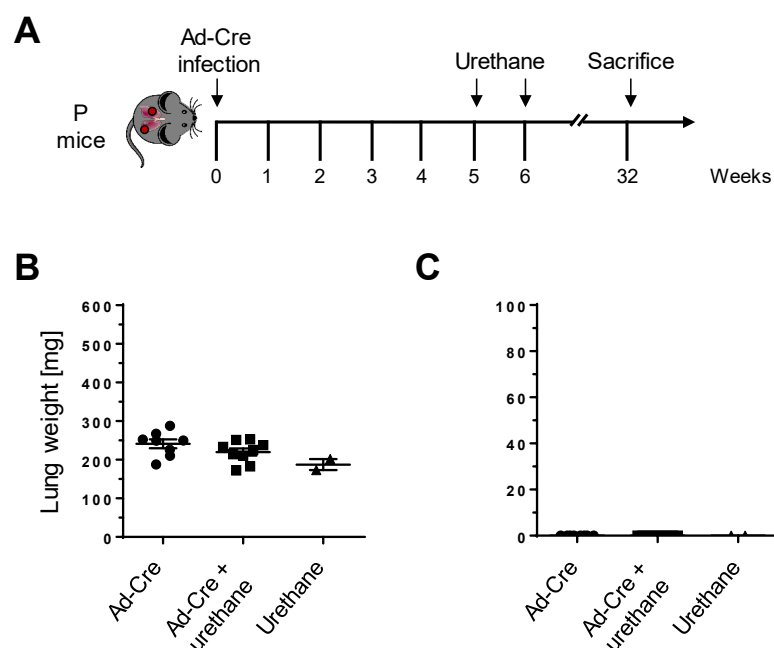


Figure 3.38: P mice do not develop tumours, even with the addition of urethane after the Ad-Cre infection.

(A) Experimental treatment schedule is shown. P mice were subjected to intranasal administration of Ad-Cre to induce the expression of oncogenic *Tp53*^{R172H}. Mice were injected urethane at 1 g/kg at the indicated times (Ad-Cre: n=8 mice; Ad-Cre + urethane: n=9 mice; urethane: n=2 mice).

(B) Mice were sacrificed at the indicated time and the lungs were weighted.

(C) Paraffin-embedded sections of lungs from all mice were stained with H&E and subjected to pathological examination to quantify the tumour burden as the percentage of total lung area occupied by tumour tissue.

Data are shown as means \pm SEM. Dots represent lungs of individual mice. Statistical analysis was performed using one-way ANOVA.

3.5.2. Carcinogen exposure before the oncogenic expression of *Kras* and *Tp53* increases tumour growth

Second, the effect of urethane exposure before the expression of *Kras*^{G12D} and *Tp53*^{R172H} was investigated. In this way, the impact of the *Kras*^{Q61L} mutations induced by urethane and the *Kras*^{G12D} mutations induced by Ad-Cre on tumour development and heterogeneity could be evaluated. As mentioned before, C57BL/6 mice are resistant to lung tumour induction by urethane and strain-specific differences in the NK gene complex have been shown to contribute to this (Kreisel et al., 2012). To inhibit the immunosurveillance for carcinogen-induced NSCLC exerted by NK cells, a depleting antibody against these cells (anti-NK1.1) was administered before the

injection of urethane, which was done 6 and 7 weeks prior to the infection with Ad-Cre (Figure 3.39). Mice were sacrificed when they reached the euthanasia criteria, 24 weeks after the Ad-Cre infection. Mice that received anti-NK1.1 and urethane treatment but were not infected with Ad-Cre and thus did not express oncogenic *Kras*^{G12D} and *Tp53*^{R172H} did not develop any tumours, indicating that the depletion of NK cells is not sufficient to overcome the carcinogen resistance of C57BL/6 mice (Figure 3.39 B, C and D). Treatment with urethane before the infection with Ad-Cre led to a significant increase in the lung weight of KP mice (Figure 3.39 B). The tumour burden in these mice was bigger than in KP mice not treated with urethane, with 50-60% of the lung area being occupied by the tumour on average (Figure 3.39 C) as opposed to 10-15% in the untreated KP mice, even if the latter were sacrificed at a later time-point after the Ad-Cre infection (Figure 3.37 C). Interestingly, there were no significant differences in lung weight or tumour burden between mice that received the NK cell-depleting antibody before the injection of urethane and those that did not (Figure 3.39 B and C). These results suggest that urethane induces some changes in the cells, that, albeit not sufficient to cause the oncogenic transformation by themselves, when combined with the expression of mutated driver genes like *Kras* and *Tp53* lead to the development of aggressive NSCLC tumours.

The previous experiment was also carried out in P mice. These animals were treated with urethane in the presence of the NK cell-depleting antibody and subsequently infected with Ad-Cre 6 weeks after the last urethane injection (Figure 3.40 A). Mice were euthanized 24 weeks after the Ad-Cre infection. Treatment with the anti-NK1.1 antibody and urethane before the Ad-Cre infection did not impact on the lung weight, as the lungs of these mice were of similar size as the lungs of Ad-Cre only or Ad-Cre and urethane-treated mice (Figure 3.40 B). Like the untreated P mice, and in contrast to KP mice, P mice treated with anti-NK1.1 and urethane did not develop any tumour (Figure 3.40 C). These results highlight the crucial role of *Kras*^{G12D} mutations in lung tumourigenesis.

In conclusion, treatment with the carcinogen urethane increased the tumour burden of KP mice both when administered before and after the induction of mutated *Kras* and *Tp53*. Whole exome sequencing of these tumours will determine whether the higher tumour burden also correlates with an increased mutational load and consequently whether these novel mouse models can serve as iGEMMs of NSCLC.

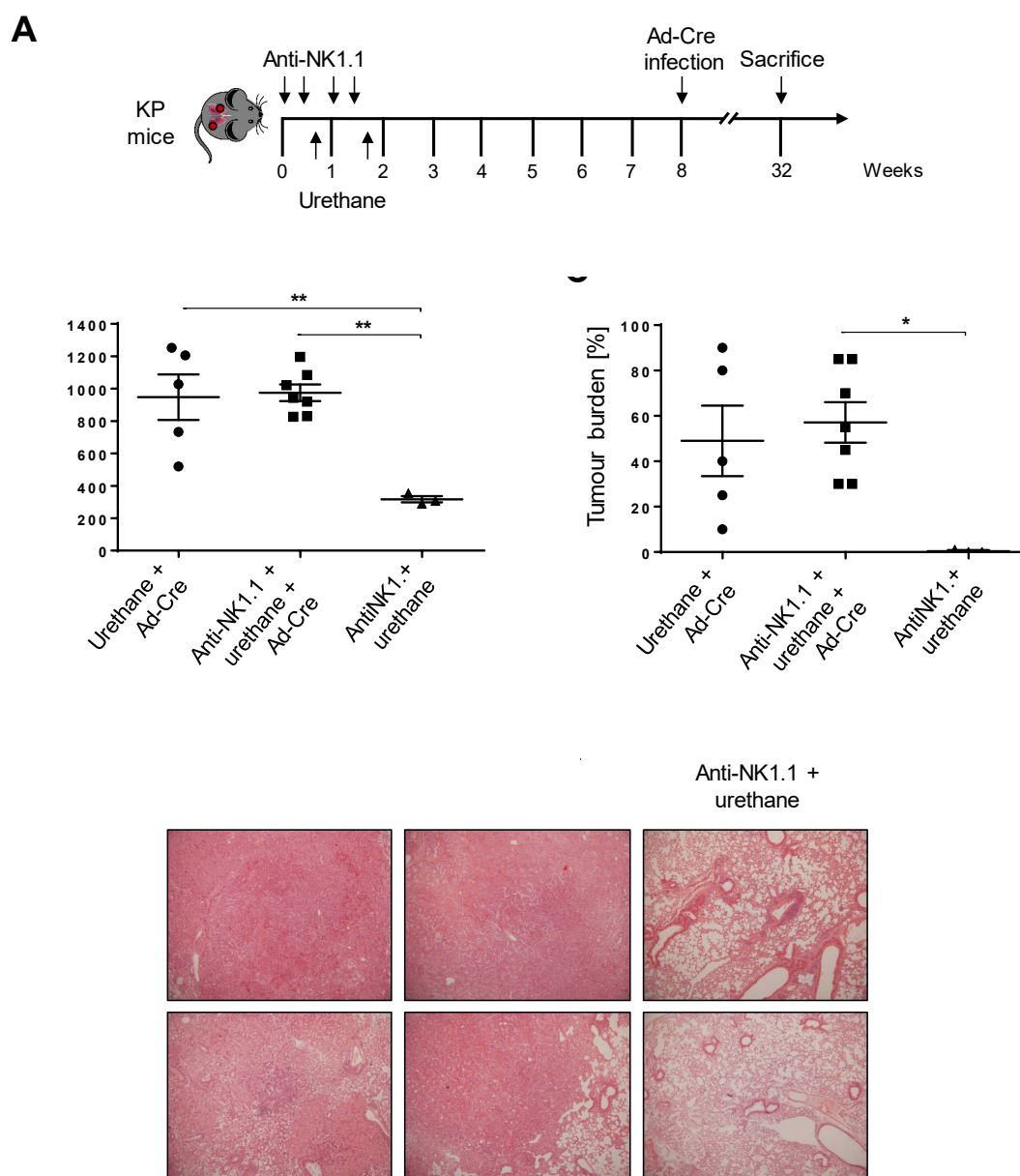


Figure 3.39: The injection of urethane before the induction of the oncogenic expression of *Kras* and *Tp53* in the KP model leads to increased tumour burden.

(A) Experimental treatment schedule is shown. KP mice were treated with anti-NK1.1 antibody [200 µg/mouse] and urethane [1 g/kg] and subjected to intranasal administration of Ad-Cre to induce the expression of oncogenic *Kras*^{G12D} and *Tp53*^{R172H} at the indicated times (urethane + Ad-Cre: n=5 mice; Anti-NK1.1 + urethane + Ad-Cre: n=7 mice; Anti-NK1.1 + urethane: n=3 mice).

(B) Mice were sacrificed at the endpoint and the lungs were weighted as a measure of their tumour content. Data are presented as means ± SEM. Dots represent lungs from individual mice.

(C) Paraffin-embedded sections of lungs from all mice were stained with H&E and subjected to pathological examination to quantify the tumour burden as the percentage of total lung area occupied by tumour tissue. Data are presented as means ± SEM. Dots represent lungs from individual mice.

(Figure legend continues on next page)

(D) Representative histological images of H&E-stained paraffin-embedded lung sections of two mice per group are shown.

Statistical analysis was performed using one-way ANOVA. * $p \leq 0.05$, ** $p \leq 0.01$

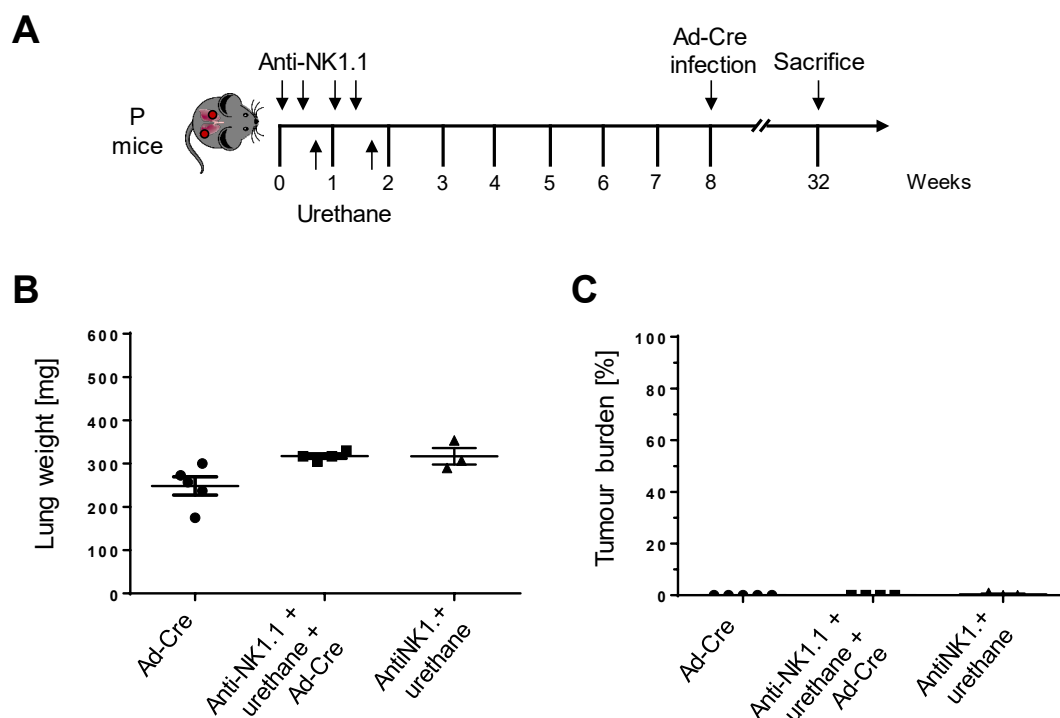


Figure 3.40: The injection of urethane before the expression of mutated *Tp53* does not lead to any tumour formation.

(A) Experimental treatment schedule is shown. P mice were treated with anti-NK1.1 antibody [200 $\mu\text{g}/\text{mouse}$] and urethane [1 g/kg] and subjected to intranasal administration of Ad-Cre to induce the expression of oncogenic *Tp53*^{R172H} at the indicated time (Ad-Cre: n=5 mice; Anti-NK1.1 + urethane + Ad-Cre: n=4 mice; Anti-NK1.1 + urethane: n=3 mice).

(B) Mice were sacrificed at the humane endpoint and the lungs were weighted as a measure of their tumour content.

(C) Paraffin-embedded sections of lungs from all mice were stained with H&E and subjected to pathological examination to quantify the tumour burden as the percentage of total lung area occupied by tumour tissue.

Data are presented as means \pm SEM. Dots represent lungs from individual mice. Statistical analysis was performed using one-way ANOVA.

4. DISCUSSION

4.1. The combination of TRAIL and Dinaciclib is an effective anti-cancer therapy

The discovery that TRAIL, in contrast to other death ligands, could kill cancer cells specifically without harming non-transformed cells sparked the development of TRAs for their clinical application (Ashkenazi et al., 1999; Walczak et al., 1999). Nevertheless, the initial excitement regarding the potential of TRAIL monotherapy as an effective anti-cancer option was soon dampened by the realisation that many tumours are resistant to TRAIL (Todaro et al., 2008; Lemke et al., 2014a; Tuthill et al., 2015). Since then, several means to overcome TRAIL resistance in cancer cells have been investigated, as detailed in section 1.1.5. Recent work in our laboratory identified CDK9 inhibition as the most potent sensitiser to TRAIL-induced apoptosis to date (Lemke et al., 2014a). The CDK9 inhibitor SNS-032 synergised with TRAIL to induce apoptosis in TRAIL-resistant NSCLC cell lines. Similarly, tumour burden in human NSCLC xenografts was reduced by this combination therapy *in vivo*. However, SNS-032 is not a well-tolerated drug and its clinical application has not progressed from phase 1. Indeed, in a phase 1 trial, 74% of CLL patients and 78% of MM patients suffered from grade 3 and 4 toxicities, with the most common ones being tumour lysis syndrome and myelosuppression, including neutropenia, thrombocytopenia, and anaemia (Tong et al., 2010). Similarly, another phase 1 study enrolling SNS-032 had to be terminated during dose-escalation due to the adverse effects (Heath et al., 2008).

Yet, the pharmaceutical industry has developed optimised CDK9 inhibitors that are better tolerated by patients. Currently, the CDK9 inhibitor that is most advanced in the clinic is Dinaciclib, having reached phase 3 testing in CLL (Ghia et al., 2017). Interestingly, in a phase 2 RCT in NSCLC patients, Dinaciclib was well tolerated but it failed to show any significant anti-tumour activity as compared to the Erlotinib arm (Stephenson et al., 2014). Consequently, further studies with Dinaciclib as a single agent for NSCLC were not pursued and, instead, combination strategies are being tested. In light of this, in this thesis, the anti-tumour efficacy of the combination of TRAIL and Dinaciclib was evaluated.

4.1.1. Dinaciclib is a potent sensitiser to TRAIL-induced cell death in many cancers

In line with other numerous reports (Koschny et al., 2007; Todaro et al., 2008; Lemke et al., 2014a; Tuthill et al., 2015), most of the cell lines tested in this thesis are resistant to TRAIL monotherapy. Importantly, however, the results presented in this work show that Dinaciclib overcomes TRAIL resistance in multiple solid tumour types including NSCLC, mesothelioma, melanoma, liver cancer, breast cancer, pancreatic cancer, colorectal cancer, ovarian cancer and cervical cancer (Figure 3.4, 3.5, 3.6 and 3.9). Moreover, comparing Dinaciclib with SNS-032 revealed that even though both inhibitors have the same IC_{50} for CDK9 (Conroy et al., 2009; Parry et al., 2010), Dinaciclib appears to be a more potent sensitiser to TRAIL-induced apoptosis (Figures 3.1 and 3.2). Of note, the concentration at which Dinaciclib efficiently sensitises cancer cells to TRAIL-induced cell death, 25 nM, is commonly reached and sustained in the plasma of patients (Gojo et al., 2013). Thereby, these data provide a robust proof of principle for the testing of TRAIL and Dinaciclib combination therapy in preclinical animal models of a broad range of diseases.

Many of the currently available therapeutic options for cancer patients rely on the expression of specific molecular targets. As such, targeted therapies are designed against certain oncogenic drivers like EGFR (Pollack et al., 1999) and chemotherapy mostly triggers apoptosis by the induction of DNA damage that is sensed by p53 (Lowe et al., 1994). Consequently, the loss of expression of those factors, which is frequently observed in cancer, renders these therapeutic strategies ineffective. In contrast, this work shows that Dinaciclib sensitises NSCLC and melanoma cell lines to TRAIL-induced apoptosis regardless of their mutational background (Figure 3.4, 3.5, 3.6 and 3.9). Hence, the combination of TRAIL and Dinaciclib could be a treatment option for those tumours in which targeted therapy is not available or chemotherapy does not work.

Alternatively, tumours with molecular characteristics for which targeted therapies are available could receive those as a first-line treatment. Despite initial response to the therapy, tumours invariably evolve to acquire resistance mechanisms that allow them to survive during these treatments. For example, melanoma cells have been shown to develop secondary resistance to B-raf and MEK inhibitors by reactivation of the MAPK or PI3K-Akt pathways (Emery et al., 2009; Johannessen et al., 2010; Nazarian

et al., 2010; Shi et al., 2014). In this thesis, treatment of targeted therapy-conditioned melanoma cell lines revealed that the combination of TRAIL and Dinaciclib is similarly efficient in parental cells than in cells that had become resistant to B-raf or MEK inhibitor treatment (Figure 3.9). Therefore, the novel therapeutic combination treatment explored here could be employed as a second-line treatment to overcome targeted therapy resistance.

Similarly, the efficacy of chemotherapy in cancer treatment is also limited by the development of resistance. For instance, cancer cells often upregulate their DNA repair machinery as a resistance mechanism to the induction of DNA damage by platinum-based cytotoxic agents (Duesberg et al., 2000; Kwon et al., 2007; Usanova et al., 2010). The DNA damage induced by these drugs is also known to induce p53-dependent transcription of pro-apoptotic Bcl-2 family members that trigger apoptosis via the mitochondrial pathway (Oda et al., 2000; Nakano and Vousden, 2001; Chipuk et al., 2004) and thus, cancer cells can alter the profile of Bcl-2 proteins to evade chemotherapy-induced cell death (Cetintas et al., 2012). Interestingly, whilst parental A375 melanoma cells are TRAIL-resistant, treatment of cisplatin-resistant A375 cells with TRAIL monotherapy induces apoptosis (Figure 3.9). TRAIL sensitivity of cisplatin-resistant NSCLC and ovarian cancer cells has previously been reported (Seah et al., 2015). These authors suggested peroxynitrite to be a critical factor in amplifying the caspase activation signalling downstream of TRAIL-R in cisplatin-resistant cells, although the exact mechanism remains unknown. Nevertheless, TRAIL sensitivity of cisplatin-resistant cells seems to be cell type-dependent since cisplatin-resistant IGR-37 cells employed here are resistant to TRAIL-induced apoptosis. On the other hand, co-treatment with TRAIL and Dinaciclib kills both cisplatin-resistant cell lines, suggesting that, although a wider range of cell lines needs to be tested, this combination therapy could overcome chemotherapy resistance.

In the context of resistance, an aspect not explored in this thesis is the possible molecular mechanism that cancer cells could employ to escape from the combined treatment with TRAIL and Dinaciclib. Although the assessment of clonogenic survival has been performed in this work, demonstrating that TRAIL and Dinaciclib co-treatment dampens the long-term survival of cancer cells (Figures 3.7 and 3.10), the experimental design followed does not allow the study of the development of resistance. For instance, cells were treated with the combination of TRAIL and Dinaciclib for one day and subsequently the media was washed, assessing the

survival 7 days later. In order to investigate whether any surviving cell could develop resistance to the combined treatment, it would be interesting to maintain the cells under sustained pressure of TRAIL engagement and CDK9 inhibition for a longer period. The evaluation of the clones selected under these circumstances could be informative of potential resistance mechanism arising in cancer cells against the novel combination therapy proposed here. A possible mechanism of resistance could be the promotion of Dinaciclib efflux, which is a strategy used by the tumour cells to diminish the intracellular concentration of many chemotherapeutic compounds. This efflux is mediated by the ATP-binding cassette (ABC) transporters, which are transmembrane proteins driving substrates across the cell membrane and are frequently abundantly expressed in cancer cells, playing an important role in multi-drug resistance (MDR) (Gottesman et al., 2002). Notably, Dinaciclib has been shown to be a substrate of two of these transporters, namely multi-drug resistance protein 1 (MDR1, also known as P-glycoprotein and ABCB1 and breast cancer resistance protein (BCRP), also known as ABCG2) (Cihalova et al., 2015). In that study, the authors reported that the overexpression of ABCB1 and ABCG2 conferred resistance to Dinaciclib in MDCKII cells. Thereby, a low ABC transporter expression could be a marker of patients that are more likely to respond to TRAIL and Dinaciclib combined treatment. If this resistance to Dinaciclib was acquired during treatment, a strategy to overcome it and thus render cancer cells sensitive to TRAIL-induced apoptosis again would be the addition of MDR1 inhibitors like zosuquidar and tariquidar, although the toxicity of the combined treatment with TRAIL, Dinaciclib and the MDR1 inhibitor would need to be carefully tested. Furthermore, gene expression analysis conducted in a study by Feldmann and colleagues demonstrated that the Notch and Transforming Growth Factor- β (TGF- β) pathways were enriched in Dinaciclib-resistant pancreatic xenografts as compared to the sensitive ones (Feldmann et al., 2011). The upregulation of these pathways involved in pancreatic carcinogenesis could represent alternative mechanisms of resistance to Dinaciclib, but more research in this direction is required to identify the precise mechanisms that can drive resistance to TRAIL and Dinaciclib combined treatment and how to overcome them.

4.1.2. Dinaciclib breaks the resistance to TRAIL-induced apoptosis by downregulating Mcl-1 and FLIP

Despite being mainly known for their role in regulating cell cycle, CDKs are a diverse family of proteins with a broad range of functions. Since the discovery of CDK9 as the signalling hub of transcriptional governance (Marshall and Price, 1995), its inhibition has received great attention as a strategy that could inhibit the increased proliferation of cancer cells. It is important to mention that overexpression of CDK9 is often observed in tumours, likely to maintain a high transcription rate in the rapidly proliferating cancer cells. For example, a 1.8-fold increase in CDK9 protein expression is observed in NSCLC tumours in comparison to surrounding non-transformed tissue and 3.4-fold increase in colorectal cancer (Walczak laboratory, unpublished data). Therefore, CDK9 inhibition particularly affects cancer cells over normal cells. By not allowing cells to progress from the pausing of RNA Pol II that happens after transcription initiation (explained in detail in section 1.2.2), this inhibition stops the elongation of all mRNA transcripts. Nevertheless, short-lived proteins, whose levels decrease quickly, are particularly affected by the inhibition of CDK9 since they need to be transcribed more often. Amongst these rapid-turnover proteins there are several crucial apoptotic regulators. For example, CDK9 inhibition by Dinaciclib has been shown to induce the downregulation of the Bcl-2 family members Mcl-1 and Bcl-XL (Fu et al., 2011; Booher et al., 2014; Chen et al., 2016; Inoue-Yamauchi et al., 2017). Moreover, work done in our laboratory revealed that CDK9 inhibition suppresses the transcription of Mcl-1 and FLIP (Lemke et al., 2014a). Importantly, concomitant downregulation of FLIP and Mcl-1 was shown to be required and sufficient for CDK9-induced TRAIL sensitisation since the overexpression of both factors prevented SNS-032-mediated sensitisation. In the work presented here, Mcl-1 and FLIP downregulation is observed following Dinaciclib, as well as SNS-032 treatment. However, Bcl-XL expression does not seem to be affected by this treatment, at least in the cell lines tested (Figure 3.3).

Despite its name, TRAIL-induced signalling is versatile and, in addition to apoptosis, it can also elicit a different modality of programmed cell death, caspase-independent RIPK1- and RIPK3-mediated necroptosis (Jouan-Lanhouet et al., 2012; Voigt et al., 2014; Goodall et al., 2016). The fact that two anti-apoptotic factors are downregulated after Dinaciclib treatment suggests that the cell death induced by TRAIL and Dinaciclib co-treatment is apoptosis but does not formally prove it. Nonetheless, the

apoptotic nature of the cell death induced by the combination of TRAIL and Dinaciclib was confirmed by the addition of the caspase inhibitor zVAD, which blocks this cell death (Figure 3.11 and 3.12).

In summary, the results to date suggest that CDK9 inhibition by Dinaciclib breaks TRAIL resistance through a dual mechanism. On one hand, downregulation of FLIP enables efficient activation of caspase-8 and, on the other hand, suppression of Mcl-1 facilitates the induction of the mitochondrial apoptotic pathway (Figure 4.1).

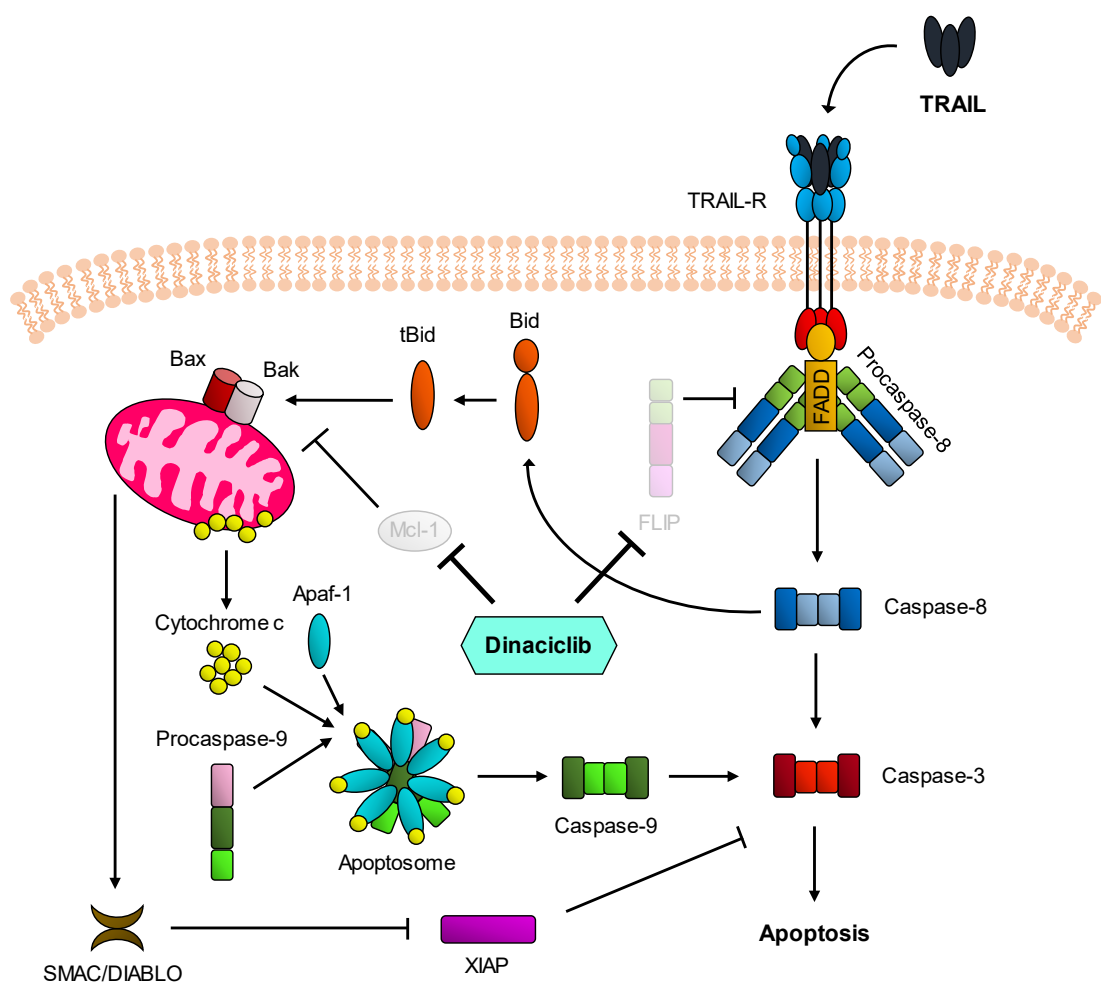


Figure 4.1: Model of Dinaciclib-mediated sensitisation to TRAIL-induced apoptosis.

By inhibiting CDK9 activity, Dinaciclib blocks the transcriptional elongation of Mcl-1 and FLIP, which are anti-apoptotic factors conferring resistance to TRAIL-induced apoptosis. The downregulation of these two factors allows the TRAIL-induced signalling cascade to be fully activated, leading to the triggering of apoptosis.

4.1.3. TRAIL- and Dinaciclib-comprising therapy shows preclinical activity in NSCLC mouse models

In order to evaluate the therapeutic potential of the combination therapy proposed in this work in NSCLC mouse models, it was first important to assess its safety and tolerability. In patients, Dinaciclib is generally safe and well tolerated. The main adverse effects are diarrhoea, vomiting, nausea, fatigue, anaemia, thrombocytopenia and neutropenia (Nemunaitis et al., 2013; Mita et al., 2014; Stephenson et al., 2014; Flynn et al., 2015; Mita et al., 2017). This gastrointestinal and haematological toxicity pattern highlights the effect of the CDK9 inhibitor on rapidly cycling cells and is reminiscent of cytotoxic chemotherapy. On the other hand, izTRAIL has previously been shown to be nontoxic *in vivo* (Walczak et al., 1999; Ganten et al., 2006). This thesis shows that, in mice, the combined treatment with TRAIL and Dinaciclib is well tolerated since they do not lose weight during the course of the treatment (Figure 3.15). Similarly, the therapy does not induce liver toxicity as indicated by the unaltered ALT levels in serum as compared to the vehicle-treated mice.

The work presented here demonstrates the anti-tumour efficacy of the combined TRAIL and Dinaciclib treatment in different *in vivo* models of NSCLC. First, TRAIL and Dinaciclib co-treatment delays the growth of subcutaneously transplanted tumours and prolongs the survival of the mice (Figure 3.16). Moreover, the combination therapy completely eradicates established lung tumours in an orthotopic xenograft model of lung cancer (Figure 3.17). In this model, A549 NSCLC cells are injected into the vein of SCID Beige mice, from where they migrate into the lungs. It was interesting to observe that, *in vivo*, TRAIL monotherapy causes a significant reduction in these tumours while A549 cells are resistant to TRAIL-induced apoptosis *in vitro*. The mechanism responsible for this difference remains enigmatic. A possible explanation could be that A549 cells become more sensitive to TRAIL-induced apoptosis when present in the lungs of the mice as compared to when cultured *in vitro*. For instance, a previous study from our laboratory reported that detachment of skin carcinoma cells from a solid surface sensitised them to TRAIL (Grosse-Wilde et al., 2008). It also seems feasible that the action of TRAIL on the tumour microenvironment is responsible for the anti-tumour effect observed. SCID Beige mice are severely immunodeficient, lacking T and B cells as well as having defective NK cells (MacDougall et al., 1990). Thereby, TRAIL could be mediating its anti-tumour effect via the myeloid immune system. For example, by inducing the death of MDSCs

or tumour-associated macrophages (TAMs), which have both been shown to die by caspase-8-dependent apoptosis through TRAIL-R2 (Germano et al., 2013; Condamine et al., 2014). An alternative hypothesis would be that in this metastasis-mimicking mouse model, cancer progression highly relies on the supply of the tumour vessels and hence, TRAIL-mediated apoptosis of tumour endothelial cells causes the reduction in tumour growth. In fact, pro-apoptotic activation of TRAIL-R2 on tumour endothelial cells has been demonstrated to disrupt the vasculature and reduce the growth of Lewis lung carcinoma tumours (Wilson et al., 2012).

To date, the most widely used mouse model of NSCLC is the KP model since it is the one that most closely resembles the progression and the histological features of the human disease. In these mice, treatment with TRAIL and Dinaciclib after the tumours are established, significantly reduces the tumour burden as compared to the vehicle-treated mice (Figure 3.18). Dinaciclib monotherapy also shows some anti-tumour effect as observed by a decreased lung weight, although the tumour burden of Dinaciclib-treated mice is not significantly different from that of vehicle-receiving animals. Analysing the effect of the therapy on the survival of mice revealed that the monotherapy with TRAIL or Dinaciclib prolongs survival (Figure 3.19). Nevertheless, this effect is more pronounced and statistically significant when both agents are administered in combination, demonstrating the synergistic anti-tumour effect of TRAIL and Dinaciclib treatment in the KP lung cancer model.

The anti-tumour effect of Dinaciclib was also observed in KP mice-derived cell lines. In some of these cell lines, Dinaciclib alone induces a pronounced reduction in their viability (Figure 3.22). In most of them, however, the addition of TRAIL further decreases their viability. Although the reduction in viability by Dinaciclib monotherapy could also be due to slower proliferation, and a more detailed analysis should be performed in KP cells, it is likely due to cell death since Dinaciclib-treated human NSCLC A549 and H322 cells showed some SYTOX positivity (Figure 3.12). This cell death has an apoptotic nature as it can be prevented by pre-incubation with zVAD. This is in line with previous studies showing that Dinaciclib can induce apoptosis (Fu et al., 2011; Chen et al., 2016). Fu and colleagues showed that upon Dinaciclib treatment, an upregulation of Bax, Bim, cytochrome c and caspase-9 was observed in osteosarcoma cell lines, suggesting that Dinaciclib activates the mitochondrial apoptotic pathway (Fu et al., 2011). More recently, however, activation of both extrinsic and intrinsic apoptotic pathways was reported in CLL cells, as

demonstrated by caspase-8 and caspase-9 activation (Chen et al., 2016). Yet, CDK9 is not the only CDK targeted by Dinaciclib, which also inhibits CDK1, CDK2 and CDK5 (Parry et al., 2010). CDK1 and CDK2 control the G2-M and G1-S transitions of the cell cycle, respectively, and their inhibition by Dinaciclib has been reported to mediate anaphase catastrophe, a lethal event in which cells with supernumerary centrosomes segregate their chromosomes into more than two daughter cells, resulting in non-viable daughter cells that die apoptotically (Danilov et al., 2016). The induction of cell death by Dinaciclib monotherapy, however, appears to be cell type-dependent whereas its combination with TRAIL elicits a more robust and constant activation of cell death and thus, is a better strategy to pursue.

Interestingly, the only clinical trial conducted so far with Dinaciclib in lung cancer, showed no activity as monotherapy in previously treated NSCLC (Stephenson et al., 2014). The median time to progression following treatment with Dinaciclib was 1.49 months, compared to 1.58 months with Erlotinib. In accordance with this, in the human solid tumour cell lines tested in this thesis, treatment with Dinaciclib alone had very little or no effect. Considering, as discussed in section 4.4, that the KP model does not accurately mimic the heterogeneous nature and the high mutational burden of human NSCLC (de Bruin et al., 2014; Alexandrov et al., 2016), it seems possible that the moderate benefit observed by Dinaciclib monotherapy in the KP model does not translate into clinical benefit in patients. However, the more robust tumour burden reduction as well as prolonged survival of the combined TRAIL and Dinaciclib therapy, has the potential to increase the survival of NSCLC patients.

Despite the development of targeted therapies for NSCLC patients harbouring targetable mutations and immunotherapy when for tumours expressing high levels of PD-L1, platinum-based chemotherapy is still the most frequently used first-line treatment for lung cancer (Hanna et al., 2017; Gandhi et al., 2018). Consequently, many novel therapies are tested in combination with chemotherapeutic drugs. The work presented here shows that the combination of TRAIL and Dinaciclib does not synergise with Carboplatin, a platinum-based chemotherapeutic agent (Figure 3.20). Indeed, the survival of the mice receiving the triple combination of TRAIL, Dinaciclib and Carboplatin is shorter than those receiving TRAIL and Dinaciclib. To determine if this is due to the triple combination being toxic, it should be tested in mice not bearing tumours, to analyse if there is any weight loss and if the liver enzymes, indicative of hepatotoxicity, change with the treatment. The comparison of Carboplatin to the

TRAIL and Dinaciclib combination treatment revealed that the latter leads to a longer median survival. Nevertheless, the number of mice in these groups should be increased and the experiment repeated in order to draw solid conclusions.

4.2. TRAIL and Dinaciclib treatment modulates the activity of the immune system

Comparing the different mouse models employed for the testing of the efficacy of TRAIL and Dinaciclib co-treatment revealed remarkable differences between immunocompetent and immunocompromised mice. Whereas Dinaciclib monotherapy does not have any anti-tumour activity in immunocompromised SCID Beige or *Rag1*^{-/-} mice, it reduces the tumour growth in immunocompetent mice. On the other hand, combined TRAIL and Dinaciclib treatment shows anti-tumour activity regardless of the presence of a complete immune system. This observation was interesting as, in a phase 2 NSCLC trial, patients treated with Dinaciclib developed neutropenia and leukopenia, suggesting that this drug affects the immune system (Stephenson et al., 2014). In line with this, previous studies have shown that CDK9 inhibition induces apoptosis in leukocyte (Hellvard et al., 2016) and neutrophil (Wang et al., 2012b; Hoodless et al., 2016) subsets, hence modulating the immune response.

Furthermore, the TRAIL/TRAIL-R system is also known to modulate the tumour immune microenvironment and it has been shown to induce the killing of tumour-supportive immune cells in addition to the cancer cells. For instance, several studies have reported that TAMs and MDSCs express TRAIL-Rs, which could be potential targets for selectively eliminating these cells (Germano et al., 2013; Condamine et al., 2014). Similarly, TRAIL was shown to reduce the number of intratumour Tregs by promoting their apoptosis (Diao et al., 2013).

In view of the aforementioned observations, it was hypothesised that TRAIL and Dinaciclib treatment not only kills cancer cells but could also modulate the immune microenvironment by inducing the death of tumour supportive immune cells and, therefore, facilitate the recruitment and activation of CTLs and NK cells. To test this, the tumour microenvironment of KP mice treated with TRAIL and Dinaciclib was immune-profiled. The analysis of the different immune subsets revealed that treatment with Dinaciclib alone or in combination with TRAIL induces a prominent

reduction in the tumour-infiltrating leukocytes in KP mice (Figure 3.23). This is in accordance with the leukopenia that has been reported as an adverse effect in clinical trials with Dinaciclib (Mita et al., 2014; Stephenson et al., 2014; Kumar et al., 2015; Mita et al., 2017). The decrease in the number of leukocytes in the tumour microenvironment could be due to less CD45 positive cells being recruited or, alternatively, as a consequence of more cells dying. In support of the latter, both CDK9 inhibition and TRAIL have been shown to induce the death of a number of immune cells, as explained above. On the other hand, CDK9 has been shown to regulate the pro-inflammatory transcription factor NF- κ B (Barboric et al., 2001) and treatment with the CDK9 inhibitor Flavopiridol inhibited the transcription of NF- κ B in endothelial cells, resulting in a reduction in their intercellular adhesion molecule 1 (ICAM-1) expression (Schmerwitz et al., 2011). Given the crucial role of this protein in leukocyte recruitment from the blood vessels to the tumours, it seems possible that CDK9 inhibition could be inhibiting the recruitment of these cells.

When analysing individual immune cell subsets, the most striking change upon TRAIL and Dinaciclib treatment was the increase in the number and proliferation of NK cells. This is interesting since the TRAIL/TRAIL-R system is known to play a key role in NK cell-mediated immunosurveillance (Kayagaki et al., 1999b). For instance, NK cells can suppress liver and lung metastases in a TRAIL-dependent fashion (Smyth et al., 2001). Moreover, a recent study reported that Dinaciclib enhances NK cell cytotoxicity against AML by downregulating the expression of inhibitory NK ligand human leukocyte antigen (HLA)-E on leukaemia cells (Yun et al., 2019). Nevertheless, the pharmacological depletion of NK cells before the treatment with the combination of TRAIL and Dinaciclib demonstrated that this subset does not mediate, at least entirely, the anti-tumour effect induced by TRAIL and Dinaciclib treatment in our model since the combination therapy is still effective in the absence of NK cells (Figure 3.24). The

Besides innate immunity effectors such as NK cells, the adaptive immunity also participates in the immune surveillance and the inhibition of tumour growth (Mortellaro and Ricciardi-Castagnoli, 2011; Vesely et al., 2011). The adaptive immunity is elicited by humoral and cellular responses mediated by B and T cells, respectively. Interestingly, TRAIL has been demonstrated to be critically involved in maintaining tolerance to the T cell response (Bossi et al., 2015). Moreover, CDK1, CDK2 and CDK5, targeted by Dinaciclib, have been shown to play a role in T cell proliferation

and migration (Wells and Morawski, 2014). Considering this, it was hypothesised that TRAIL and Dinaciclib treatment could be modulating the tumour microenvironment by affecting cells of the adaptive immune system. This was tested by comparing the anti-tumour response to TRAIL and Dinaciclib in KP59 tumours in *WT* versus *Rag1^{-/-}* mice, which produce no mature T or B cells (Mombaerts et al., 1992). Whilst Dinaciclib induces a significant tumour reduction in *WT* mice, this effect is prevented in *Rag1^{-/-}* mice, indicating that, for its action *in vivo*, it requires the presence of the adaptive immunity (Figure 3.26). This is in line with the results obtained in SCID Beige mice, which also lack T and B cells (MacDougall et al., 1990), in which Dinaciclib monotherapy does not have any anti-tumour activity.

In contrast, the anti-tumour activity of combined TRAIL and Dinaciclib therapy is only partially rescued in *Rag1^{-/-}* mice, suggesting that the combination therapy mediates its *in vivo* efficacy both through adaptive immunity-dependent and -independent mechanisms. This highlights the differences between the anti-tumour activity of TRAIL and Dinaciclib combination and Dinaciclib monotreatment. Considering that a recent report showed that encapsulated Dinaciclib in PD-L1-targeted lipid nanoparticles led to a robust depletion of tumour-associated myeloid cells (Zhang et al., 2019) and that, as mentioned before, TRAIL has been reported to induce apoptosis in MDSCs (Condamine et al., 2014), the role of the myeloid immune compartment in the anti-tumour activity of the combined TRAIL and Dinaciclib treatment should be further explored. To this end, it would be interesting to perform experiments in mouse models deficient for different myeloid subsets.

At this point, the contribution of T and/or B cells to the anti-tumour activity mediated by Dinaciclib cannot be dissected. Whereas the multifaceted effects of cancer-associated T cells have been intensively studied, less is known about tumour-infiltrating B cells, whose role remains controversial. Some studies have shown the ability of B cells to induce and maintain an anti-tumour activity (Germain et al., 2014), while others have reported that B cells exist in immunosuppressive subtypes (Fremd et al., 2013; Affara et al., 2014; Bodogai et al., 2015). Interestingly, CDK9 levels change during B cell differentiation and activation, with its expression being higher in memory cells and activated B cells than in naïve cells (De Falco et al., 2008).

Nevertheless, more recent evidence points towards T cells as the key players in Dinaciclib-mediated anti-tumour activity. Dinaciclib has been shown to induce a type I IFN signature within the tumours, which is known to promote antigen presentation

and priming of anti-tumour T cells (Hossain et al., 2018). Furthermore, RNA sequencing (RNA-seq) data has revealed the upregulation of class I HLA upon CDK9 inhibition (Zhang et al., 2018). Of note, HLA governs a critical step in cancer-specific neoantigen presentation and cytolytic T cell response by presenting intracellular peptides on the cell surface for recognition by TCRs. Thereby, it seems likely that Dinaciclib enhances an antitumour T cell response, although the exact mechanism remains elusive. In the KP model used here, Dinaciclib alone or in combination with TRAIL does not induce any apparent increase in the number of T cells. Similar results have been reported by Hossain and colleagues, who showed no change in the number of T cells upon Dinaciclib treatment in a CT26 colorectal cancer model (Hossain et al., 2018). Using the CDK9 inhibitor SNS-032, however, an increase in the percentage of CD3 positive T cells from the total CD45 positive cells has been reported in an ID8 ovarian cancer model (Zhang et al., 2018). Yet, this increase in percentage does not necessarily reflect an increase in the total number of T cells, as it could be due to a change in a different immune subset. Even though the recruitment of T cells does not seem to be affected by Dinaciclib, it would be interesting to analyse the expression of activation markers such as CD69 in these cells, as an increased activation status of T cells could be responsible for the enhanced antitumour response.

Given the results obtained in this work, together with those reported by others, I propose that Dinaciclib would enhance the anti-tumour immunity of CTLs. The molecular mechanism by which this is achieved remains to be explored. Dinaciclib could be having an effect directly on the tumour cells by increasing their neoantigen presentation or it could be inducing immunogenic cell death in cancer cells, which is characterised by the release or cell-surface expression of highly immunostimulatory damage-associated molecular patterns (DAMPs) by the dying tumour cells. Some of the hallmarks of immunogenic cell death include surface calreticulin expression, and the release of adenosine triphosphate (ATP) and high mobility group box 1 (HMGB1), all of which have been observed upon Dinaciclib treatment (Hossain et al., 2018). Alternatively, Dinaciclib could be increasing the activation of intratumour CTLs by augmenting their IFN γ or granzyme production.

On the other hand, the combined action of TRAIL and Dinaciclib would lead to the direct killing of tumour cells. As such, this dual mechanism would boost the anti-tumour activity of the combined treatment. Importantly, in cases in which the immune

system is compromised, TRAIL and Dinaciclib co-treatment-mediated direct killing of the cancer cells would still be possible.

In light of the work presented in this thesis, it is tempting to speculate that the combination of TRAIL and Dinaciclib would synergise with ICB. This type of immunotherapy is one of the most exciting recent breakthroughs in cancer treatment, with anti-PD-1 and anti-PD-L1 showing striking durable control of advanced NSCLC (Borghaei et al., 2015; Brahmer et al., 2015; Garon et al., 2015). Nevertheless, in a substantial proportion of cancer patients, including NSCLC, ICB either does not work or exerts very limited effects. It is now clear that the pre-existing tumour immune environment plays a crucial role in the responsiveness to treatment with the presence of tumour infiltrating lymphocytes, the expression of PD-L1, a high mutational load, and the expression of neoantigens having been shown to act as positive prognostic factors (Herbst et al., 2014; Tumei et al., 2014; Garon et al., 2015; Rizvi et al., 2015; Schumacher and Schreiber, 2015; Hugo et al., 2016; Pfirschke et al., 2016). Interestingly, Dinaciclib has already been shown to synergise with anti-PD-1 in syngeneic colorectal and bladder cancer models, which did not respond to Dinaciclib monotherapy (Hossain et al., 2018). Similarly, CDK9 inhibition by SNS-032 sensitised to anti-PD-1 therapy in an ovarian syngeneic mouse model (Zhang et al., 2018). Moreover, inhibition of BRD4, which is also targeted by Dinaciclib as discussed in the next section, has been reported to cooperate with PD-1 blockade to reduce the tumour in the KP model (Adeegbe et al., 2018). Thereby, I deem it likely that the combined treatment with TRAIL, Dinaciclib and anti-PD-1 would achieve pronounced and long-lasting anti-tumour responses.

4.3. Combined inhibition of CDK9 and BRD4 is required to sensitise some cancer cells to TRAIL-induced apoptosis

The comparison of different CDK9 inhibitors in cell lines derived from KP mice revealed an interesting observation. Whereas KP cells are sensitised to TRAIL-induced apoptosis by Dinaciclib, SNS-032 or NVP-2 do not break the resistance to TRAIL in these cells (Figure 3.30). This was unexpected since SNS-032 has the same IC_{50} for CDK9 as Dinaciclib, 4 nM (Conroy et al., 2009; Parry et al., 2010) and NVP-2 targets CDK9 specifically with an IC_{50} lower than 0.5 nM (Olson et al., 2018).

Furthermore, in contrast to Dinaciclib, CDK9 knockdown by different means does not sensitise different KP cells to TRAIL-induced apoptosis, regardless of their *Tp53* status (Figure 3.31 and 3.32). These results were surprising because they are not in accordance with the sensitisation to TRAIL observed in different human cancer cell lines by specific CDK9 inhibition or knockdown (section 3.4.1 and (Lemke et al., 2014a)). The caveat of siRNA or shRNA-mediated knockdown is that the downregulation of the target might be incomplete, and, although the knockdown looks efficient by Western Blotting, remaining protein levels could still be sufficient to mediate the resistance to TRAIL-induced apoptosis. In order to overcome this, it would be optimal to generate CDK9 KO cells. However, this has turned out to be unsuccessful, likely because of CDK9's essential role in transcriptional elongation, which renders deficient cells not viable. In line with this, mouse KOs of CDK9 and its associated proteins are embryonically lethal (Kohoutek et al., 2009).

The results mentioned above support the hypothesis that Dinaciclib inhibits additional targets other than CDK9, which also mediates resistance to TRAIL-induced apoptosis. Importantly, this additional target is not any of the other CDKs inhibited by Dinaciclib, since the downregulation of none of them in combination with the downregulation of CDK9 sensitises KP394T4 cells to TRAIL-mediated cell death (Figure 3.31). A literature search revealed that Dinaciclib can also bind to the acetyl-lysine binding site of BRD4, although with lower affinity, with an IC_{50} of 19 μ M (Martin et al., 2013; Ember et al., 2014; Mishra et al., 2014). This was interesting since BRD4, which binds to acetylated histones via its bromodomain, is known to positively regulate transcriptional elongation by binding through its C-terminal domain to P-TEFb and bringing it in close proximity with RNA Pol II (Jang et al., 2005; Yang et al., 2005). Moreover, BRD4 was reported to be an atypical kinase that activates transcription by directly phosphorylating RNA Pol II CTD at Ser2 (Devaiah et al., 2012). Yet, a more recent work has corrected this by showing that it is not able to phosphorylate the CTD of RNA Pol II in absence of the P-TEFb (Lu et al., 2015).

Consequently, the requirement of concomitant BRD4 and CDK9 inhibition for TRAIL sensitisation was tested. Interestingly, the combined inhibition of CDK9 and BRD4 sensitises different KP cell lines to TRAIL-induced apoptosis (Figure 3.33). In order to demonstrate that the concomitant inhibition of CDK9 and BRD4 is not only required but sufficient to break the resistance to TRAIL-induced apoptosis, the best strategy would be to generate CDK9 and BRD4 double KO cells. However, although BRD4

KO has been reported to be viable in skin squamous cell carcinoma cells (Xiang et al., 2018), no BRD4 KO KP cells could be obtained. Alternatively, a PROTAC-based approach was selected. Consistent with the results using pharmacological inhibitors, concomitant degradation of CDK9 and BRD4 sensitises tumour cells to TRAIL-induced apoptosis (Figure 3.35), confirming that the inhibition of CDK9 and BRD4 is required to break the resistance to TRAIL in KP cells. In order to validate this, the overexpression of both proteins should be performed, which, according to the data presented here, should confer resistance to TRAIL-induced apoptosis in these cells.

Interestingly, BRD4 inhibition by JQ1 has been shown to enhance TRAIL-induced apoptosis by downregulating FLIP in NSCLC cell lines (Klingbeil et al., 2016). In contrast, in the work presented here, BRD4 inhibition by JQ1, or its degradation by MZ1, does not achieve any sensitisation to TRAIL-induced cell death, even at concentrations of 1000 ng/ml (Figure 3.34). Accordingly, no substantial downregulation in the levels of FLIP is observed at 10 μ M of JQ1 or MZ1. These discrepancies are most likely due to differences between the cell lines, since in the work by Klingbeil and colleagues, NSCLC cell lines displayed varied sensitivities to JQ1-mediated sensitisation to TRAIL-induced apoptosis. Notably, previous work in our laboratory demonstrated that concomitant downregulation of FLIP and Mcl-1 is required for TRAIL sensitisation, as the knockdown of FLIP was not sufficient to sensitise to TRAIL-induced apoptosis (Lemke et al., 2014a). The JQ1-induced FLIP downregulation and consequent TRAIL sensitisation has also been reported in a different study by Yao and colleagues, who showed that these effects are independent of BRD4 (Yao et al., 2015). In that study, JQ1, but not the genetic suppression of BRD4, decreased FLIP levels by promoting its proteasomal degradation. Although the exact mechanism has not been elucidated, this highlights BRD4-independent functions of JQ1. Importantly, in the work presented in this thesis, treatment with JQ1 results in a similar sensitisation to TRAIL-induced apoptosis than BRD4 degradation, indicating that it is indeed BRD4 what mediates resistance to TRAIL.

In the work shown here, selective CDK9 inhibition has been demonstrated to not be sufficient to overcome TRAIL resistance in all cell lines. Whilst in some cell lines, CDK9 inhibition sensitises them to TRAIL-induced apoptosis, some others need the additional inhibition of BRD4, which has been identified here to also mediate resistance to TRAIL-induced apoptosis. Importantly, Dinaciclib, by concomitantly

inhibiting CDK9 and BRD4, sensitises all the cell lines tested so far to TRAIL-induced apoptosis and hence, it seems like the best agent discovered to date to break the inherent or acquired resistance of cancer cells to TRAIL-induced apoptosis. In contrast, selective CDK9 inhibitors like NVP-2 do not achieve such broad sensitisation to TRAIL, and thereby their clinical application in combination with TRAIL might be more limited.

Mechanistically, the downregulation of FLIP and Mcl-1, and thus, the sensitivity to TRAIL, is dictated by the ability to achieve the inhibition of the phosphorylation of the Ser2 of the CTD of RNA Pol II and consequently prevent the transcription pause release. According to the current dogma, inhibition of CDK9, the catalytically active subunit of the P-TEFb, should be sufficient to achieve the sensitisation to TRAIL. Nevertheless, the work presented here shows that this is not always the case, since in some cellular systems, the concomitant inhibition of BRD4 is required. The requirement for the simultaneous inhibition of CDK9 and BRD4 could be due to a compensatory mechanism. Interestingly, Lu and colleagues described that upon sustained CDK9 inhibition, a strong increase in one of its target genes, *MYC*, was observed (Lu et al., 2015). This was achieved by amplified BRD4-mediated recruitment of P-TEFb from its inhibitory 7SK snRNP complex and enhanced CDK9 activity. Therefore, only simultaneous inhibition of both CDK9 and BRD4 could achieve efficient inhibition of transcriptional elongation.

The fact that BRD4 inhibition does not sensitise cells to TRAIL-induced apoptosis indicates that transcriptional elongation can still happen in its absence. This might be explained by the transient release of free P-TEFb from the 7SK snRNP that has been reported upon JQ1 inhibition (Bartholomeeusen et al., 2012). In the absence of BRD4, or when its binding to the chromatin is inhibited, P-TEFb could still be recruited to the transcription complex by other transcription factors. In fact, evidence indicates that the super elongation complex (SEC) can also bind to P-TEFb (Lin et al., 2010; Lu et al., 2016). Interestingly, members of the SEC have been observed to be upregulated upon JQ1 treatment, suggesting a balancing mechanism in which SEC is upregulated in response to BRD4 inhibition to rescue RNA Pol II elongation (Decker et al., 2017).

Altogether, these data suggest the existence of a complementary and compensatory relationship between CDK9 and BRD4 to ensure transcriptional elongation. Consistent with this, BET inhibitors have been shown to synergise with CDK9 inhibitors (Baker et al., 2015; Moreno et al., 2017). The work presented here

demonstrates that the concomitant inhibition of CDK9 and BRD4, like that achieved by Dinaciclib, results in a more broad sensitisation to TRAIL-induced apoptosis than selective CDK9 inhibition. However, the exact mechanism as to why and how this compensatory relationship between CDK9 and BRD4 differs between different cellular systems remains to be explored.

4.4. KP mice treated with urethane could serve as a novel iGEMM for NSCLC

Several lung cancer evolution studies over the last years have helped to investigate the heterogeneous nature of human NSCLC (de Bruin et al., 2014). It is now well established that both exogenous mutational processes such as smoking as well as endogenous processes like the upregulation of APOBEC cytidine deaminases contribute to the large mutational burden found in NSCLC (Lee et al., 2010; Alexandrov et al., 2013; Roberts et al., 2013; Alexandrov et al., 2016). Currently available mouse models of this disease, however, do not recapitulate this high tumour burden. In fact, tumours from *Kras*-driven LAC GEMMs like the KP model used in this thesis have been shown to contain dramatically lower mutational rates than their human counterparts (Westcott et al., 2015; McFadden et al., 2016). As such, these mouse models do not faithfully mimic the human disease. This is particularly relevant for the development of immunotherapies since it has been demonstrated that tumours with increased tumour mutational burden present more neoantigens and, thereby, are more immunogenic (Rizvi et al., 2015; Hellmann et al., 2018).

In order to overcome the aforementioned limitations of current GEMMs of NSCLC, it was hypothesised that the combination of the carcinogen urethane with the KP mouse model would lead to the development of tumours with an increased mutational burden, mimicking the human disease closer. The preliminary results obtained in this thesis show that treatment of KP mice with urethane both before and after the initiation of the tumours results in increased tumour burden (Figures 3.37 and 3.39). Whole exome sequencing will be next performed in those tumour samples with the aim of quantifying the mutations arising in each model. Furthermore, the tumours will also be immune-profiled in order to determine their immune infiltration. In accordance with their low mutational burden, current KP models have been shown to be poorly

infiltrated with T cells and, consequently to be resistant to ICB (DuPage et al., 2011; Lastwika et al., 2016; Pfirschke et al., 2016; Akbay et al., 2017). On the basis of the hypothesis presented here, KP mice treated with urethane should contain a bigger mutational burden and hence, contain more tumour infiltrating lymphocytes and show some response to ICB therapy.

Although the current hypothesis in the immunotherapy field is, as mentioned above, that tumours with increased tumour burden are more immunogenic, recent reports have questioned this direct correlation. Tumours containing similar levels of mutational burden have been shown to exhibit variable immune responses (Rooney et al., 2015), while some cancer with low mutational burden still respond to ICB (Miao et al., 2018). Moreover, Hugo and colleagues reported that tumour mutational burden could not reliably predict the response to anti-PD-1 therapy in melanoma patients, suggesting that additional factors contribute to T cell reactivity (Hugo et al., 2016). Interestingly, the intratumour heterogeneity, defined as the tumour clonal diversity, has been also associated with tumour immune surveillance. In fact, low intratumour heterogeneity, with a higher clonal neoantigen burden, has been correlated with the response to ICB as well as with improved survival of the patients (McGranahan et al., 2016; McDonald et al., 2019; Rosenthal et al., 2019; Wolf et al., 2019). Consequently, it would be interesting to analyse distinct tumour nodules arising in different locations of the lung and compare them to each other to determine the effect of urethane in the tumour heterogeneity.

4.5. Summary and outlook

Cancer cell resistance to TRAIL-induced apoptosis limits the application of TRAIL-R agonists, which will likely only be effective in combination with a potent TRAIL sensitiser. On the basis of the results presented in this thesis, I propose Dinaciclib as a powerful therapeutic agent to overcome TRAIL resistance. Indeed, the data shown here demonstrate the anti-cancer activity of the combination of TRAIL and Dinaciclib in many solid tumour types including, importantly, chemotherapy- and targeted therapy resistant cancer cells.

Interestingly, I show that Dinaciclib is a more powerful sensitiser to TRAIL-induced apoptosis than previously tested CDK9 inhibitors like SNS-032. Crucial for its broad

applicability, Dinaciclib seems to inhibit BRD4 in addition to CDK9, which allows the inhibition of transcriptional elongation in a wide range of cellular types.

Although Dinaciclib shows single-agent activity in some tumour types, it has been reported to not be effective in many others (Hossain et al., 2018). Similarly, it has not shown any clinical benefit in clinical trials in solid tumours yet (Stephenson et al., 2014). In contrast, I have observed anti-tumour activity by the combined treatment of TRAIL and Dinaciclib in all the tumour types tested to date. Furthermore, it has been shown in this thesis that this novel synergistic therapy is effective *in vivo* in mouse models of NSCLC, making it a promising therapeutic option for these patients. Consequently, I propose the clinical testing of TRAs in combination with Dinaciclib in patients with NSCLC.

In addition to sensitising cancer cells to TRAIL-induced apoptosis, this novel therapy seems to also elicit anti-tumour effects via the tumour immune microenvironment. The results obtained in this thesis, together with those of others, suggest that Dinaciclib requires the function of the adaptive immunity for its anti-tumour activity. Based on these data, I hypothesise that the combination of TRAs and Dinaciclib could synergise with ICB. Yet, this warrants further investigation. Of note, the iGEMMs that are currently under development as explained in this thesis, will be of much use for the testing of this hypothesis.

In order to take the combination of TRAs with Dinaciclib into the clinic, it would be important to find which patients are most likely to benefit from this therapy. As explained in the introduction, TRAIL exerts pro-tumourigenic functions both in a cancer cell-autonomous manner and by promoting a tumour-supportive immune microenvironment (von Karstedt et al., 2015; Hartwig et al., 2017). Thereby, although it seems opposing to the therapeutic strategy proposed in this thesis, the blockade of the TRAIL/TRAIL-R system could be beneficial in some cancers. Further work is needed to find biomarkers that can determine with patients should be treated with a TRAIL-R agonist- or antagonist-based therapy.

ACKNOWLEDGEMENTS

First, I would like to thank to Prof Henning Walczak for taking me on board and giving me the chance to work in such a stimulating and demanding environment. Thanks a lot for the guidance and the constant challenge, which has made me grow a lot scientifically.

Furthermore, I would like to express my gratitude to Cancer Research UK for funding my PhD and making this work possible.

I am also thankful to Dr Pablo Rodriguez-Viciano for being my secondary supervisor and together with Prof Richard Jenner assessing my upgrade and giving helpful advice.

Moreover, I would like to thank:

- Jayne Holby and the staff at the Cruciform Biological Services Unit for animal husbandry and technical support.
- Lorraine Lawrence for the histology service.
- Mona EL-Bahrawy for tumour burden quantification.

In addition, I am extremely grateful to all the former and current members of the Walczak lab. Thanks for the great working atmosphere, the constant support and all the good moments in and outside the lab. In particular, I want to thank:

- Antonella Montinaro for her inestimable help throughout my PhD, for teaching me everything, answering all my constant questions, correcting my thesis and being a great partner in this project.
- Torsten Hartwig for being an awesome teammate and all the helpful discussions.
- Diego de Miguel for being the best bench neighbour, all the scientific input and correcting my thesis. Thanks for being always there during these intense years, all the shared adventures and your friendship.
- Aditya Shroff for all the shared moments during late evenings and weekends in the lab, at the pub and in conferences. You have become a great friend.
- Elodie Lafont, Sebastian Kupka, Alexis Betrancourt and Song Chen for being great lab neighbours and all the nice chats in the lab and at the pub.

- Lucia Taraborrelli and Maureen Spit for the great times at the gym and in the dance floor.
- Lynet Nyoni and Rute Ferreira for being great lunch buddies. Thanks Rute for correcting my thesis as well.
- Silvia von Karstedt for taking me under her wing in the beginning and all the shared drinks.
- Eva Rieser and Nieves Peltzer for being so kind and always ready to help.
- Aida Sarr for genotyping the mice.
- Verónica Dominguez for her administrative help.

I am also very grateful to all the people I have met at the UCL Cancer Institute, for making this experience much more enjoyable. Thank you Enrique, Manolo, Isa, Celia, Elena, Arman, Juanjo, Amandeep, Simon, Isabelle, Jo, Maria and all the rest for all the fun Friday nights spent at the pub after work.

Last but not least, special thanks go to my family and friends:

- All my friends back home, for always being there, no matter how far I am or how many things I miss.
- Laura, for sharing this PhD experience with me, the constant support and being the best flatmate. This London adventure would not have been the same without your friendship.
- My aunts and uncle, for their unconditional love and support.
- Valentí, for making me laugh constantly and correcting my thesis. Thank you for your love and for keeping me sane through these intense last years.
- My dad, for always believing in me. *Aita, eres mi ejemplo de superación y trabajo duro. Gracias por apoyarme siempre en todas mis decisiones y creer en mí más que yo misma.*

Amatxu, esta tesis va por ti.

REFERENCES

- Adams, J.M., and Cory, S. (2007). The Bcl-2 apoptotic switch in cancer development and therapy. *Oncogene* 26, 1324-1337.
- Adeegbe, D.O., Liu, S., Hattersley, M.M., Bowden, M., Zhou, C.W., Li, S., Vlahos, R., Grondine, M., Dolgalev, I., Ivanova, E.V., Quinn, M.M., Gao, P., Hammerman, P.S., Bradner, J.E., Diehl, J.A., Rustgi, A.K., Bass, A.J., Tsigos, A., Freeman, G.J., Chen, H., and Wong, K.K. (2018). BET Bromodomain Inhibition Cooperates with PD-1 Blockade to Facilitate Antitumor Response in Kras-Mutant Non-Small Cell Lung Cancer. *Cancer Immunol Res* 6, 1234-1245.
- Affara, N.I., Ruffell, B., Medler, T.R., Gunderson, A.J., Johansson, M., Bornstein, S., Bergsland, E., Steinhoff, M., Li, Y., Gong, Q., Ma, Y., Wiesen, J.F., Wong, M.H., Kulesz-Martin, M., Irving, B., and Coussens, L.M. (2014). B cells regulate macrophage phenotype and response to chemotherapy in squamous carcinomas. *Cancer Cell* 25, 809-821.
- Agata, Y., Kawasaki, A., Nishimura, H., Ishida, Y., Tsubata, T., Yagita, H., and Honjo, T. (1996). Expression of the PD-1 antigen on the surface of stimulated mouse T and B lymphocytes. *Int Immunol* 8, 765-772.
- Aggarwal, B.B. (2003). Signalling pathways of the TNF superfamily: a double-edged sword. *Nat Rev Immunol* 3, 745-756.
- Aggarwal, B.B., Gupta, S.C., and Kim, J.H. (2012). Historical perspectives on tumor necrosis factor and its superfamily: 25 years later, a golden journey. *Blood* 119, 651-665.
- Ahn, S.H., Kim, M., and Buratowski, S. (2004). Phosphorylation of serine 2 within the RNA polymerase II C-terminal domain couples transcription and 3' end processing. *Mol Cell* 13, 67-76.
- Akbay, E.A., Koyama, S., Liu, Y., Dries, R., Bufe, L.E., Silkes, M., Alam, M.M., Magee, D.M., Jones, R., Jinushi, M., Kulkarni, M., Carretero, J., Wang, X., Warner-Hatten, T., Cavanaugh, J.D., Osa, A., Kumanogoh, A., Freeman, G.J., Awad, M.M., Christiani, D.C., Bueno, R., Hammerman, P.S., Dranoff, G., and Wong, K.K. (2017). Interleukin-17A Promotes Lung Tumor Progression through Neutrophil Attraction to Tumor Sites and Mediating Resistance to PD-1 Blockade. *J Thorac Oncol* 12, 1268-1279.
- Akhtar, M.S., Heidemann, M., Tietjen, J.R., Zhang, D.W., Chapman, R.D., Eick, D., and Ansari, A.Z. (2009). TFIIH kinase places bivalent marks on the carboxy-terminal domain of RNA polymerase II. *Mol Cell* 34, 387-393.
- Albert, T.K., Rigault, C., Eickhoff, J., Baumgart, K., Antrecht, C., Klebl, B., Mittler, G., and Meisterernst, M. (2014). Characterization of molecular and cellular functions of the cyclin-dependent kinase CDK9 using a novel specific inhibitor. *Br J Pharmacol* 171, 55-68.
- Alexandrov, L.B., Ju, Y.S., Haase, K., Van Loo, P., Martincorena, I., Nik-Zainal, S., Totoki, Y., Fujimoto, A., Nakagawa, H., Shibata, T., Campbell, P.J., Vineis, P., Phillips, D.H., and Stratton, M.R. (2016). Mutational signatures associated with tobacco smoking in human cancer. *Science* 354, 618-622.
- Alexandrov, L.B., Nik-Zainal, S., Wedge, D.C., Aparicio, S.A., Behjati, S., Biankin, A.V., Bignell, G.R., Bolli, N., Borg, A., Borresen-Dale, A.L., Boyault, S., Burkhardt, B., Butler, A.P., Caldas, C., Davies, H.R., Desmedt, C., Eils, R., Eyfjord, J.E., Foekens, J.A., Greaves, M., Hosoda, F., Hutter, B., Ilcic, T., Imbeaud, S., Imielinski, M., Jager, N., Jones, D.T., Jones, D., Knappskog, S., Kool, M., Lakhani, S.R., Lopez-Otin, C., Martin, S., Munshi, N.C., Nakamura,

H., Northcott, P.A., Pajic, M., Papaemmanuil, E., Paradiso, A., Pearson, J.V., Puente, X.S., Raine, K., Ramakrishna, M., Richardson, A.L., Richter, J., Rosenstiel, P., Schlesner, M., Schumacher, T.N., Span, P.N., Teague, J.W., Totoki, Y., Tutt, A.N., Valdes-Mas, R., van Buuren, M.M., van 't Veer, L., Vincent-Salomon, A., Waddell, N., Yates, L.R., Australian Pancreatic Cancer Genome, I., Consortium, I.B.C., Consortium, I.M.-S., PedBrain, I., Zucman-Rossi, J., Futreal, P.A., McDermott, U., Lichter, P., Meyerson, M., Grimmond, S.M., Siebert, R., Campo, E., Shibata, T., Pfister, S.M., Campbell, P.J., and Stratton, M.R. (2013). Signatures of mutational processes in human cancer. *Nature* **500**, 415-421.

Alnemri, E.S., Livingston, D.J., Nicholson, D.W., Salvesen, G., Thornberry, N.A., Wong, W.W., and Yuan, J. (1996). Human ICE/CED-3 protease nomenclature. *Cell* **87**, 171.

Antonia, S.J., Villegas, A., Daniel, D., Vicente, D., Murakami, S., Hui, R., Kurata, T., Chiappori, A., Lee, K.H., de Wit, M., Cho, B.C., Bourhaba, M., Quantin, X., Tokito, T., Mekhail, T., Planchard, D., Kim, Y.C., Karapetis, C.S., Huret, S., Ostoros, G., Kubota, K., Gray, J.E., Paz-Ares, L., de Castro Carpeno, J., Faivre-Finn, C., Reck, M., Vansteenkiste, J., Spigel, D.R., Wadsworth, C., Melillo, G., Taboada, M., Dennis, P.A., Ozguroglu, M., and Investigators, P. (2018). Overall Survival with Durvalumab after Chemoradiotherapy in Stage III NSCLC. *N Engl J Med* **379**, 2342-2350.

Ashkenazi, A. (2015). Targeting the extrinsic apoptotic pathway in cancer: lessons learned and future directions. *J Clin Invest* **125**, 487-489.

Ashkenazi, A., Pai, R.C., Fong, S., Leung, S., Lawrence, D.A., Marsters, S.A., Blackie, C., Chang, L., McMurtrey, A.E., Hebert, A., DeForge, L., Koumenis, I.L., Lewis, D., Harris, L., Bussiere, J., Koeppen, H., Shahrokh, Z., and Schwall, R.H. (1999). Safety and antitumor activity of recombinant soluble Apo2 ligand. *J Clin Invest* **104**, 155-162.

Azijli, K., Yuvaraj, S., Peppelenbosch, M.P., Wurdinger, T., Dekker, H., Joore, J., van Dijk, E., Quax, W.J., Peters, G.J., de Jong, S., and Kruijt, F.A. (2012). Kinome profiling of non-canonical TRAIL signaling reveals RIP1-Src-STAT3-dependent invasion in resistant non-small cell lung cancer cells. *J Cell Sci* **125**, 4651-4661.

Bagella, L., MacLachlan, T.K., Buono, R.J., Pisano, M.M., Giordano, A., and De Luca, A. (1998). Cloning of murine CDK9/PITALRE and its tissue-specific expression in development. *J Cell Physiol* **177**, 206-213.

Bagella, L., Stiegler, P., De Luca, A., Siracusa, L.D., and Giordano, A. (2000). Genomic organization, promoter analysis, and chromosomal mapping of the mouse gene encoding Cdk9. *J Cell Biochem* **78**, 170-178.

Baker, A., Gregory, G.P., Verbrugge, I., Kats, L., Hilton, J.J., Vidacs, E., Lee, E.M., Lock, R.B., Zuber, J., Shortt, J., and Johnstone, R.W. (2016). The CDK9 Inhibitor Dinaciclib Exerts Potent Apoptotic and Antitumor Effects in Preclinical Models of MLL-Rearranged Acute Myeloid Leukemia. *Cancer Res* **76**, 1158-1169.

Baker, E.K., Taylor, S., Gupte, A., Sharp, P.P., Walia, M., Walsh, N.C., Zannettino, A.C., Chalk, A.M., Burns, C.J., and Walkley, C.R. (2015). BET inhibitors induce apoptosis through a MYC independent mechanism and synergise with CDK inhibitors to kill osteosarcoma cells. *Sci Rep* **5**, 10120.

Balkwill, F.R., and Mantovani, A. (2012). Cancer-related inflammation: common themes and therapeutic opportunities. *Semin Cancer Biol* **22**, 33-40.

Bang, Y.J. (2011). The potential for crizotinib in non-small cell lung cancer: a perspective review. *Ther Adv Med Oncol* **3**, 279-291.

- Barboric, M., Lenasi, T., Chen, H., Johansen, E.B., Guo, S., and Peterlin, B.M. (2009). 7SK snRNP/P-TEFb couples transcription elongation with alternative splicing and is essential for vertebrate development. *Proc Natl Acad Sci U S A* *106*, 7798-7803.
- Barboric, M., Nissen, R.M., Kanazawa, S., Jabrane-Ferrat, N., and Peterlin, B.M. (2001). NF-kappaB binds P-TEFb to stimulate transcriptional elongation by RNA polymerase II. *Mol Cell* *8*, 327-337.
- Bartholomeeusen, K., Xiang, Y., Fujinaga, K., and Peterlin, B.M. (2012). Bromodomain and extra-terminal (BET) bromodomain inhibition activate transcription via transient release of positive transcription elongation factor b (P-TEFb) from 7SK small nuclear ribonucleoprotein. *J Biol Chem* *287*, 36609-36616.
- Belch, A., Sharma, A., Spencer, A., Tarantolo, S., Bahlis, N.J., Doval, D., Gallant, G., Kumm, E., Klein, J., and Chanan-Khan, A. (2010). A Multicenter Randomized Phase II Trial of Mapatumumab, a TRAIL-R1 Agonist Monoclonal Antibody, In Combination with Bortezomib In Patients with Relapsed/Refractory Multiple Myeloma (MM). *Blood* *116*, Abstracts 5031.
- Belyanskaya, L.L., Ziogas, A., Hopkins-Donaldson, S., Kurtz, S., Simon, H.U., Stahel, R., and Zangemeister-Wittke, U. (2008). TRAIL-induced survival and proliferation of SCLC cells is mediated by ERK and dependent on TRAIL-R2/DR5 expression in the absence of caspase-8. *Lung Cancer* *60*, 355-365.
- Berg, D., Lehne, M., Muller, N., Siegmund, D., Munkel, S., Sebald, W., Pfizenmaier, K., and Wajant, H. (2007). Enforced covalent trimerization increases the activity of the TNF ligand family members TRAIL and CD95L. *Cell Death Differ* *14*, 2021-2034.
- Bettayeb, K., Tirado, O.M., Marionneau-Lambot, S., Ferandin, Y., Lozach, O., Morris, J.C., Mateo-Lozano, S., Drucekes, P., Schachtele, C., Kubbutat, M.H., Liger, F., Marquet, B., Joseph, B., Echaliier, A., Endicott, J.A., Notario, V., and Meijer, L. (2007). Meriolins, a new class of cell death inducing kinase inhibitors with enhanced selectivity for cyclin-dependent kinases. *Cancer Res* *67*, 8325-8334.
- Beyer, K., Baukloh, A.K., Stoyanova, A., Kamphues, C., Sattler, A., and Kotsch, K. (2019). Interactions of Tumor Necrosis Factor-Related Apoptosis-Inducing Ligand (TRAIL) with the Immune System: Implications for Inflammation and Cancer. *Cancers (Basel)* *11*.
- Bisgrove, D.A., Mahmoudi, T., Henklein, P., and Verdin, E. (2007). Conserved P-TEFb-interacting domain of BRD4 inhibits HIV transcription. *Proc Natl Acad Sci U S A* *104*, 13690-13695.
- Bodmer, J.L., Meier, P., Tschopp, J., and Schneider, P. (2000). Cysteine 230 is essential for the structure and activity of the cytotoxic ligand TRAIL. *J Biol Chem* *275*, 20632-20637.
- Bodogai, M., Moritoh, K., Lee-Chang, C., Hollander, C.M., Sherman-Baust, C.A., Wersto, R.P., Araki, Y., Miyoshi, I., Yang, L., Trinchieri, G., and Biragyn, A. (2015). Immunosuppressive and Prometastatic Functions of Myeloid-Derived Suppressive Cells Rely upon Education from Tumor-Associated B Cells. *Cancer Res* *75*, 3456-3465.
- Boldin, M.P., Goncharov, T.M., Goltsev, Y.V., and Wallach, D. (1996). Involvement of MACH, a novel MORT1/FADD-interacting protease, in Fas/APO-1- and TNF receptor-induced cell death. *Cell* *85*, 803-815.
- Boldin, M.P., Varfolomeev, E.E., Pancer, Z., Mett, I.L., Camonis, J.H., and Wallach, D. (1995). A novel protein that interacts with the death domain of Fas/APO1 contains a sequence motif related to the death domain. *J Biol Chem* *270*, 7795-7798.

Booher, R.N., Hatch, H., Dolinski, B.M., Nguyen, T., Harmonay, L., Al-Assaad, A.S., Ayers, M., Nebozhyn, M., Loboda, A., Hirsch, H.A., Zhang, T., Shi, B., Merkel, C.E., Angagaw, M.H., Wang, Y., Long, B.J., Lennon, X.Q., Miselis, N., Pucci, V., Monahan, J.W., Lee, J., Kondic, A.G., Im, E.K., Mauro, D., Blanchard, R., Gilliland, G., Fawell, S.E., Zavel, L., Schuller, A.G., and Strack, P. (2014). MCL1 and BCL-xL levels in solid tumors are predictive of dinaciclib-induced apoptosis. *PLoS One* 9, e108371.

Borghaei, H., Paz-Ares, L., Horn, L., Spigel, D.R., Steins, M., Ready, N.E., Chow, L.Q., Vokes, E.E., Felip, E., Holgado, E., Barlesi, F., Kohlhaufl, M., Arrieta, O., Burgio, M.A., Fayette, J., Lena, H., Poddubskaya, E., Gerber, D.E., Gettinger, S.N., Rudin, C.M., Rizvi, N., Crino, L., Blumenschein, G.R., Jr., Antonia, S.J., Dorange, C., Harbison, C.T., Graf Finckenstein, F., and Brahmer, J.R. (2015). Nivolumab versus Docetaxel in Advanced Nonsquamous Non-Small-Cell Lung Cancer. *N Engl J Med* 373, 1627-1639.

Bossen, C., Ingold, K., Tardivel, A., Bodmer, J.L., Gaide, O., Hertig, S., Ambrose, C., Tschopp, J., and Schneider, P. (2006). Interactions of tumor necrosis factor (TNF) and TNF receptor family members in the mouse and human. *J Biol Chem* 281, 13964-13971.

Bossi, F., Bernardi, S., Zauli, G., Secchiero, P., and Fabris, B. (2015). TRAIL modulates the immune system and protects against the development of diabetes. *J Immunol Res* 2015, 680749.

Bott, M., Brevet, M., Taylor, B.S., Shimizu, S., Ito, T., Wang, L., Creaney, J., Lake, R.A., Zakowski, M.F., Reva, B., Sander, C., Delsite, R., Powell, S., Zhou, Q., Shen, R., Olshen, A., Rusch, V., and Ladanyi, M. (2011). The nuclear deubiquitinase BAP1 is commonly inactivated by somatic mutations and 3p21.1 losses in malignant pleural mesothelioma. *Nat Genet* 43, 668-672.

Brahmer, J., Reckamp, K.L., Baas, P., Crino, L., Eberhardt, W.E., Poddubskaya, E., Antonia, S., Pluzanski, A., Vokes, E.E., Holgado, E., Waterhouse, D., Ready, N., Gainor, J., Aren Frontera, O., Havel, L., Steins, M., Garassino, M.C., Aerts, J.G., Domine, M., Paz-Ares, L., Reck, M., Baudelet, C., Harbison, C.T., Lestini, B., and Spigel, D.R. (2015). Nivolumab versus Docetaxel in Advanced Squamous-Cell Non-Small-Cell Lung Cancer. *N Engl J Med* 373, 123-135.

Bratton, S.B., Lewis, J., Butterworth, M., Duckett, C.S., and Cohen, G.M. (2002). XIAP inhibition of caspase-3 preserves its association with the Apaf-1 apoptosome and prevents CD95- and Bax-induced apoptosis. *Cell Death Differ* 9, 881-892.

Brosh, R., and Rotter, V. (2009). When mutants gain new powers: news from the mutant p53 field. *Nat Rev Cancer* 9, 701-713.

Brunner, M.C., Chambers, C.A., Chan, F.K., Hanke, J., Winoto, A., and Allison, J.P. (1999). CTLA-4-Mediated inhibition of early events of T cell proliferation. *J Immunol* 162, 5813-5820.

Buratowski, S. (2003). The CTD code. *Nat Struct Biol* 10, 679-680.

Buratowski, S., Hahn, S., Guarente, L., and Sharp, P.A. (1989). Five intermediate complexes in transcription initiation by RNA polymerase II. *Cell* 56, 549-561.

Burns, T.F., and El-Deiry, W.S. (2001). Identification of inhibitors of TRAIL-induced death (ITIDs) in the TRAIL-sensitive colon carcinoma cell line SW480 using a genetic approach. *J Biol Chem* 276, 37879-37886.

Cai, Z., Jitkaew, S., Zhao, J., Chiang, H.C., Choksi, S., Liu, J., Ward, Y., Wu, L.G., and Liu, Z.G. (2014). Plasma membrane translocation of trimerized MLKL protein is required for TNF-induced necroptosis. *Nat Cell Biol* 16, 55-65.

- Camidge, D.R., Herbst, R.S., Gordon, M.S., Eckhardt, S.G., Kurzrock, R., Durbin, B., Ing, J., Tohny, T.M., Sager, J., Ashkenazi, A., Bray, G., and Mendelson, D. (2010). A phase I safety and pharmacokinetic study of the death receptor 5 agonistic antibody PRO95780 in patients with advanced malignancies. *Clin Cancer Res* 16, 1256-1263.
- Campbell, J.D., Alexandrov, A., Kim, J., Wala, J., Berger, A.H., Pedamallu, C.S., Shukla, S.A., Guo, G., Brooks, A.N., Murray, B.A., Imielinski, M., Hu, X., Ling, S., Akbani, R., Rosenberg, M., Cibulskis, C., Ramachandran, A., Collisson, E.A., Kwiatkowski, D.J., Lawrence, M.S., Weinstein, J.N., Verhaak, R.G., Wu, C.J., Hammerman, P.S., Cherniack, A.D., Getz, G., Cancer Genome Atlas Research, N., Artyomov, M.N., Schreiber, R., Govindan, R., and Meyerson, M. (2016). Distinct patterns of somatic genome alterations in lung adenocarcinomas and squamous cell carcinomas. *Nat Genet* 48, 607-616.
- Cancer Genome Atlas Research, N. (2014). Comprehensive molecular profiling of lung adenocarcinoma. *Nature* 511, 543-550.
- Canon, J., Rex, K., Saiki, A.Y., Mohr, C., Cooke, K., Bagal, D., Gaida, K., Holt, T., Knutson, C.G., Koppada, N., Lanman, B.A., Werner, J., Rapaport, A.S., San Miguel, T., Ortiz, R., Osgood, T., Sun, J.R., Zhu, X., McCarter, J.D., Volak, L.P., Houk, B.E., Fakih, M.G., O'Neil, B.H., Price, T.J., Falchook, G.S., Desai, J., Kuo, J., Govindan, R., Hong, D.S., Ouyang, W., Henary, H., Arvedson, T., Cee, V.J., and Lipford, J.R. (2019). The clinical KRAS(G12C) inhibitor AMG 510 drives anti-tumour immunity. *Nature*.
- Carbone, D.P., Gandara, D.R., Antonia, S.J., Zielinski, C., and Paz-Ares, L. (2015). Non-Small-Cell Lung Cancer: Role of the Immune System and Potential for Immunotherapy. *J Thorac Oncol* 10, 974-984.
- Carbone, D.P., Reck, M., Paz-Ares, L., Creelan, B., Horn, L., Steins, M., Felip, E., van den Heuvel, M.M., Ciuleanu, T.E., Badin, F., Ready, N., Hiltermann, T.J.N., Nair, S., Juergens, R., Peters, S., Minenza, E., Wrangle, J.M., Rodriguez-Abreu, D., Borghaei, H., Blumenschein, G.R., Jr., Villaruz, L.C., Havel, L., Krejci, J., Corral Jaime, J., Chang, H., Geese, W.J., Bhagavatheeswaran, P., Chen, A.C., Socinski, M.A., and CheckMate, I. (2017). First-Line Nivolumab in Stage IV or Recurrent Non-Small-Cell Lung Cancer. *N Engl J Med* 376, 2415-2426.
- Carswell, E.A., Old, L.J., Kassel, R.L., Green, S., Fiore, N., and Williamson, B. (1975). An endotoxin-induced serum factor that causes necrosis of tumors. *Proc Natl Acad Sci U S A* 72, 3666-3670.
- Cetintas, V.B., Kucukaslan, A.S., Kosova, B., Tetik, A., Selvi, N., Cok, G., Gunduz, C., and Eroglu, Z. (2012). Cisplatin resistance induced by decreased apoptotic activity in non-small-cell lung cancer cell lines. *Cell Biol Int* 36, 261-265.
- Cha, S.S., Kim, M.S., Choi, Y.H., Sung, B.J., Shin, N.K., Shin, H.C., Sung, Y.C., and Oh, B.H. (1999). 2.8 Å resolution crystal structure of human TRAIL, a cytokine with selective antitumor activity. *Immunity* 11, 253-261.
- Chai, J., Du, C., Wu, J.W., Kyin, S., Wang, X., and Shi, Y. (2000). Structural and biochemical basis of apoptotic activation by Smac/DIABLO. *Nature* 406, 855-862.
- Chang, D.W., Xing, Z., Pan, Y., Algeciras-Schimmich, A., Barnhart, B.C., Yaish-Ohad, S., Peter, M.E., and Yang, X. (2002). c-FLIP(L) is a dual function regulator for caspase-8 activation and CD95-mediated apoptosis. *EMBO J* 21, 3704-3714.
- Chaudhary, P.M., Eby, M., Jasmin, A., Bookwalter, A., Murray, J., and Hood, L. (1997). Death receptor 5, a new member of the TNFR family, and DR4 induce FADD-dependent apoptosis and activate the NF-kappaB pathway. *Immunity* 7, 821-830.

Cheah, C.Y., Belada, D., Fanale, M.A., Janikova, A., Czucman, M.S., Flinn, I.W., Kapp, A.V., Ashkenazi, A., Kelley, S., Bray, G.L., Holden, S., and Seymour, J.F. (2015). Dulanermin with rituximab in patients with relapsed indolent B-cell lymphoma: an open-label phase 1b/2 randomised study. *Lancet Haematol* 2, e166-174.

Chen, R., Keating, M.J., Gandhi, V., and Plunkett, W. (2005). Transcription inhibition by flavopiridol: mechanism of chronic lymphocytic leukemia cell death. *Blood* 106, 2513-2519.

Chen, W., Zhou, Z., Li, L., Zhong, C.Q., Zheng, X., Wu, X., Zhang, Y., Ma, H., Huang, D., Li, W., Xia, Z., and Han, J. (2013). Diverse sequence determinants control human and mouse receptor interacting protein 3 (RIP3) and mixed lineage kinase domain-like (MLKL) interaction in necroptotic signaling. *J Biol Chem* 288, 16247-16261.

Chen, X., Li, W., Ren, J., Huang, D., He, W.T., Song, Y., Yang, C., Li, W., Zheng, X., Chen, P., and Han, J. (2014a). Translocation of mixed lineage kinase domain-like protein to plasma membrane leads to necrotic cell death. *Cell Res* 24, 105-121.

Chen, Y., Germano, S., Clements, C., Samuel, J., Shelmani, G., Jayne, S., Dyer, M.J., and Macip, S. (2016). Pro-survival signal inhibition by CDK inhibitor dinaciclib in Chronic Lymphocytic Leukaemia. *Br J Haematol* 175, 641-651.

Chen, Z., Fillmore, C.M., Hammerman, P.S., Kim, C.F., and Wong, K.K. (2014b). Non-small-cell lung cancers: a heterogeneous set of diseases. *Nat Rev Cancer* 14, 535-546.

Cheng, A.L., Kang, Y.K., He, A.R., Lim, H.Y., Ryou, B.Y., Hung, C.H., Sheen, I.S., Izumi, N., Austin, T., Wang, Q., Greenberg, J., Shiratori, S., Beckman, R.A., Kudo, M., and Investigators' Study, G. (2015). Safety and efficacy of tigatuzumab plus sorafenib as first-line therapy in subjects with advanced hepatocellular carcinoma: A phase 2 randomized study. *J Hepatol* 63, 896-904.

Chinnaiyan, A.M., O'Rourke, K., Tewari, M., and Dixit, V.M. (1995). FADD, a novel death domain-containing protein, interacts with the death domain of Fas and initiates apoptosis. *Cell* 81, 505-512.

Chipuk, J.E., Kuwana, T., Bouchier-Hayes, L., Droin, N.M., Newmeyer, D.D., Schuler, M., and Green, D.R. (2004). Direct activation of Bax by p53 mediates mitochondrial membrane permeabilization and apoptosis. *Science* 303, 1010-1014.

Cho, E.J., Kobor, M.S., Kim, M., Greenblatt, J., and Buratowski, S. (2001). Opposing effects of Ctk1 kinase and Fcp1 phosphatase at Ser 2 of the RNA polymerase II C-terminal domain. *Genes Dev* 15, 3319-3329.

Cidado, J., Boiko, S., Proia, T., Ferguson, D., Criscione, S.W., San Martin, M., Pop-Damkov, P., Su, N., Roamio Franklin, V.N., Sekhar Reddy Chilamakuri, C., D'Santos, C.S., Shao, W., Saeh, J.C., Koch, R., Weinstock, D.M., Zinda, M., Fawell, S.E., and Drew, L. (2019). AZD4573 is a highly selective CDK9 inhibitor that suppresses Mcl-1 and induces apoptosis in hematological cancer cells. *Clin Cancer Res*.

Cihalova, D., Ceckova, M., Kucera, R., Klimes, J., and Staud, F. (2015). Dinaciclib, a cyclin-dependent kinase inhibitor, is a substrate of human ABCB1 and ABCG2 and an inhibitor of human ABCC1 in vitro. *Biochem Pharmacol* 98, 465-472.

Ciprotti, M., Tebbutt, N.C., Lee, F.T., Lee, S.T., Gan, H.K., McKee, D.C., O'Keefe, G.J., Gong, S.J., Chong, G., Hopkins, W., Chappell, B., Scott, F.E., Brechbiel, M.W., Tse, A.N., Jansen, M., Matsumura, M., Kotsuma, M., Watanabe, R., Venhaus, R., Beckman, R.A., Greenberg, J., and Scott, A.M. (2015). Phase I Imaging and Pharmacodynamic Trial of CS-1008 in Patients With Metastatic Colorectal Cancer. *J Clin Oncol* 33, 2609-2616.

- Ciuleanu, T., Bazin, I., Lungulescu, D., Miron, L., Bondarenko, I., Deptala, A., Rodriguez-Torres, M., Giantonio, B., Fox, N.L., Wissel, P., Egger, J., Ding, M., Kalyani, R.N., Humphreys, R., Gribbin, M., and Sun, W. (2016). A randomized, double-blind, placebo-controlled phase II study to assess the efficacy and safety of mapatumumab with sorafenib in patients with advanced hepatocellular carcinoma. *Ann Oncol* 27, 680-687.
- Clohessy, J.G., Zhuang, J., de Boer, J., Gil-Gomez, G., and Brady, H.J. (2006). Mcl-1 interacts with truncated Bid and inhibits its induction of cytochrome c release and its role in receptor-mediated apoptosis. *J Biol Chem* 281, 5750-5759.
- Cohn, A.L., Taberero, J., Maurel, J., Nowara, E., Sastre, J., Chuah, B.Y., Kopp, M.V., Sakaeva, D.D., Mitchell, E.P., Dubey, S., Suzuki, S., Hei, Y.J., Galimi, F., McCaffery, I., Pan, Y., Loberg, R., Cottrell, S., and Choo, S.P. (2013). A randomized, placebo-controlled phase 2 study of ganitumab or conatumumab in combination with FOLFIRI for second-line treatment of mutant KRAS metastatic colorectal cancer. *Ann Oncol* 24, 1777-1785.
- Condamine, T., Kumar, V., Ramachandran, I.R., Youn, J.I., Celis, E., Finnberg, N., El-Deiry, W.S., Winograd, R., Vonderheide, R.H., English, N.R., Knight, S.C., Yagita, H., McCaffrey, J.C., Antonia, S., Hockstein, N., Witt, R., Masters, G., Bauer, T., and Gabrilovich, D.I. (2014). ER stress regulates myeloid-derived suppressor cell fate through TRAIL-R-mediated apoptosis. *J Clin Invest* 124, 2626-2639.
- Conroy, A., Stockett, D.E., Walker, D., Arkin, M.R., Hoch, U., Fox, J.A., and Hawtin, R.E. (2009). SNS-032 is a potent and selective CDK 2, 7 and 9 inhibitor that drives target modulation in patient samples. *Cancer Chemother Pharmacol* 64, 723-732.
- Cretney, E., Takeda, K., Yagita, H., Glaccum, M., Peschon, J.J., and Smyth, M.J. (2002). Increased susceptibility to tumor initiation and metastasis in TNF-related apoptosis-inducing ligand-deficient mice. *J Immunol* 168, 1356-1361.
- Cristofanon, S., and Fulda, S. (2012). ABT-737 promotes tBid mitochondrial accumulation to enhance TRAIL-induced apoptosis in glioblastoma cells. *Cell Death Dis* 3, e432.
- Danilov, A.V., Hu, S., Orr, B., Godek, K., Mustachio, L.M., Sekula, D., Liu, X., Kawakami, M., Johnson, F.M., Compton, D.A., Freemantle, S.J., and Dmitrovsky, E. (2016). Dinaciclib Induces Anaphase Catastrophe in Lung Cancer Cells via Inhibition of Cyclin-Dependent Kinases 1 and 2. *Mol Cancer Ther* 15, 2758-2766.
- Davison, B.L., Egly, J.M., Mulvihill, E.R., and Chambon, P. (1983). Formation of stable preinitiation complexes between eukaryotic class B transcription factors and promoter sequences. *Nature* 301, 680-686.
- de Bruin, E.C., McGranahan, N., Mitter, R., Salm, M., Wedge, D.C., Yates, L., Jamal-Hanjani, M., Shafi, S., Murugaesu, N., Rowan, A.J., Gronroos, E., Muhammad, M.A., Horswell, S., Gerlinger, M., Varela, I., Jones, D., Marshall, J., Voet, T., Van Loo, P., Rasi, D.M., Rintoul, R.C., Janes, S.M., Lee, S.M., Forster, M., Ahmad, T., Lawrence, D., Falzon, M., Capitanio, A., Harkins, T.T., Lee, C.C., Tom, W., Teefe, E., Chen, S.C., Begum, S., Rabinowitz, A., Phillimore, B., Spencer-Dene, B., Stamp, G., Szallasi, Z., Matthews, N., Stewart, A., Campbell, P., and Swanton, C. (2014). Spatial and temporal diversity in genomic instability processes defines lung cancer evolution. *Science* 346, 251-256.
- De Falco, G., Leucci, E., Onnis, A., Bellan, C., Tigli, C., Wirths, S., Cerino, G., Cocco, M., Crupi, D., De Luca, A., Lanzavecchia, A., Tosi, P., Leoncini, L., and Giordano, A. (2008). Cdk9/Cyclin T1 complex: a key player during the activation/differentiation process of normal lymphoid B cells. *J Cell Physiol* 215, 276-282.

- Decker, T.M., Kluge, M., Krebs, S., Shah, N., Blum, H., Friedel, C.C., and Eick, D. (2017). Transcriptome analysis of dominant-negative Brd4 mutants identifies Brd4-specific target genes of small molecule inhibitor JQ1. *Sci Rep* 7, 1684.
- Declercq, W., Vanden Berghe, T., and Vandenabeele, P. (2009). RIP kinases at the crossroads of cell death and survival. *Cell* 138, 229-232.
- Degli-Esposti, M.A., Dougall, W.C., Smolak, P.J., Waugh, J.Y., Smith, C.A., and Goodwin, R.G. (1997a). The novel receptor TRAIL-R4 induces NF-kappaB and protects against TRAIL-mediated apoptosis, yet retains an incomplete death domain. *Immunity* 7, 813-820.
- Degli-Esposti, M.A., Smolak, P.J., Walczak, H., Waugh, J., Huang, C.P., DuBose, R.F., Goodwin, R.G., and Smith, C.A. (1997b). Cloning and characterization of TRAIL-R3, a novel member of the emerging TRAIL receptor family. *J Exp Med* 186, 1165-1170.
- Degterev, A., Hitomi, J., Gemscheid, M., Ch'en, I.L., Korkina, O., Teng, X., Abbott, D., Cuny, G.D., Yuan, C., Wagner, G., Hedrick, S.M., Gerber, S.A., Lugovskoy, A., and Yuan, J. (2008). Identification of RIP1 kinase as a specific cellular target of necrostatins. *Nat Chem Biol* 4, 313-321.
- Demetri, G.D., Le Cesne, A., Chawla, S.P., Brodowicz, T., Maki, R.G., Bach, B.A., Smethurst, D.P., Bray, S., Hei, Y.J., and Blay, J.Y. (2012). First-line treatment of metastatic or locally advanced unresectable soft tissue sarcomas with conatumumab in combination with doxorubicin or doxorubicin alone: a phase I/II open-label and double-blind study. *Eur J Cancer* 48, 547-563.
- Desai, B.M., Villanueva, J., Nguyen, T.T., Lioni, M., Xiao, M., Kong, J., Krepler, C., Vultur, A., Flaherty, K.T., Nathanson, K.L., Smalley, K.S., and Herlyn, M. (2013). The anti-melanoma activity of dinaciclib, a cyclin-dependent kinase inhibitor, is dependent on p53 signaling. *PLoS One* 8, e59588.
- Devaiah, B.N., Lewis, B.A., Cherman, N., Hewitt, M.C., Albrecht, B.K., Robey, P.G., Ozato, K., Sims, R.J., 3rd, and Singer, D.S. (2012). BRD4 is an atypical kinase that phosphorylates serine2 of the RNA polymerase II carboxy-terminal domain. *Proc Natl Acad Sci U S A* 109, 6927-6932.
- Deveraux, Q.L., Takahashi, R., Salvesen, G.S., and Reed, J.C. (1997). X-linked IAP is a direct inhibitor of cell-death proteases. *Nature* 388, 300-304.
- Dey, A., Chitsaz, F., Abbasi, A., Misteli, T., and Ozato, K. (2003). The double bromodomain protein Brd4 binds to acetylated chromatin during interphase and mitosis. *Proc Natl Acad Sci U S A* 100, 8758-8763.
- Dey, J., Deckwerth, T.L., Kerwin, W.S., Casalini, J.R., Merrell, A.J., Grenley, M.O., Burns, C., Ditzler, S.H., Dixon, C.P., Beirne, E., Gillespie, K.C., Kleinman, E.F., and Klinghoffer, R.A. (2017). Voruciclib, a clinical stage oral CDK9 inhibitor, represses MCL-1 and sensitizes high-risk Diffuse Large B-cell Lymphoma to BCL2 inhibition. *Sci Rep* 7, 18007.
- Diao, Z., Shi, J., Zhu, J., Yuan, H., Ru, Q., Liu, S., Liu, Y., and Zheng, D. (2013). TRAIL suppresses tumor growth in mice by inducing tumor-infiltrating CD4(+)CD25 (+) Treg apoptosis. *Cancer Immunol Immunother* 62, 653-663.
- Dickens, L.S., Boyd, R.S., Jukes-Jones, R., Hughes, M.A., Robinson, G.L., Fairall, L., Schwabe, J.W., Cain, K., and Macfarlane, M. (2012). A death effector domain chain DISC model reveals a crucial role for caspase-8 chain assembly in mediating apoptotic cell death. *Mol Cell* 47, 291-305.

- Diehl, G.E., Yue, H.H., Hsieh, K., Kuang, A.A., Ho, M., Morici, L.A., Lenz, L.L., Cado, D., Riley, L.W., and Winoto, A. (2004). TRAIL-R as a negative regulator of innate immune cell responses. *Immunity* **21**, 877-889.
- Dohrman, A., Russell, J.Q., Cuenin, S., Fortner, K., Tschopp, J., and Budd, R.C. (2005). Cellular FLIP long form augments caspase activity and death of T cells through heterodimerization with and activation of caspase-8. *J Immunol* **175**, 311-318.
- Doi, T., Murakami, H., Ohtsu, A., Fuse, N., Yoshino, T., Yamamoto, N., Boku, N., Onozawa, Y., Hsu, C.P., Gorski, K.S., Friberg, G., Kawaguchi, T., and Sasaki, T. (2011). Phase 1 study of conatumumab, a pro-apoptotic death receptor 5 agonist antibody, in Japanese patients with advanced solid tumors. *Cancer Chemother Pharmacol* **68**, 733-741.
- Dondelinger, Y., Declercq, W., Montessuit, S., Roelandt, R., Goncalves, A., Bruggeman, I., Hulpiau, P., Weber, K., Sehon, C.A., Marquis, R.W., Bertin, J., Gough, P.J., Savvides, S., Martinou, J.C., Bertrand, M.J., and Vandenabeele, P. (2014). MLKL compromises plasma membrane integrity by binding to phosphatidylinositol phosphates. *Cell Rep* **7**, 971-981.
- Dorothee, G., Vergnon, I., Menez, J., Echchakir, H., Grunenwald, D., Kubin, M., Chouaib, S., and Mami-Chouaib, F. (2002). Tumor-infiltrating CD4+ T lymphocytes express APO2 ligand (APO2L)/TRAIL upon specific stimulation with autologous lung carcinoma cells: role of IFN-alpha on APO2L/TRAIL expression and -mediated cytotoxicity. *J Immunol* **169**, 809-817.
- Drosten, M., and Barbacid, M. (2016). Modeling K-Ras-driven lung adenocarcinoma in mice: preclinical validation of therapeutic targets. *J Mol Med (Berl)* **94**, 121-135.
- Duesberg, P., Stindl, R., and Hehlmann, R. (2000). Explaining the high mutation rates of cancer cells to drug and multidrug resistance by chromosome reassortments that are catalyzed by aneuploidy. *Proc Natl Acad Sci U S A* **97**, 14295-14300.
- DuPage, M., Cheung, A.F., Mazumdar, C., Winslow, M.M., Bronson, R., Schmidt, L.M., Crowley, D., Chen, J., and Jacks, T. (2011). Endogenous T cell responses to antigens expressed in lung adenocarcinomas delay malignant tumor progression. *Cancer Cell* **19**, 72-85.
- DuPage, M., Dooley, A.L., and Jacks, T. (2009). Conditional mouse lung cancer models using adenoviral or lentiviral delivery of Cre recombinase. *Nat Protoc* **4**, 1064-1072.
- Eberhardy, S.R., and Farnham, P.J. (2001). c-Myc mediates activation of the cad promoter via a post-RNA polymerase II recruitment mechanism. *J Biol Chem* **276**, 48562-48571.
- Ehrhardt, H., Fulda, S., Schmid, I., Hiscott, J., Debatin, K.M., and Jeremias, I. (2003). TRAIL induced survival and proliferation in cancer cells resistant towards TRAIL-induced apoptosis mediated by NF-kappaB. *Oncogene* **22**, 3842-3852.
- El-Zawahry, A., McKillop, J., and Voelkel-Johnson, C. (2005). Doxorubicin increases the effectiveness of Apo2L/TRAIL for tumor growth inhibition of prostate cancer xenografts. *BMC Cancer* **5**, 2.
- Elmallah, M.I.Y., and Micheau, O. (2019). Epigenetic Regulation of TRAIL Signaling: Implication for Cancer Therapy. *Cancers (Basel)* **11**.
- Ember, S.W., Zhu, J.Y., Olesen, S.H., Martin, M.P., Becker, A., Berndt, N., Georg, G.I., and Schonbrunn, E. (2014). Acetyl-lysine binding site of bromodomain-containing protein 4 (BRD4) interacts with diverse kinase inhibitors. *ACS Chem Biol* **9**, 1160-1171.
- Emery, C.M., Vijayendran, K.G., Zipser, M.C., Sawyer, A.M., Niu, L., Kim, J.J., Hatton, C., Chopra, R., Oberholzer, P.A., Karpova, M.B., MacConaill, L.E., Zhang, J., Gray, N.S., Sellers,

- W.R., Dummer, R., and Garraway, L.A. (2009). MEK1 mutations confer resistance to MEK and B-RAF inhibition. *Proc Natl Acad Sci U S A* *106*, 20411-20416.
- Emery, J.G., McDonnell, P., Burke, M.B., Deen, K.C., Lyn, S., Silverman, C., Dul, E., Appelbaum, E.R., Eichman, C., DiPrinzio, R., Dodds, R.A., James, I.E., Rosenberg, M., Lee, J.C., and Young, P.R. (1998). Osteoprotegerin is a receptor for the cytotoxic ligand TRAIL. *J Biol Chem* *273*, 14363-14367.
- Engle, J.A., and Kolesar, J.M. (2014). Afatinib: A first-line treatment for selected patients with metastatic non-small-cell lung cancer. *Am J Health Syst Pharm* *71*, 1933-1938.
- Evans, T., Rosenthal, E.T., Youngblom, J., Distel, D., and Hunt, T. (1983). Cyclin: a protein specified by maternal mRNA in sea urchin eggs that is destroyed at each cleavage division. *Cell* *33*, 389-396.
- Fabre, C., Gobbi, M., Ezzili, C., Zoubir, M., Sablin, M.P., Small, K., Im, E., Shinwari, N., Zhang, D., Zhou, H., and Le Tourneau, C. (2014). Clinical study of the novel cyclin-dependent kinase inhibitor dinaciclib in combination with rituximab in relapsed/refractory chronic lymphocytic leukemia patients. *Cancer Chemother Pharmacol* *74*, 1057-1064.
- Fakler, M., Loeder, S., Vogler, M., Schneider, K., Jeremias, I., Debatin, K.M., and Fulda, S. (2009). Small molecule XIAP inhibitors cooperate with TRAIL to induce apoptosis in childhood acute leukemia cells and overcome Bcl-2-mediated resistance. *Blood* *113*, 1710-1722.
- Falco, G.D., Neri, L.M., Falco, M.D., Bellan, C., Yu, Z., Luca, A.D., Leoncini, L., and Giordano, A. (2002). Cdk9, a member of the cdc2-like family of kinases, binds to gp130, the receptor of the IL-6 family of cytokines. *Oncogene* *21*, 7464-7470.
- Fandy, T.E., Ross, D.D., Gore, S.D., and Srivastava, R.K. (2007). Flavopiridol synergizes TRAIL cytotoxicity by downregulation of FLIPL. *Cancer Chemother Pharmacol* *60*, 313-319.
- Fang, F., Wang, A.P., and Yang, S.F. (2005). Antitumor activity of a novel recombinant mutant human tumor necrosis factor-related apoptosis-inducing ligand. *Acta Pharmacol Sin* *26*, 1373-1381.
- Fanger, N.A., Maliszewski, C.R., Schooley, K., and Griffith, T.S. (1999). Human dendritic cells mediate cellular apoptosis via tumor necrosis factor-related apoptosis-inducing ligand (TRAIL). *J Exp Med* *190*, 1155-1164.
- Feldmann, G., Mishra, A., Bisht, S., Karikari, C., Garrido-Laguna, I., Rasheed, Z., Ottenhof, N.A., Dadon, T., Alvarez, H., Fendrich, V., Rajeshkumar, N.V., Matsui, W., Brossart, P., Hidalgo, M., Bannerji, R., Maitra, A., and Nelkin, B.D. (2011). Cyclin-dependent kinase inhibitor Dinaciclib (SCH727965) inhibits pancreatic cancer growth and progression in murine xenograft models. *Cancer Biol Ther* *12*, 598-609.
- Feng, S., Yang, Y., Mei, Y., Ma, L., Zhu, D.E., Hoti, N., Castanares, M., and Wu, M. (2007). Cleavage of RIP3 inactivates its caspase-independent apoptosis pathway by removal of kinase domain. *Cell Signal* *19*, 2056-2067.
- Filippakopoulos, P., Qi, J., Picaud, S., Shen, Y., Smith, W.B., Fedorov, O., Morse, E.M., Keates, T., Hickman, T.T., Fellettar, I., Philpott, M., Munro, S., McKeown, M.R., Wang, Y., Christie, A.L., West, N., Cameron, M.J., Schwartz, B., Heightman, T.D., La Thangue, N., French, C.A., Wiest, O., Kung, A.L., Knapp, S., and Bradner, J.E. (2010). Selective inhibition of BET bromodomains. *Nature* *468*, 1067-1073.
- Finnberg, N., Klein-Szanto, A.J., and El-Deiry, W.S. (2008). TRAIL-R deficiency in mice promotes susceptibility to chronic inflammation and tumorigenesis. *J Clin Invest* *118*, 111-123.

Fischer, K., Al-Sawaf, O., Bahlo, J., Fink, A.M., Tandon, M., Dixon, M., Robrecht, S., Warburton, S., Humphrey, K., Samoylova, O., Liberati, A.M., Pinilla-Ibarz, J., Opat, S., Sivcheva, L., Le Du, K., Fogliatto, L.M., Niemann, C.U., Weinkove, R., Robinson, S., Kipps, T.J., Boettcher, S., Tausch, E., Humerickhouse, R., Eichhorst, B., Wendtner, C.M., Langerak, A.W., Kreuzer, K.A., Ritgen, M., Goede, V., Stilgenbauer, S., Mobasher, M., and Hallek, M. (2019). Venetoclax and Obinutuzumab in Patients with CLL and Coexisting Conditions. *N Engl J Med* **380**, 2225-2236.

Fisher, R.P. (2005). Secrets of a double agent: CDK7 in cell-cycle control and transcription. *J Cell Sci* **118**, 5171-5180.

Flynn, J., Jones, J., Johnson, A.J., Andritsos, L., Maddocks, K., Jaglowski, S., Hessler, J., Grever, M.R., Im, E., Zhou, H., Zhu, Y., Zhang, D., Small, K., Bannerji, R., and Byrd, J.C. (2015). Dinaciclib is a novel cyclin-dependent kinase inhibitor with significant clinical activity in relapsed and refractory chronic lymphocytic leukemia. *Leukemia* **29**, 1524-1529.

Foley, J.F., Anderson, M.W., Stoner, G.D., Gaul, B.W., Hardisty, J.F., and Maronpot, R.R. (1991). Proliferative lesions of the mouse lung: progression studies in strain A mice. *Exp Lung Res* **17**, 157-168.

Forero-Torres, A., Infante, J.R., Waterhouse, D., Wong, L., Vickers, S., Arrowsmith, E., He, A.R., Hart, L., Trent, D., Wade, J., Jin, X., Wang, Q., Austin, T., Rosen, M., Beckman, R., von Roemeling, R., Greenberg, J., and Saleh, M. (2013). Phase 2, multicenter, open-label study of tigatuzumab (CS-1008), a humanized monoclonal antibody targeting death receptor 5, in combination with gemcitabine in chemotherapy-naïve patients with unresectable or metastatic pancreatic cancer. *Cancer Med* **2**, 925-932.

Forero-Torres, A., Shah, J., Wood, T., Posey, J., Carlisle, R., Copigneaux, C., Luo, F.R., Wojtowicz-Praga, S., Percent, I., and Saleh, M. (2010). Phase I trial of weekly tigatuzumab, an agonistic humanized monoclonal antibody targeting death receptor 5 (DR5). *Cancer Biother Radiopharm* **25**, 13-19.

Forero-Torres, A., Varley, K.E., Abramson, V.G., Li, Y., Vaklavas, C., Lin, N.U., Liu, M.C., Rugo, H.S., Nanda, R., Storniolo, A.M., Traina, T.A., Patil, S., Van Poznak, C.H., Nangia, J.R., Irvin, W.J., Jr., Krontiras, H., De Los Santos, J.F., Haluska, P., Grizzle, W., Myers, R.M., Wolff, A.C., and Translational Breast Cancer Research, C. (2015). TBCRC 019: A Phase II Trial of Nanoparticle Albumin-Bound Paclitaxel with or without the Anti-Death Receptor 5 Monoclonal Antibody Tigatuzumab in Patients with Triple-Negative Breast Cancer. *Clin Cancer Res* **21**, 2722-2729.

Forero, A., Bendell, J.C., Kumar, P., Janisch, L., Rosen, M., Wang, Q., Copigneaux, C., Desai, M., Senaldi, G., and Maitland, M.L. (2017). First-in-human study of the antibody DR5 agonist DS-8273a in patients with advanced solid tumors. *Invest New Drugs* **35**, 298-306.

Freeman, G.J., Long, A.J., Iwai, Y., Bourque, K., Chernova, T., Nishimura, H., Fitz, L.J., Malenkovich, N., Okazaki, T., Byrne, M.C., Horton, H.F., Fouser, L., Carter, L., Ling, V., Bowman, M.R., Carreno, B.M., Collins, M., Wood, C.R., and Honjo, T. (2000). Engagement of the PD-1 immunoinhibitory receptor by a novel B7 family member leads to negative regulation of lymphocyte activation. *J Exp Med* **192**, 1027-1034.

Fremd, C., Schuetz, F., Sohn, C., Beckhove, P., and Domschke, C. (2013). B cell-regulated immune responses in tumor models and cancer patients. *Oncoimmunology* **2**, e25443.

Frew, A.J., Lindemann, R.K., Martin, B.P., Clarke, C.J., Sharkey, J., Anthony, D.A., Banks, K.M., Haynes, N.M., Gangatirkar, P., Stanley, K., Bolden, J.E., Takeda, K., Yagita, H., Secrist, J.P., Smyth, M.J., and Johnstone, R.W. (2008). Combination therapy of established cancer using a histone deacetylase inhibitor and a TRAIL receptor agonist. *Proc Natl Acad Sci U S A* **105**, 11317-11322.

- Fu, W., Ma, L., Chu, B., Wang, X., Bui, M.M., Gemmer, J., Altiok, S., and Pledger, W.J. (2011). The cyclin-dependent kinase inhibitor SCH 727965 (dinaciclib) induces the apoptosis of osteosarcoma cells. *Mol Cancer Ther* 10, 1018-1027.
- Fuchs, C.S., Fakih, M., Schwartzberg, L., Cohn, A.L., Yee, L., Dreisbach, L., Kozloff, M.F., Hei, Y.J., Galimi, F., Pan, Y., Haddad, V., Hsu, C.P., Sabin, A., and Saltz, L. (2013). TRAIL receptor agonist conatumumab with modified FOLFOX6 plus bevacizumab for first-line treatment of metastatic colorectal cancer: A randomized phase 1b/2 trial. *Cancer* 119, 4290-4298.
- Fujinaga, K., Irwin, D., Huang, Y., Taube, R., Kurosu, T., and Peterlin, B.M. (2004). Dynamics of human immunodeficiency virus transcription: P-TEFb phosphorylates RD and dissociates negative effectors from the transactivation response element. *Mol Cell Biol* 24, 787-795.
- Fulda, S., and Debatin, K.M. (2002). IFN γ sensitizes for apoptosis by upregulating caspase-8 expression through the Stat1 pathway. *Oncogene* 21, 2295-2308.
- Fulda, S., Meyer, E., and Debatin, K.M. (2002a). Inhibition of TRAIL-induced apoptosis by Bcl-2 overexpression. *Oncogene* 21, 2283-2294.
- Fulda, S., Wick, W., Weller, M., and Debatin, K.M. (2002b). Smac agonists sensitize for Apo2L/TRAIL- or anticancer drug-induced apoptosis and induce regression of malignant glioma in vivo. *Nat Med* 8, 808-815.
- Gandhi, L., Rodriguez-Abreu, D., Gadgeel, S., Esteban, E., Felip, E., De Angelis, F., Domine, M., Clingan, P., Hochmair, M.J., Powell, S.F., Cheng, S.Y., Bischoff, H.G., Peled, N., Grossi, F., Jennens, R.R., Reck, M., Hui, R., Garon, E.B., Boyer, M., Rubio-Viqueira, B., Novello, S., Kurata, T., Gray, J.E., Vida, J., Wei, Z., Yang, J., Raftopoulos, H., Pietanza, M.C., and Garassino, M.C. (2018). Pembrolizumab plus Chemotherapy in Metastatic Non-Small-Cell Lung Cancer. *N Engl J Med* 378, 2078-2092.
- Ganten, T.M., Koschny, R., Sykora, J., Schulze-Bergkamen, H., Buchler, P., Haas, T.L., Schader, M.B., Untergasser, A., Stremmel, W., and Walczak, H. (2006). Preclinical differentiation between apparently safe and potentially hepatotoxic applications of TRAIL either alone or in combination with chemotherapeutic drugs. *Clin Cancer Res* 12, 2640-2646.
- Garon, E.B., Rizvi, N.A., Hui, R., Leighl, N., Balmanoukian, A.S., Eder, J.P., Patnaik, A., Aggarwal, C., Gubens, M., Horn, L., Carcereny, E., Ahn, M.J., Felip, E., Lee, J.S., Hellmann, M.D., Hamid, O., Goldman, J.W., Soria, J.C., Dolled-Filhart, M., Rutledge, R.Z., Zhang, J., Luceford, J.K., Rangwala, R., Lubiniecki, G.M., Roach, C., Emancipator, K., Gandhi, L., and Investigators, K.-. (2015). Pembrolizumab for the treatment of non-small-cell lung cancer. *N Engl J Med* 372, 2018-2028.
- Geng, C., Hou, J., Zhao, Y., Ke, X., Wang, Z., Qiu, L., Xi, H., Wang, F., Wei, N., Liu, Y., Yang, S., Wei, P., Zheng, X., Huang, Z., Zhu, B., and Chen, W.M. (2014). A multicenter, open-label phase II study of recombinant CPT (Circularly Permuted TRAIL) plus thalidomide in patients with relapsed and refractory multiple myeloma. *Am J Hematol* 89, 1037-1042.
- Gerlinger, M., Rowan, A.J., Horswell, S., Math, M., Larkin, J., Endesfelder, D., Gronroos, E., Martinez, P., Matthews, N., Stewart, A., Tarpey, P., Varela, I., Phillimore, B., Begum, S., McDonald, N.Q., Butler, A., Jones, D., Raine, K., Latimer, C., Santos, C.R., Nohadani, M., Eklund, A.C., Spencer-Dene, B., Clark, G., Pickering, L., Stamp, G., Gore, M., Szallasi, Z., Downward, J., Futreal, P.A., and Swanton, C. (2012). Intratumor heterogeneity and branched evolution revealed by multiregion sequencing. *N Engl J Med* 366, 883-892.
- Germain, C., Gnjatic, S., Tamzalit, F., Knockaert, S., Remark, R., Goc, J., Lepelley, A., Becht, E., Katsahian, S., Bizouard, G., Validire, P., Damotte, D., Alifano, M., Magdeleinat, P., Cremer, I., Teillaud, J.L., Fridman, W.H., Sautes-Fridman, C., and Dieu-Nosjean, M.C. (2014).

Presence of B cells in tertiary lymphoid structures is associated with a protective immunity in patients with lung cancer. *Am J Respir Crit Care Med* 189, 832-844.

Germano, G., Frapolli, R., Belgiovine, C., Anselmo, A., Pesce, S., Liguori, M., Erba, E., Ubaldi, S., Zucchetti, M., Pasqualini, F., Nebuloni, M., van Rooijen, N., Mortarini, R., Beltrame, L., Marchini, S., Fuso Nerini, I., Sanfilippo, R., Casali, P.G., Pilotti, S., Galmarini, C.M., Anichini, A., Mantovani, A., D'Incalci, M., and Allavena, P. (2013). Role of macrophage targeting in the antitumor activity of trabectedin. *Cancer Cell* 23, 249-262.

Ghia, P., Scarfo, L., Perez, S., Pathiraja, K., Derosier, M., Small, K., McCrary Sisk, C., and Patton, N. (2017). Efficacy and safety of dinaciclib vs ofatumumab in patients with relapsed/refractory chronic lymphocytic leukemia. *Blood* 129, 1876-1878.

Gibellini, D., Borderi, M., De Crignis, E., Cicola, R., Vescini, F., Caudarella, R., Chiodo, F., and Re, M.C. (2007). RANKL/OPG/TRAIL plasma levels and bone mass loss evaluation in antiretroviral naive HIV-1-positive men. *J Med Virol* 79, 1446-1454.

Gilchrist, D.A., Dos Santos, G., Fargo, D.C., Xie, B., Gao, Y., Li, L., and Adelman, K. (2010). Pausing of RNA polymerase II disrupts DNA-specified nucleosome organization to enable precise gene regulation. *Cell* 143, 540-551.

Glover-Cutter, K., Larochelle, S., Erickson, B., Zhang, C., Shokat, K., Fisher, R.P., and Bentley, D.L. (2009). TFIIH-associated Cdk7 kinase functions in phosphorylation of C-terminal domain Ser7 residues, promoter-proximal pausing, and termination by RNA polymerase II. *Mol Cell Biol* 29, 5455-5464.

Godin-Heymann, N., Ulkus, L., Brannigan, B.W., McDermott, U., Lamb, J., Maheswaran, S., Settleman, J., and Haber, D.A. (2008). The T790M "gatekeeper" mutation in EGFR mediates resistance to low concentrations of an irreversible EGFR inhibitor. *Mol Cancer Ther* 7, 874-879.

Goh, K.C., Novotny-Diermayr, V., Hart, S., Ong, L.C., Loh, Y.K., Cheong, A., Tan, Y.C., Hu, C., Jayaraman, R., William, A.D., Sun, E.T., Dymock, B.W., Ong, K.H., Ethirajulu, K., Burrows, F., and Wood, J.M. (2012). TG02, a novel oral multi-kinase inhibitor of CDKs, JAK2 and FLT3 with potent anti-leukemic properties. *Leukemia* 26, 236-243.

Gojo, I., Sadowska, M., Walker, A., Feldman, E.J., Iyer, S.P., Baer, M.R., Sausville, E.A., Lapidus, R.G., Zhang, D., Zhu, Y., Jou, Y.M., Poon, J., Small, K., and Bannerji, R. (2013). Clinical and laboratory studies of the novel cyclin-dependent kinase inhibitor dinaciclib (SCH 727965) in acute leukemias. *Cancer Chemother Pharmacol* 72, 897-908.

Golks, A., Brenner, D., Fritsch, C., Krammer, P.H., and Lavrik, I.N. (2005). c-FLIPR, a new regulator of death receptor-induced apoptosis. *J Biol Chem* 280, 14507-14513.

Gong, Y.N., Guy, C., Olauson, H., Becker, J.U., Yang, M., Fitzgerald, P., Linkermann, A., and Green, D.R. (2017). ESCRT-III Acts Downstream of MLKL to Regulate Necroptotic Cell Death and Its Consequences. *Cell* 169, 286-300 e216.

Goodall, M.L., Fitzwalter, B.E., Zahedi, S., Wu, M., Rodriguez, D., Mulcahy-Levy, J.M., Green, D.R., Morgan, M., Cramer, S.D., and Thorburn, A. (2016). The Autophagy Machinery Controls Cell Death Switching between Apoptosis and Necroptosis. *Dev Cell* 37, 337-349.

Gottesman, M.M., Fojo, T., and Bates, S.E. (2002). Multidrug resistance in cancer: role of ATP-dependent transporters. *Nat Rev Cancer* 2, 48-58.

Govindan, R., Ding, L., Griffith, M., Subramanian, J., Dees, N.D., Kanchi, K.L., Maher, C.A., Fulton, R., Fulton, L., Wallis, J., Chen, K., Walker, J., McDonald, S., Bose, R., Ornitz, D.,

- Xiong, D., You, M., Dooling, D.J., Watson, M., Mardis, E.R., and Wilson, R.K. (2012). Genomic landscape of non-small cell lung cancer in smokers and never-smokers. *Cell* **150**, 1121-1134.
- Grana, X., De Luca, A., Sang, N., Fu, Y., Claudio, P.P., Rosenblatt, J., Morgan, D.O., and Giordano, A. (1994). PITALRE, a nuclear CDC2-related protein kinase that phosphorylates the retinoblastoma protein in vitro. *Proc Natl Acad Sci U S A* **91**, 3834-3838.
- Graves, J.D., Kordich, J.J., Huang, T.H., Piasecki, J., Bush, T.L., Sullivan, T., Foltz, I.N., Chang, W., Douangpanya, H., Dang, T., O'Neill, J.W., Mallari, R., Zhao, X., Branstetter, D.G., Rossi, J.M., Long, A.M., Huang, X., and Holland, P.M. (2014). Apo2L/TRAIL and the death receptor 5 agonist antibody AMG 655 cooperate to promote receptor clustering and antitumor activity. *Cancer Cell* **26**, 177-189.
- Greco, F.A., Bonomi, P., Crawford, J., Kelly, K., Oh, Y., Halpern, W., Lo, L., Gallant, G., and Klein, J. (2008). Phase 2 study of mapatumumab, a fully human agonistic monoclonal antibody which targets and activates the TRAIL receptor-1, in patients with advanced non-small cell lung cancer. *Lung Cancer* **61**, 82-90.
- Gregory, G.P., Hogg, S.J., Kats, L.M., Vidacs, E., Baker, A.J., Gilan, O., Lefebure, M., Martin, B.P., Dawson, M.A., Johnstone, R.W., and Shortt, J. (2015). CDK9 inhibition by dinaciclib potently suppresses Mcl-1 to induce durable apoptotic responses in aggressive MYC-driven B-cell lymphoma in vivo. *Leukemia* **29**, 1437-1441.
- Griffith, T.S., Wiley, S.R., Kubin, M.Z., Sedger, L.M., Maliszewski, C.R., and Fanger, N.A. (1999). Monocyte-mediated tumoricidal activity via the tumor necrosis factor-related cytokine, TRAIL. *J Exp Med* **189**, 1343-1354.
- Grosse-Wilde, A., Voloshanenko, O., Bailey, S.L., Longton, G.M., Schaefer, U., Csernok, A.I., Schutz, G., Greiner, E.F., Kemp, C.J., and Walczak, H. (2008). TRAIL-R deficiency in mice enhances lymph node metastasis without affecting primary tumor development. *J Clin Invest* **118**, 100-110.
- Gupta, K., Sari-Ak, D., Haffke, M., Trowitzsch, S., and Berger, I. (2016). Zooming in on Transcription Preinitiation. *J Mol Biol* **428**, 2581-2591.
- Guseva, N.V., Rokhlin, O.W., Taghiyev, A.F., and Cohen, M.B. (2008). Unique resistance of breast carcinoma cell line T47D to TRAIL but not anti-Fas is linked to p43cFLIP(L). *Breast Cancer Res Treat* **107**, 349-357.
- Haas, T.L., Emmerich, C.H., Gerlach, B., Schmukle, A.C., Cordier, S.M., Rieser, E., Feltham, R., Vince, J., Warnken, U., Wenger, T., Koschny, R., Komander, D., Silke, J., and Walczak, H. (2009). Recruitment of the linear ubiquitin chain assembly complex stabilizes the TNF-R1 signaling complex and is required for TNF-mediated gene induction. *Mol Cell* **36**, 831-844.
- Hanahan, D., and Weinberg, R.A. (2011). Hallmarks of cancer: the next generation. *Cell* **144**, 646-674.
- Hanna, N., Johnson, D., Temin, S., Baker, S., Jr., Brahmer, J., Ellis, P.M., Giaccone, G., Hesketh, P.J., Jaiyesimi, I., Leighl, N.B., Riely, G.J., Schiller, J.H., Schneider, B.J., Smith, T.J., Tashbar, J., Biermann, W.A., and Masters, G. (2017). Systemic Therapy for Stage IV Non-Small-Cell Lung Cancer: American Society of Clinical Oncology Clinical Practice Guideline Update. *J Clin Oncol* **35**, 3484-3515.
- Hartwig, T., Montinaro, A., von Karstedt, S., Sevko, A., Surinova, S., Chakravarthy, A., Taraborrelli, L., Draber, P., Lafont, E., Arce Vargas, F., El-Bahrawy, M.A., Quezada, S.A., and Walczak, H. (2017). The TRAIL-Induced Cancer Secretome Promotes a Tumor-Supportive Immune Microenvironment via CCR2. *Mol Cell* **65**, 730-742 e735.

- Havlicek, L., Hanus, J., Vesely, J., Leclerc, S., Meijer, L., Shaw, G., and Strnad, M. (1997). Cytokinin-derived cyclin-dependent kinase inhibitors: synthesis and cdc2 inhibitory activity of olomoucine and related compounds. *J Med Chem* *40*, 408-412.
- He, Y., Fang, J., Taatjes, D.J., and Nogales, E. (2013). Structural visualization of key steps in human transcription initiation. *Nature* *495*, 481-486.
- Heath, E.I., Bible, K., Martell, R.E., Adelman, D.C., and Lorusso, P.M. (2008). A phase 1 study of SNS-032 (formerly BMS-387032), a potent inhibitor of cyclin-dependent kinases 2, 7 and 9 administered as a single oral dose and weekly infusion in patients with metastatic refractory solid tumors. *Invest New Drugs* *26*, 59-65.
- Hecht, S.S., Isaacs, S., and Trushin, N. (1994). Lung tumor induction in A/J mice by the tobacco smoke carcinogens 4-(methylnitrosamino)-1-(3-pyridyl)-1-butanone and benzo[a]pyrene: a potentially useful model for evaluation of chemopreventive agents. *Carcinogenesis* *15*, 2721-2725.
- Hellmann, M.D., Nathanson, T., Rizvi, H., Creelan, B.C., Sanchez-Vega, F., Ahuja, A., Ni, A., Novik, J.B., Mangarin, L.M.B., Abu-Akeel, M., Liu, C., Sauter, J.L., Rekhman, N., Chang, E., Callahan, M.K., Chaft, J.E., Voss, M.H., Tenet, M., Li, X.M., Covello, K., Renninger, A., Vitazka, P., Geese, W.J., Borghaei, H., Rudin, C.M., Antonia, S.J., Swanton, C., Hammerbacher, J., Merghoub, T., McGranahan, N., Snyder, A., and Wolchok, J.D. (2018). Genomic Features of Response to Combination Immunotherapy in Patients with Advanced Non-Small-Cell Lung Cancer. *Cancer Cell* *33*, 843-852 e844.
- Hellvard, A., Zeitlmann, L., Heiser, U., Kehlen, A., Niestroj, A., Demuth, H.U., Koziel, J., Delaleu, N., Jan, P., and Mydel, P. (2016). Inhibition of CDK9 as a therapeutic strategy for inflammatory arthritis. *Sci Rep* *6*, 31441.
- Henry, C.M., and Martin, S.J. (2017). Caspase-8 Acts in a Non-enzymatic Role as a Scaffold for Assembly of a Pro-inflammatory "FADDosome" Complex upon TRAIL Stimulation. *Mol Cell* *65*, 715-729 e715.
- Henson, E.S., Gibson, E.M., Villanueva, J., Bristow, N.A., Haney, N., and Gibson, S.B. (2003). Increased expression of Mcl-1 is responsible for the blockage of TRAIL-induced apoptosis mediated by EGF/ErbB1 signaling pathway. *J Cell Biochem* *89*, 1177-1192.
- Herbst, R.S., Eckhardt, S.G., Kurzrock, R., Ebbinghaus, S., O'Dwyer, P.J., Gordon, M.S., Novotny, W., Goldwasser, M.A., Tohny, T.M., Lum, B.L., Ashkenazi, A., Jubb, A.M., and Mendelson, D.S. (2010a). Phase I dose-escalation study of recombinant human Apo2L/TRAIL, a dual proapoptotic receptor agonist, in patients with advanced cancer. *J Clin Oncol* *28*, 2839-2846.
- Herbst, R.S., Heymach, J.V., and Lippman, S.M. (2008). Lung cancer. *N Engl J Med* *359*, 1367-1380.
- Herbst, R.S., Kurzrock, R., Hong, D.S., Valdivieso, M., Hsu, C.P., Goyal, L., Juan, G., Hwang, Y.C., Wong, S., Hill, J.S., Friberg, G., and LoRusso, P.M. (2010b). A first-in-human study of conatumumab in adult patients with advanced solid tumors. *Clin Cancer Res* *16*, 5883-5891.
- Herbst, R.S., Soria, J.C., Kowanetz, M., Fine, G.D., Hamid, O., Gordon, M.S., Sosman, J.A., McDermott, D.F., Powderly, J.D., Gettinger, S.N., Kohrt, H.E., Horn, L., Lawrence, D.P., Rost, S., Leabman, M., Xiao, Y., Mokatrini, A., Koeppen, H., Hegde, P.S., Mellman, I., Chen, D.S., and Hodi, F.S. (2014). Predictive correlates of response to the anti-PD-L1 antibody MPDL3280A in cancer patients. *Nature* *515*, 563-567.
- Herr, I., Wilhelm, D., Meyer, E., Jeremias, I., Angel, P., and Debatin, K.M. (1999). JNK/SAPK activity contributes to TRAIL-induced apoptosis. *Cell Death Differ* *6*, 130-135.

- Hildebrand, J.M., Tanzer, M.C., Lucet, I.S., Young, S.N., Spall, S.K., Sharma, P., Pierotti, C., Garnier, J.M., Dobson, R.C., Webb, A.I., Tripaydonis, A., Babon, J.J., Mulcair, M.D., Scanlon, M.J., Alexander, W.S., Wilks, A.F., Czabotar, P.E., Lessene, G., Murphy, J.M., and Silke, J. (2014). Activation of the pseudokinase MLKL unleashes the four-helix bundle domain to induce membrane localization and necroptotic cell death. *Proc Natl Acad Sci U S A* *111*, 15072-15077.
- Hinz, S., Trauzold, A., Boenicke, L., Sandberg, C., Beckmann, S., Bayer, E., Walczak, H., Kalthoff, H., and Ungefroren, H. (2000). Bcl-XL protects pancreatic adenocarcinoma cells against CD95- and TRAIL-receptor-mediated apoptosis. *Oncogene* *19*, 5477-5486.
- Holler, N., Zaru, R., Micheau, O., Thome, M., Attinger, A., Valitutti, S., Bodmer, J.L., Schneider, P., Seed, B., and Tschopp, J. (2000). Fas triggers an alternative, caspase-8-independent cell death pathway using the kinase RIP as effector molecule. *Nat Immunol* *1*, 489-495.
- Holohan, C., Van Schaeybroeck, S., Longley, D.B., and Johnston, P.G. (2013). Cancer drug resistance: an evolving paradigm. *Nat Rev Cancer* *13*, 714-726.
- Hoodless, L.J., Lucas, C.D., Duffin, R., Denvir, M.A., Haslett, C., Tucker, C.S., and Rossi, A.G. (2016). Genetic and pharmacological inhibition of CDK9 drives neutrophil apoptosis to resolve inflammation in zebrafish in vivo. *Sci Rep* *5*, 36980.
- Hoogwater, F.J., Nijkamp, M.W., Smakman, N., Steller, E.J., Emmink, B.L., Westendorp, B.F., Raats, D.A., Sprick, M.R., Schaefer, U., Van Houdt, W.J., De Bruijn, M.T., Schackmann, R.C., Derksen, P.W., Medema, J.P., Walczak, H., Borel Rinkes, I.H., and Kranenburg, O. (2010). Oncogenic K-Ras turns death receptors into metastasis-promoting receptors in human and mouse colorectal cancer cells. *Gastroenterology* *138*, 2357-2367.
- Hopkins-Donaldson, S., Ziegler, A., Kurtz, S., Bigosch, C., Kandioler, D., Ludwig, C., Zangemeister-Wittke, U., and Stahel, R. (2003). Silencing of death receptor and caspase-8 expression in small cell lung carcinoma cell lines and tumors by DNA methylation. *Cell Death Differ* *10*, 356-364.
- Hossain, D.M.S., Javaid, S., Cai, M., Zhang, C., Sawant, A., Hinton, M., Sathe, M., Grein, J., Blumenschein, W., Pinheiro, E.M., and Chackerian, A. (2018). Dinaciclib induces immunogenic cell death and enhances anti-PD1-mediated tumor suppression. *J Clin Invest* *128*, 644-654.
- Hotte, S.J., Hirte, H.W., Chen, E.X., Siu, L.L., Le, L.H., Corey, A., Iacobucci, A., MacLean, M., Lo, L., Fox, N.L., and Oza, A.M. (2008). A phase 1 study of mapatumumab (fully human monoclonal antibody to TRAIL-R1) in patients with advanced solid malignancies. *Clin Cancer Res* *14*, 3450-3455.
- Hou, J., Qiu, L., Zhao, Y., Zhang, X., Liu, Y., Wang, Z., Zhou, F., Leng, Y., Yang, S., Xi, H., Wang, F., Zhu, B., Chen, W., Wei, P., and Zheng, X. (2018). A Phase1b Dose Escalation Study of Recombinant Circularly Permuted TRAIL in Patients With Relapsed or Refractory Multiple Myeloma. *Am J Clin Oncol* *41*, 1008-1014.
- Huang, C.H., Lujambio, A., Zuber, J., Tschaharganeh, D.F., Doran, M.G., Evans, M.J., Kitzing, T., Zhu, N., de Stanchina, E., Sawyers, C.L., Armstrong, S.A., Lewis, J.S., Sherr, C.J., and Lowe, S.W. (2014). CDK9-mediated transcription elongation is required for MYC addiction in hepatocellular carcinoma. *Genes Dev* *28*, 1800-1814.
- Huang, D., Zheng, X., Wang, Z.A., Chen, X., He, W.T., Zhang, Y., Xu, J.G., Zhao, H., Shi, W., Wang, X., Zhu, Y., and Han, J. (2017). The MLKL Channel in Necroptosis Is an Octamer Formed by Tetramers in a Dyadic Process. *Mol Cell Biol* *37*.

- Huang, S., and Sinicrope, F.A. (2008). BH3 mimetic ABT-737 potentiates TRAIL-mediated apoptotic signaling by unsequestering Bim and Bak in human pancreatic cancer cells. *Cancer Res* **68**, 2944-2951.
- Huet, H.A., Growney, J.D., Johnson, J.A., Li, J., Bilic, S., Ostrom, L., Zafari, M., Kowal, C., Yang, G., Royo, A., Jensen, M., Dombrecht, B., Meerschaert, K.R., Kolkman, J.A., Cromie, K.D., Mosher, R., Gao, H., Schuller, A., Isaacs, R., Sellers, W.R., and Ettenberg, S.A. (2014). Multivalent nanobodies targeting death receptor 5 elicit superior tumor cell killing through efficient caspase induction. *MAbs* **6**, 1560-1570.
- Hughes, M.A., Powley, I.R., Jukes-Jones, R., Horn, S., Feoktistova, M., Fairall, L., Schwabe, J.W., Leverkus, M., Cain, K., and MacFarlane, M. (2016). Co-operative and Hierarchical Binding of c-FLIP and Caspase-8: A Unified Model Defines How c-FLIP Isoforms Differentially Control Cell Fate. *Mol Cell* **61**, 834-849.
- Hugo, W., Zaretsky, J.M., Sun, L., Song, C., Moreno, B.H., Hu-Lieskovan, S., Berent-Maoz, B., Pang, J., Chmielowski, B., Cherry, G., Seja, E., Lomeli, S., Kong, X., Kelley, M.C., Sosman, J.A., Johnson, D.B., Ribas, A., and Lo, R.S. (2016). Genomic and Transcriptomic Features of Response to Anti-PD-1 Therapy in Metastatic Melanoma. *Cell* **165**, 35-44.
- Hymowitz, S.G., Christinger, H.W., Fuh, G., Ultsch, M., O'Connell, M., Kelley, R.F., Ashkenazi, A., and de Vos, A.M. (1999). Triggering cell death: the crystal structure of Apo2L/TRAIL in a complex with death receptor 5. *Mol Cell* **4**, 563-571.
- Hymowitz, S.G., O'Connell, M.P., Ultsch, M.H., Hurst, A., Totpal, K., Ashkenazi, A., de Vos, A.M., and Kelley, R.F. (2000). A unique zinc-binding site revealed by a high-resolution X-ray structure of homotrimeric Apo2L/TRAIL. *Biochemistry* **39**, 633-640.
- Ichikawa, K., Liu, W., Zhao, L., Wang, Z., Liu, D., Ohtsuka, T., Zhang, H., Mountz, J.D., Koopman, W.J., Kimberly, R.P., and Zhou, T. (2001). Tumoricidal activity of a novel anti-human DR5 monoclonal antibody without hepatocyte cytotoxicity. *Nat Med* **7**, 954-960.
- Ikeda, T., Hirata, S., Fukushima, S., Matsunaga, Y., Ito, T., Uchino, M., Nishimura, Y., and Senju, S. (2010). Dual effects of TRAIL in suppression of autoimmunity: the inhibition of Th1 cells and the promotion of regulatory T cells. *J Immunol* **185**, 5259-5267.
- Inoue-Yamauchi, A., Jeng, P.S., Kim, K., Chen, H.C., Han, S., Ganesan, Y.T., Ishizawa, K., Jebiwott, S., Dong, Y., Pietanza, M.C., Hellmann, M.D., Kris, M.G., Hsieh, J.J., and Cheng, E.H. (2017). Targeting the differential addiction to anti-apoptotic BCL-2 family for cancer therapy. *Nat Commun* **8**, 16078.
- Inoue, S., MacFarlane, M., Harper, N., Wheat, L.M., Dyer, M.J., and Cohen, G.M. (2004). Histone deacetylase inhibitors potentiate TNF-related apoptosis-inducing ligand (TRAIL)-induced apoptosis in lymphoid malignancies. *Cell Death Differ* **11 Suppl 2**, S193-206.
- Irmeler, M., Thome, M., Hahne, M., Schneider, P., Hofmann, K., Steiner, V., Bodmer, J.L., Schroter, M., Burns, K., Mattmann, C., Rimoldi, D., French, L.E., and Tschopp, J. (1997). Inhibition of death receptor signals by cellular FLIP. *Nature* **388**, 190-195.
- Ishimura, N., Isomoto, H., Bronk, S.F., and Gores, G.J. (2006). Trail induces cell migration and invasion in apoptosis-resistant cholangiocarcinoma cells. *Am J Physiol Gastrointest Liver Physiol* **290**, G129-136.
- Itoh, N., Yonehara, S., Ishii, A., Yonehara, M., Mizushima, S., Sameshima, M., Hase, A., Seto, Y., and Nagata, S. (1991). The polypeptide encoded by the cDNA for human cell surface antigen Fas can mediate apoptosis. *Cell* **66**, 233-243.

- Jackson, E.L., Olive, K.P., Tuveson, D.A., Bronson, R., Crowley, D., Brown, M., and Jacks, T. (2005). The differential effects of mutant p53 alleles on advanced murine lung cancer. *Cancer Res* 65, 10280-10288.
- Jackson, E.L., Willis, N., Mercer, K., Bronson, R.T., Crowley, D., Montoya, R., Jacks, T., and Tuveson, D.A. (2001). Analysis of lung tumor initiation and progression using conditional expression of oncogenic K-ras. *Genes Dev* 15, 3243-3248.
- Jain, N., Gandhi, V., and Wierda, W. (2019). Ibrutinib and Venetoclax for First-Line Treatment of CLL. Reply. *N Engl J Med* 381, 789.
- Janes, M.R., Zhang, J., Li, L.S., Hansen, R., Peters, U., Guo, X., Chen, Y., Babbar, A., Firdaus, S.J., Darjania, L., Feng, J., Chen, J.H., Li, S., Li, S., Long, Y.O., Thach, C., Liu, Y., Zariéh, A., Ely, T., Kucharski, J.M., Kessler, L.V., Wu, T., Yu, K., Wang, Y., Yao, Y., Deng, X., Zarrinkar, P.P., Brehmer, D., Dhanak, D., Lorenzi, M.V., Hu-Lowe, D., Patricelli, M.P., Ren, P., and Liu, Y. (2018). Targeting KRAS Mutant Cancers with a Covalent G12C-Specific Inhibitor. *Cell* 172, 578-589 e517.
- Jang, M.K., Mochizuki, K., Zhou, M., Jeong, H.S., Brady, J.N., and Ozato, K. (2005). The bromodomain protein Brd4 is a positive regulatory component of P-TEFb and stimulates RNA polymerase II-dependent transcription. *Mol Cell* 19, 523-534.
- Janssen, E.M., Droin, N.M., Lemmens, E.E., Pinkoski, M.J., Bensinger, S.J., Ehst, B.D., Griffith, T.S., Green, D.R., and Schoenberger, S.P. (2005). CD4⁺ T-cell help controls CD8⁺ T-cell memory via TRAIL-mediated activation-induced cell death. *Nature* 434, 88-93.
- Jeffrey, P.D., Russo, A.A., Polyak, K., Gibbs, E., Hurwitz, J., Massague, J., and Pavletich, N.P. (1995). Mechanism of CDK activation revealed by the structure of a cyclinA-CDK2 complex. *Nature* 376, 313-320.
- Jeronimo, C., and Robert, F. (2014). Kin28 regulates the transient association of Mediator with core promoters. *Nat Struct Mol Biol* 21, 449-455.
- Jin, Z., and El-Deiry, W.S. (2006). Distinct signaling pathways in TRAIL- versus tumor necrosis factor-induced apoptosis. *Mol Cell Biol* 26, 8136-8148.
- Jo, M., Kim, T.H., Seol, D.W., Esplen, J.E., Dorko, K., Billiar, T.R., and Strom, S.C. (2000). Apoptosis induced in normal human hepatocytes by tumor necrosis factor-related apoptosis-inducing ligand. *Nat Med* 6, 564-567.
- Johannessen, C.M., Boehm, J.S., Kim, S.Y., Thomas, S.R., Wardwell, L., Johnson, L.A., Emery, C.M., Stransky, N., Cogdill, A.P., Barretina, J., Caponigro, G., Hieronymus, H., Murray, R.R., Salehi-Ashtiani, K., Hill, D.E., Vidal, M., Zhao, J.J., Yang, X., Alkan, O., Kim, S., Harris, J.L., Wilson, C.J., Myer, V.E., Finan, P.M., Root, D.E., Roberts, T.M., Golub, T., Flaherty, K.T., Dummer, R., Weber, B.L., Sellers, W.R., Schlegel, R., Wargo, J.A., Hahn, W.C., and Garraway, L.A. (2010). COT drives resistance to RAF inhibition through MAP kinase pathway reactivation. *Nature* 468, 968-972.
- Johnson, A.J., Yeh, Y.Y., Smith, L.L., Wagner, A.J., Hessler, J., Gupta, S., Flynn, J., Jones, J., Zhang, X., Bannerji, R., Grever, M.R., and Byrd, J.C. (2012). The novel cyclin-dependent kinase inhibitor dinaciclib (SCH727965) promotes apoptosis and abrogates microenvironmental cytokine protection in chronic lymphocytic leukemia cells. *Leukemia* 26, 2554-2557.
- Johnson, L., Greenbaum, D., Cichowski, K., Mercer, K., Murphy, E., Schmitt, E., Bronson, R.T., Umanoff, H., Edelman, W., Kucherlapati, R., and Jacks, T. (1997). K-ras is an essential gene in the mouse with partial functional overlap with N-ras. *Genes Dev* 11, 2468-2481.

- Johnson, L., Mercer, K., Greenbaum, D., Bronson, R.T., Crowley, D., Tuveson, D.A., and Jacks, T. (2001). Somatic activation of the K-ras oncogene causes early onset lung cancer in mice. *Nature* *410*, 1111-1116.
- Jonkers, J., Meuwissen, R., van der Gulden, H., Peterse, H., van der Valk, M., and Berns, A. (2001). Synergistic tumor suppressor activity of BRCA2 and p53 in a conditional mouse model for breast cancer. *Nat Genet* *29*, 418-425.
- Jordan, E.J., Kim, H.R., Arcila, M.E., Barron, D., Chakravarty, D., Gao, J., Chang, M.T., Ni, A., Kundra, R., Jonsson, P., Jayakumaran, G., Gao, S.P., Johnsen, H.C., Hanrahan, A.J., Zehir, A., Rekhtman, N., Ginsberg, M.S., Li, B.T., Yu, H.A., Paik, P.K., Drilon, A., Hellmann, M.D., Reales, D.N., Benayed, R., Rusch, V.W., Kris, M.G., Chaft, J.E., Baselga, J., Taylor, B.S., Schultz, N., Rudin, C.M., Hyman, D.M., Berger, M.F., Solit, D.B., Ladanyi, M., and Riely, G.J. (2017). Prospective Comprehensive Molecular Characterization of Lung Adenocarcinomas for Efficient Patient Matching to Approved and Emerging Therapies. *Cancer Discov* *7*, 596-609.
- Jost, P.J., Grabow, S., Gray, D., McKenzie, M.D., Nachbur, U., Huang, D.C., Bouillet, P., Thomas, H.E., Borner, C., Silke, J., Strasser, A., and Kaufmann, T. (2009). XIAP discriminates between type I and type II FAS-induced apoptosis. *Nature* *460*, 1035-1039.
- Jouan-Lanhouet, S., Arshad, M.I., Piquet-Pellorce, C., Martin-Chouly, C., Le Moigne-Muller, G., Van Herreweghe, F., Takahashi, N., Sergent, O., Lagadic-Gossmann, D., Vandenabeele, P., Samson, M., and Dimanche-Boitrel, M.T. (2012). TRAIL induces necroptosis involving RIPK1/RIPK3-dependent PARP-1 activation. *Cell Death Differ* *19*, 2003-2014.
- Kanazawa, S., Soucek, L., Evan, G., Okamoto, T., and Peterlin, B.M. (2003). c-Myc recruits P-TEFb for transcription, cellular proliferation and apoptosis. *Oncogene* *22*, 5707-5711.
- Karl, I., Jossberger-Werner, M., Schmidt, N., Horn, S., Goebeler, M., Leverkus, M., Wajant, H., and Giner, T. (2014). TRAF2 inhibits TRAIL- and CD95L-induced apoptosis and necroptosis. *Cell Death Dis* *5*, e1444.
- Kasinski, A.L., and Slack, F.J. (2012). miRNA-34 prevents cancer initiation and progression in a therapeutically resistant K-ras and p53-induced mouse model of lung adenocarcinoma. *Cancer Res* *72*, 5576-5587.
- Kawano, R., Nishisaka, T., Takeshima, Y., Yonehara, S., and Inai, K. (1995). Role of point mutation of the K-ras gene in tumorigenesis of B6C3F1 mouse lung lesions induced by urethane. *Jpn J Cancer Res* *86*, 802-810.
- Kayagaki, N., Yamaguchi, N., Nakayama, M., Eto, H., Okumura, K., and Yagita, H. (1999a). Type I interferons (IFNs) regulate tumor necrosis factor-related apoptosis-inducing ligand (TRAIL) expression on human T cells: A novel mechanism for the antitumor effects of type I IFNs. *J Exp Med* *189*, 1451-1460.
- Kayagaki, N., Yamaguchi, N., Nakayama, M., Takeda, K., Akiba, H., Tsutsui, H., Okumura, H., Nakanishi, K., Okumura, K., and Yagita, H. (1999b). Expression and function of TNF-related apoptosis-inducing ligand on murine activated NK cells. *J Immunol* *163*, 1906-1913.
- Kazandjian, D., Blumenthal, G.M., Chen, H.Y., He, K., Patel, M., Justice, R., Keegan, P., and Pazdur, R. (2014). FDA approval summary: crizotinib for the treatment of metastatic non-small cell lung cancer with anaplastic lymphoma kinase rearrangements. *Oncologist* *19*, e5-11.
- Kazandjian, D., Suzman, D.L., Blumenthal, G., Mushti, S., He, K., Libeg, M., Keegan, P., and Pazdur, R. (2016). FDA Approval Summary: Nivolumab for the Treatment of Metastatic Non-Small Cell Lung Cancer With Progression On or After Platinum-Based Chemotherapy. *Oncologist* *21*, 634-642.

- Keir, M.E., Liang, S.C., Guleria, I., Latchman, Y.E., Qipo, A., Albacker, L.A., Koulmanda, M., Freeman, G.J., Sayegh, M.H., and Sharpe, A.H. (2006). Tissue expression of PD-L1 mediates peripheral T cell tolerance. *J Exp Med* 203, 883-895.
- Kelley, S.K., and Ashkenazi, A. (2004). Targeting death receptors in cancer with Apo2L/TRAIL. *Curr Opin Pharmacol* 4, 333-339.
- Kelley, S.K., Harris, L.A., Xie, D., Deforge, L., Totpal, K., Bussiere, J., and Fox, J.A. (2001). Preclinical studies to predict the disposition of Apo2L/tumor necrosis factor-related apoptosis-inducing ligand in humans: characterization of in vivo efficacy, pharmacokinetics, and safety. *J Pharmacol Exp Ther* 299, 31-38.
- Khuder, S.A. (2001). Effect of cigarette smoking on major histological types of lung cancer: a meta-analysis. *Lung Cancer* 31, 139-148.
- Khuder, S.A., and Mutgi, A.B. (2001). Effect of smoking cessation on major histologic types of lung cancer. *Chest* 120, 1577-1583.
- Khunger, A., Khunger, M., and Velcheti, V. (2018). Dabrafenib in combination with trametinib in the treatment of patients with BRAF V600-positive advanced or metastatic non-small cell lung cancer: clinical evidence and experience. *Ther Adv Respir Dis* 12, 1753466618767611.
- Kim, D.M., Koo, S.Y., Jeon, K., Kim, M.H., Lee, J., Hong, C.Y., and Jeong, S. (2003). Rapid induction of apoptosis by combination of flavopiridol and tumor necrosis factor (TNF)-alpha or TNF-related apoptosis-inducing ligand in human cancer cell lines. *Cancer Res* 63, 621-626.
- Kim, E.H., Kim, S.U., Shin, D.Y., and Choi, K.S. (2004). Roscovitine sensitizes glioma cells to TRAIL-mediated apoptosis by downregulation of survivin and XIAP. *Oncogene* 23, 446-456.
- Kindler, H.L., Richards, D.A., Garbo, L.E., Garon, E.B., Stephenson, J.J., Jr., Rocha-Lima, C.M., Safran, H., Chan, D., Kocs, D.M., Galimi, F., McGreivy, J., Bray, S.L., Hei, Y., Feigal, E.G., Loh, E., and Fuchs, C.S. (2012). A randomized, placebo-controlled phase 2 study of ganitumab (AMG 479) or conatumumab (AMG 655) in combination with gemcitabine in patients with metastatic pancreatic cancer. *Ann Oncol* 23, 2834-2842.
- Kipps, T.J., Eradat, H., Grosicki, S., Catalano, J., Cosolo, W., Dyagil, I.S., Yalamanchili, S., Chai, A., Sahasranaman, S., Punnoose, E., Hurst, D., and Pylypenko, H. (2015). A phase 2 study of the BH3 mimetic BCL2 inhibitor navitoclax (ABT-263) with or without rituximab, in previously untreated B-cell chronic lymphocytic leukemia. *Leuk Lymphoma* 56, 2826-2833.
- Kischkel, F.C., Hellbardt, S., Behrmann, I., Germer, M., Pawlita, M., Krammer, P.H., and Peter, M.E. (1995). Cytotoxicity-dependent APO-1 (Fas/CD95)-associated proteins form a death-inducing signaling complex (DISC) with the receptor. *EMBO J* 14, 5579-5588.
- Kischkel, F.C., Lawrence, D.A., Chuntharapai, A., Schow, P., Kim, K.J., and Ashkenazi, A. (2000). Apo2L/TRAIL-dependent recruitment of endogenous FADD and caspase-8 to death receptors 4 and 5. *Immunity* 12, 611-620.
- Kischkel, F.C., Lawrence, D.A., Tinel, A., LeBlanc, H., Virmani, A., Schow, P., Gazdar, A., Blenis, J., Arnott, D., and Ashkenazi, A. (2001). Death receptor recruitment of endogenous caspase-10 and apoptosis initiation in the absence of caspase-8. *J Biol Chem* 276, 46639-46646.
- Klingbeil, O., Lesche, R., Gelato, K.A., Haendler, B., and Lejeune, P. (2016). Inhibition of BET bromodomain-dependent XIAP and FLIP expression sensitizes KRAS-mutated NSCLC to pro-apoptotic agents. *Cell Death Dis* 7, e2365.

- Koga, Y., Matsuzaki, A., Suminoe, A., Hattori, H., and Hara, T. (2004). Neutrophil-derived TNF-related apoptosis-inducing ligand (TRAIL): a novel mechanism of antitumor effect by neutrophils. *Cancer Res* 64, 1037-1043.
- Kohoutek, J., Li, Q., Blazek, D., Luo, Z., Jiang, H., and Peterlin, B.M. (2009). Cyclin T2 is essential for mouse embryogenesis. *Mol Cell Biol* 29, 3280-3285.
- Kondo, T., Suda, T., Fukuyama, H., Adachi, M., and Nagata, S. (1997). Essential roles of the Fas ligand in the development of hepatitis. *Nat Med* 3, 409-413.
- Koschny, R., Ganten, T.M., Sykora, J., Haas, T.L., Sprick, M.R., Kolb, A., Stremmel, W., and Walczak, H. (2007). TRAIL/bortezomib cotreatment is potentially hepatotoxic but induces cancer-specific apoptosis within a therapeutic window. *Hepatology* 45, 649-658.
- Koschny, R., Holland, H., Sykora, J., Erdal, H., Krupp, W., Bauer, M., Bockmuehl, U., Ahnert, P., Meixensberger, J., Stremmel, W., Walczak, H., and Ganten, T.M. (2010). Bortezomib sensitizes primary human esthesioneuroblastoma cells to TRAIL-induced apoptosis. *J Neurooncol* 97, 171-185.
- Kreisel, D., Gelman, A.E., Higashikubo, R., Lin, X., Vikis, H.G., White, J.M., Toth, K.A., Deshpande, C., Carreno, B.M., You, M., Taffner, S.M., Yokoyama, W.M., Bui, J.D., Schreiber, R.D., and Krupnick, A.S. (2012). Strain-specific variation in murine natural killer gene complex contributes to differences in immunosurveillance for urethane-induced lung cancer. *Cancer Res* 72, 4311-4317.
- Kreuz, S., Siegmund, D., Scheurich, P., and Wajant, H. (2001). NF-kappaB inducers upregulate cFLIP, a cycloheximide-sensitive inhibitor of death receptor signaling. *Mol Cell Biol* 21, 3964-3973.
- Krueger, A., Schmitz, I., Baumann, S., Krammer, P.H., and Kirchhoff, S. (2001). Cellular FLICE-inhibitory protein splice variants inhibit different steps of caspase-8 activation at the CD95 death-inducing signaling complex. *J Biol Chem* 276, 20633-20640.
- Kumar, S.K., LaPlant, B., Chng, W.J., Zonder, J., Callander, N., Fonseca, R., Fruth, B., Roy, V., Erlichman, C., Stewart, A.K., and Mayo Phase, C. (2015). Dinaciclib, a novel CDK inhibitor, demonstrates encouraging single-agent activity in patients with relapsed multiple myeloma. *Blood* 125, 443-448.
- Kwon, H.C., Roh, M.S., Oh, S.Y., Kim, S.H., Kim, M.C., Kim, J.S., and Kim, H.J. (2007). Prognostic value of expression of ERCC1, thymidylate synthase, and glutathione S-transferase P1 for 5-fluorouracil/oxaliplatin chemotherapy in advanced gastric cancer. *Ann Oncol* 18, 504-509.
- Lacey, D.L., Timms, E., Tan, H.L., Kelley, M.J., Dunstan, C.R., Burgess, T., Elliott, R., Colombero, A., Elliott, G., Scully, S., Hsu, H., Sullivan, J., Hawkins, N., Davy, E., Capparelli, C., Eli, A., Qian, Y.X., Kaufman, S., Sarosi, I., Shalhoub, V., Senaldi, G., Guo, J., Delaney, J., and Boyle, W.J. (1998). Osteoprotegerin ligand is a cytokine that regulates osteoclast differentiation and activation. *Cell* 93, 165-176.
- Lafont, E., Kantari-Mimoun, C., Draber, P., De Miguel, D., Hartwig, T., Reichert, M., Kupka, S., Shimizu, Y., Taraborrelli, L., Spit, M., Sprick, M.R., and Walczak, H. (2017). The linear ubiquitin chain assembly complex regulates TRAIL-induced gene activation and cell death. *EMBO J* 36, 1147-1166.
- Lalaoui, N., Morle, A., Merino, D., Jacquemin, G., Iessi, E., Morizot, A., Shirley, S., Robert, B., Solary, E., Garrido, C., and Micheau, O. (2011). TRAIL-R4 promotes tumor growth and resistance to apoptosis in cervical carcinoma HeLa cells through AKT. *PLoS One* 6, e19679.

- Larkins, E., Blumenthal, G.M., Yuan, W., He, K., Sridhara, R., Subramaniam, S., Zhao, H., Liu, C., Yu, J., Goldberg, K.B., McKee, A.E., Keegan, P., and Pazdur, R. (2017). FDA Approval Summary: Pembrolizumab for the Treatment of Recurrent or Metastatic Head and Neck Squamous Cell Carcinoma with Disease Progression on or After Platinum-Containing Chemotherapy. *Oncologist* 22, 873-878.
- Larochelle, S., Amat, R., Glover-Cutter, K., Sanso, M., Zhang, C., Allen, J.J., Shokat, K.M., Bentley, D.L., and Fisher, R.P. (2012). Cyclin-dependent kinase control of the initiation-to-elongation switch of RNA polymerase II. *Nat Struct Mol Biol* 19, 1108-1115.
- Lastwika, K.J., Wilson, W., 3rd, Li, Q.K., Norris, J., Xu, H., Ghazarian, S.R., Kitagawa, H., Kawabata, S., Taube, J.M., Yao, S., Liu, L.N., Gills, J.J., and Dennis, P.A. (2016). Control of PD-L1 Expression by Oncogenic Activation of the AKT-mTOR Pathway in Non-Small Cell Lung Cancer. *Cancer Res* 76, 227-238.
- Lavrik, I., Krueger, A., Schmitz, I., Baumann, S., Weyd, H., Krammer, P.H., and Kirchhoff, S. (2003). The active caspase-8 heterotetramer is formed at the CD95 DISC. *Cell Death Differ* 10, 144-145.
- Leach, D.R., Krummel, M.F., and Allison, J.P. (1996). Enhancement of antitumor immunity by CTLA-4 blockade. *Science* 271, 1734-1736.
- Lecis, D., Drago, C., Manzoni, L., Seneci, P., Scolastico, C., Mastrangelo, E., Bolognesi, M., Anichini, A., Kashkar, H., Walczak, H., and Delia, D. (2010). Novel SMAC-mimetics synergistically stimulate melanoma cell death in combination with TRAIL and Bortezomib. *Br J Cancer* 102, 1707-1716.
- Lee, C.L., Moding, E.J., Huang, X., Li, Y., Woodlief, L.Z., Rodrigues, R.C., Ma, Y., and Kirsch, D.G. (2012). Generation of primary tumors with Flp recombinase in FRT-flanked p53 mice. *Dis Model Mech* 5, 397-402.
- Lee, D.K., Duan, H.O., and Chang, C. (2001). Androgen receptor interacts with the positive elongation factor P-TEFb and enhances the efficiency of transcriptional elongation. *J Biol Chem* 276, 9978-9984.
- Lee, M.W., Park, S.C., Yang, Y.G., Yim, S.O., Chae, H.S., Bach, J.H., Lee, H.J., Kim, K.Y., Lee, W.B., and Kim, S.S. (2002). The involvement of reactive oxygen species (ROS) and p38 mitogen-activated protein (MAP) kinase in TRAIL/Apo2L-induced apoptosis. *FEBS Lett* 512, 313-318.
- Lee, W., Jiang, Z., Liu, J., Haverty, P.M., Guan, Y., Stinson, J., Yue, P., Zhang, Y., Pant, K.P., Bhatt, D., Ha, C., Johnson, S., Kennemer, M.I., Mohan, S., Nazarenko, I., Watanabe, C., Sparks, A.B., Shames, D.S., Gentleman, R., de Sauvage, F.J., Stern, H., Pandita, A., Ballinger, D.G., Drmanac, R., Modrusan, Z., Seshagiri, S., and Zhang, Z. (2010). The mutation spectrum revealed by paired genome sequences from a lung cancer patient. *Nature* 465, 473-477.
- Legler, K., Hauser, C., Egberts, J.H., Willms, A., Heneweer, C., Boretius, S., Rocken, C., Gluer, C.C., Becker, T., Kluge, M., Hill, O., Gieffers, C., Fricke, H., Kalthoff, H., Lemke, J., and Trauzold, A. (2018). The novel TRAIL-receptor agonist APG350 exerts superior therapeutic activity in pancreatic cancer cells. *Cell Death Dis* 9, 445.
- Lehnert, C., Weiswange, M., Jeremias, I., Bayer, C., Grunert, M., Debatin, K.M., and Strauss, G. (2014). TRAIL-receptor costimulation inhibits proximal TCR signaling and suppresses human T cell activation and proliferation. *J Immunol* 193, 4021-4031.

- Lemke, J., Noack, A., Adam, D., Tchikov, V., Bertsch, U., Roder, C., Schutze, S., Wajant, H., Kalthoff, H., and Trauzold, A. (2010). TRAIL signaling is mediated by DR4 in pancreatic tumor cells despite the expression of functional DR5. *J Mol Med (Berl)* 88, 729-740.
- Lemke, J., von Karstedt, S., Abd El Hay, M., Conti, A., Arce, F., Montinaro, A., Papenfuss, K., El-Bahrawy, M.A., and Walczak, H. (2014a). Selective CDK9 inhibition overcomes TRAIL resistance by concomitant suppression of cFlip and Mcl-1. *Cell Death Differ* 21, 491-502.
- Lemke, J., von Karstedt, S., Zinngrebe, J., and Walczak, H. (2014b). Getting TRAIL back on track for cancer therapy. *Cell Death Differ* 21, 1350-1364.
- Leng, Y., Hou, J., Jin, J., Zhang, M., Ke, X., Jiang, B., Pan, L., Yang, L., Zhou, F., Wang, J., Wang, Z., Liu, L., Li, W., Shen, Z., Qiu, L., Chang, N., Li, J., Liu, J., Pang, H., Meng, H., Wei, P., Jiang, H., Liu, Y., Zheng, X., Yang, S., and Chen, W. (2017). Circularly permuted TRAIL plus thalidomide and dexamethasone versus thalidomide and dexamethasone for relapsed/refractory multiple myeloma: a phase 2 study. *Cancer Chemother Pharmacol* 79, 1141-1149.
- Leng, Y., Qiu, L., Hou, J., Zhao, Y., Zhang, X., Yang, S., Xi, H., Huang, Z., Pan, L., and Chen, W. (2016). Phase II open-label study of recombinant circularly permuted TRAIL as a single-agent treatment for relapsed or refractory multiple myeloma. *Chin J Cancer* 35, 86.
- Leong, S., Cohen, R.B., Gustafson, D.L., Langer, C.J., Camidge, D.R., Padavic, K., Gore, L., Smith, M., Chow, L.Q., von Mehren, M., O'Bryant, C., Hariharan, S., Diab, S., Fox, N.L., Miceli, R., and Eckhardt, S.G. (2009). Mapatumumab, an antibody targeting TRAIL-R1, in combination with paclitaxel and carboplatin in patients with advanced solid malignancies: results of a phase I and pharmacokinetic study. *J Clin Oncol* 27, 4413-4421.
- Li, H., Zhu, H., Xu, C.J., and Yuan, J. (1998). Cleavage of BID by caspase 8 mediates the mitochondrial damage in the Fas pathway of apoptosis. *Cell* 94, 491-501.
- Li, L., Thomas, R.M., Suzuki, H., De Brabander, J.K., Wang, X., and Harran, P.G. (2004). A small molecule Smac mimic potentiates TRAIL- and TNFalpha-mediated cell death. *Science* 305, 1471-1474.
- Li, Q., Price, J.P., Byers, S.A., Cheng, D., Peng, J., and Price, D.H. (2005). Analysis of the large inactive P-TEFb complex indicates that it contains one 7SK molecule, a dimer of HEXIM1 or HEXIM2, and two P-TEFb molecules containing Cdk9 phosphorylated at threonine 186. *J Biol Chem* 280, 28819-28826.
- Lin, C., Smith, E.R., Takahashi, H., Lai, K.C., Martin-Brown, S., Florens, L., Washburn, M.P., Conaway, J.W., Conaway, R.C., and Shilatifard, A. (2010). AFF4, a component of the ELL/P-TEFb elongation complex and a shared subunit of MLL chimeras, can link transcription elongation to leukemia. *Mol Cell* 37, 429-437.
- Lin, P.S., Dubois, M.F., and Dahmus, M.E. (2002a). TFIIIF-associating carboxyl-terminal domain phosphatase dephosphorylates phosphoserines 2 and 5 of RNA polymerase II. *J Biol Chem* 277, 45949-45956.
- Lin, X., Taube, R., Fujinaga, K., and Peterlin, B.M. (2002b). P-TEFb containing cyclin K and Cdk9 can activate transcription via RNA. *J Biol Chem* 277, 16873-16878.
- Lin, Y., Devin, A., Cook, A., Keane, M.M., Kelliher, M., Lipkowitz, S., and Liu, Z.G. (2000). The death domain kinase RIP is essential for TRAIL (Apo2L)-induced activation of I κ B kinase and c-Jun N-terminal kinase. *Mol Cell Biol* 20, 6638-6645.
- Lin, Y., Devin, A., Rodriguez, Y., and Liu, Z.G. (1999). Cleavage of the death domain kinase RIP by caspase-8 prompts TNF-induced apoptosis. *Genes Dev* 13, 2514-2526.

- Linkermann, A., and Green, D.R. (2014). Necroptosis. *N Engl J Med* **370**, 455-465.
- Liu, H., and Herrmann, C.H. (2005). Differential localization and expression of the Cdk9 42k and 55k isoforms. *J Cell Physiol* **203**, 251-260.
- Locksley, R.M., Killeen, N., and Lenardo, M.J. (2001). The TNF and TNF receptor superfamilies: integrating mammalian biology. *Cell* **104**, 487-501.
- Lowe, S.W., Bodis, S., McClatchey, A., Remington, L., Ruley, H.E., Fisher, D.E., Housman, D.E., and Jacks, T. (1994). p53 status and the efficacy of cancer therapy in vivo. *Science* **266**, 807-810.
- Lu, H., Xue, Y., Yu, G.K., Arias, C., Lin, J., Fong, S., Faure, M., Weisburd, B., Ji, X., Mercier, A., Sutton, J., Luo, K., Gao, Z., and Zhou, Q. (2015). Compensatory induction of MYC expression by sustained CDK9 inhibition via a BRD4-dependent mechanism. *Elife* **4**, e06535.
- Lu, X., Zhu, X., Li, Y., Liu, M., Yu, B., Wang, Y., Rao, M., Yang, H., Zhou, K., Wang, Y., Chen, Y., Chen, M., Zhuang, S., Chen, L.F., Liu, R., and Chen, R. (2016). Multiple P-TEFbs cooperatively regulate the release of promoter-proximally paused RNA polymerase II. *Nucleic Acids Res* **44**, 6853-6867.
- Luo, S.Y., and Lam, D.C. (2013). Oncogenic driver mutations in lung cancer. *Transl Respir Med* **1**, 6.
- Luo, X., Budihardjo, I., Zou, H., Slaughter, C., and Wang, X. (1998). Bid, a Bcl2 interacting protein, mediates cytochrome c release from mitochondria in response to activation of cell surface death receptors. *Cell* **94**, 481-490.
- MacCallum, D.E., Melville, J., Frame, S., Watt, K., Anderson, S., Gianella-Borradori, A., Lane, D.P., and Green, S.R. (2005). Seliciclib (CYC202, R-Roscovitin) induces cell death in multiple myeloma cells by inhibition of RNA polymerase II-dependent transcription and down-regulation of Mcl-1. *Cancer Res* **65**, 5399-5407.
- MacDougall, J.R., Croy, B.A., Chapeau, C., and Clark, D.A. (1990). Demonstration of a splenic cytotoxic effector cell in mice of genotype SCID/SCID.BG/BG. *Cell Immunol* **130**, 106-117.
- MacFarlane, M., Ahmad, M., Srinivasula, S.M., Fernandes-Alnemri, T., Cohen, G.M., and Alnemri, E.S. (1997). Identification and molecular cloning of two novel receptors for the cytotoxic ligand TRAIL. *J Biol Chem* **272**, 25417-25420.
- MacFarlane, M., Inoue, S., Kohlhaas, S.L., Majid, A., Harper, N., Kennedy, D.B., Dyer, M.J., and Cohen, G.M. (2005a). Chronic lymphocytic leukemic cells exhibit apoptotic signaling via TRAIL-R1. *Cell Death Differ* **12**, 773-782.
- MacFarlane, M., Kohlhaas, S.L., Sutcliffe, M.J., Dyer, M.J., and Cohen, G.M. (2005b). TRAIL receptor-selective mutants signal to apoptosis via TRAIL-R1 in primary lymphoid malignancies. *Cancer Res* **65**, 11265-11270.
- Malkinson, A.M. (1989). The genetic basis of susceptibility to lung tumors in mice. *Toxicology* **54**, 241-271.
- Malumbres, M. (2014). Cyclin-dependent kinases. *Genome Biol* **15**, 122.
- Manenti, G., and Dragani, T.A. (2005). Pas1 haplotype-dependent genetic predisposition to lung tumorigenesis in rodents: a meta-analysis. *Carcinogenesis* **26**, 875-882.

- Manzo, F., Nebbioso, A., Miceli, M., Conte, M., De Bellis, F., Carafa, V., Franci, G., Tambaro, F.P., and Altucci, L. (2009). TNF-related apoptosis-inducing ligand: signalling of a 'smart' molecule. *Int J Biochem Cell Biol* *41*, 460-466.
- Mariani, S.M., Matiba, B., Armandola, E.A., and Krammer, P.H. (1997). Interleukin 1 beta-converting enzyme related proteases/caspases are involved in TRAIL-induced apoptosis of myeloma and leukemia cells. *J Cell Biol* *137*, 221-229.
- Marshall, N.F., and Price, D.H. (1995). Purification of P-TEFb, a transcription factor required for the transition into productive elongation. *J Biol Chem* *270*, 12335-12338.
- Marsters, S.A., Sheridan, J.P., Pitti, R.M., Huang, A., Skubatch, M., Baldwin, D., Yuan, J., Gurney, A., Goddard, A.D., Godowski, P., and Ashkenazi, A. (1997). A novel receptor for Apo2L/TRAIL contains a truncated death domain. *Curr Biol* *7*, 1003-1006.
- Martin, M.P., Olesen, S.H., Georg, G.I., and Schonbrunn, E. (2013). Cyclin-dependent kinase inhibitor dinaciclib interacts with the acetyl-lysine recognition site of bromodomains. *ACS Chem Biol* *8*, 2360-2365.
- Massey, T.E., Devereux, T.R., Maronpot, R.R., Foley, J.F., and Anderson, M.W. (1995). High frequency of K-ras mutations in spontaneous and vinyl carbamate-induced lung tumors of relatively resistant B6CF1 (C57BL/6J x BALB/cJ) mice. *Carcinogenesis* *16*, 1065-1069.
- McCann, C., Crawford, N., Majkut, J., Holohan, C., Armstrong, C.W.D., Maxwell, P.J., Ong, C.W., LaBonte, M.J., McDade, S.S., Waugh, D.J., and Longley, D.B. (2018). Cytoplasmic FLIP(S) and nuclear FLIP(L) mediate resistance of castrate-resistant prostate cancer to apoptosis induced by IAP antagonists. *Cell Death Dis* *9*, 1081.
- McCormick, F. (2015). The potential of targeting Ras proteins in lung cancer. *Expert Opin Ther Targets* *19*, 451-454.
- McDonald, K.A., Kawaguchi, T., Qi, Q., Peng, X., Asaoka, M., Young, J., Opyrchal, M., Yan, L., Patnaik, S., Otsuji, E., and Takabe, K. (2019). Tumor Heterogeneity Correlates with Less Immune Response and Worse Survival in Breast Cancer Patients. *Ann Surg Oncol* *26*, 2191-2199.
- McFadden, D.G., Politi, K., Bhutkar, A., Chen, F.K., Song, X., Pirun, M., Santiago, P.M., Kim-Kiselak, C., Platt, J.T., Lee, E., Hodges, E., Rosebrock, A.P., Bronson, R.T., Succi, N.D., Hannon, G.J., Jacks, T., and Varmus, H. (2016). Mutational landscape of EGFR-, MYC-, and Kras-driven genetically engineered mouse models of lung adenocarcinoma. *Proc Natl Acad Sci U S A* *113*, E6409-E6417.
- McGranahan, N., Furness, A.J., Rosenthal, R., Ramskov, S., Lyngaa, R., Saini, S.K., Jamal-Hanjani, M., Wilson, G.A., Birkbak, N.J., Hiley, C.T., Watkins, T.B., Shafi, S., Murugaesu, N., Mitter, R., Akarca, A.U., Linares, J., Marafioti, T., Henry, J.Y., Van Allen, E.M., Miao, D., Schilling, B., Schadendorf, D., Garraway, L.A., Makarov, V., Rizvi, N.A., Snyder, A., Hellmann, M.D., Merghoub, T., Wolchok, J.D., Shukla, S.A., Wu, C.J., Peggs, K.S., Chan, T.A., Hadrup, S.R., Quezada, S.A., and Swanton, C. (2016). Clonal neoantigens elicit T cell immunoreactivity and sensitivity to immune checkpoint blockade. *Science* *351*, 1463-1469.
- Medema, J.P., Scaffidi, C., Kischkel, F.C., Shevchenko, A., Mann, M., Krammer, P.H., and Peter, M.E. (1997). FLICE is activated by association with the CD95 death-inducing signaling complex (DISC). *EMBO J* *16*, 2794-2804.
- Meijer, L., Borgne, A., Mulner, O., Chong, J.P., Blow, J.J., Inagaki, N., Inagaki, M., Delcros, J.G., and Moulinoux, J.P. (1997). Biochemical and cellular effects of roscovitine, a potent and selective inhibitor of the cyclin-dependent kinases cdc2, cdk2 and cdk5. *Eur J Biochem* *243*, 527-536.

- Merchant, M.S., Geller, J.I., Baird, K., Chou, A.J., Galli, S., Charles, A., Amaoko, M., Rhee, E.H., Price, A., Wexler, L.H., Meyers, P.A., Widemann, B.C., Tsokos, M., and Mackall, C.L. (2012). Phase I trial and pharmacokinetic study of lexatumumab in pediatric patients with solid tumors. *J Clin Oncol* 30, 4141-4147.
- Merino, D., Kelly, G.L., Lessene, G., Wei, A.H., Roberts, A.W., and Strasser, A. (2018). BH3-Mimetic Drugs: Blazing the Trail for New Cancer Medicines. *Cancer Cell* 34, 879-891.
- Merino, D., Lalaoui, N., Morizot, A., Schneider, P., Solary, E., and Micheau, O. (2006). Differential inhibition of TRAIL-mediated DR5-DISC formation by decoy receptors 1 and 2. *Mol Cell Biol* 26, 7046-7055.
- Meurette, O., Huc, L., Rebillard, A., Le Moigne, G., Lagadic-Gossmann, D., and Dimanche-Boitrel, M.T. (2005). TRAIL (TNF-related apoptosis-inducing ligand) induces necrosis-like cell death in tumor cells at acidic extracellular pH. *Ann N Y Acad Sci* 1056, 379-387.
- Meurette, O., Rebillard, A., Huc, L., Le Moigne, G., Merino, D., Micheau, O., Lagadic-Gossmann, D., and Dimanche-Boitrel, M.T. (2007). TRAIL induces receptor-interacting protein 1-dependent and caspase-dependent necrosis-like cell death under acidic extracellular conditions. *Cancer Res* 67, 218-226.
- Miao, D., Margolis, C.A., Gao, W., Voss, M.H., Li, W., Martini, D.J., Norton, C., Bosse, D., Wankowicz, S.M., Cullen, D., Horak, C., Wind-Rotolo, M., Tracy, A., Giannakis, M., Hodi, F.S., Drake, C.G., Ball, M.W., Allaf, M.E., Snyder, A., Hellmann, M.D., Ho, T., Motzer, R.J., Signoretti, S., Kaelin, W.G., Jr., Choueiri, T.K., and Van Allen, E.M. (2018). Genomic correlates of response to immune checkpoint therapies in clear cell renal cell carcinoma. *Science* 359, 801-806.
- Micheau, O., Thome, M., Schneider, P., Holler, N., Tschopp, J., Nicholson, D.W., Briand, C., and Grutter, M.G. (2002). The long form of FLIP is an activator of caspase-8 at the Fas death-inducing signaling complex. *J Biol Chem* 277, 45162-45171.
- Micheau, O., and Tschopp, J. (2003). Induction of TNF receptor I-mediated apoptosis via two sequential signaling complexes. *Cell* 114, 181-190.
- Mishra, N.K., Urick, A.K., Ember, S.W., Schonbrunn, E., and Pomerantz, W.C. (2014). Fluorinated aromatic amino acids are sensitive ¹⁹F NMR probes for bromodomain-ligand interactions. *ACS Chem Biol* 9, 2755-2760.
- Mita, M.M., Joy, A.A., Mita, A., Sankhala, K., Jou, Y.M., Zhang, D., Statkevich, P., Zhu, Y., Yao, S.L., Small, K., Bannerji, R., and Shapiro, C.L. (2014). Randomized phase II trial of the cyclin-dependent kinase inhibitor dinaciclib (MK-7965) versus capecitabine in patients with advanced breast cancer. *Clin Breast Cancer* 14, 169-176.
- Mita, M.M., Mita, A.C., Moseley, J.L., Poon, J., Small, K.A., Jou, Y.M., Kirschmeier, P., Zhang, D., Zhu, Y., Statkevich, P., Sankhala, K.K., Sarantopoulos, J., Cleary, J.M., Chirieac, L.R., Rodig, S.J., Bannerji, R., and Shapiro, G.I. (2017). Phase 1 safety, pharmacokinetic and pharmacodynamic study of the cyclin-dependent kinase inhibitor dinaciclib administered every three weeks in patients with advanced malignancies. *Br J Cancer* 117, 1258-1268.
- Mitri, Z., Karakas, C., Wei, C., Briones, B., Simmons, H., Ibrahim, N., Alvarez, R., Murray, J.L., Keyomarsi, K., and Moulder, S. (2015). A phase 1 study with dose expansion of the CDK inhibitor dinaciclib (SCH 727965) in combination with epirubicin in patients with metastatic triple negative breast cancer. *Invest New Drugs* 33, 890-894.
- Mitsiades, N., Mitsiades, C.S., Poulaki, V., Chauhan, D., Richardson, P.G., Hideshima, T., Munshi, N., Treon, S.P., and Anderson, K.C. (2002). Biologic sequelae of nuclear factor-kappaB blockade in multiple myeloma: therapeutic applications. *Blood* 99, 4079-4086.

- Molinsky, J., Klanova, M., Koc, M., Beranova, L., Andera, L., Ludvikova, Z., Bohmova, M., Gasova, Z., Strnad, M., Ivanek, R., Trneny, M., Necas, E., Zivny, J., and Klener, P. (2013). Roscovitine sensitizes leukemia and lymphoma cells to tumor necrosis factor-related apoptosis-inducing ligand-induced apoptosis. *Leuk Lymphoma* *54*, 372-380.
- Mom, C.H., Verweij, J., Oldenhuis, C.N., Gietema, J.A., Fox, N.L., Miceli, R., Eskens, F.A., Loos, W.J., de Vries, E.G., and Sleijfer, S. (2009). Mapatumumab, a fully human agonistic monoclonal antibody that targets TRAIL-R1, in combination with gemcitabine and cisplatin: a phase I study. *Clin Cancer Res* *15*, 5584-5590.
- Mombaerts, P., Iacomini, J., Johnson, R.S., Herrup, K., Tonegawa, S., and Papaioannou, V.E. (1992). RAG-1-deficient mice have no mature B and T lymphocytes. *Cell* *68*, 869-877.
- Mompean, M., Li, W., Li, J., Laage, S., Siemer, A.B., Bozkurt, G., Wu, H., and McDermott, A.E. (2018). The Structure of the Necrosome RIPK1-RIPK3 Core, a Human Hetero-Amyloid Signaling Complex. *Cell* *173*, 1244-1253 e1210.
- Moreno, N., Holsten, T., Mertins, J., Zhogbi, A., Johann, P., Kool, M., Meisterernst, M., and Kerl, K. (2017). Combined BRD4 and CDK9 inhibition as a new therapeutic approach in malignant rhabdoid tumors. *Oncotarget* *8*, 84986-84995.
- Morizot, A., Merino, D., Lalaoui, N., Jacquemin, G., Granci, V., Iessi, E., Lanneau, D., Bouyer, F., Solary, E., Chauffert, B., Saas, P., Garrido, C., and Micheau, O. (2011). Chemotherapy overcomes TRAIL-R4-mediated TRAIL resistance at the DISC level. *Cell Death Differ* *18*, 700-711.
- Mortellaro, A., and Ricciardi-Castagnoli, P. (2011). From vaccine practice to vaccine science: the contribution of human immunology to the prevention of infectious disease. *Immunol Cell Biol* *89*, 332-339.
- Mucha, S.R., Rizzani, A., Gerbes, A.L., Camaj, P., Thasler, W.E., Bruns, C.J., Eichhorst, S.T., Gallmeier, E., Kolligs, F.T., Goke, B., and De Toni, E.N. (2009). JNK inhibition sensitises hepatocellular carcinoma cells but not normal hepatocytes to the TNF-related apoptosis-inducing ligand. *Gut* *58*, 688-698.
- Muhlenbeck, F., Haas, E., Schwenzler, R., Schubert, G., Grell, M., Smith, C., Scheurich, P., and Wajant, H. (1998). TRAIL/Apo2L activates c-Jun NH2-terminal kinase (JNK) via caspase-dependent and caspase-independent pathways. *J Biol Chem* *273*, 33091-33098.
- Munshi, A., Pappas, G., Honda, T., McDonnell, T.J., Younes, A., Li, Y., and Meyn, R.E. (2001). TRAIL (APO-2L) induces apoptosis in human prostate cancer cells that is inhibitable by Bcl-2. *Oncogene* *20*, 3757-3765.
- Murphy, J.M., Czabotar, P.E., Hildebrand, J.M., Lucet, I.S., Zhang, J.G., Alvarez-Diaz, S., Lewis, R., Lalaoui, N., Metcalf, D., Webb, A.I., Young, S.N., Varghese, L.N., Tannahill, G.M., Hatchell, E.C., Majewski, I.J., Okamoto, T., Dobson, R.C., Hilton, D.J., Babon, J.J., Nicola, N.A., Strasser, A., Silke, J., and Alexander, W.S. (2013). The pseudokinase MLKL mediates necroptosis via a molecular switch mechanism. *Immunity* *39*, 443-453.
- Muzio, M., Chinnaiyan, A.M., Kischkel, F.C., O'Rourke, K., Shevchenko, A., Ni, J., Scaffidi, C., Bretz, J.D., Zhang, M., Gentz, R., Mann, M., Krammer, P.H., Peter, M.E., and Dixit, V.M. (1996). FLICE, a novel FADD-homologous ICE/CED-3-like protease, is recruited to the CD95 (Fas/APO-1) death-inducing signaling complex. *Cell* *85*, 817-827.
- Nakano, K., and Vousden, K.H. (2001). PUMA, a novel proapoptotic gene, is induced by p53. *Mol Cell* *7*, 683-694.

- Narita, T., Ishida, T., Ito, A., Masaki, A., Kinoshita, S., Suzuki, S., Takino, H., Yoshida, T., Ri, M., Kusumoto, S., Komatsu, H., Imada, K., Tanaka, Y., Takaori-Kondo, A., Inagaki, H., Scholz, A., Lienau, P., Kuroda, T., Ueda, R., and Iida, S. (2017). Cyclin-dependent kinase 9 is a novel specific molecular target in adult T-cell leukemia/lymphoma. *Blood* 130, 1114-1124.
- Nauts, H.C., Swift, W.E., and Coley, B.L. (1946). The treatment of malignant tumors by bacterial toxins as developed by the late William B. Coley, M.D., reviewed in the light of modern research. *Cancer Res* 6, 205-216.
- Nazarian, R., Shi, H., Wang, Q., Kong, X., Koya, R.C., Lee, H., Chen, Z., Lee, M.K., Attar, N., Sazegar, H., Chodon, T., Nelson, S.F., McArthur, G., Sosman, J.A., Ribas, A., and Lo, R.S. (2010). Melanomas acquire resistance to B-RAF(V600E) inhibition by RTK or N-RAS upregulation. *Nature* 468, 973-977.
- Nebbio, A., Clarke, N., Voltz, E., Germain, E., Ambrosino, C., Bontempo, P., Alvarez, R., Schiavone, E.M., Ferrara, F., Bresciani, F., Weisz, A., de Lera, A.R., Gronemeyer, H., and Altucci, L. (2005). Tumor-selective action of HDAC inhibitors involves TRAIL induction in acute myeloid leukemia cells. *Nat Med* 11, 77-84.
- Nemunaitis, J.J., Small, K.A., Kirschmeier, P., Zhang, D., Zhu, Y., Jou, Y.M., Statkevich, P., Yao, S.L., and Bannerji, R. (2013). A first-in-human, phase 1, dose-escalation study of dinaciclib, a novel cyclin-dependent kinase inhibitor, administered weekly in subjects with advanced malignancies. *J Transl Med* 11, 259.
- Nguyen, V.T., Kiss, T., Michels, A.A., and Bensaude, O. (2001). 7SK small nuclear RNA binds to and inhibits the activity of CDK9/cyclin T complexes. *Nature* 414, 322-325.
- Nuzum, E.O., Malkinson, A.M., and Beer, D.G. (1990). Specific Ki-ras codon 61 mutations may determine the development of urethan-induced mouse lung adenomas or adenocarcinomas. *Mol Carcinog* 3, 287-295.
- O'Donnell, M.A., Legarda-Addison, D., Skountzos, P., Yeh, W.C., and Ting, A.T. (2007). Ubiquitination of RIP1 regulates an NF-kappaB-independent cell-death switch in TNF signaling. *Curr Biol* 17, 418-424.
- Oberst, A., Dillon, C.P., Weinlich, R., McCormick, L.L., Fitzgerald, P., Pop, C., Hakem, R., Salvesen, G.S., and Green, D.R. (2011). Catalytic activity of the caspase-8-FLIP(L) complex inhibits RIPK3-dependent necrosis. *Nature* 471, 363-367.
- Oda, E., Ohki, R., Murasawa, H., Nemoto, J., Shibue, T., Yamashita, T., Tokino, T., Taniguchi, T., and Tanaka, N. (2000). Noxa, a BH3-only member of the Bcl-2 family and candidate mediator of p53-induced apoptosis. *Science* 288, 1053-1058.
- Odogwu, L., Mathieu, L., Blumenthal, G., Larkins, E., Goldberg, K.B., Griffin, N., Bijwaard, K., Lee, E.Y., Philip, R., Jiang, X., Rodriguez, L., McKee, A.E., Keegan, P., and Pazdur, R. (2018). FDA Approval Summary: Dabrafenib and Trametinib for the Treatment of Metastatic Non-Small Cell Lung Cancers Harboring BRAF V600E Mutations. *Oncologist* 23, 740-745.
- Oehm, A., Behrmann, I., Falk, W., Pawlita, M., Maier, G., Klas, C., Li-Weber, M., Richards, S., Dhein, J., Trauth, B.C., Ponsting, H., and Krammer, P.H. (1992). Purification and molecular cloning of the APO-1 cell surface antigen, a member of the tumor necrosis factor/nerve growth factor receptor superfamily. Sequence identity with the Fas antigen. *J Biol Chem* 267, 10709-10715.
- Ogasawara, J., Watanabe-Fukunaga, R., Adachi, M., Matsuzawa, A., Kasugai, T., Kitamura, Y., Itoh, N., Suda, T., and Nagata, S. (1993). Lethal effect of the anti-Fas antibody in mice. *Nature* 364, 806-809.

Ohno, J., Horio, Y., Sekido, Y., Hasegawa, Y., Takahashi, M., Nishizawa, J., Saito, H., Ishikawa, F., and Shimokata, K. (2001). Telomerase activation and p53 mutations in urethane-induced A/J mouse lung tumor development. *Carcinogenesis* 22, 751-756.

Olson, C.M., Jiang, B., Erb, M.A., Liang, Y., Doctor, Z.M., Zhang, Z., Zhang, T., Kwiatkowski, N., Boukhali, M., Green, J.L., Haas, W., Nomanbhoy, T., Fischer, E.S., Young, R.A., Bradner, J.E., Winter, G.E., and Gray, N.S. (2018). Pharmacological perturbation of CDK9 using selective CDK9 inhibition or degradation. *Nat Chem Biol* 14, 163-170.

Ortiz-Ferron, G., Yerbes, R., Eramo, A., Lopez-Perez, A.I., De Maria, R., and Lopez-Rivas, A. (2008). Roscovitine sensitizes breast cancer cells to TRAIL-induced apoptosis through a pleiotropic mechanism. *Cell Res* 18, 664-676.

Ouyang, X., Shi, M., Jie, F., Bai, Y., Shen, P., Yu, Z., Wang, X., Huang, C., Tao, M., Wang, Z., Xie, C., Wu, Q., Shu, Y., Han, B., Zhang, F., Zhang, Y., Hu, C., Ma, X., Liang, Y., Wang, A., Lu, B., Shi, Y., Chen, J., Zhuang, Z., Wang, J., Huang, J., Wang, C., Bai, C., Zhou, X., Li, Q., Chen, F., Yu, H., and Feng, J. (2018). Phase III study of dulanermin (recombinant human tumor necrosis factor-related apoptosis-inducing ligand/Apo2 ligand) combined with vinorelbine and cisplatin in patients with advanced non-small-cell lung cancer. *Invest New Drugs* 36, 315-322.

Pai-Scherf, L., Blumenthal, G.M., Li, H., Subramaniam, S., Mishra-Kalyani, P.S., He, K., Zhao, H., Yu, J., Paciga, M., Goldberg, K.B., McKee, A.E., Keegan, P., and Pazdur, R. (2017). FDA Approval Summary: Pembrolizumab for Treatment of Metastatic Non-Small Cell Lung Cancer: First-Line Therapy and Beyond. *Oncologist* 22, 1392-1399.

Palacios, C., Yerbes, R., and Lopez-Rivas, A. (2006). Flavopiridol induces cellular FLICE-inhibitory protein degradation by the proteasome and promotes TRAIL-induced early signaling and apoptosis in breast tumor cells. *Cancer Res* 66, 8858-8869.

Pan, G., Ni, J., Wei, Y.F., Yu, G., Gentz, R., and Dixit, V.M. (1997a). An antagonist decoy receptor and a death domain-containing receptor for TRAIL. *Science* 277, 815-818.

Pan, G., O'Rourke, K., Chinnaiyan, A.M., Gentz, R., Ebner, R., Ni, J., and Dixit, V.M. (1997b). The receptor for the cytotoxic ligand TRAIL. *Science* 276, 111-113.

Pan, G., O'Rourke, K., and Dixit, V.M. (1998). Caspase-9, Bcl-XL, and Apaf-1 form a ternary complex. *J Biol Chem* 273, 5841-5845.

Pan, Y., Xu, R., Peach, M., Huang, C.P., Branstetter, D., Novotny, W., Herbst, R.S., Eckhardt, S.G., and Holland, P.M. (2011). Evaluation of pharmacodynamic biomarkers in a Phase 1a trial of dulanermin (rhApo2L/TRAIL) in patients with advanced tumours. *Br J Cancer* 105, 1830-1838.

Papadopoulos, K.P., Isaacs, R., Bilic, S., Kentsch, K., Huet, H.A., Hofmann, M., Rasco, D., Kundamal, N., Tang, Z., Cooksey, J., and Mahipal, A. (2015). Unexpected hepatotoxicity in a phase I study of TAS266, a novel tetravalent agonistic Nanobody(R) targeting the DR5 receptor. *Cancer Chemother Pharmacol* 75, 887-895.

Paparidis, N.F., Durvale, M.C., and Canduri, F. (2017). The emerging picture of CDK9/P-TEFb: more than 20 years of advances since PITALRE. *Mol Biosyst* 13, 246-276.

Park, D.S., Farinelli, S.E., and Greene, L.A. (1996). Inhibitors of cyclin-dependent kinases promote survival of post-mitotic neuronally differentiated PC12 cells and sympathetic neurons. *J Biol Chem* 271, 8161-8169.

Parry, D., Guzi, T., Shanahan, F., Davis, N., Prabhavalkar, D., Wiswell, D., Seghezzi, W., Paruch, K., Dwyer, M.P., Doll, R., Nomeir, A., Windsor, W., Fischmann, T., Wang, Y., Oft, M.,

- Chen, T., Kirschmeier, P., and Lees, E.M. (2010). Dinaciclib (SCH 727965), a novel and potent cyclin-dependent kinase inhibitor. *Mol Cancer Ther* 9, 2344-2353.
- Paz-Ares, L., Balint, B., de Boer, R.H., van Meerbeeck, J.P., Wierzbicki, R., De Souza, P., Galimi, F., Haddad, V., Sabin, T., Hei, Y.J., Pan, Y., Cottrell, S., Hsu, C.P., and RamLau, R. (2013). A randomized phase 2 study of paclitaxel and carboplatin with or without conatumumab for first-line treatment of advanced non-small-cell lung cancer. *J Thorac Oncol* 8, 329-337.
- Peng, J., Marshall, N.F., and Price, D.H. (1998). Identification of a cyclin subunit required for the function of *Drosophila* P-TEFb. *J Biol Chem* 273, 13855-13860.
- Pfirschke, C., Engblom, C., Rickelt, S., Cortez-Retamozo, V., Garris, C., Pucci, F., Yamazaki, T., Poirier-Colame, V., Newton, A., Redouane, Y., Lin, Y.J., Wojtkiewicz, G., Iwamoto, Y., Mino-Kenudson, M., Huynh, T.G., Hynes, R.O., Freeman, G.J., Kroemer, G., Zitvogel, L., Weissleder, R., and Pittet, M.J. (2016). Immunogenic Chemotherapy Sensitizes Tumors to Checkpoint Blockade Therapy. *Immunity* 44, 343-354.
- Pillai, M.R., Collison, L.W., Wang, X., Finkelstein, D., Rehg, J.E., Boyd, K., Szymczak-Workman, A.L., Doggett, T., Griffith, T.S., Ferguson, T.A., and Vignali, D.A. (2011). The plasticity of regulatory T cell function. *J Immunol* 187, 4987-4997.
- Pitti, R.M., Marsters, S.A., Ruppert, S., Donahue, C.J., Moore, A., and Ashkenazi, A. (1996). Induction of apoptosis by Apo-2 ligand, a new member of the tumor necrosis factor cytokine family. *J Biol Chem* 271, 12687-12690.
- Piyathilake, C.J., Frost, A.R., Weiss, H., Manne, U., Heimburger, D.C., and Grizzle, W.E. (2000). The expression of Ep-CAM (17-1A) in squamous cell cancers of the lung. *Hum Pathol* 31, 482-487.
- Plaschka, C., Nozawa, K., and Cramer, P. (2016). Mediator Architecture and RNA Polymerase II Interaction. *J Mol Biol* 428, 2569-2574.
- Plummer, R., Attard, G., Pacey, S., Li, L., Razak, A., Perrett, R., Barrett, M., Judson, I., Kaye, S., Fox, N.L., Halpern, W., Corey, A., Calvert, H., and de Bono, J. (2007). Phase 1 and pharmacokinetic study of lexatumumab in patients with advanced cancers. *Clin Cancer Res* 13, 6187-6194.
- Pollack, V.A., Savage, D.M., Baker, D.A., Tsaparikos, K.E., Sloan, D.E., Moyer, J.D., Barbacci, E.G., Pustilnik, L.R., Smolarek, T.A., Davis, J.A., Vaidya, M.P., Arnold, L.D., Doty, J.L., Iwata, K.K., and Morin, M.J. (1999). Inhibition of epidermal growth factor receptor-associated tyrosine phosphorylation in human carcinomas with CP-358,774: dynamics of receptor inhibition in situ and antitumor effects in athymic mice. *J Pharmacol Exp Ther* 291, 739-748.
- Pop, C., Oberst, A., Drag, M., Van Raam, B.J., Riedl, S.J., Green, D.R., and Salvesen, G.S. (2011). FLIP(L) induces caspase 8 activity in the absence of interdomain caspase 8 cleavage and alters substrate specificity. *Biochem J* 433, 447-457.
- Quarato, G., Guy, C.S., Grace, C.R., Llambi, F., Nourse, A., Rodriguez, D.A., Wakefield, R., Frase, S., Moldoveanu, T., and Green, D.R. (2016). Sequential Engagement of Distinct MLKL Phosphatidylinositol-Binding Sites Executes Necroptosis. *Mol Cell* 61, 589-601.
- Rahl, P.B., Lin, C.Y., Seila, A.C., Flynn, R.A., McCuine, S., Burge, C.B., Sharp, P.A., and Young, R.A. (2010). c-Myc regulates transcriptional pause release. *Cell* 141, 432-445.
- Ran, F.A., Hsu, P.D., Wright, J., Agarwala, V., Scott, D.A., and Zhang, F. (2013). Genome engineering using the CRISPR-Cas9 system. *Nat Protoc* 8, 2281-2308.

- Ravi, R., Bedi, G.C., Engstrom, L.W., Zeng, Q., Mookerjee, B., Gelinas, C., Fuchs, E.J., and Bedi, A. (2001). Regulation of death receptor expression and TRAIL/Apo2L-induced apoptosis by NF-kappaB. *Nat Cell Biol* 3, 409-416.
- Ray, M., Salgia, R., and Vokes, E.E. (2009). The role of EGFR inhibition in the treatment of non-small cell lung cancer. *Oncologist* 14, 1116-1130.
- Reck, M., Krzakowski, M., Chmielowska, E., Sebastian, M., Hadler, D., Fox, T., Wang, Q., Greenberg, J., Beckman, R.A., and von Pawel, J. (2013). A randomized, double-blind, placebo-controlled phase 2 study of tigatuzumab (CS-1008) in combination with carboplatin/paclitaxel in patients with chemotherapy-naive metastatic/unresectable non-small cell lung cancer. *Lung Cancer* 82, 441-448.
- Ren, X., Ye, F., Jiang, Z., Chu, Y., Xiong, S., and Wang, Y. (2007). Involvement of cellular death in TRAIL/DR5-dependent suppression induced by CD4(+)CD25(+) regulatory T cells. *Cell Death Differ* 14, 2076-2084.
- Riedl, S.J., and Shi, Y. (2004). Molecular mechanisms of caspase regulation during apoptosis. *Nat Rev Mol Cell Biol* 5, 897-907.
- Riley, J.S., Hutchinson, R., McArt, D.G., Crawford, N., Holohan, C., Paul, I., Van Schaeybroeck, S., Salto-Tellez, M., Johnston, P.G., Fennell, D.A., Gately, K., O'Byrne, K., Cummins, R., Kay, E., Hamilton, P., Stasik, I., and Longley, D.B. (2013). Prognostic and therapeutic relevance of FLIP and procaspase-8 overexpression in non-small cell lung cancer. *Cell Death Dis* 4, e951.
- Rimel, J.K., and Taatjes, D.J. (2018). The essential and multifunctional TFIIH complex. *Protein Sci* 27, 1018-1037.
- Rizvi, N.A., Hellmann, M.D., Snyder, A., Kvistborg, P., Makarov, V., Havel, J.J., Lee, W., Yuan, J., Wong, P., Ho, T.S., Miller, M.L., Rekhman, N., Moreira, A.L., Ibrahim, F., Bruggeman, C., Gasmi, B., Zappasodi, R., Maeda, Y., Sander, C., Garon, E.B., Merghoub, T., Wolchok, J.D., Schumacher, T.N., and Chan, T.A. (2015). Cancer immunology. Mutational landscape determines sensitivity to PD-1 blockade in non-small cell lung cancer. *Science* 348, 124-128.
- Roberts, S.A., Lawrence, M.S., Klimczak, L.J., Grimm, S.A., Fargo, D., Stojanov, P., Kiezun, A., Kryukov, G.V., Carter, S.L., Saksena, G., Harris, S., Shah, R.R., Resnick, M.A., Getz, G., and Gordenin, D.A. (2013). An APOBEC cytidine deaminase mutagenesis pattern is widespread in human cancers. *Nat Genet* 45, 970-976.
- Rocha Lima, C.M., Bayraktar, S., Flores, A.M., MacIntyre, J., Montero, A., Baranda, J.C., Wallmark, J., Portera, C., Raja, R., Stern, H., Royer-Joo, S., and Amler, L.C. (2012). Phase Ib study of drozitumab combined with first-line mFOLFOX6 plus bevacizumab in patients with metastatic colorectal cancer. *Cancer Invest* 30, 727-731.
- Rodenhuis, S., and Slebos, R.J. (1992). Clinical significance of ras oncogene activation in human lung cancer. *Cancer Res* 52, 2665s-2669s.
- Rodriguez, D.A., Weinlich, R., Brown, S., Guy, C., Fitzgerald, P., Dillon, C.P., Oberst, A., Quarato, G., Low, J., Cripps, J.G., Chen, T., and Green, D.R. (2016). Characterization of RIPK3-mediated phosphorylation of the activation loop of MLKL during necroptosis. *Cell Death Differ* 23, 76-88.
- Rooney, M.S., Shukla, S.A., Wu, C.J., Getz, G., and Hacohen, N. (2015). Molecular and genetic properties of tumors associated with local immune cytolytic activity. *Cell* 160, 48-61.
- Rosenthal, R., Cadieux, E.L., Salgado, R., Bakir, M.A., Moore, D.A., Hiley, C.T., Lund, T., Tanic, M., Reading, J.L., Joshi, K., Henry, J.Y., Ghorani, E., Wilson, G.A., Birkbak, N.J., Jamal-

- Hanjani, M., Veeriah, S., Szallasi, Z., Loi, S., Hellmann, M.D., Feber, A., Chain, B., Herrero, J., Quezada, S.A., Demeulemeester, J., Van Loo, P., Beck, S., McGranahan, N., Swanton, C., and consortium, T.R. (2019). Neoantigen-directed immune escape in lung cancer evolution. *Nature* **567**, 479-485.
- Rozanov, D.V., Savinov, A.Y., Golubkov, V.S., Rozanova, O.L., Postnova, T.I., Sergienko, E.A., Vasile, S., Aleshin, A.E., Rega, M.F., Pellicchia, M., and Strongin, A.Y. (2009). Engineering a leucine zipper-TRAIL homotrimer with improved cytotoxicity in tumor cells. *Mol Cancer Ther* **8**, 1515-1525.
- Russell, P., and Nurse, P. (1986). *Schizosaccharomyces pombe* and *Saccharomyces cerevisiae*: a look at yeasts divided. *Cell* **45**, 781-782.
- Sausville, E.A., and Burger, A.M. (2006). Contributions of human tumor xenografts to anticancer drug development. *Cancer Res* **66**, 3351-3354, discussion 3354.
- Sawadogo, M., and Roeder, R.G. (1985). Interaction of a gene-specific transcription factor with the adenovirus major late promoter upstream of the TATA box region. *Cell* **43**, 165-175.
- Sayers, T.J., Brooks, A.D., Koh, C.Y., Ma, W., Seki, N., Raziuddin, A., Blazar, B.R., Zhang, X., Elliott, P.J., and Murphy, W.J. (2003). The proteasome inhibitor PS-341 sensitizes neoplastic cells to TRAIL-mediated apoptosis by reducing levels of c-FLIP. *Blood* **102**, 303-310.
- Scaffidi, C., Schmitz, I., Krammer, P.H., and Peter, M.E. (1999). The role of c-FLIP in modulation of CD95-induced apoptosis. *J Biol Chem* **274**, 1541-1548.
- Schmerwitz, U.K., Sass, G., Khandoga, A.G., Joore, J., Mayer, B.A., Berberich, N., Totzke, F., Krombach, F., Tiegs, G., Zahler, S., Vollmar, A.M., and Furst, R. (2011). Flavopiridol protects against inflammation by attenuating leukocyte-endothelial interaction via inhibition of cyclin-dependent kinase 9. *Arterioscler Thromb Vasc Biol* **31**, 280-288.
- Schneider, P., Bodmer, J.L., Thome, M., Hofmann, K., Holler, N., and Tschopp, J. (1997a). Characterization of two receptors for TRAIL. *FEBS Lett* **416**, 329-334.
- Schneider, P., Olson, D., Tardivel, A., Browning, B., Lugovskoy, A., Gong, D., Dobles, M., Hertig, S., Hofmann, K., Van Vlijmen, H., Hsu, Y.M., Burkly, L.C., Tschopp, J., and Zheng, T.S. (2003). Identification of a new murine tumor necrosis factor receptor locus that contains two novel murine receptors for tumor necrosis factor-related apoptosis-inducing ligand (TRAIL). *J Biol Chem* **278**, 5444-5454.
- Schneider, P., Thome, M., Burns, K., Bodmer, J.L., Hofmann, K., Kataoka, T., Holler, N., and Tschopp, J. (1997b). TRAIL receptors 1 (DR4) and 2 (DR5) signal FADD-dependent apoptosis and activate NF-kappaB. *Immunity* **7**, 831-836.
- Schrank, Z., Chhabra, G., Lin, L., Iderzorig, T., Osude, C., Khan, N., Kuckovic, A., Singh, S., Miller, R.J., and Puri, N. (2018). Current Molecular-Targeted Therapies in NSCLC and Their Mechanism of Resistance. *Cancers (Basel)* **10**.
- Schug, Z.T., Gonzalez, F., Houtkooper, R.H., Vaz, F.M., and Gottlieb, E. (2011). BID is cleaved by caspase-8 within a native complex on the mitochondrial membrane. *Cell Death Differ* **18**, 538-548.
- Schumacher, T.N., and Schreiber, R.D. (2015). Neoantigens in cancer immunotherapy. *Science* **348**, 69-74.

- Screaton, G.R., Mongkolsapaya, J., Xu, X.N., Cowper, A.E., McMichael, A.J., and Bell, J.I. (1997). TRICK2, a new alternatively spliced receptor that transduces the cytotoxic signal from TRAIL. *Curr Biol* 7, 693-696.
- Seah, S., Low, I.C., Hirpara, J.L., Sachaphibulkij, K., Kroemer, G., Brenner, C., and Pervaiz, S. (2015). Activation of surrogate death receptor signaling triggers peroxynitrite-dependent execution of cisplatin-resistant cancer cells. *Cell Death Dis* 6, e1926.
- Sedger, L.M., Glaccum, M.B., Schuh, J.C., Kanaly, S.T., Williamson, E., Kayagaki, N., Yun, T., Smolak, P., Le, T., Goodwin, R., and Gliniak, B. (2002). Characterization of the in vivo function of TNF-alpha-related apoptosis-inducing ligand, TRAIL/Apo2L, using TRAIL/Apo2L gene-deficient mice. *Eur J Immunol* 32, 2246-2254.
- Senderowicz, A.M., Headlee, D., Stinson, S.F., Lush, R.M., Kalil, N., Villalba, L., Hill, K., Steinberg, S.M., Figg, W.D., Tompkins, A., Arbuck, S.G., and Sausville, E.A. (1998). Phase I trial of continuous infusion flavopiridol, a novel cyclin-dependent kinase inhibitor, in patients with refractory neoplasms. *J Clin Oncol* 16, 2986-2999.
- Shalini, S., Dorstyn, L., Dawar, S., and Kumar, S. (2015). Old, new and emerging functions of caspases. *Cell Death Differ* 22, 526-539.
- Shamimi-Noori, S., Yeow, W.S., Ziauddin, M.F., Xin, H., Tran, T.L., Xie, J., Loehfelm, A., Patel, P., Yang, J., Schrupp, D.S., Fang, B.L., and Nguyen, D.M. (2008). Cisplatin enhances the antitumor effect of tumor necrosis factor-related apoptosis-inducing ligand gene therapy via recruitment of the mitochondria-dependent death signaling pathway. *Cancer Gene Ther* 15, 356-370.
- Sheridan, J.P., Marsters, S.A., Pitti, R.M., Gurney, A., Skubatch, M., Baldwin, D., Ramakrishnan, L., Gray, C.L., Baker, K., Wood, W.I., Goddard, A.D., Godowski, P., and Ashkenazi, A. (1997). Control of TRAIL-induced apoptosis by a family of signaling and decoy receptors. *Science* 277, 818-821.
- Shi, H., Hugo, W., Kong, X., Hong, A., Koya, R.C., Moriceau, G., Chodon, T., Guo, R., Johnson, D.B., Dahlman, K.B., Kelley, M.C., Kefford, R.F., Chmielowski, B., Glaspy, J.A., Sosman, J.A., van Baren, N., Long, G.V., Ribas, A., and Lo, R.S. (2014). Acquired resistance and clonal evolution in melanoma during BRAF inhibitor therapy. *Cancer Discov* 4, 80-93.
- Shimizu, Y., Taraborrelli, L., and Walczak, H. (2015). Linear ubiquitination in immunity. *Immunol Rev* 266, 190-207.
- Shimkin, M.B., and Stoner, G.D. (1975). Lung tumors in mice: application to carcinogenesis bioassay. *Adv Cancer Res* 21, 1-58.
- Shore, S.M., Byers, S.A., Dent, P., and Price, D.H. (2005). Characterization of Cdk9(55) and differential regulation of two Cdk9 isoforms. *Gene* 350, 51-58.
- Shore, S.M., Byers, S.A., Maury, W., and Price, D.H. (2003). Identification of a novel isoform of Cdk9. *Gene* 307, 175-182.
- Siegel, R.L., Miller, K.D., and Jemal, A. (2019). Cancer statistics, 2019. *CA Cancer J Clin* 69, 7-34.
- Simonet, W.S., Lacey, D.L., Dunstan, C.R., Kelley, M., Chang, M.S., Luthy, R., Nguyen, H.Q., Wooden, S., Bennett, L., Boone, T., Shimamoto, G., DeRose, M., Elliott, R., Colombero, A., Tan, H.L., Trail, G., Sullivan, J., Davy, E., Bucay, N., Renshaw-Gegg, L., Hughes, T.M., Hill, D., Pattison, W., Campbell, P., Sander, S., Van, G., Tarpley, J., Derby, P., Lee, R., and Boyle, W.J. (1997). Osteoprotegerin: a novel secreted protein involved in the regulation of bone density. *Cell* 89, 309-319.

- Singh, H.D., Otano, I., Rombouts, K., Singh, K.P., Peppas, D., Gill, U.S., Bottcher, K., Kennedy, P.T.F., Oben, J., Pinzani, M., Walczak, H., Fusai, G., Rosenberg, W.M.C., and Maini, M.K. (2017). TRAIL regulatory receptors constrain human hepatic stellate cell apoptosis. *Sci Rep* 7, 5514.
- Smith, C.A., Farrah, T., and Goodwin, R.G. (1994). The TNF receptor superfamily of cellular and viral proteins: activation, costimulation, and death. *Cell* 76, 959-962.
- Smyth, M.J., Cretney, E., Takeda, K., Wiltrot, R.H., Sedger, L.M., Kayagaki, N., Yagita, H., and Okumura, K. (2001). Tumor necrosis factor-related apoptosis-inducing ligand (TRAIL) contributes to interferon gamma-dependent natural killer cell protection from tumor metastasis. *J Exp Med* 193, 661-670.
- Snyder, A., Makarov, V., Merghoub, T., Yuan, J., Zaretsky, J.M., Desrichard, A., Walsh, L.A., Postow, M.A., Wong, P., Ho, T.S., Hollmann, T.J., Bruggeman, C., Kannan, K., Li, Y., Elipenahli, C., Liu, C., Harbison, C.T., Wang, L., Ribas, A., Wolchok, J.D., and Chan, T.A. (2014). Genetic basis for clinical response to CTLA-4 blockade in melanoma. *N Engl J Med* 371, 2189-2199.
- Sogaard, T.M., and Svejstrup, J.Q. (2007). Hyperphosphorylation of the C-terminal repeat domain of RNA polymerase II facilitates dissociation of its complex with mediator. *J Biol Chem* 282, 14113-14120.
- Solca, F., Dahl, G., Zoephel, A., Bader, G., Sanderson, M., Klein, C., Kraemer, O., Himmelsbach, F., Haakma, E., and Adolf, G.R. (2012). Target binding properties and cellular activity of afatinib (BIBW 2992), an irreversible ErbB family blocker. *J Pharmacol Exp Ther* 343, 342-350.
- Son, J.K., Varadarajan, S., and Bratton, S.B. (2010). TRAIL-activated stress kinases suppress apoptosis through transcriptional upregulation of MCL-1. *Cell Death Differ* 17, 1288-1301.
- Soria, J.C., Mark, Z., Zatloukal, P., Szima, B., Albert, I., Juhasz, E., Pujol, J.L., Kozielski, J., Baker, N., Smethurst, D., Hei, Y.J., Ashkenazi, A., Stern, H., Amler, L., Pan, Y., and Blackhall, F. (2011). Randomized phase II study of dulanermin in combination with paclitaxel, carboplatin, and bevacizumab in advanced non-small-cell lung cancer. *J Clin Oncol* 29, 4442-4451.
- Soria, J.C., Smit, E., Khayat, D., Besse, B., Yang, X., Hsu, C.P., Reese, D., Wiezorek, J., and Blackhall, F. (2010). Phase 1b study of dulanermin (recombinant human Apo2L/TRAIL) in combination with paclitaxel, carboplatin, and bevacizumab in patients with advanced non-squamous non-small-cell lung cancer. *J Clin Oncol* 28, 1527-1533.
- Sprick, M.R., Rieser, E., Stahl, H., Grosse-Wilde, A., Weigand, M.A., and Walczak, H. (2002). Caspase-10 is recruited to and activated at the native TRAIL and CD95 death-inducing signalling complexes in a FADD-dependent manner but can not functionally substitute caspase-8. *EMBO J* 21, 4520-4530.
- Sprick, M.R., Weigand, M.A., Rieser, E., Rauch, C.T., Juo, P., Blenis, J., Krammer, P.H., and Walczak, H. (2000). FADD/MORT1 and caspase-8 are recruited to TRAIL receptors 1 and 2 and are essential for apoptosis mediated by TRAIL receptor 2. *Immunity* 12, 599-609.
- Squires, M.S., Feltell, R.E., Wallis, N.G., Lewis, E.J., Smith, D.M., Cross, D.M., Lyons, J.F., and Thompson, N.T. (2009). Biological characterization of AT7519, a small-molecule inhibitor of cyclin-dependent kinases, in human tumor cell lines. *Mol Cancer Ther* 8, 324-332.
- Srivastava, R.K., Kurzrock, R., and Shankar, S. (2010). MS-275 sensitizes TRAIL-resistant breast cancer cells, inhibits angiogenesis and metastasis, and reverses epithelial-mesenchymal transition in vivo. *Mol Cancer Ther* 9, 3254-3266.

Stadel, D., Mohr, A., Ref, C., MacFarlane, M., Zhou, S., Humphreys, R., Bachem, M., Cohen, G., Moller, P., Zwacka, R.M., Debatin, K.M., and Fulda, S. (2010). TRAIL-induced apoptosis is preferentially mediated via TRAIL receptor 1 in pancreatic carcinoma cells and profoundly enhanced by XIAP inhibitors. *Clin Cancer Res* 16, 5734-5749.

Stephenson, J.J., Nemunaitis, J., Joy, A.A., Martin, J.C., Jou, Y.M., Zhang, D., Statkevich, P., Yao, S.L., Zhu, Y., Zhou, H., Small, K., Bannerji, R., and Edelman, M.J. (2014). Randomized phase 2 study of the cyclin-dependent kinase inhibitor dinaciclib (MK-7965) versus erlotinib in patients with non-small cell lung cancer. *Lung Cancer* 83, 219-223.

Sun, L., Wang, H., Wang, Z., He, S., Chen, S., Liao, D., Wang, L., Yan, J., Liu, W., Lei, X., and Wang, X. (2012). Mixed lineage kinase domain-like protein mediates necrosis signaling downstream of RIP3 kinase. *Cell* 148, 213-227.

Sun, X., Yin, J., Starovasnik, M.A., Fairbrother, W.J., and Dixit, V.M. (2002). Identification of a novel homotypic interaction motif required for the phosphorylation of receptor-interacting protein (RIP) by RIP3. *J Biol Chem* 277, 9505-9511.

Swanton, C., and Govindan, R. (2016). Clinical Implications of Genomic Discoveries in Lung Cancer. *N Engl J Med* 374, 1864-1873.

Takeda, K., Hayakawa, Y., Smyth, M.J., Kayagaki, N., Yamaguchi, N., Kakuta, S., Iwakura, Y., Yagita, H., and Okumura, K. (2001). Involvement of tumor necrosis factor-related apoptosis-inducing ligand in surveillance of tumor metastasis by liver natural killer cells. *Nat Med* 7, 94-100.

Takeda, K., Smyth, M.J., Cretney, E., Hayakawa, Y., Kayagaki, N., Yagita, H., and Okumura, K. (2002). Critical role for tumor necrosis factor-related apoptosis-inducing ligand in immune surveillance against tumor development. *J Exp Med* 195, 161-169.

Taniai, M., Grambihler, A., Higuchi, H., Werneburg, N., Bronk, S.F., Farrugia, D.J., Kaufmann, S.H., and Gores, G.J. (2004). Mcl-1 mediates tumor necrosis factor-related apoptosis-inducing ligand resistance in human cholangiocarcinoma cells. *Cancer Res* 64, 3517-3524.

Tartaglia, L.A., Ayres, T.M., Wong, G.H., and Goeddel, D.V. (1993). A novel domain within the 55 kd TNF receptor signals cell death. *Cell* 74, 845-853.

Thome, M., and Tschopp, J. (2001). Regulation of lymphocyte proliferation and death by FLIP. *Nat Rev Immunol* 1, 50-58.

Todaro, M., Lombardo, Y., Francipane, M.G., Alea, M.P., Cammareri, P., Iovino, F., Di Stefano, A.B., Di Bernardo, C., Agrusa, A., Condorelli, G., Walczak, H., and Stassi, G. (2008). Apoptosis resistance in epithelial tumors is mediated by tumor-cell-derived interleukin-4. *Cell Death Differ* 15, 762-772.

Tokunaga, F., Sakata, S., Saeki, Y., Satomi, Y., Kirisako, T., Kamei, K., Nakagawa, T., Kato, M., Murata, S., Yamaoka, S., Yamamoto, M., Akira, S., Takao, T., Tanaka, K., and Iwai, K. (2009). Involvement of linear polyubiquitylation of NEMO in NF-kappaB activation. *Nat Cell Biol* 11, 123-132.

Tolcher, A.W., Mita, M., Meropol, N.J., von Mehren, M., Patnaik, A., Padavic, K., Hill, M., Mays, T., McCoy, T., Fox, N.L., Halpern, W., Corey, A., and Cohen, R.B. (2007). Phase I pharmacokinetic and biologic correlative study of mapatumumab, a fully human monoclonal antibody with agonist activity to tumor necrosis factor-related apoptosis-inducing ligand receptor-1. *J Clin Oncol* 25, 1390-1395.

Tong, W.G., Chen, R., Plunkett, W., Siegel, D., Sinha, R., Harvey, R.D., Badros, A.Z., Popplewell, L., Coutre, S., Fox, J.A., Mahadocon, K., Chen, T., Kegley, P., Hoch, U., and

- Wierda, W.G. (2010). Phase I and pharmacologic study of SNS-032, a potent and selective Cdk2, 7, and 9 inhibitor, in patients with advanced chronic lymphocytic leukemia and multiple myeloma. *J Clin Oncol* 28, 3015-3022.
- Tracey, K.J., Lowry, S.F., and Cerami, A. (1988). Cachetin/TNF-alpha in septic shock and septic adult respiratory distress syndrome. *Am Rev Respir Dis* 138, 1377-1379.
- Trarbach, T., Moehler, M., Heinemann, V., Kohne, C.H., Przyborek, M., Schulz, C., Sneller, V., Gallant, G., and Kanzler, S. (2010). Phase II trial of mapatumumab, a fully human agonistic monoclonal antibody that targets and activates the tumour necrosis factor apoptosis-inducing ligand receptor-1 (TRAIL-R1), in patients with refractory colorectal cancer. *Br J Cancer* 102, 506-512.
- Trauth, B.C., Klas, C., Peters, A.M., Matzku, S., Moller, P., Falk, W., Debatin, K.M., and Krammer, P.H. (1989). Monoclonal antibody-mediated tumor regression by induction of apoptosis. *Science* 245, 301-305.
- Truneh, A., Sharma, S., Silverman, C., Khandekar, S., Reddy, M.P., Deen, K.C., McLaughlin, M.M., Srinivasula, S.M., Livi, G.P., Marshall, L.A., Alnemri, E.S., Williams, W.V., and Doyle, M.L. (2000). Temperature-sensitive differential affinity of TRAIL for its receptors. DR5 is the highest affinity receptor. *J Biol Chem* 275, 23319-23325.
- Tsai, K.L., Sato, S., Tomomori-Sato, C., Conaway, R.C., Conaway, J.W., and Asturias, F.J. (2013). A conserved Mediator-CDK8 kinase module association regulates Mediator-RNA polymerase II interaction. *Nat Struct Mol Biol* 20, 611-619.
- Tumeh, P.C., Harview, C.L., Yearley, J.H., Shintaku, I.P., Taylor, E.J., Robert, L., Chmielowski, B., Spasic, M., Henry, G., Ciobanu, V., West, A.N., Carmona, M., Kivork, C., Seja, E., Cherry, G., Gutierrez, A.J., Grogan, T.R., Mateus, C., Tomasic, G., Glaspy, J.A., Emerson, R.O., Robins, H., Pierce, R.H., Elashoff, D.A., Robert, C., and Ribas, A. (2014). PD-1 blockade induces responses by inhibiting adaptive immune resistance. *Nature* 515, 568-571.
- Tuthill, M.H., Montinaro, A., Zinngrebe, J., Prieske, K., Draber, P., Prieske, S., Newsom-Davis, T., von Karstedt, S., Graves, J., and Walczak, H. (2015). TRAIL-R2-specific antibodies and recombinant TRAIL can synergise to kill cancer cells. *Oncogene* 34, 2138-2144.
- Usanova, S., Piee-Staffa, A., Sied, U., Thomale, J., Schneider, A., Kaina, B., and Koberle, B. (2010). Cisplatin sensitivity of testis tumour cells is due to deficiency in interstrand-crosslink repair and low ERCC1-XPF expression. *Mol Cancer* 9, 248.
- Valley, C.C., Lewis, A.K., Mudaliar, D.J., Perlmutter, J.D., Braun, A.R., Karim, C.B., Thomas, D.D., Brody, J.R., and Sachs, J.N. (2012). Tumor necrosis factor-related apoptosis-inducing ligand (TRAIL) induces death receptor 5 networks that are highly organized. *J Biol Chem* 287, 21265-21278.
- van der Sloot, A.M., Tur, V., Szegezdi, E., Mullally, M.M., Cool, R.H., Samali, A., Serrano, L., and Quax, W.J. (2006). Designed tumor necrosis factor-related apoptosis-inducing ligand variants initiating apoptosis exclusively via the DR5 receptor. *Proc Natl Acad Sci U S A* 103, 8634-8639.
- Vanden Berghe, T., Linkermann, A., Jouan-Lanhouet, S., Walczak, H., and Vandenabeele, P. (2014). Regulated necrosis: the expanding network of non-apoptotic cell death pathways. *Nat Rev Mol Cell Biol* 15, 135-147.
- Varfolomeev, E., Maecker, H., Sharp, D., Lawrence, D., Renz, M., Vucic, D., and Ashkenazi, A. (2005). Molecular determinants of kinase pathway activation by Apo2 ligand/tumor necrosis factor-related apoptosis-inducing ligand. *J Biol Chem* 280, 40599-40608.

- Vercammen, D., Brouckaert, G., Denecker, G., Van de Craen, M., Declercq, W., Fiers, W., and Vandennebeele, P. (1998). Dual signaling of the Fas receptor: initiation of both apoptotic and necrotic cell death pathways. *J Exp Med* *188*, 919-930.
- Vesely, M.D., Kershaw, M.H., Schreiber, R.D., and Smyth, M.J. (2011). Natural innate and adaptive immunity to cancer. *Annu Rev Immunol* *29*, 235-271.
- Vikis, H.G., Rymaszewski, A.L., and Tichelaar, J.W. (2013). Mouse models of chemically-induced lung carcinogenesis. *Front Biosci (Elite Ed)* *5*, 939-946.
- Vilimanovich, U., and Bumbasirevic, V. (2008). TRAIL induces proliferation of human glioma cells by c-FLIPL-mediated activation of ERK1/2. *Cell Mol Life Sci* *65*, 814-826.
- Vitovski, S., Phillips, J.S., Sayers, J., and Croucher, P.I. (2007). Investigating the interaction between osteoprotegerin and receptor activator of NF-kappaB or tumor necrosis factor-related apoptosis-inducing ligand: evidence for a pivotal role for osteoprotegerin in regulating two distinct pathways. *J Biol Chem* *282*, 31601-31609.
- Voigt, S., Philipp, S., Davarnia, P., Winoto-Morbach, S., Roder, C., Arenz, C., Trauzold, A., Kabelitz, D., Schutze, S., Kalthoff, H., and Adam, D. (2014). TRAIL-induced programmed necrosis as a novel approach to eliminate tumor cells. *BMC Cancer* *14*, 74.
- von Karstedt, S., Conti, A., Nobis, M., Montinaro, A., Hartwig, T., Lemke, J., Legler, K., Annewanter, F., Campbell, A.D., Taraborrelli, L., Grosse-Wilde, A., Coy, J.F., El-Bahrawy, M.A., Bergmann, F., Koschny, R., Werner, J., Ganten, T.M., Schweiger, T., Hoetzenecker, K., Kenessey, I., Hegedus, B., Bergmann, M., Hauser, C., Egberts, J.H., Becker, T., Rocken, C., Kalthoff, H., Trauzold, A., Anderson, K.I., Sansom, O.J., and Walczak, H. (2015). Cancer cell-autonomous TRAIL-R signaling promotes KRAS-driven cancer progression, invasion, and metastasis. *Cancer Cell* *27*, 561-573.
- von Karstedt, S., Montinaro, A., and Walczak, H. (2017). Exploring the TRAILs less travelled: TRAIL in cancer biology and therapy. *Nat Rev Cancer* *17*, 352-366.
- von Pawel, J., Harvey, J.H., Spigel, D.R., Dediu, M., Reck, M., Cebotaru, C.L., Humphreys, R.C., Gribbin, M.J., Fox, N.L., and Camidge, D.R. (2014). Phase II trial of mapatumumab, a fully human agonist monoclonal antibody to tumor necrosis factor-related apoptosis-inducing ligand receptor 1 (TRAIL-R1), in combination with paclitaxel and carboplatin in patients with advanced non-small-cell lung cancer. *Clin Lung Cancer* *15*, 188-196 e182.
- Wada, T., Takagi, T., Yamaguchi, Y., Ferdous, A., Imai, T., Hirose, S., Sugimoto, S., Yano, K., Hartzog, G.A., Winston, F., Buratowski, S., and Handa, H. (1998). DSIF, a novel transcription elongation factor that regulates RNA polymerase II processivity, is composed of human Spt4 and Spt5 homologs. *Genes Dev* *12*, 343-356.
- Wainberg, Z.A., Messersmith, W.A., Peddi, P.F., Kapp, A.V., Ashkenazi, A., Royer-Joo, S., Portera, C.C., and Kozloff, M.F. (2013). A phase 1B study of dulanermin in combination with modified FOLFOX6 plus bevacizumab in patients with metastatic colorectal cancer. *Clin Colorectal Cancer* *12*, 248-254.
- Wakelee, H.A., Patnaik, A., Sikic, B.I., Mita, M., Fox, N.L., Miceli, R., Ullrich, S.J., Fisher, G.A., and Tolcher, A.W. (2010). Phase I and pharmacokinetic study of lexatumumab (HGS-ETR2) given every 2 weeks in patients with advanced solid tumors. *Ann Oncol* *21*, 376-381.
- Walczak, H., Degli-Esposti, M.A., Johnson, R.S., Smolak, P.J., Waugh, J.Y., Boiani, N., Timour, M.S., Gerhart, M.J., Schooley, K.A., Smith, C.A., Goodwin, R.G., and Rauch, C.T. (1997). TRAIL-R2: a novel apoptosis-mediating receptor for TRAIL. *EMBO J* *16*, 5386-5397.

- Walczak, H., Iwai, K., and Dikic, I. (2012). Generation and physiological roles of linear ubiquitin chains. *BMC Biol* 10, 23.
- Walczak, H., Miller, R.E., Ariail, K., Gliniak, B., Griffith, T.S., Kubin, M., Chin, W., Jones, J., Woodward, A., Le, T., Smith, C., Smolak, P., Goodwin, R.G., Rauch, C.T., Schuh, J.C., and Lynch, D.H. (1999). Tumoricidal activity of tumor necrosis factor-related apoptosis-inducing ligand in vivo. *Nat Med* 5, 157-163.
- Walsby, E., Pratt, G., Shao, H., Abbas, A.Y., Fischer, P.M., Bradshaw, T.D., Brennan, P., Fegan, C., Wang, S., and Pepper, C. (2014). A novel Cdk9 inhibitor preferentially targets tumor cells and synergizes with fludarabine. *Oncotarget* 5, 375-385.
- Walunas, T.L., Lenschow, D.J., Bakker, C.Y., Linsley, P.S., Freeman, G.J., Green, J.M., Thompson, C.B., and Bluestone, J.A. (1994). CTLA-4 can function as a negative regulator of T cell activation. *Immunity* 1, 405-413.
- Wang, G., Zhan, Y., Wang, H., and Li, W. (2012a). ABT-263 sensitizes TRAIL-resistant hepatocarcinoma cells by downregulating the Bcl-2 family of anti-apoptotic protein. *Cancer Chemother Pharmacol* 69, 799-805.
- Wang, H., Davis, J.S., and Wu, X. (2014a). Immunoglobulin Fc domain fusion to TRAIL significantly prolongs its plasma half-life and enhances its antitumor activity. *Mol Cancer Ther* 13, 643-650.
- Wang, H., Sun, L., Su, L., Rizo, J., Liu, L., Wang, L.F., Wang, F.S., and Wang, X. (2014b). Mixed lineage kinase domain-like protein MLKL causes necrotic membrane disruption upon phosphorylation by RIP3. *Mol Cell* 54, 133-146.
- Wang, K., Hampson, P., Hazeldine, J., Krystof, V., Strnad, M., Pechan, P., and M, J. (2012b). Cyclin-dependent kinase 9 activity regulates neutrophil spontaneous apoptosis. *PLoS One* 7, e30128.
- Wang, T.T., and Jeng, J. (2000). Coordinated regulation of two TRAIL-R2/KILLER/DR5 mRNA isoforms by DNA damaging agents, serum and 17beta-estradiol in human breast cancer cells. *Breast Cancer Res Treat* 61, 87-96.
- Warzocha, K., Bienvenu, J., Coiffier, B., and Salles, G. (1995). Mechanisms of action of the tumor necrosis factor and lymphotoxin ligand-receptor system. *Eur Cytokine Netw* 6, 83-96.
- Wei, M.C., Lindsten, T., Mootha, V.K., Weiler, S., Gross, A., Ashiya, M., Thompson, C.B., and Korsmeyer, S.J. (2000). tBID, a membrane-targeted death ligand, oligomerizes BAK to release cytochrome c. *Genes Dev* 14, 2060-2071.
- Wei, P., Garber, M.E., Fang, S.M., Fischer, W.H., and Jones, K.A. (1998). A novel CDK9-associated C-type cyclin interacts directly with HIV-1 Tat and mediates its high-affinity, loop-specific binding to TAR RNA. *Cell* 92, 451-462.
- Weinlich, R., Oberst, A., Dillon, C.P., Janke, L.J., Milasta, S., Lukens, J.R., Rodriguez, D.A., Gurung, P., Savage, C., Kanneganti, T.D., and Green, D.R. (2013). Protective roles for caspase-8 and cFLIP in adult homeostasis. *Cell Rep* 5, 340-348.
- Weinstock, C., Khozin, S., Suzman, D., Zhang, L., Tang, S., Wahby, S., Goldberg, K.B., Kim, G., and Pazdur, R. (2017). U.S. Food and Drug Administration Approval Summary: Atezolizumab for Metastatic Non-Small Cell Lung Cancer. *Clin Cancer Res* 23, 4534-4539.
- Wells, A.D., and Morawski, P.A. (2014). New roles for cyclin-dependent kinases in T cell biology: linking cell division and differentiation. *Nat Rev Immunol* 14, 261-270.

- Went, P.T., Lugli, A., Meier, S., Bundi, M., Mirlacher, M., Sauter, G., and Dirnhofer, S. (2004). Frequent EpCam protein expression in human carcinomas. *Hum Pathol* 35, 122-128.
- Werneburg, N.W., Guicciardi, M.E., Bronk, S.F., Kaufmann, S.H., and Gores, G.J. (2007). Tumor necrosis factor-related apoptosis-inducing ligand activates a lysosomal pathway of apoptosis that is regulated by Bcl-2 proteins. *J Biol Chem* 282, 28960-28970.
- Westcott, P.M., Halliwill, K.D., To, M.D., Rashid, M., Rust, A.G., Keane, T.M., Delrosario, R., Jen, K.Y., Gurley, K.E., Kemp, C.J., Fredlund, E., Quigley, D.A., Adams, D.J., and Balmain, A. (2015). The mutational landscapes of genetic and chemical models of Kras-driven lung cancer. *Nature* 517, 489-492.
- Wiley, S.R., Schooley, K., Smolak, P.J., Din, W.S., Huang, C.P., Nicholl, J.K., Sutherland, G.R., Smith, T.D., Rauch, C., Smith, C.A., and Goodwin, R.G. (1995). Identification and characterization of a new member of the TNF family that induces apoptosis. *Immunity* 3, 673-682.
- Wilson, N.S., Yang, A., Yang, B., Couto, S., Stern, H., Gogineni, A., Pitti, R., Marsters, S., Weimer, R.M., Singh, M., and Ashkenazi, A. (2012). Proapoptotic activation of death receptor 5 on tumor endothelial cells disrupts the vasculature and reduces tumor growth. *Cancer Cell* 22, 80-90.
- Wolf, Y., Bartok, O., Patkar, S., Eli, G.B., Cohen, S., Litchfield, K., Levy, R., Jimenez-Sanchez, A., Trabish, S., Lee, J.S., Karathia, H., Barnea, E., Day, C.P., Cinnamon, E., Stein, I., Solomon, A., Bitton, L., Perez-Guijarro, E., Dubovik, T., Shen-Orr, S.S., Miller, M.L., Merlino, G., Levin, Y., Pikarsky, E., Eisenbach, L., Admon, A., Swanton, C., Ruppin, E., and Samuels, Y. (2019). UVB-Induced Tumor Heterogeneity Diminishes Immune Response in Melanoma. *Cell* 179, 219-235 e221.
- Wong, K.H., Jin, Y., and Struhl, K. (2014). TFIIH phosphorylation of the Pol II CTD stimulates mediator dissociation from the preinitiation complex and promoter escape. *Mol Cell* 54, 601-612.
- Wu, G.S., Burns, T.F., McDonald, E.R., 3rd, Jiang, W., Meng, R., Krantz, I.D., Kao, G., Gan, D.D., Zhou, J.Y., Muschel, R., Hamilton, S.R., Spinner, N.B., Markowitz, S., Wu, G., and el-Deiry, W.S. (1997). KILLER/DR5 is a DNA damage-inducible p53-regulated death receptor gene. *Nat Genet* 17, 141-143.
- Wu, G.S., Burns, T.F., Zhan, Y., Alnemri, E.S., and El-Deiry, W.S. (1999). Molecular cloning and functional analysis of the mouse homologue of the KILLER/DR5 tumor necrosis factor-related apoptosis-inducing ligand (TRAIL) death receptor. *Cancer Res* 59, 2770-2775.
- Wu, S.Y., and Chiang, C.M. (2007). The double bromodomain-containing chromatin adaptor Brd4 and transcriptional regulation. *J Biol Chem* 282, 13141-13145.
- Wu, Y., Giaisi, M., Kohler, R., Chen, W.M., Krammer, P.H., and Li-Weber, M. (2017). Rocaglamide breaks TRAIL-resistance in human multiple myeloma and acute T-cell leukemia in vivo in a mouse xenograft model. *Cancer Lett* 389, 70-77.
- Xiang, H., Nguyen, C.B., Kelley, S.K., Dybdal, N., and Escandon, E. (2004). Tissue distribution, stability, and pharmacokinetics of Apo2 ligand/tumor necrosis factor-related apoptosis-inducing ligand in human colon carcinoma COLO205 tumor-bearing nude mice. *Drug Metab Dispos* 32, 1230-1238.
- Xiang, T., Bai, J.Y., She, C., Yu, D.J., Zhou, X.Z., and Zhao, T.L. (2018). Bromodomain protein BRD4 promotes cell proliferation in skin squamous cell carcinoma. *Cell Signal* 42, 106-113.

- Yamada, T., Yamaguchi, Y., Inukai, N., Okamoto, S., Mura, T., and Handa, H. (2006). P-TEFb-mediated phosphorylation of hSpt5 C-terminal repeats is critical for processive transcription elongation. *Mol Cell* *21*, 227-237.
- Yamaguchi, Y., Takagi, T., Wada, T., Yano, K., Furuya, A., Sugimoto, S., Hasegawa, J., and Handa, H. (1999). NELF, a multisubunit complex containing RD, cooperates with DSIF to repress RNA polymerase II elongation. *Cell* *97*, 41-51.
- Yang, Z., Yik, J.H., Chen, R., He, N., Jang, M.K., Ozato, K., and Zhou, Q. (2005). Recruitment of P-TEFb for stimulation of transcriptional elongation by the bromodomain protein Brd4. *Mol Cell* *19*, 535-545.
- Yang, Z., Zhu, Q., Luo, K., and Zhou, Q. (2001). The 7SK small nuclear RNA inhibits the CDK9/cyclin T1 kinase to control transcription. *Nature* *414*, 317-322.
- Yao, W., Yue, P., Khuri, F.R., and Sun, S.Y. (2015). The BET bromodomain inhibitor, JQ1, facilitates c-FLIP degradation and enhances TRAIL-induced apoptosis independent of BRD4 and c-Myc inhibition. *Oncotarget* *6*, 34669-34679.
- Yin, T., Lallena, M.J., Kreklau, E.L., Fales, K.R., Carballares, S., Torres, R., Wishart, G.N., Ajamie, R.T., Cronier, D.M., Iversen, P.W., Meier, T.I., Foreman, R.T., Zeckner, D., Sissons, S.E., Halstead, B.W., Lin, A.B., Donoho, G.P., Qian, Y., Li, S., Wu, S., Aggarwal, A., Ye, X.S., Starling, J.J., Gaynor, R.B., de Dios, A., and Du, J. (2014). A novel CDK9 inhibitor shows potent antitumor efficacy in preclinical hematologic tumor models. *Mol Cancer Ther* *13*, 1442-1456.
- Yokosuka, T., Takamatsu, M., Kobayashi-Imanishi, W., Hashimoto-Tane, A., Azuma, M., and Saito, T. (2012). Programmed cell death 1 forms negative costimulatory microclusters that directly inhibit T cell receptor signaling by recruiting phosphatase SHP2. *J Exp Med* *209*, 1201-1217.
- Yonehara, S., Ishii, A., and Yonehara, M. (1989). A cell-killing monoclonal antibody (anti-Fas) to a cell surface antigen co-downregulated with the receptor of tumor necrosis factor. *J Exp Med* *169*, 1747-1756.
- You, M., Candrian, U., Maronpot, R.R., Stoner, G.D., and Anderson, M.W. (1989). Activation of the Ki-ras protooncogene in spontaneously occurring and chemically induced lung tumors of the strain A mouse. *Proc Natl Acad Sci U S A* *86*, 3070-3074.
- Younes, A., Vose, J.M., Zelenetz, A.D., Smith, M.R., Burris, H.A., Ansell, S.M., Klein, J., Halpern, W., Miceli, R., Kumm, E., Fox, N.L., and Czuczman, M.S. (2010). A Phase 1b/2 trial of mapatumumab in patients with relapsed/refractory non-Hodgkin's lymphoma. *Br J Cancer* *103*, 1783-1787.
- Young, N.P., Crowley, D., and Jacks, T. (2011). Uncoupling cancer mutations reveals critical timing of p53 loss in sarcomagenesis. *Cancer Res* *71*, 4040-4047.
- Yu, H.A., Sima, C.S., Huang, J., Solomon, S.B., Rimner, A., Paik, P., Pietanza, M.C., Azzoli, C.G., Rizvi, N.A., Krug, L.M., Miller, V.A., Kris, M.G., and Riely, G.J. (2013). Local therapy with continued EGFR tyrosine kinase inhibitor therapy as a treatment strategy in EGFR-mutant advanced lung cancers that have developed acquired resistance to EGFR tyrosine kinase inhibitors. *J Thorac Oncol* *8*, 346-351.
- Yu, J.W., Jeffrey, P.D., and Shi, Y. (2009). Mechanism of procaspase-8 activation by c-FLIPL. *Proc Natl Acad Sci U S A* *106*, 8169-8174.
- Yudkovsky, N., Ranish, J.A., and Hahn, S. (2000). A transcription reinitiation intermediate that is stabilized by activator. *Nature* *408*, 225-229.

- Yun, H.D., Schirm, D.K., Felices, M., Miller, J.S., and Eckfeldt, C.E. (2019). Dinaciclib enhances natural killer cell cytotoxicity against acute myelogenous leukemia. *Blood Adv* 3, 2448-2452.
- Zengerle, M., Chan, K.H., and Ciulli, A. (2015). Selective Small Molecule Induced Degradation of the BET Bromodomain Protein BRD4. *ACS Chem Biol* 10, 1770-1777.
- Zerafa, N., Westwood, J.A., Cretney, E., Mitchell, S., Waring, P., Iezzi, M., and Smyth, M.J. (2005). Cutting edge: TRAIL deficiency accelerates hematological malignancies. *J Immunol* 175, 5586-5590.
- Zhang, H., Pandey, S., Travers, M., Sun, H., Morton, G., Madzo, J., Chung, W., Khowsathit, J., Perez-Leal, O., Barrero, C.A., Merali, C., Okamoto, Y., Sato, T., Pan, J., Garriga, J., Bhanu, N.V., Simithy, J., Patel, B., Huang, J., Raynal, N.J., Garcia, B.A., Jacobson, M.A., Kadoch, C., Merali, S., Zhang, Y., Childers, W., Abou-Gharbia, M., Karanicolas, J., Baylin, S.B., Zahnow, C.A., Jelinek, J., Grana, X., and Issa, J.J. (2018). Targeting CDK9 Reactivates Epigenetically Silenced Genes in Cancer. *Cell* 175, 1244-1258 e1226.
- Zhang, L., and Fang, B. (2005). Mechanisms of resistance to TRAIL-induced apoptosis in cancer. *Cancer Gene Ther* 12, 228-237.
- Zhang, P., Miska, J., Lee-Chang, C., Rashidi, A., Panek, W.K., An, S., Zannikou, M., Lopez-Rosas, A., Han, Y., Xiao, T., Pituch, K.C., Kanojia, D., Balyasnikova, I.V., and Lesniak, M.S. (2019). Therapeutic targeting of tumor-associated myeloid cells synergizes with radiation therapy for glioblastoma. *Proc Natl Acad Sci U S A* 116, 23714-23723.
- Zhang, X.D., Borrow, J.M., Zhang, X.Y., Nguyen, T., and Hersey, P. (2003). Activation of ERK1/2 protects melanoma cells from TRAIL-induced apoptosis by inhibiting Smac/DIABLO release from mitochondria. *Oncogene* 22, 2869-2881.
- Zhang, X.D., Zhang, X.Y., Gray, C.P., Nguyen, T., and Hersey, P. (2001). Tumor necrosis factor-related apoptosis-inducing ligand-induced apoptosis of human melanoma is regulated by smac/DIABLO release from mitochondria. *Cancer Res* 61, 7339-7348.
- Zhao, J., Jitkaew, S., Cai, Z., Choksi, S., Li, Q., Luo, J., and Liu, Z.G. (2012). Mixed lineage kinase domain-like is a key receptor interacting protein 3 downstream component of TNF-induced necrosis. *Proc Natl Acad Sci U S A* 109, 5322-5327.
- Zhu, Y., Pe'ery, T., Peng, J., Ramanathan, Y., Marshall, N., Marshall, T., Amendt, B., Mathews, M.B., and Price, D.H. (1997). Transcription elongation factor P-TEFb is required for HIV-1 tat transactivation in vitro. *Genes Dev* 11, 2622-2632.